UNIVERSITEIT VAN PRETORIA
UNIVERSITY OF PRETORIA
YUNIBESITHI YA PRETORIA

Role of African horsesickness virus protein NS3 in cytotoxicity and virus induced cytopathology

by

Tracy Leonora Meiring

Submitted in partial fulfilment of the requirements for the degree
Philosophiae Doctor

in the Faculty of Natural & Agricultural Science
University of Pretoria

Pretoria
February 2009

DECLARATION

I, Tracy Leonora Meiring declare that the thesis/dissertation, which I hereby submit for the degree Philosophiae Doctor at the University of Pretoria, is my own work and has not previously been submitted by me for a degree at this or any other tertiary institution.

Signature:
Date:

ACKNOWLEDGEMENTS

I would like to express my sincere appreciation and thanks to the following people:

Dr Vida van Staden for her valuable guidance, motivation, and support throughout this study

Prof Henk Huismans for his leadership, support and critical advice

Flip Wege for his excellent technical assistance with cell culture

Alan Hall and Chris van der Merwe at the Laboratory for Microscopy and Microanalysis at the University of Pretoria (UP)

Renate Zipfel, Gladys Shabangu and Mia Beyleveld at the Sequencing facility (UP)

Dr Marco Romito and Dr A.C. Potgieter at the Onderstepoort Veterinary Institute

The Department of Biochemistry (UP) for the use of their facilities

My fellow colleagues in the Orbivirus Research group and Department of Genetics (UP) for their interest and support

The National Research Foundation for financial assistance

My family and friends for their encouragement and understanding

SUMMARY

Role of African horsesickness virus protein NS3 in cytotoxicity and virus induced cytopathology

by

Tracy Leonora Meiring

Supervisor: Dr Vida van Staden
Department of Genetics
University of Pretoria

Co-supervisor: Prof Henk Huismans
Department of Genetics
University of Pretoria

For the degree PhD

The viral determinants of African horsesickness virus (AHSV) cytopathology are not well understood. Several AHSV proteins may play a role, including non-structural protein NS3, a cytotoxic membrane protein that localises to sites of virus release and plasma membrane disorganisation in infected cells. AHSV NS3 is highly variable and clusters into three phylogenetic groups, termed α, β and γ. In chapter 2 we examined the role of NS3 in determining the phenotypic characteristics observed during AHSV infection of cells. Three AHSV strains, AHSV-2 (γ NS3), AHSV-3 (β NS3) and AHSV-4 (α NS3), were shown to have quantitatively different phenotypes in Vero cells. To investigate the contribution of NS3 to these differences, reassortants were generated between these strains in which the S10 genome segment encoding NS3 was exchanged, alone or in combination with other segments. Exchange of NS3 resulted in changes in virus release and membrane permeability, indicating an important role for NS3 in these viral properties. The cytopathic effect and decreased viability of infected cells was not associated with NS3 alone and it is likely that a number of viral and host factors contribute to these complex phenotypes.

In chapter 3 the cytolytic effect of the NS3 proteins of the orbiviruses AHSV, bluetongue virus (BTV) and equine encephalosis virus (EEV) were compared. Inducible expression in *Escherichia coli* (*E. coli*) showed differences in cytotoxicity, with EEV NS3 having a greater lytic effect than

AHSV and BTV NS3. Cytotoxicity was linked to increased membrane permeability of the cells as confirmed by an increased uptake of membrane impermeant compounds. When expressed in insect cells however all three NS3 proteins caused a marked but equivalent decrease in cell viability. Although the orbivirus NS3 proteins have similar predicted secondary structures, differences could lie in structural stability and association with membranes of specific cell types, which impacts on cytotoxicity. To determine the regions within AHSV NS3 that mediate cytotoxicity, a series of truncated mutants of NS3 where constructed and expressed in *E. coli*. The combined presence of both hydrophobic domains of AHSV NS3 was found to be critical for membrane permeabilisation and cytotoxicity.

In chapter 4 the AHSV-2, AHSV-3 and AHSV-4 NS3 proteins (from the γ, β and α NS3 clades) were compared to examine the impact of sequence variation in NS3 on structure and function. The proteins were expressed in the baculovirus expression system as both wild-type proteins and C-terminal eGFP (enhanced green fluorescent protein) fusions. Exogenous addition of the baculovirus expressed proteins to Vero cells resulted in different permeabilisation levels that could be linked to that induced by the AHSV strains. Cell viability and membrane association assays in insect cells showed that all three proteins were equivalently cytotoxic and membrane associated. The subcellular localisation of the eGFP-NS3 fusion proteins was examined by confocal fluorescent imaging of live cells. NS3 localised to the plasma membrane, and as distinct punctuate foci in the perinuclear region. This suggests localisation to the internal membrane systems of cells and has important implications for the function of this membrane permeabilising protein.

LIST OF ABBREVIATIONS

aa	amino acid
AHS	African horsesickness
AHSV	African horsesickness virus
amp	ampicillin
BHK	baby hamster kidney cells
bp	base pairs
BTV	bluetongue virus
^{o}C	degrees Celsius
cDNA	complementary deoxyribonucleic acid
Ci	Curie
CLP	core-like particle
cm^2	centimetre squared
CPE	cytopathic effect
CPM	counts per minute
Da	Dalton
DEPC	diethylpyrocarbonate
DLP	double-layered particle
DNA	deoxyribonucleic acid
dNTP	deoxyribonucleotide triphosphate
ds	double-stranded
DTT	dithiothreitol
EC	endothelial cells
EDTA	ethylenediaminetetra-acetic acid
EEV	equine encephalosis virus
eGFP	enhanced green fluorescent protein
EHDV	epizootic haemorrhagic disease virus
ER	endoplasmic reticulum
et al.	*et alibi*
EtBr	ethidium bromide
FCS	foetal calf serum
Fig.	figure
g	gravitational force
G	gauge
gal	galactosidase
gent	gentamycin
GFP	green fluorescent protein
GST	glutathione S-transferase
h	hour/s
HD	hydrophobic domain
HIV	human immunodeficiency virus
Hyg B	hygromycin B
i.e.	that is
IgG	immunoglobulin class G
IgY	immunoglobulin class Y
IPTG	isopropyl-β-D thiogalactopyranoside
k	kilo
kan	kanamycin
kb	kilobase pairs
kDa	kilodalton
LB	Luria-Bertani medium
M	molar
MEM	minimal essential medium Eagle
min	minute/s
ml	millilitre

mM	millimolar
MMOH	methyl mercuric hydroxide
MOI	multiplicity of infection
mRNA	messenger RNA
NaCl	sodium chloride
ND	not done
ng	nanograms
NLS	nuclear localisation signal
nm	nanometers
NS	non-structural
OD_{600}	optical density at 600 nm
OIE	Office International des Epizooties
ORF	open reading frame
OVI	Onderstepoort Veterinary Institute
P	Particulate
PAGE	polyacrylamide gel electrophoresis
PBS	phosphate buffered saline
PCR	polymerase chain reaction
PEG	polyethylene glycol
pfu	plaque-forming units
p.i.	post infection
PMSF	phenylmethylsulphonyl fluoride
PSB	protein solvent buffer
rif	rifampicin
RNA	ribonucleic acid
rpm	revolutions per minute
S	supernatant
S1-S10	segments 1 to 10 (refers to orbiviruses)
^{35}S	radiolabelled sulphur
SD	standard deviation
SDS	sodium dodecyl sulphate
sec	second/s
Sf9	*Spodoptera frugiperda* insect cells
siRNA	small interfering RNA
ss	single-stranded
TEMED	N,N,N',N'-tetramethylethylene diamine
tet	tetracycline
TM	transmembrane
TMHMM	TransMembrane Hidden Markov Model
Tris	Tris hydroxymethyl aminomethane
UHQ	ultra high quality water
µg	micrograms
µl	microlitres
µm	micrometers
U	units
UP	University of Pretoria
UV	ultraviolet
V	volts
VIB	viral inclusion body
VLP	virus-like particle
VMP	viral membrane protein
VP	virus protein
VPS	vacuolar protein sorting
v/v	volume per volume
v/w	volume per weight
X-gal	5-bromo-4-chloro-3-indolyl-β-D-galactopyranoside

LIST OF BUFFERS

Hypotonic buffer:

10 mM Tris, 0.2 mM $MgCl_2$ [pH 7.4]

NTE:

100 mM NaCl, 10 mM Tris, 1 mM EDTA [pH 7.4]

PBS:

137 mM NaCl, 2.7 mM KCl, 4.3 mM $Na_2HPO_4.7H_20$, 1.4 mM KH_2PO_4 [pH 7.3]

PSB (2x):

125 mM Tris-HCl [pH 6.8], 4% SDS, 20% glycerol, 10% 2-mercaptoethanol

TGS:

25 mM Tris-HCl [pH 8.3], 192 mM glycine, 0.1% SDS

Transfer buffer:

25 mM Tris, 192 mM glycine

Tris-glycine buffer:

25 mM Tris, 250 mM glycine

TABLE OF CONTENTS

CHAPTER 1: LITERATURE REVIEW

1.1. INTRODUCTION

Since the discovery of viruses as 'filterable disease agents', approximately 110 years ago, the field has expanded enormously with viruses continually being discovered in many different species. The currently identified and characterised viruses probably represent only a fraction of the viral diversity, or virosphere, predicted to be present in the biosphere. Suttle (2005) proposes that viruses are the most abundant biological entities on the planet and are, in terms of biomass, second only to prokaryotes. These recent insights imply that, in most cases, excessive virulence in viruses is an exception, and probably an evolutionary dead-end strategy. It is, nonetheless, these virulent viruses that have received most of our attention because of their devastating disease causing capabilities. Remarkable progress has been made in our understanding of exactly how these viruses cause disease, the myriad strategies they use to multiply within their hosts, the subtle and often surprising interactions that exist between them and their hosts, and the diverse tactics they employ to evade detection and eradication by their hosts' defence systems.

The focus of this investigation is a virus that causes one of the most lethal viral diseases of equids, African horsesickness (AHS). This review will summarise the progress that has been made in research on African horsesickness virus (AHSV), and will highlight the need for further investigation into the viral factors that contribute to the molecular basis of AHS disease and pathogenesis. The emphasis of this review will be on the non-structural AHSV protein NS3 that has been implicated by previous studies to be a potentially important factor in disease pathogenesis and virulence. Viral proteins that share similar structural and/or functional characteristics to AHSV NS3 will also be discussed.

1.2. AFRICAN HORSESICKNESS (AHS)

1.2.1. History and current status of AHS

Although the first known historical report of a disease resembling AHS was in Yemen in 1327, the disease almost certainly originated in Africa (Coetzer & Guthrie, 2004). Here it was probably first recognised following the introduction of horses into central and east Africa. In southern Africa, were AHS is endemic today, the first serious outbreak occurred in 1719 when over 1 700 horses died. Over the subsequent years at least 10 major and numerous lesser outbreaks have been recorded in this region. The most severe outbreak occurred in South Africa in 1854 causing the death of over 70 000 horses. The incidence, range and severity of outbreaks in this region has decreased greatly over the past century probably relating to the decline in horse and zebra

numbers, and the introduction of AHS vaccines. The disease has made incursions into other areas including the Middle East, Arabia, India and Pakistan between 1959 and 1961, North Africa and Spain from 1955 to 1956, and Spain, Portugal and Morocco in 1987 to 1991 (Mellor & Hamblin, 2004).

The pioneering work on AHS and the discovery of the etiological agent, African horsesickness virus (AHSV), occurred in the early 1900s. M'Fadyean showed that AHS was transmissible through filtered bacteria-free blood from an infected horse, his results were confirmed and expanded on by Sir Arnold Theiler in 1901. Theiler commenced research on AHSV, demonstrating the plurality of the virus strains and their impact on vaccination, as well as describing the disease forms of AHS (Theiler, 1921). In the late 1960s Dr Verwoerd at the Onderstepoort Veterinary Research Institute showed that AHSV had a segmented double stranded RNA (dsRNA) genome. Since this early work research into AHSV, and other related dsRNA viruses, has expanded greatly and will be outlined later in this review.

Currently there is no specific treatment available for AHS. Animals that recover from infections show life-long immunity to the serotype they were infected with and partial immunity to similar serotypes (Erasmus, 1998). Prevention and control measures include the restriction of animal movement, slaughter of viraemic animals, stabling susceptible horses at the times at which the vector is most active (at twilight and during the night), vector control (insecticides and repellents) and vaccination (Mellor & Hamblin, 2004). The only widely available commercial AHSV vaccines are supplied by Onderstepoort Biological Products, Onderstepoort, South Africa (www.obpvaccines.co.za). These vaccines are polyvalent attenuated cell culture adapted viruses. Adult horses in southern Africa, excluding regions of the Western Cape province, are vaccinated annually in spring in an attempt to prevent disease and control outbreaks (Coetzer & Guthrie, 2004). Monovalent vaccines are sometimes additionally administered during outbreaks. Concerns over the safety and efficacy of these vaccines have been raised following cases of alleged vaccine failure and vaccine-induced disease. Analysis of AHSV isolates from three post-vaccination horses that died or exhibited AHS symptoms, revealed reassortment of the vaccine but reassortants were found not to be pathogenic or lethal when administered to susceptible horses (Von Teichman & Smit, 2008). Further large scale studies would however have to be conducted to determine the frequency of vaccine reassortment, and the potential association of the vaccine with AHS disease and AHS-induced death.

During AHS outbreaks, or potential outbreaks, the detection and serotyping of AHSV is crucial and should occur timeously. Although the clinical signs and lesions typical of AHS are specific they can be confused with other diseases. Rapid serotyping is also essential for the selection of

the correct vaccine serotype for efficient control of the spread of the disease, particularly when the outbreak occurs in a non-endemic area (Koekemoer *et al.*, 2000). Several techniques have therefore been tailored for the detection of the AHSV RNA segments, antigens and antibodies. These include, for example, a novel real time PCR assay developed for the detection and serotyping of AHSV within two to three hours (Rodriguez-Sanchez *et al.*, 2008).

1.2.2. Host range and transmission

Many species of vertebrate are susceptible to AHSV infection, including zebras, horses, mules, donkeys, dogs, camels and elephants. Signs of clinical infection are rarely seen in zebras and they have long been considered to be the natural vertebrate host and reservoir of AHSV. They are believed to play a vital role in the persistence of the virus in Africa. The introduction of zebras, with sub-clinical infection, into a safari park close to Madrid is the likely cause of the outbreak of AHS in Spain in 1987. Horses, mules and donkeys are not considered long-term reservoirs, involved in the permanent persistence of the virus, because of the high mortality rate frequently recorded, particularly in horses (Mellor & Hamblin, 2004).

AHS is not contagious, and the virus is transmitted by *Culicoides* biting midges of which the most important vectors in Africa are *C. imicola* and *C. bolitinos* (Venter *et al.,* 2000). The insect is most active during the summer, when the optimal conditions of warm weather, high rainfall and wind occur. *Culicoides imicola* breeds in wet soil and in years of heavy rain its population can increase over 200-fold (Meiswinkel, 1998). The spread of the virus has been limited by the climatic conditions favoured by these insects (Meiswinkel, 1998; Mellor *et al.*, 1998). *Culicoides imicola* is common throughout Africa and south east Asia, and is now known to be widespread across the southern parts of Europe (Mellor & Hamblin, 2004). Climate change however may increase the vector range and so doing raise the possibility of the international spread of AHS (Purse *et al.*, 2005; Gould & Higgs, 2009).

1.2.3. AHS disease forms and pathogenesis

African horsesickness has four clinicopathological forms: horsesickness fever, cardiac form, pulmonary form and mixed form. Horsesickness fever is characterised by a remittent mild to moderate fever and is often subclinical with no associated mortality. It occurs frequently following infection with less virulent strains of virus or when some degree of immunity exists (for example horses that have been vaccinated with or exposed to a heterologous serotype). This is the only form of disease exhibited by zebra. The cardiac (sub-acute) form is characterised by fever (lasting 3-6 days), subcutaneous oedema of the head, neck and chest and supraorbital fossa, and

haemorrhages of the eyes and ventral tongue surface. Death is as a result of cardiac failure. Mortality rates with this form range from 50 to 60%. The pulmonary (peracute) form develops rapidly (1 to 3 days), with marked depression, fever, increased respiratory rate, severely laboured breathing, profuse sweating and coughing spasms. A frothy, serofibrinous fluid may exude from the nostrils. The mortality rate in horses with this form is high, exceeding 95%, and death is due to a lack of oxygen. The mixed form of AHS is the most common and is a combination of the cardiac and pulmonary forms with mortality rates between 50 and 90% (Coetzer & Guthrie, 2004; Mellor & Hamblin, 2004).

The form of disease in infected horses may be the result of a variety of factors, including the route of infection, tropism of sub-populations of virus particles, host immune status, permissivity and genetic susceptibility (Laegreid *et al.*, 1993). However, the principal determinant of the clinical form of the disease was shown in experimentally infected naive horses to be the viral virulence phenotype (Laegreid *et al.*, 1993).

The clinical and molecular basis of AHS pathogenesis is not well understood. The key pathological features of AHS are oedema, effusion and haemorrhage, and the clinical signs are thought to develop as a result of damage to the circulatory and respiratory systems (Mellor & Hamblin, 2004). On infection of the vertebrate host initial virus multiplication occurs in local lymph nodes and the virus is then spread throughout the body via the circulatory system. This primary viraemia enables the virus to infect target organs; namely the lungs, spleen, other tissues of the lymphoid system, and various endothelial cells (EC). Replication of the virus in these tissues then leads to secondary viraemia that usually coincides with the onset of fever (Mellor & Hamblin, 2004). In experimentally infected horses, with the peracute form of disease, viral antigen is found mainly in the cardio-vascular and lymphatic systems. In these horses AHSV antigen was located primarily in EC of capillaries, and small venous and arteriolar vessels, particularly of cardiopulmonary tissues suggesting that EC are the main target of AHSV infection during the late stages of this form of the disease (Wohlsein *et al.*, 1997). AHSV has been shown to infect pulmonary microvascular EC, causing pronounced cell swelling, discontinuity of the plasma membrane and loss of structural detail in severely affected cells (Laegreid *et al.*, 1992a). Skowneck *et al.* (1995) suggest that it is the loss of the EC barrier function that results in the development of the prominent pathological features. Damage to EC and loss of integrity of intercellular junctions could result in loss of EC barrier function and the subsequent development of oedema (Laegreid *et al.*, 1992a; Skowronek *et al.*, 1995; Gomez-Villamandos *et al.*, 1999). Virulence variants of AHSV have also been shown to differ in their ability to infect and damage cultured EC (Laegreid *et al.*, 1992b).

1.3. AFRICAN HORSESICKNESS VIRUS (AHSV)

1.3.1. Classification

AHSV is a member of the genus *Orbivirus* in the family *Reoviridae*. Members of the *Orbivirus* genus frequently have similar morphological and molecular characteristics but distinct host ranges and pathobiological properties (Roy, 1996). The prototype orbivirus, bluetongue virus (BTV), is similar in molecular constitution and morphology to AHSV but causes disease in cattle and sheep (Mellor & Hamblin, 2004). Another closely related orbivirus, equine encephalosis virus (EEV), infects equids but disease is subclinical (Coetzer & Erasmus, 1994). Biting midges (*Culicoides* spp.) are the principal vectors for all three of these orbiviruses.

Nine serotypes of AHSV have been identified that are antigenically distinct based on neutralisation studies of the major outer capsid viral protein VP2 (Howell, 1962).

1.3.2. Genome

Orbiviruses are characterised by a genome consisting of 10 double-stranded (ds) RNA segments of different sizes encoding at least seven structural (VP1-VP7) and four non-structural proteins, NS1, NS2, NS3 and NS3A (Bremer, 1976; Huismans, 1979; Mertens *et al.*, 1984; Mertens, 2004). The dsRNA genome segments are enclosed within the inner core of the virus and are never exposed in the cytoplasm (Mertens & Diprose, 2004). The total AHSV genome is approximately 18 kilobase pairs (kb) in length. The 5' non-coding regions of the genome segments are 12 to 35 base pairs (bp) in length and the 3' non-coding regions 29 to 100 bp. Partial inverted complementarity is observed between the 5' and 3' end sequences within each AHSV segment, indicating the potential for the formation of secondary structure in the single stranded (ss) RNA forms (Roy *et al.*, 1994).

1.3.3. Structural proteins

The mature AHSV virion is a non-enveloped icosahedral particle composed of two distinct layers; a core or inner capsid surrounded by an outer capsid (Roy *et al.*, 1994).

1.3.3.1. Outer capsid proteins

The outer capsid of AHSV is composed of structural proteins VP2 and VP5. VP2 (encoded by segment 2) is the major component of the outer shell of the virus particle and is involved in virus-

cell attachment and penetration (Roy *et al.*, 1994). The full-length VP2 genes of all nine AHSV serotypes have been cloned, expressed and the protein sequences aligned. Sequence homology varied between 47.6 and 71.4 % indicating that VP2 is the most variable AHSV protein (Potgieter *et al.*, 2003). The major serotype-specific neutralising epitopes of AHSV are located on VP2 (Burrage *et al.*, 1993; Martinez-Torrecuadrada *et al.*, 1994; Martinez-Torrecuadrada & Casal, 1995; Bentley *et al.*, 2000; Martinez-Torrecuadrada *et al.*, 2001). Recombinant baculovirus expressed VP2, alone or in combination with VP5 and/or VP7, provided full protection against AHSV challenge in horses (Martinez-Torrecuadrada *et al.*, 1996; Roy *et al.*, 1996; Stone-Marschat *et al.*, 1996). The insolubility and aggregation of the protein have however made the development of VP2 subunit vaccines problematic (Du Plessis *et al.*, 1998). AHSV serotype 4 VP2 and VP5 have successfully been expressed from individual alphavirus-based vaccine vectors, initial tests however failed to induce a neutralising antibody response in horses (MacLachlan *et al.*, 2007).

AHSV VP5 is encoded by segment 6 and its biological function remains unknown, although it is probably analogous to that of its BTV counterpart (Martinez-Torrecuadrada *et al.*, 1999). In BTV, VP5 is believed to play an important role during cell entry. Following attachment to the membrane the virus enters the cell via the clathrin-dependant endocytic pathway. The virus is then internalised into early endosomes where separation of the outer and inner capsid layers is induced by low pH (Forzan *et al.*, 2007). The transcriptionally active core is then delivered into the cell cytoplasm. Purified BTV VP5 was shown to permeabilise both mammalian and *Culicoides* cell membranes (Hassan *et al.*, 2001) and to act as a fusion protein, at low pH, when fused to a transmembrane anchor and expressed on the cell surface (Forzan *et al.*, 2004). Both permeabilisation and fusion activities are mediated by two N-terminal amphipathic helixes. BTV VP5 is believed therefore to play a major role in destabilising the membrane of the endocytosed vesicle allowing the release of the viral core into the cytoplasm (Hassan *et al.*, 2001; Forzan *et al.*, 2004). AHSV VP5 contains similar amphipathic helix motifs and appears to be cytotoxic when expressed in insect cells (Roy *et al.*, 1994).

1.3.3.2. Inner capsid proteins

The genome of AHSV is encapsidated by an inner core particle composed of two major structural proteins (VP7 and VP3) and three core-associated enzymes (VP1, VP4 and VP6). The genome remains within the inner core throughout the replication cycle (Mertens & Diprose, 2004). This is essential as direct contact between the dsRNA and the host cell cytoplasm would activate an array of host antiviral mechanisms and degradation by nucleases. In BTV the core particle has been studied to atomic resolution by X-ray crystallography, revealing important information with

regard to the organisation of VP3 and VP7, the packaging of the genome within the core, as well as how the simultaneous and repeated transcription of all 10 genome segments occurs within the confined interior of the core (Grimes *et al.*, 1998; Mertens & Diprose, 2004).

VP3 and VP7 (encoded by segments 3 and 7 respectively) are highly conserved between members of the O*rbivirus* genus and contain the group-specific antigenic determinants (Roy, 1996). When AHSV VP3 and VP7 were co-expressed in insect cells they aggregated to form empty core-like particles (CLP) (Maree *et al.*, 1998). When expressed alone in insect cells AHSV VP7 forms hexagonal crystalline structures due to its insoluble and hydrophobic nature (Chuma *et al.*, 1992).

VP1 and VP4 (encoded by segment 1 and 4 respectively) are considered to have replicase-transcriptase and guanyl transferase activity respectively, analogous to BTV VP1 and VP4 (Roy *et al.*, 1994). VP6 (encoded by segment 9) is believed to act as the viral helicase catalysing the unwinding of the dsRNA segments prior to transcription. The protein shares a degree of sequence similarity to an *E. coli* helicase (Turnbull *et al.*, 1996) and has the ability to bind both single-stranded (ss) and ds RNA and DNA (De Waal & Huismans, 2005). A recent study revealed the potential for a second open reading frame (ORF) on genome segment 9 (Firth, 2008), whether this ORF is expressed, and what functional role the encoded protein may play, remains to be experimentally investigated. VP1, VP4 and VP6 therefore provide the enzymatic machinery needed to convert dsRNA into a translatable mRNA, as well as synthesizing a negative RNA strand from a positive RNA template to reform the dsRNA genome segments in progeny virus cores.

1.3.4. Non-structural proteins

AHSV NS1 is encoded by segment 5. NS1 is highly conserved; a comparison of NS1 sequences from AHSV serotypes 4, 6 and 9 revealed 95 to 98% amino acid homology (Maree & Huismans, 1997). The protein is synthesised in large amounts (up to 25% of the total viral proteins in BTV-infected cells) and forms the characteristic tubules that are observed in orbiviral infected cells throughout the infection cycle (Huismans & Els, 1979). NS1 contains several conserved cysteine residues that are believed to be of functional significance in forming the highly ordered helical assemblies. Of the 16 cysteine residues found in AHSV NS1 9 are conserved at the same site in BTV NS1 (Maree & Huismans, 1997). Mutational analysis of BTV NS1 revealed that both the conserved cysteines at residues 337 and 340 as well as the N- and C-termini are essential for tubule formation (Monastyrskaya *et al.*, 1994). The exact function of NS1, and the tubular structures formed by this protein, is not yet clear but studies on BTV NS1 suggest an involvement

in virus morphogenesis (Owens *et al.*, 2004). The use of the tubular structures of NS1 as an immunogen delivery system is being investigated (Ghosh *et al.*, 2002a; Ghosh *et al.*, 2002b; Murphy & Roy, 2008).

AHSV NS2 is encoded by segment 8 and is highly conserved (Van Staden & Huismans, 1991). The protein forms dense granular bodies in recombinant baculovirus infected cells (Uitenweerde *et al.*, 1995). These structures are similar to the virus inclusion bodies (VIBs) observed in the cytoplasm of AHSV infected cells. VIBs are the virus factories where viral replication and core assembly occur. NS2 is therefore believed to be involved in virus assembly by forming a matrix within the cytoplasm to which cores, viral proteins and ssRNA rapidly associate and where core assembly occurs. AHSV NS2 furthermore has ssRNA binding ability and is therefore thought to be directly involved in viral mRNA recruitment to these inclusion sites (Uitenweerde *et al.*, 1995). BTV NS2 has been found to recognise different RNA structures and to contain several RNA-binding domains. This may be the basis for the discrimination between viral RNAs and may explain how a single copy of each RNA segment is selected for incorporation into cores during virus assembly (Fillmore *et al.*, 2002; Butan *et al.*, 2004; Lymperopoulos *et al.*, 2006). NS2 is the only phosphorylated viral protein in infected cells (Devaney *et al.*, 1988). In BTV phosphorylation of NS2 is necessary for VIB formation. De-phosphorylation of the protein is thought to result in the disassembly of VIBs allowing the release of assembled cores for the attachment of the outer capsid proteins and subsequent viral release (Modrof *et al.*, 2005; Kar *et al.*, 2007).

NS3 and NS3A are encoded by the smallest RNA genome segment, S10, from alternative start codons in the same open reading frame (Van Staden & Huismans, 1991). NS3 contains 10 additional N-terminal amino acids (aa) that are absent in NS3A. Conserved regions within NS3 include: (i) the initiation codon for NS3A, (ii) a proline-rich region between aa 22 and 34, (iii) a highly conserved region (CR) between aa 46 and 90 (iv) two hydrophobic domains (HD) from aa 116-137 and 154-170 proposed to be transmembrane regions (TM) (Van Staden *et al.*, 1995) and (v) a highly variable, hydrophilic region (aa 139-158) between the HDs (Van Niekerk *et al.*, 2003; Quan *et al.*, 2008). These conserved domains are also present in NS3 from other orbiviruses, such as BTV and EEV (Van Niekerk *et al.*, 2003).

NS3 is a membrane associated protein expressed at low levels in infected cells (Van Staden *et al.*, 1995). The protein is proposed to be involved in virus release based on its presence at sites of membrane damage and virus exit in AHSV-infected cells (Stoltz *et al.*, 1996). When expressed in insect cells NS3 causes a cytotoxic effect (Van Staden *et al.*, 1995). The mechanism by which NS3 causes cell death is unknown, but may be as a result of the modification of the permeability of the cell membrane. Cytotoxicity was found to be dependant on the membrane association of

the protein, which is mediated by its two hydrophobic transmembrane domains (Van Niekerk *et al.*, 2001a). The cytotoxic nature of NS3, and its potential role in virus release, suggests a possible involvement in pathogenicity and virulence.

Unlike NS1 and NS2, NS3 is a highly variable protein with amino acid variation of up to 28% within and 37% across serotypes (Van Niekerk *et al.*, 2001b). This makes NS3 the second most variable AHSV protein after the outer capsid protein VP2. The reason for this high level of variation is unknown. Comparison of the nucleotide sequence of S10 revealed the presence of three distinct phylogenetic groups, termed clades α, β and γ (Sailleau *et al.*, 1997; Martin *et al.*, 1998; Van Niekerk *et al.*, 2001b; Quan *et al.*, 2008). Analysis of reassortant AHSV viruses indicated that the origin of the S10 gene, i.e. whether it groups into the α, β or γ clade, could contribute to the virulence phenotype and release characteristics of the virus (Martin *et al.*, 1998; O'Hara *et al.*, 1998).

Since NS3 is the focus of this investigation the functional analogues in other members of the *Reoviridae* family, namely BTV NS3 and rotavirus NSP4, will be discussed in the following sections.

1.4. BLUETONGUE VIRUS NS3

BTV NS3 is the cognate protein to AHSV NS3 in the prototype orbivirus, BTV. This orbivirus has been extensively studied and the findings have served as a model and directed research on related dsRNA viruses. A brief outline of the findings with regard to the life cycle of BTV, and the role played by the various BTV proteins, will therefore firstly be given here.

1.4.1. BTV life cycle

During the BTV life cycle cell attachment, and cell tropism, are mediated by the binding of VP2 to a cellular receptor in susceptible cells (Hassan & Roy, 1999). The virus then enters the cell through clathrin-mediated endocytosis and is incorporated into early endosomes (Forzan *et al.*, 2007). The low pH environment within these endosomes causes degradation of VP2 and triggers conformational modifications in VP5 that allow the protein to associate with and possibly permeabilise the endosomal membrane (Hassan *et al.*, 2001). This is thought to facilitate the release of the transcriptionally active core into the cytoplasm while VP5 is retained in the endosomes (Forzan *et al.*, 2007). The core particle consists of a protective layer of VP7 and VP3 proteins, the enzymes (VP1, VP4 and VP6) necessary for transcription, capping and helicase activity, and the ten dsRNA genome segments. Once in the cytoplasm the core enzymes

immediately initiate transcription of each of the genome segments into full-length positive sense ssRNA. The newly synthesised methylated and capped mRNA strands exit the core, are translated by the host cell machinery and used as templates for negative strand synthesis during the formation of the progeny virus genome (Mertens & Diprose, 2004).

Following viral protein synthesis, phosphorylated NS2 condenses with viral ssRNA to form viral inclusion bodies (VIBs). The core structural proteins localise to these VIBs where they form subcores and cores. The ssRNA is packaged within these cores and converted to dsRNA (Mertens & Diprose, 2004). During the final stages of virus assembly the outer capsid proteins, VP2 and VP5, are attached to the cores at the surface of VIBs. De-phosphorylation of NS2 in the VIBs then leads to the release of the newly formed progeny virions (Modrof *et al.*, 2005). An alternative model for the final stages of virus production was recently proposed, where VP5 associates with lipid rafts in the plasma membrane, and core particles are transported to these sites for the final assembly of the outer capsid proteins (Bhattacharya & Roy, 2008). Once the outer capsid is attached the viral protein NS3 has been proposed to mediate release by a variety of mechanisms as will be discussed in the following section.

1.4.2. Role of BTV NS3 in the viral life cycle

The smallest genome segment of BTV, as in AHSV, encodes two related proteins NS3 and NS3A from two overlapping in-phase open reading frames (Van Dijk & Huismans, 1988). BTV NS3 sequences however, in contrast to AHSV NS3, are highly conserved amongst serotypes (Van Niekerk *et al.*, 2003; Balasuriya *et al.*, 2008). Variation of BTV NS3 is thought to be limited by structural and functional constraints (Pierce *et al.*, 1998; Balasuriya *et al.*, 2008). Recombinant baculovirus expressed BTV NS3 and NS3A reacted strongly with sera from sheep following infection with homologous and heterologous BTV serotypes, suggesting that they are highly conserved group-specific antigens (French *et al.*, 1989).

BTV NS3 and NS3A are integral membrane glycoproteins (Wu *et al.*, 1992) associated with lipid membranes in infected cells (Hyatt *et al.*, 1991; Bansal *et al.*, 1998). Electron microscopic examination of BTV-infected cells showed that NS3 was associated with areas of membrane perturbation and that the presence of the protein correlated with BTV release (Hyatt *et al.*, 1991). Recombinant baculovirus expression of BTV virus-like particles (VLPs) together with NS3/NS3A resulted in the budding and release of these particles from infected cells. Release of VLPs did not occur in the absence of NS3, or when NS1 was co-expressed with the VLPs. NS3 is therefore involved in the release of BTV from infected cells (Hyatt *et al.*, 1993).

BTV may be released from cells by lysis or budding, and several studies have implicated NS3 in both release strategies. Beaton *et al.* (2002) showed that the C-terminal domain of NS3 interacts with the outermost BTV capsid protein VP2, while an amphipathic α-helix in the N-terminal domain interacts with a cellular protein p11 (currently called S100A10). The p11 protein, together with p36 (currently called annexin A2), forms a heterotetramer molecule known as the annexin II complex (or Calpactin complex). Annexins, such as annexin A2, exhibit binding to phospholipids and membranes in various tissues while S100A10 has the ability to bind cytoskeletal proteins, such as actin. The annexin II complex can therefore link membranes and/or vesicles to cytoskeletal proteins and so regulate membrane organisation (Miwa *et al.*, 2008). This complex has been implicated in cellular processes such as exocytosis and correct trafficking of proteins out of the cell. NS3 was found to interact with p11 at the same site as p36 thereby outcompeting this molecule. The addition of a peptide representing the 14 N-terminal aa of NS3 to BTV-infected C6/36 insect cells severely reduced the amount of virus released, confirming the physiological relevance of the interaction between NS3 and p11. A model for the NS3-mediated non-lytic release of BTV was therefore proposed (Fig. 1.1). In this model NS3 enables virus egress by acting as a receptor for assembled virions and recruiting them to the existing host cell export machinery (Beaton *et al.*, 2002).

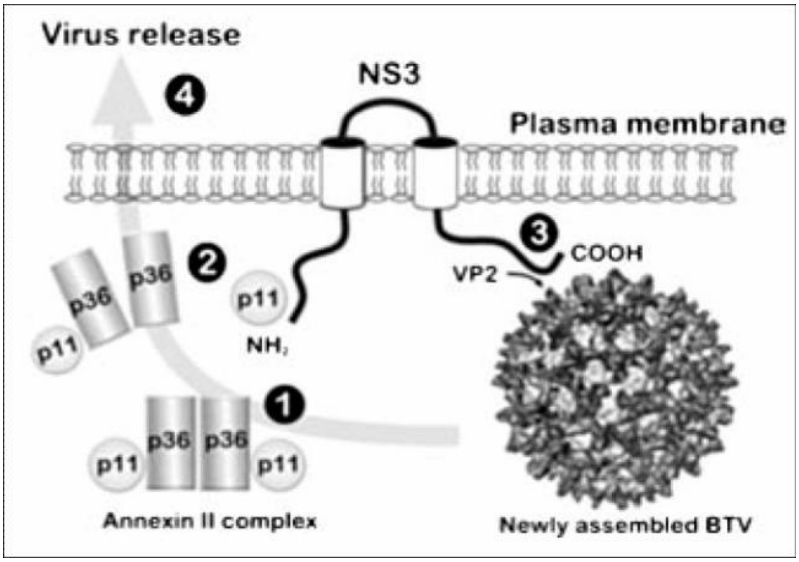

Fig.1.1 A model for the role of BTV NS3 in virus release (Beaton *et al.*, 2002). (1) p11 and p36 form a heterotetramer known as the annexin II complex involved in cellular exocytosis. (2) The N terminus of NS3 interacts with p11, either alone or it may displace one copy of p36 in the heterotetramer so forming a partial annexin II complex. (3) Newly assemble mature virions bind to NS3 via an interaction between the C terminus of NS3 and the outer capsid protein VP2. (4) The virions can now engage with the exocytic machinery via contact with the p11/annexin II complex and non-lytic virus release occurs.

An additional route for the non-lytic release of BTV was proposed when it was found that NS3 binds to and co-localises with Tsg101. This protein forms part of the ESCRT-I (endosomal sorting complex required for transport) complex in the vacuolar protein sorting (VPS) pathway. BTV NS3 interacts with Tsg101 of both mammalian and insect origins, and the interaction is mediated by a conserved PSAP late-domain motif in the conserved proline rich region of NS3. Furthermore, knockdown of Tsg101 by small interfering RNA (siRNA) in BTV-infected cells resulted in a significant reduction in the amount of virus released (Wirblich *et al.*, 2006). BTV NS3 therefore interacts with multiple cellular release factors so facilitating virus budding from infected cells (Fig.1.2).

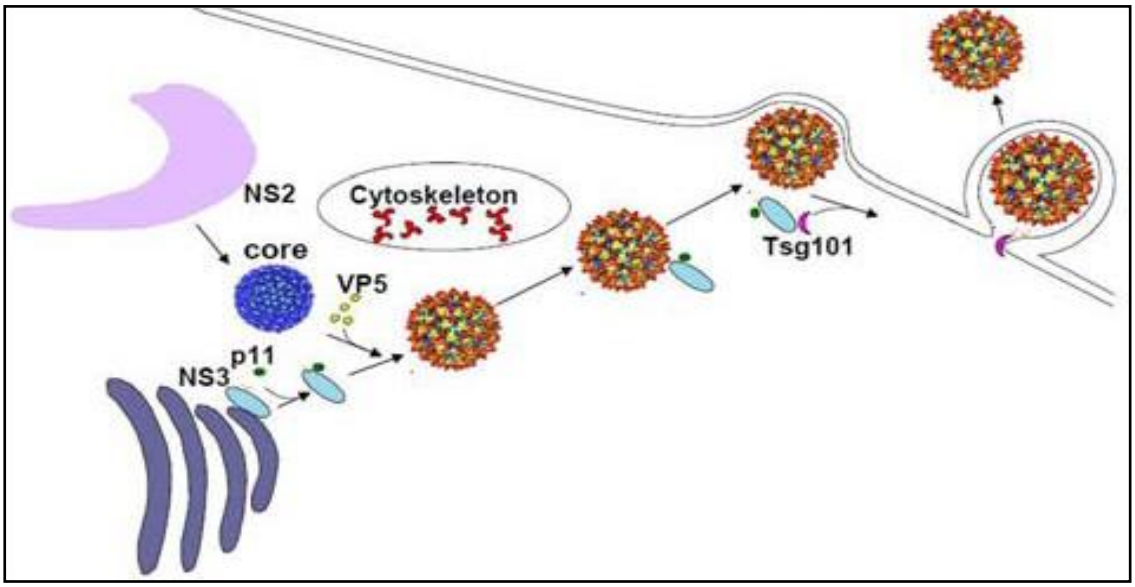

Fig.1.2 A schematic representation of how NS3 may facilitate the non-lytic release of BTV from infected cells through its interaction with the cellular release factors, p11 and Tsg101, and the BTV outer capsid protein VP2 (Roy, 2008).

Han and Harty (2004) demonstrated that NS3 forms homo-oligomers, increases membrane permeability and is targeted to the Golgi apparatus and plasma membrane of cells. The integrity of TM1, but not TM2, was found to be critical for both Golgi targeting and plasma membrane permeabilisation. They concluded that NS3 has viroporin-like properties that may contribute to the role of NS3 in lytic virus release through destabilisation of the plasma membrane. This activity may also contribute to cytopathicity in infected cells and viral pathogenesis.

It has recently been proposed that NS3 may additionally play a role in the final steps of virus assembly through its interaction with VP2 (Beaton *et al.*, 2002) and VP5, where it may keep the two outer capsid proteins in close proximity for assembly onto cores (Bhattacharya & Roy, 2008).

1.5. ROTAVIRUS NSP4

Rotavirus is a member of the *Reoviridae* family and has been the focus of much investigation because of its devastating impact on human health. The rotavirus encoded protein NSP4 is the cognate protein to NS3 of orbiviruses and may share many functional similarities to these proteins. The findings regarding this protein and the role that it plays in the viral life cycle will therefore be discussed here.

NSP4 (encoded by rotavirus genome segment 10) is a relatively small protein, the full length protein being only 175 aa. Structural domains within the protein include: (i) two high mannose N-glycosylation sites at asparagines 8 and 18, (ii) three HDs (H1, H2 and H3) (aa 1-85), (iii) a single membrane spanning or transmembrane domain (formed by H2), (iv) an α-helical coiled-coil structure that allows NSP4 to assemble into homotetramers (between aa 95-137) and (v) a relatively long cytoplasmic tail (aa 45-175) (Taylor *et al.*, 1996; Estes, 2001). The cytoplasmic tail or C-terminal region contains many of the domains responsible for the functions assigned to NSP4.

NSP4 varies by 19.4% between serotypes (Kirkwood & Palombo, 1997) which is significantly less than that observed within the AHSV NS3 protein (Van Niekerk *et al.*, 2001b). Sequence analysis of NSP4 from human and animal rotaviruses has revealed the presence of 4 distinct genetic groups or alleles, termed NSP4 genotypes A to D (Ciarlet *et al.*, 2000).

NSP4 was first identified as a glycosylated 28 kDa integral membrane protein in the ER membrane (Estes, 2001). The protein has subsequently been identified in and associated with a variety of compartments and structures within cells including the ER-Golgi intermediate compartment, autophagosomes (Berkova *et al.*, 2006), raft membranes such as the plasma membrane caveolae (Storey *et al.*, 2007) and microtubules (Xu *et al.*, 2000). NSP4 has also been found to be secreted from rotavirus-infected cells. Both a 7 kDa cleavage product of NSP4 (aa 112-175) (Zhang *et al.*, 2000) and a novel soluble form of NSP4 that has undergone additional posttranslational modifications (Bugarcic & Taylor, 2006) were identified in the media of infected cells. The protein is therefore both cell-associated (intracellular NSP4, iNSP4) and secreted from cells (extracellular NSP4, eNSP4). The fact that NSP4 has different forms, and is localised to different regions within and outside the cell, allows the protein to serve multiple functions during infection.

NSP4 has been found to play several pivotal roles during both rotavirus morphogenesis and rotavirus-induced pathogenesis (Estes, 2001). A putative role for NSP4 in modulating rotavirus

replication was also proposed when it was found that NSP4 depletion by siRNA caused a significant increase in viral transcription late in the infection cycle (Silvestri *et al.*, 2005). How NSP4 aids morphogenesis and contributes to pathogenesis will be discussed in greater detail in the following sections.

1.5.1. Role of NSP4 in rotavirus morphogenesis

During rotavirus morphogenesis immature double layered particles (DLPs) are synthesised within viroplasms in the cytoplasm. These DLPs must then bud into the ER where the final steps of virus maturation occur yielding infectious triple-layered particles (TLPs). In the ER membrane NSP4 is anchored in such a way that the C-terminus projects into the cytoplasm. This cytoplasmic tail acts as a receptor for newly synthesised DLPs and facilitates their translocation into the ER lumen (Estes, 2001). This receptor activity is mediated by the interaction between the last 17 to 20 aa of NSP4 and VP6 in the DLP (O'Brien *et al.*, 2000). When NSP4 synthesis is blocked in rotavirus infected cells almost no viral particles are assembled. The levels and distribution of several other viral proteins, including VP6, are also severely affected (Lopez *et al.*, 2005).

During budding into the ER DLPs acquire a transient lipid envelope that contains NSP4 and the outer capsid protein VP7. Once inside the ER the lipid envelope and NSP4 are lost allowing for the condensation of VP7 and the assembly of the outer capsid layer. In the mature virus the glycoprotein VP7 forms a smooth surface from which VP4 projects as spike-like structures (Estes, 2001). The stage at which VP4 is incorporated into the virion is not yet clear and may differ in different cell lines. Rotavirus assembly and release has been studied most extensively in MA104 (a rhesus monkey epithelial cell line) cells. Here most if not all of the final steps of virus assembly occur in the ER, where the incorporation of VP4 is thought to coincide with budding (Maass & Atkinson, 1990). Mature viruses then remain associated with the ER until being released by cell lysis (Estes, 2001). An alternative mode of virus assembly and release was however observed in Caco-2 cells, a well differentiated polarised cell line of human intestinal origin (Jourdan *et al.*, 1997; Sapin *et al.*, 2002).

Jourdan and co-workers (1997) found that the release of rotavirus from polarised intestinal Caco-2 cells occurred prior to any cell lysis, did not involve the Golgi apparatus or lysosomes and that the virus was associated with smooth vesicles within the cell. Sapin *et al.* (2002) later showed that VP4 associates with rafts (specialized membrane microdomains enriched in cholesterol and sphingolipids) within these cells as early as 3 hours post infection, and at a later stage other structural proteins and NSP4 were also found in these rafts. Rafts purified from these cells

contained infectious virus. In these cells, VP4 assembly with the rest of the viral particle occurs outside the ER via an association of VP7-coated DLPs with VP4-containing lipid rafts at the plasma membrane (Delmas *et al.*, 2004a; Delmas *et al.*, 2004b). Besides serving as platforms for the final stages of virus assembly these lipid rafts may also provide targeting of the mature virus to the cell membrane in a pathway that bypasses the Golgi apparatus, the classic exocytic pathway (Sapin *et al.*, 2002; Chwetzoff & Trugnan, 2006).

Several lines of evidence have shown that some portion of NSP4 resides in cellular lipid rafts; Triton X-100 resistant lipid rafts from rotavirus-infected Caco-2 cells contained NSP4 (Sapin *et al.*, 2002; Cuadras *et al.*, 2006), NSP4 (aa 114 to 135) has been shown to bind to caveolin-1, a marker of detergent resistant membrane fractions called caveolae (Parr *et al.*, 2006; Mir *et al.*, 2007), and full-length NSP4 has been detected in plasma membrane caveolae (Storey *et al.*, 2007). NSP4 within these rafts may function as a receptor to recruit DLPs and other viral proteins. VP7, NSP4 and VP4 have been shown to form complexes (Maass & Atkinson, 1990), and NSP4 binds VP4 (mediated by aa 112-148) (Au *et al.*, 1993). Furthermore, NSP4 silencing decreased the association of virus particles with rafts (Cuadras *et al.*, 2006). Rafts may also serve as a transport mechanism for NSP4 from the ER to the plasma membrane (Storey *et al.*, 2007).

NSP4 has also been shown to interact with parts of the ER molecular chaperone and folding systems. NSP4 binds to protein disulphide isomerase (PDI) (Mirazimi & Svensson, 1998) and calnexin (Mirazimi *et al.*, 1998), and also upregulates BiP (GRP78) and endoplasmin (GRP94) (Xu *et al.*, 1998). The main function of these molecular chaperones and folding enzymes is to prevent any non-specific interactions between newly synthesised proteins, to maintain these proteins in a proper state for folding and to mark incorrectly folded proteins for degradation. These proteins thus act as a quality control checkpoint in the ER. The significance of the interaction between NSP4 and this system to virus assembly is unknown but siRNA silencing of these chaperones during rotavirus infection has shown them to be necessary for quality control during rotavirus morphogenesis from MA104 cells (Maruri-Avidal *et al.*, 2008).

1.5.1. Role of NSP4 in rotavirus pathogenesis

The key pathological feature of rotavirus infection is age-dependant diarrhoea. The development of diarrhoea is a multifactorial process involving changes in the Ca^{2+} dependant processes of water and electrolyte secretion, as well as the induction of cell death in the different cell types that form the intestinal epithelium. Several properties of NSP4 have implicated this protein as a virulence factor involved in rotavirus pathogenesis. These include the ability to induce diarrhoea

in the absence of other viral proteins, increase cytosolic calcium ion concentration, induce the expression of nitric oxide synthase, destabilise membranes and disorganise the cell cytoskeleton. Each of these activities and their potential role in pathogenesis will be discussed here.

The most significant finding linking NSP4 to pathogenesis was the discovery that purified NSP4 alone induced diarrhoea when administered to young mice (Ball *et al.*, 1996). Antibodies directed against NSP4 have, furthermore, been found to block both rotaviral- and NSP4-induced diarrhoea in mice (Hou *et al.*, 2008). This enterotoxic activity is associated with a region of the protein between aa 114-135. A peptide representing this region was sufficient to illicit the same diarrhoea inducing effect as the full length protein (Ball *et al.*, 1996), and site-directed mutations between aa 131 and 140 caused a loss of function. NSP4 from virulent and avirulent rotaviruses, that had aa changes in this region, were found to differ greatly in their diarrhoea inducing activities (Zhang *et al.*, 1998). This region interacts with membranes but does not cause membrane destabilisation (Huang *et al.*, 2004). The mechanism of induction of diarrhoea by eNSP4 is believed to be a result of the activation of signal transduction pathways, such as phospholipase C-IP_3, that increases intracellular calcium levels and leads to chloride secretion. A recent study showed that NSP4 binds to integrin alpha1 and alpha2 on the surface of polarized intestinal epithelial (Caco-2) cells triggering this signalling cascade (Seo *et al.*, 2008).

Intracellular expression of NSP4, as a recombinant in insect or mammalian cells, was found to result in an increase in cytoplasmic Ca^{2+} concentration (Tian *et al.*, 1994; Berkova *et al.*, 2003). Silencing NSP4 expression in infected cells prevented the increase in cytosolic Ca^{2+} and plasma membrane permeability to Ca^{2+} normally observed during rotavirus infection and decreased virus yield by more than 90% (Zambrano *et al.*, 2008). The mechanism by which iNSP4 increases plasma membrane permeability to Ca^{2+} is currently unknown. This activity is however known to be independent of the phospholipase C-IP_3 signal transduction pathway used by eNSP4 (Tian *et al.*, 1994; Berkova *et al.*, 2003).

Expression of NSP4 in mammalian (Newton *et al.*, 1997) and *E. coli* (Browne *et al.*, 2000) cells has profound effects on cell viability and membrane stability. This membrane destabilising activity is associated with a membrane-proximal region (residues 48-91) which includes a potential cationic amphipathic helix. It has been proposed that this may be the mechanism used by iNSP4 to increase membrane permeability to Ca^{2+} (Ruiz *et al.*, 2005). Ruiz and co-workers (2005) showed that when glycosylation and membrane trafficking in rotavirus-infected cells where blocked, by tunicamycin and brefeldin A respectively, the increase in Ca^{2+} permeability was inhibited. This indicated that a glycosylated membrane targeted protein was responsible for this activity, the most likely candidate being NSP4.

Both intra- and extracellular NSP4 therefore affect Ca^{2+} homeostasis in cells. The concentration of Ca^{2+} in cells is normally tightly regulated as it controls many essential processes within the cell. Modification of Ca^{2+} homeostasis has been related to cytotoxicity and cell death, and is probably the root cause of the cytopathological effects induced by infection. Alterations to Ca^{2+} concentrations may also be part of the basis of the physiological alterations in the intestine induced by rotavirus which finally lead to diarrhoea (Zambrano *et al.*, 2008).

NSP4 may also alter aqueous secretion in intestinal cells through its ability to inhibit the Na-D-glucose symporter SGLT1 involved in water resorption (Halaihel *et al.*, 2000) and also by inducing the expression of nitric oxide (NO) synthase; an enzyme responsible for the synthesis of NO which is a possible modulator of aqueous secretion (Borghan *et al.*, 2007).

NSP4 has also been found to bind to as well as rearrange different components of the cell cytoskeleton. The protein has been identified along microtubule-like structures and found to block membrane trafficking along microtubules between the ER and the Golgi (Xu *et al.*, 2000). Expression of NSP4 has been found to increase F-actin levels and induce actin rearrangement (Berkova *et al.*, 2007). Both of the above activities may contribute to pathogenesis by interfering with cellular processes dependant on the cytoskeleton, such as endo- and exocytosis, receptor internalization, channel activity and ion gradients.

NSP4 is thus a striking example of not only how multiple functions can be mediated by a single relatively small protein, but also of how a single viral protein can significantly influence, and indeed may be the major determinant of, viral cytopathology and pathogenesis.

1.5. ALTERATION OF MEMBRANE PERMEABILITY BY ANIMAL VIRUSES

Cytolytic animal viruses induce severe adverse effects on susceptible host cells, resulting in profound morphological and biochemical changes, and eventual cell degeneration. These detrimental effects have been linked to the alteration of the host cell membrane permeability, a feature typically observed during viral infection of mammalian cells (Carrasco, 1995).

Increased permeability of the cell to ions and low-molecular-weight compounds changes the cellular ion homeostasis, disrupts the membrane potential and allows the release of essential compounds from the cell. Besides the consequences for the infected cell, membrane permeabilisation can play numerous functions in the viral life cycle. The alteration of ion concentration within the cell may promote viral protein synthesis. The translation of mRNAs from

several cytolytic animal viruses has been found to be fairly resistant to high sodium concentrations with the result that translation of viral mRNA may be promoted over cellular mRNA translation (Garry *et al.*, 1979). Changes in ion concentration may provide an ideal environment for virion assembly. The disruption of the cell membrane could facilitate virus budding and virus spread to surrounding cells. Disorganisation of cellular membranes may lead to the development of the cytopathic effect (CPE) and subsequent cell lysis (Carrasco, 1995; Gonzalez & Carrasco, 2003). Changes in cell homeostasis have also recently been implicated in modulating the cell death programme (Franco *et al.*, 2006).

Several viral gene products may be directly or indirectly responsible for this activity, including viral proteases and glycoproteins. For naked viruses, the intracellular accumulation of viral particles and the expression of large amounts of viral products have often been thought to cause non-specific membrane damage possibly leading to enhanced permeability, cell lysis and release of new progeny. However, increasing evidence has indicated that in a large number of animal viruses a single cytotoxic viral protein or viroporin is specifically responsible for the modification of membrane integrity at late stages of infection (Gonzalez & Carrasco, 2003). Viroporins are virus encoded proteins that when expressed individually cause an increase in membrane permeability to ions and other small molecules (Carrasco, 1995). Several endomembrane systems within the cell may be affected, including the plasma membrane, the ER and the Golgi complex. Examples of viroporins are given in Table 1.1.

Table 1.1 List of viroporins (modified from Gonzalez & Carrasco, 2003)

Virus family	**Viroporins**
Togaviridae	SFV (Semliki forest virus) 6K, Sindbis virus 6K, Ross River virus 6K
Picornaviridae	Poliovirus 2B, Coxsackievirus 2B, Poliovirus 3A
Retroviridae	HIV-1 (human immunodeficiency virus type 1) Vpu
Paramyxoviridae	HRSV (human respiratory syncytial virus) SH
Orthomyxoviridae	Influenza A virus M2
Reoviridae	ARV (avian reovirus) p10
Flaviviridae	HCV (Hepatitis C virus) p7
Phycodnaviridae	PBCV-1 (*Paramecium bursaria* chlorella virus) Kcv
Rhabdoviridae	BEFV (bovine ephemeral fever virus) alpha 10p
Coronaviridae	MHV (murine hepatitis virus) E, SARS-CoV (severe acute respiratory syndrome coronavirus) E

Viroporins are typically small proteins (60-120 aa) that interact directly with membranes. A variety of structural features identified in viroporins may then contribute to the destabilisation of the membrane. The best characterised viroporins are integral membrane proteins that contain a hydrophobic domain that forms an amphipathic α-helix. Upon insertion into the membrane, and oligomerisation of the protein, the hydrophilic residues in this amphipathic helix form a hydrophilic pore, while the hydrophobic residues interact with phospholipids in the membrane. Other viroporins contain an additional hydrophobic domain that interacts with and potentially disturbs the lipid bilayer. The presence of basic amino acids within or surrounding the hydrophobic domain in some viroporins may furthermore have a detergent like effect on membranes (Gonzalez & Carrasco, 2003).

Selected examples of viroporins, and their role in the viral life cycle, will be discussed in the following section.

6K proteins of alphaviruses

Sindbis virus and Semliki forest virus are enveloped, positive sense RNA cytolytic viruses of animals in the *Alphavirus* genus. Late in Sindbis virus infection an increase in intracellular Na^+ ion concentration occurs as a result of changes in cell permeability. This correlates with a substantial decrease in host protein synthesis, while virus protein synthesis continues and appears to favour these conditions (Ulug *et al.*, 1996). These intracellular conditions, therefore, lead to the preferential expression of the virus proteins over the host cell proteins. Changes in the permeability of the membrane of infected cells have been associated with an accessory protein named 6K protein.

6K proteins are small hydrophobic α-helical proteins that associate with membranes. In eukaryotic cells the expression of 6K increases membrane permeability to the translation inhibitor Hygromycin B (Sanz *et al.*, 2003; Madan *et al.*, 2005b; Madan *et al.*, 2008). Inducible expression in *E. coli* leads to leakage of the bacterial cell membrane and cell death (Sanz *et al.*, 1994). 6K proteins, produced synthetically or in *E. coli*, are incorporated into planar lipid bilayers forming cation selective ion channels, increasing membrane conductance (Melton *et al.*, 2002).

Reverse genetics studies on Semliki forest virus, where the entire gene encoding the 6K protein was deleted, indicated that virus replication was not abrogated but that the final assembly and budding of progeny virions were defective. In the absence of 6K virus binding, internalisation, uncoating, replication and the formation of nucleocapsids occurred, but the newly formed nucleocapsids accumulated at the plasma membrane (Loewy *et al.*, 1995; Sanz *et al.*, 2003). In

HIV-1 mutants expressing truncated variants of the HIV-1 viroporin, Vpu, a similar effect was noted. Here the virus was still capable of replication but the final assembly and exit of virus particles was affected with a large proportion of particles remaining cell associated (Gonzalez & Carrasco, 2001). Interestingly, the synthesis of HIV-1 Vpu in cells infected with Sindbis virus lacking the 6K gene was capable of compensating for, in part, the defects in final assembly and release caused by the absence of 6K (Gonzalez & Carrasco, 2001).

2B proteins of enteroviruses

Enteroviruses (such as poliovirus, coxsackievirus, echovirus) are members of the *Picornaviridae* family of nonenveloped, cytolytic viruses. Several functional and morphological modifications occur in host cell membranes in enterovirus infected cells. The permeability of both intracellular membranes and the plasma membrane is affected, and the enterovirus viroporin 2B protein plays a major role in these virus-induced membrane modifications (Aldabe *et al.*, 1996; De Jong *et al.*, 2004). Recombinant expression of 2B in mammalian cells induces the permeabilisation of the plasma membrane, the ER and the Golgi complex (Aldabe *et al.*, 1996; Van Kuppeveld *et al.*, 2005). 2B localises to the ER, Golgi complex and to a lesser extent to the plasma membrane (De Jong *et al.*, 2004). The 2B protein sequence contains two hydrophobic domains, predicted to form transmembrane regions that insert into the negatively charged membranes of the target organelles forming an integral hairpin loop (De Jong *et al.*, 2004).

The 2B protein of enteroviruses additionally has an anti-apoptotic function that is related to its membrane permeabilising effect. The 2B protein forms pores in the ER and Golgi membranes allowing the passage of Ca^{2+} out of these organelles thereby reducing their Ca^{2+} content. This potentially serves two different purposes. Firstly, it provides the intracellular conditions necessary for the replication of the viral RNA genome, and secondly delays the apoptotic host-cell response. ER–mitochondrial Ca^{2+} signalling occurs during the initiation of apoptosis, the reduction of calcium in the ER and Golgi by 2B therefore perturbs this signalling pathway. This activity delays the host-cell apoptotic response allowing time for the virus to replicate. The apoptotic program is not, however, blocked and at a later stage the killing of the host cell facilitates the release of the newly formed progeny virions (Van Kuppeveld *et al.*, 2005). Madan *et al.* (2008) however report that several viroporins from RNA viruses, including the 2B protein of poliovirus, are capable of inducing apoptosis when expressed individually in BHK cells. They propose that during the initial stages of virus infection, when the levels of 2B are low, apoptosis is inhibited allowing for virus replication. At later stages when expression levels of 2B are higher apoptosis is induced. This may then provide a means for the efficient spread of virions that evades the host immune inflammatory response.

E proteins of coronaviruses

The E protein from the coronaviruses, murine hepatitis virus and severe acute respiratory syndrome coronavirus (SARS-CoV), has recently been shown to have viroporin activity. The expression of the E protein permeabilises both *E. coli* and mammalian cells (Madan *et al.*, 2005a; Liao *et al.*, 2006). The protein also displays structural features characteristic of viroporins, with a highly hydrophobic domain that forms at least one amphipathic α-helix (Liao *et al.*, 2006).

Studies in which the entire ORF encoding the E protein was removed, showed that the E protein was not required for virus replication as viable and infectious progeny were produced. The titres of mutant virus were, however, greatly reduced with respect to the wild-type virus, suggesting that virion assembly or morphogenesis was less efficient and that the E protein increases assembly rate (Kuo & Masters, 2003; DeDiego *et al.*, 2007). Mutant Influenza A viruses, in which the M2 transmembrane domain responsible for ion channel activity was deleted, were also able to undergo multiple cycles of replication but grew substantially slower. This indicates the importance of M2 ion channel activity in the rate of efficient viral replication (Watanabe *et al.*, 2001). Therefore, in some cases, the expression of viroporins has been found not to be essential for progeny virus formation, their expression, however, significantly increases virus production suggesting a putative role in modulating virus production.

Recent studies have proposed that AHSV NS3 (Van Niekerk *et al.*, 2001a), BTV NS3 (Han & Harty, 2004) and rotavirus NSP4 (Ruiz *et al.*, 2005) may have viroporin-like activity based on their cytotoxic and/or membrane permeabilising effect when expressed individually. Further characterisation of their role during the viral life cycle has, however, been hindered due to the lack of a reverse genetics system for these segmented dsRNA viruses. Although following the onset of this study a reverse genetics system for BTV has been developed (Boyce *et al.*, 2008). In this study genomic segment reassortment was used as an alternative tool for studying protein function. This evolutionary mechanism, and its application in protein function studies, will therefore be discussed in the following section.

1.6. GENOME SEGMENT REASSORTMENT

RNA viruses are characterised by small and compact genomes, short generation times, large population numbers and the highest mutation rates amongst living species. The high mutation rate is due to the low, or absent, proof reading activity of their RNA-dependant RNA polymerases, which have an error rate of 10^{-3} to 10^{-5} misincorporations per nucleotide copied (Domingo & Holland, 1997). Genomic variation in RNA viruses is additionally generated through homologous

and nonhomologous recombination and, in those viruses with a segmented genome, reassortment or genetic drift. Reassortment is the exchange of genome segments between different virus strains co-infecting the same cell, and results in the formation of new strains or variants with segments from both viruses (reassortants). RNA viruses therefore generally evolve as a mixed population of related but non-identical genomes, with one or several master nucleotide genome sequence(s) or quasispecies dominating the population (Domingo *et al.*, 1996). This potentially provides the virus with a high adaptive potential in new environments where the selection of viral sub-populations with the highest fitness, even if they are in the minority, allows for rapid evolution (Briones *et al.*, 2006). The alternative replication in vertebrate and non-vertebrate hosts that occurs in arthropod transmitted viruses, however, imposes constraints on these viruses and they generally evolve slower, as has been demonstrated for sindbis virus (Greene *et al.*, 2005).

Genome segment reassortment has been shown to occur in nature for many segmented animal RNA viruses, including AHSV (Von Teichman & Smit, 2008), BTV (Kahlon *et al.*, 1983; Pierce *et al.*, 1998) and rotavirus (Iturriza-Gómara *et al.*, 2001). The ability of the AHSV and BTV viruses to reassort raises concerns over the current use of attenuated live vaccines for these viruses. This is due to the potential risk of reassortment with field strains and possible reversion to virulence. Field strains containing segments from vaccine strains have recently been detected for both viruses (Batten *et al.*, 2008; Von Teichman & Smit, 2008).

Reassortment of genome segments of BTV and AHSV has also been shown to occur *in vitro* (Ramig *et al.*, 1989; O'Hara *et al.*, 1998). Ramig and co-workers (1989) examined the constraints and kinetics of BTV reassortment in Vero cells. Reassortment was found to be an early event in the replication cycle, and non-random segregation of specific genome segments occurred. In the absence of selection pressures, the majority of the genome segments randomly segregate, segments 8 and 10, however, were found to segregate non-randomly with bias towards one parent. The basis for this non-random segregation is not known (Ramig *et al.*, 1989). Preferential selection of the genome segment encoding NSP1 from one of the parental viruses during mixed infection with rotaviruses has also been demonstrated (Mahbub Alam *et al.*, 2006). No studies have directly examined the constraints and kinetics of AHSV reassortment, or whether viral protein interactions or protein-protein function influence this.

The *in vitro* generation of reassortants, through mixed infections and/or reverse genetics, has proven to be a powerful tool in elucidating viral protein functions in many segmented RNA viruses such as reovirus (Moody & Joklik, 1989; Roner & Mutsoli, 2007), rotavirus (Tauscher & Desselberger, 1997), BTV (Cowley & Gorman, 1987) and influenza virus (Parks *et al.*, 2007;

Pappas *et al.*, 2008). In this type of analysis phenotypic traits in which the two parental strains differ are selected and, using either random genome segment reassortants or reassortants generated by reverse genetics, these phenotypes are then associated with the presence of specific genome segments. For example, co-segregation of the hemagglutination functions of BTV with the gene encoding the outer capsid protein VP2 in reassortants between two BTV serotypes that differed in their hemagglutination patterns, demonstrated that VP2 was the virus hemagglutinin (Cowley & Gorman, 1987). *In vitro* reassortment is also widely used for creating viruses with specific phenotypes for vaccine purposes (Dennehy, 2008) and in analysing the potential dangers of reassortment between attenuated vaccine strains and field strains (Parks *et al.*, 2007).

In a previous study AHSV reassortants were used to identify genome segments controlling virulence in a mouse model system. Two virus strains with avirulent and virulent phenotypes in adult Balb C mice were selected as parental strains for the generation of reassortants. Reassortants were then analysed for virulence in Balb C mice. Reassortant viruses clustered into three phenotypic groups; avirulent, virulent and those with a novel intermediate virulence. Genome segment 2, encoding the outer capsid protein VP2, from the virulent parent was present in all reassortant viruses displaying the virulent phenotype. Similarily all the avirulent reassortants had genome segment 2 from the avirulent parent. VP2, and its role in cell entry, may therefore have an important influence in determining the virulence characteristics of AHSV in the mouse model. Interestingly, all of the virulent reassortant strains also contained the genome segments encoding VP5 and NS3 from the virulent parent. These segments, however, could not be the primary determinants of the virulent phenotype as they also appeared in the other groups of viruses. They may however be necessary for the expression of the virulent phenotype. All the viruses with a novel intermediate virulence phenotype had VP2, VP5 and NS1 from the avirulent parent but NS3 from the virulent parent, indicating that although NS3 may not be the primary determinant of virulence in mice, the presence of NS3 from the virulent parent significantly increases virulence (O'Hara *et al.*, 1998).

1.7. AIMS

The virulence and pathogenesis of AHSV is likely to involve complex interactions between multiple viral and host determinants. Viral factors include those that control or influence key events during the viral life cycle, such as cell entry, rate of viral replication, virus trafficking and release. In addition to this, virus proteins that influence the cytopathic effects induced during viral infection, that alter cellular homeostasis, and that manipulate the host cell response to infection may also play a role in pathogenesis. Characterisation of the AHSV proteins that contribute to

these aspects is therefore of vital importance to understanding the molecular and cellular basis of AHS disease and its progression. In this study we focussed on AHSV NS3 due to the cytotoxic nature of the protein and its potential role in virus release. A further unique and intriguing feature of AHSV NS3 is the high variability of this protein within and across serotypes of AHSV. This is in contrast to BTV NS3, the other non-structural proteins of AHSV, and indeed most of the non-structural proteins of dsRNA viruses; which are often the most highly conserved of the viral proteins.

The central objective of this investigation was to further characterise the role that the AHSV NS3 protein plays in the viral life cycle and virus-cell interactions, such as cytopathology and cytotoxicity, that potentially contribute to the events leading to pathogenesis. The following specific aims were therefore addressed in this study:

1. To determine the contribution of NS3 to virus phenotypic properties such as virus yield, virus release, virus-induced cytopathicity and membrane permeabilisation during AHSV infection of mammalian cells.

2. To compare the membrane permeabilising and cytolytic effect of NS3 from AHSV, BTV and EEV.

3. To determine which regions within NS3 are critical to its membrane permeabilising and cytolytic effects.

4. To determine if sequence variation within NS3 influences its membrane permeabilising effect, cytotoxicity, membrane association and subcellular localisation.

CHAPTER 2: GENOME SEGMENT REASSORTMENT IDENTIFIES NS3 AS A KEY PROTEIN IN AHSV RELEASE AND MEMBRANE PERMEABILISATION

2.1. INTRODUCTION

The prominent pathological features of AHS are haemorrhages, oedema and effusion (Mellor & Hamblin, 2004). These features have been associated with changes in the morphology and permeability of pulmonary and vascular endothelial cells, the main target cells during AHSV infection (Laegreid *et al.*, 1992a). Infection of cultured endothelial cells with virulence variants of AHSV resulted in distinctly different cytopathologies (Laegreid *et al.*, 1992b). When grown in tissue culture AHSV causes severe cytopathic effects (CPE) in mammalian cells (Coetzer & Guthrie, 2004).

AHSV NS3, encoded by segment 10 (S10), is the smallest of the viral proteins and is expressed to low levels in infected cells (Van Staden *et al.*, 1995). Immunolocalisation studies of AHSV-infected Vero cells showed that NS3 was localised to the plasma membrane specifically at the perturbed areas at the sites of virus exit. NS3 was therefore proposed to be involved in virus release (Stoltz *et al.*, 1996). When expressed individually in insect or mammalian cells, both the AHSV and BTV NS3 proteins cause a cytotoxic effect (Van Staden *et al.*, 1995; Van Niekerk *et al.*, 2001a; Han & Harty, 2004). Cells expressing AHSV NS3 display degraded or absent cell membranes, cytotoxicity is therefore possibly as a result of membrane damage. Cytotoxicity was shown to be dependant on the membrane association of the protein, mediated by two hydrophobic domains (Van Niekerk *et al.*, 2001a). NS3 has been proposed to function as a viroporin that induces changes in membrane permeability, facilitates virus release, and possibly contributes to the cytopathic effect thereby potentially contributing to pathogenesis (Van Niekerk *et al.*, 2001a; Han & Harty, 2004). These findings have however never been investigated in the context of AHSV infection of cells. The first objective of this part of the study was therefore to investigate the functional significance of the NS3 protein in AHSV infection of mammalian cells, and, secondly, to determine whether the high levels of sequence variation in NS3 impacted on this.

In stark contrast to BTV NS3, that is highly conserved amongst different serotypes (Van Niekerk *et al.*, 2003; Balasuriya *et al.*, 2008) AHSV NS3 shows much more sequence diversity with up to 37% amino acid variation across all serotypes (Van Niekerk *et al.*, 2001b). Comparison of the nucleotide sequence of S10, the segment encoding NS3, shows that this variation clusters into three distinct phylogenetic groups, termed clades α, β and γ (Sailleau *et al.*, 1997; Martin *et al.*, 1998; Van Niekerk *et al.*, 2001b; Quan *et al.*, 2008).

To assess the role played by NS3 during AHSV infection a reassortant based approach was used. Three parental AHSV isolates, AHSV-2, AHSV-3 and AHSV-4, were selected based on the segregation of their NS3 proteins into the three phylogenetic clades (Van Niekerk *et al.*, 2001b) and preliminary observations by van Niekerk (2001c) that they differed in their cytopathology in

Vero cells. The NS3 proteins encoded by AHSV-2, AHSV-3 and AHSV-4 respectively represent the γ, β and α clades. From these parental strains, reassortant progeny viruses were generated by co-infections of cells and progeny plaque purifications. Reassortants in which genome segment 10 encoding NS3 was exchanged, with or without the exchange of additional segments, were identified on the basis of the migration of the dsRNA genome segments in PAGE gels and from partial sequencing of the genome segments. Reassortants and parental strains were then compared in Vero cells in terms of virus yield, virus release and viral-induced CPE as well as their effect on cell viability and cell membrane permeability to evaluate the contribution of the NS3 protein to viral phenotype.

2.2. MATERIALS AND METHODS

2.2.1. Cells and viruses

BHK-21 (ATCC CCL-10) and Vero (ATCC CCL-81) cells were obtained from ATCC (Manassa, USA). CER cells, a BHK derivative, were obtained from the Virology Division at the Onderstepoort Veterinary Institute (OVI, Onderstepoort, South Africa). BHK, Vero and CER cells were maintained in monolayers in minimal essential medium (MEM) supplemented with non-essential amino acids (Sigma), 5% foetal calf serum (FCS, Sigma) and antibiotics (60 mg/ml penicillin, 60 mg/ml streptomycin and 150 µg/ml fungizone, Highveld Biological). Cells were maintained at 37°C in 5% CO_2.

The parental virus strains used in this study were obtained from the OIE Reference Laboratory at the OVI. AHSV serotype 2 82/61 (AHSV-2) and AHSV serotype 4 HS39/97 (AHSV-4) were isolated from spleen or lung samples of dead horses; AHSV serotype 3 M322/97 (AHSV-3) from the spleen of a dead dog. These strains each encode a NS3 protein from one of the three NS3 phylogenetic clades, i.e. AHSV-2 (γ NS3), AHSV-3 (β NS3) and AHSV-4 (α NS3) (Van Niekerk *et al.*, 2001b). Single virus populations were obtained following three rounds of plaque purification in BHK cells.

2.2.2. Isolation of AHSV reassortants

BHK cells seeded on 6 well plates and grown to 80% confluency were co-infected with two parental strains at equal multiplicities of infection (MOI) of 1 or 4 plaque-forming units (pfu)/cell. The inoculum was replaced after 3 h with supplemented MEM. Supernatants were harvested at 2 to 3 days post infection (p.i.) and individual progeny viruses obtained by plaque purification. For this BHK cells seeded on 6 well plates were incubated for 1 h with diluted virus-containing supernatant in an equal volume supplemented MEM. The inoculum was removed, and cells overlaid with 2 ml of 0.7% agarose in MEM containing 5% FCS and antibiotics. Plaques were randomly selected after 3 to 4 days incubation at 37°C, resuspended in 1 ml complete medium, and amplified twice by passage in BHK cells as routinely done for the AHSV parental strains.

2.2.3. Genome segment assignment

2.2.3.1. Isolation and polyacrylamide gel electrophoresis (PAGE) of dsRNA

Viral dsRNA was isolated from infected BHK cells using TRIZOL reagent (Invitrogen) according to the manufacturer's recommendations. RNA samples were stored at 4°C in diethylpyrocarbonate (DEPC) treated water. Samples were analysed by 6, 8, 10, 12 and 14% polyacrylamide gel electrophoresis (PAGE) to identify the origins of the genome segments. Briefly, samples were concentrated in the spacer gel containing 3% acrylamide, 0.08% N, N' methylene bis-acrylamide, 64 mM Tris pH 6.7, 0.15% ammoniumperoxydisulphate, 0.15% TEMED. The RNA was then separated in the resolving gel containing 6, 8, 10, 12 or 14% acrylamide and 0.16, 0.21, 0.27, 0.32, or 0.37% N, N' methylene bis-acrylamide, 375 mM Tris pH 8.9, 0.0625 N HCl, 0.15% ammoniumperoxydisulphate, 0.05% TEMED). Electrophoresis was carried out in Tris-glycine buffer (25 mM Tris, 250 mM glycine) at 80-90V for 20 h. The gels were stained in Tris-glycine buffer containing SYBR gold nucleic acid gel stain (Molecular Probes) and viewed under a UV transilluminator.

2.2.3.2. Sequencing of genome segments

The total dsRNA was converted to cDNA using a single-primer amplification sequence-independent dsRNA method (Potgieter *et al.*, 2002) by Dr A. C. Potgieter, OVI. Full or partial individual gene segments were then amplified by PCR using gene specific primers for segments 2, 3, 5, 6, 7, 8, 9 and 10. All PCR reactions were carried out in a final volume of 50 µl containing 1.25 U Takara ExTaq, 5 µl 10 x Takara reaction buffer (including $MgCl_2$), 2.5 mM of each dNTP

and 100 pmol of each primer. Primer sequences and PCR conditions used are listed in Table 2.1. PCR amplicons were purified using a commercial purification kit (Roche) and sequenced using an ABI PRISM Big Dye Terminator Cycle Sequencing Ready Reaction kit with the primers in Table 2.1 on an ABI PRISM 3130xl Genetic Analyzer (Perkin Elmer). Sequences were aligned using AlignX, Vector NTI (Invitrogen).

Table 2.1 Primers used to PCR amplify and sequence individual gene segments of the AHSV strains and reassortants used in this study

Primer Name (Storage Code)	**5' to 3' sequence (Orientation)**	**Amplification product and PCR conditions**
HSV3VP2FOR (P3H1)	GTTTAATTCACCATGGCTTCGGAATTCG (Forward)	Full length VP2 gene on segment 2 of AHSV-3 94°C 4 minutes (min) 35 x (94°C 30 sec, 56°C 30 sec, 72°C 3 min) 72°C 7 min
HSV3VP2REV (P3I1)	GTAAGTTGATTCACATGGAGCGGGAG (Reverse)	
HS4VP2FOW (P3C8)	GTTAAATTCACTATGGCGTCCGAGTTG (Forward)	Full length VP2 gene on segment 2 of AHSV-4 94°C 4 min 35 x (94°C 30 sec, 57°C 30 sec, 72°C 3 min) 72°C 7 min
HS4VP2REV (P3C9)	GTATGTGTATTCACATGGAGCAACAG (Reverse)	
SI5 (P4E1)	GGAGATCTATGCAAGGGAATGAAAGAATAC (Forward)	Full length VP3 gene on segment 3 94°C 4 min 35 x (94°C 30 sec, 59°C 30 sec, 72°C 3 min) 72°C 7 min
SI3 (P4A1)	GGAGATCTGGCTGCTAAATCGTTGGTCG (Reverse)	
VP5IF3/9 (P6C1)	AGGAAGATCGTGTGATTG (Forward)	Bases 380 to 1160 of VP5 gene on segment 6 of AHSV-3 94°C 2 min 35 x (94°C 30 sec, 52°C 30 sec, 72°C 90 sec) 72°C 5 min
VP5IR3/9 (P6B1)	TGGCGTATGCTCTGAATG (Reverse)	
HS4VP5BamF (P6A1)	GTGGGATCCATGGGAAAGTTCACATC (Forward)	Full length VP5 gene on segment 6 of AHSV-4 94°C 2 min 35 x (94°C 30 sec, 53°C 30 sec, 72°C 90 sec) 72°C 5 min
HS5VP5EcoRIR (P6F1)	CGGAATTCAGCTATTTTCACACCATATAC (Reverse)	
AHSV4NS1BamFP (P9A2)	GCGGATCCGTTAAAGAACCTAGGCGG (Forward)	Full length NS1 gene on segment 5 94°C 2 min 35 x (94°C 30 sec, 59°C 30 sec, 72°C 90 sec) 72°C 5 min
AHSV4NS1EcoRP (P9A3)	CGGAATTCGTAAGTTTGTGAAACCAGGGGG (Reverse)	
VP7A (P8A3)	5' end of segment 7 AHSV9 (Forward)	Full length VP7 gene on segment 7 94°C 2 min 35 x (94°C 30 sec, 47°C 30 sec, 72°C 90 sec) 72°C 5 min
VP7B (P8B3)	3' end of segment 7 AHSV9 (Reverse)	
G8.1 (NS2F) (P10A1)	GTTTAAAAATCCGTTCGTCATC (Forward)	Full length NS2 gene on segment 8 94°C 2 min 35 x (94°C 30 sec, 54°C 30 sec, 72°C 90 sec) 72°C 5 min
G8.2 (NS2R) (P10B1)	GTATGTTGAAATCCGCGGTTA (Reverse)	

Primer Name (Storage Code)	5' to 3' sequence (Orientation)	Amplification product and PCR conditions
VP6.5 (P7A1)	GTAAGTTTTAAGTTGCCC (Forward)	Full length VP6 gene on segment 9 94°C 2 min 35 x (94°C 30 sec, 46°C 30 sec, 72°C 90 sec) 72°C 5 min
VP6.4 (P7B1)	GTTAAATAAGTTGTCTCATG (Reverse)	
NS3pBam (P11E3)	CGGGATCCGTTTAAATTATCCCTTG (Forward)	Full length NS3 gene on segment 10 94°C 2 min 35 x (94°C 30 sec, 59°C 30 sec, 72°C 60 sec) 72°C 5 min
NS3pEco (P11E4)	CGGAATTCGTAAGTCGTTATCCCGG (Reverse)	

2.2.4. Virus titration

The phenotypes of the parental and reassortant viruses, such as virus yield and release, were then assayed in Vero cells as previous characterisation of AHSV expression was carried out in Vero cells (Van Staden *et al.*, 1995; Stoltz *et al.*, 1996). Vero cells seeded on 6 well plates were infected with virus strains at a MOI of 10 pfu/cell for 1 h at 37°C. Unbound virus was removed by washing twice with cold serum free medium. Prewarmed supplemented medium was then added and the cells incubated at 37°C. At 24 or 48 h p.i. the cells were resuspended in the medium and collected by centrifugation at 380 g for 10 min. The resulting supernatant was diluted directly for plaque assays to quantify released virus. The cell pellets were resuspended in 2 mM Tris, incubated for 10 min at room temperature and lysed by passage through a 22G needle. Serial dilutions of lysates then allowed for the determination of the amount of cell-associated virus. Virus titres were determined by plaque assay, as described above, on CER cells. Plaques were visualised by staining with 1 ml/well 0.1% w/v neutral red (Fluka) for 2 h at 37°C. Total virus yield was calculated as the sum of released and cell-associated virus, and virus release expressed as the percentage released virus versus total virus.

2.2.5. Cytopathic effect (CPE) and cell viability

Vero cells were seeded on sterile glass coverslips in 6 well plates and infected at a MOI of 5 pfu/cell with virus strains as described above. Cells were examined for viral induced CPE at 12 hourly intervals over a 48 h period under an inverted phase-contrast light microscope. CPE was comparatively scored from slight (+) to severe (++++).

Cell viability was monitored using the CellTiter-Blue™ cell viability assay according to the manufacturer's instructions (Promega). This assay is based on the reduction of resazurin to the highly fluorescent resorufin by metabolically active cells. The metabolic capacity in non-viable cells is rapidly lost, they do not therefore reduce the indicator dye and no fluorescent signal is generated. Briefly, Vero cells seeded on 48 well plates were infected with virus strains at a MOI of 10 pfu/cell as described above. A volume of 50 µl CellTiter-Blue™ reagent was added per well at 6 hourly intervals from 0 to 48 h p.i. and cells incubated at 37°C for a further 3 h. Fluorescence ($530\text{-}570_{Ex}/580\text{-}620_{Em}$) was recorded using a Thermo Labsystems Fluoroskan Ascent FL plate reader. Background fluorescence was corrected for by including wells with serum supplemented MEM in the absence of cells. Fluorescence readings for these wells were subtracted from experimental wells. The percentage viable cells was calculated by expressing the fluorescence in wells containing the AHSV infected Vero cells as a percentage of the fluorescence in wells containing uninfected (mock) cells.

2.2.6. Hygromycin B (Hyg B) membrane permeability assay

Membrane permeabilisation assays were modified from the method described by Chang *et al.* (1999). Vero cells were infected on 48 well plates as described above. At 6, 12 and 18 h p.i. the

medium was removed and the cells washed twice with MEM without methionine. Cells were incubated for 30 min with MEM without methionine with or without Hygromycin B (Hyg B, 500 μg/ml, Roche Diagnostics). Proteins were labelled for 30 min in MEM without methionine with 2.5 μCi [^{35}S] L-methionine (Perkin Elmer) per well. Cells were washed twice with ice-cold PBS and harvested in 50 μl/well lysis buffer (150 mM NaCl, 50 mM Tris-HCl, 1 mM EDTA, 1% Nonidet P40 and protease inhibitors 1 mg/ml pefabloc SC, 0.7 μg/ml pepstatin, 1 mM phenylmethylsulphonyl fluoride (PMSF)). TCA solution (5% trichloroacetic acid in 20 mM sodium pyrophosphate) was added to precipitate proteins and the sample spotted onto fibreglass discs (GF/C, Whatman). Discs were washed with 70% ethanol and left to dry at room temperature. Discs were placed in scintillation fluid (Beckman) and counted in a Tri-Carb 2800TR Liquid Scintillation Analyzer (Perkin Elmer). The percentage permeabilised cells was calculated as counts per minute (CPM) of sample containing Hyg B divided by CPM of sample in absence of Hyg B x 100. The CPM of samples labelled in the absence of Hyg B was used a measure of total protein synthesis.

2.2.7. Statistical analysis

Mean and standard deviations (SD) were calculated, and differences in phenotype between Vero cells infected with AHSV strains and reassortants tested for significance by Student's *t* test. Pearson's product-moment correlation tests were used to calculate correlation coefficients.

2.3. RESULTS

2.3.1. Production and characterisation of AHSV reassortants

In order to generate reassortant viruses, cells were simultaneous infected with a combination of either parental strains AHSV-2 and AHSV-3, or AHSV-2 and AHSV-4, or AHSV-3 and AHSV-4 at an equal MOI. Progeny virus clones were plaque purified and amplified. In this study the primary aim was to determine the effect of NS3, encoded by the S10 gene, on the phenotype of AHSV so the selection of reassortants focussed on the exchange of the smallest genome segment 10 in relation to the serotype-determining segment 2 encoding VP2. Five putative reassortants were therefore initially identified based on the differential PAGE migration patterns of segments 2 and 10. Representative 14 and 6% polyacrylamide gels are shown in Fig. 2.1. Genome segment numbers are given based on the order of migration of the segments during agarose gel electrophoresis, the principal difference being that during PAGE segments 5 and 6 are often found to migrate in the reverse order (O'Hara *et al.*, 1998).

The parental origin of all of the genome segments of the reassortants were then identified on the basis of their PAGE profiles, and/or from partial sequencing of the genome segments following cDNA synthesis and PCR amplification of the complete genomes (see 2.2.3.2).

Table 2.2 lists the dsRNA genome segments that could be distinguished by PAGE. Segments 1 and 4 were not sequenced as their parental origins could be assigned based on their PAGE profiles, and these genes are highly conserved across all AHSV serotypes. To illustrate the differences in the migration of segment 1 of the viruses an enlargement of the upper part of the 14% gel from Fig. 2.1A is shown in Fig. 2.2. The assignment of segment 4 of reassortants between AHSV-2 and AHSV-3 was based on their differential migration during 6% PAGE, to show this an enlargement of Fig. 2.1B is given in Fig. 2.3A. PAGE analysis of the total genomic cDNA profiles of the viruses revealed that additional differences in the migration of the parental virus cDNA segments, that were not evident in the dsRNA profiles, could be distinguished. The parental origin of segment 4 of the reassortants between AHSV-2 and AHSV-4 could be assigned following 8% PAGE of the total genomic cDNA (Fig. 2.3B).

Table 2.2 The dsRNA genome segments that showed distinguishable mobility between the indicated parental strains in different percentages polyacrylamide gels

Parental strains	6% PAGE	8% PAGE	10% PAGE	12% PAGE	14% PAGE
AHSV-2 and -3	2, 4, 6, 10	2, 4, 6, 10	2, 4, 6, 10	2, 6, 10	1, 2, 6, 10
AHSV-2 and -4	2, 6, 9, 10	2, 6, 10	2, 6, 10	2, 6, 7, 10	1, 2, 6, 7,10

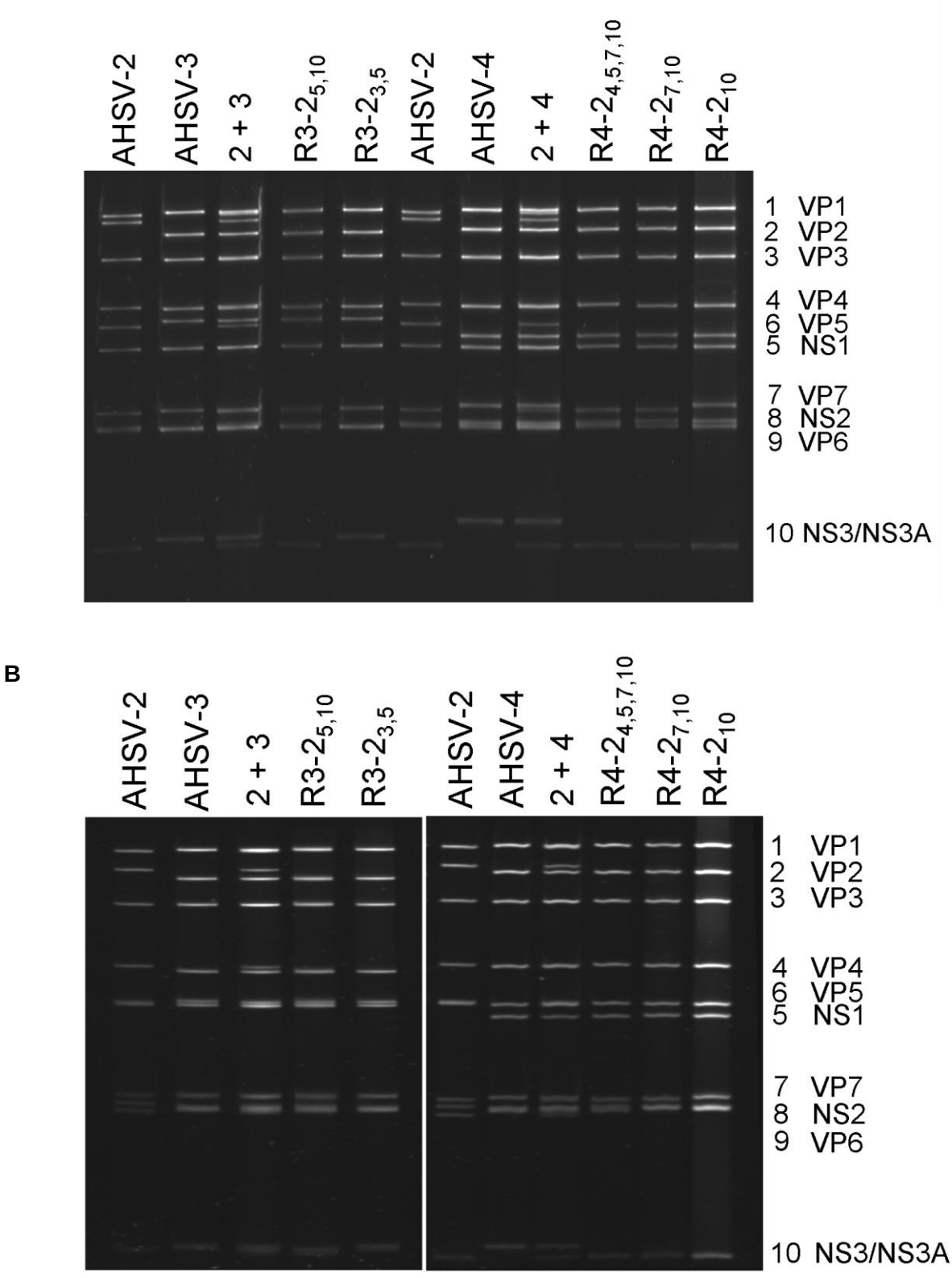

Fig. 2.1 The dsRNA profiles of AHSV-2, AHSV-3, AHSV-4 and reassortant viruses. The dsRNA was isolated from BHK cells infected with the indicated viruses and analysed in a 14% (A) or 6% (B) polyacrylamide gel stained with SYBR gold and visualised under UV illumination. Lanes 3 and 8 were loaded with a mixture of the dsRNA from the respective parental strains. Numbers 1 to 10 on the right indicate the approximate positions of the dsRNA segments; the protein encoded by each segment is also shown. The nomenclature used for the reassortants is described in the text.

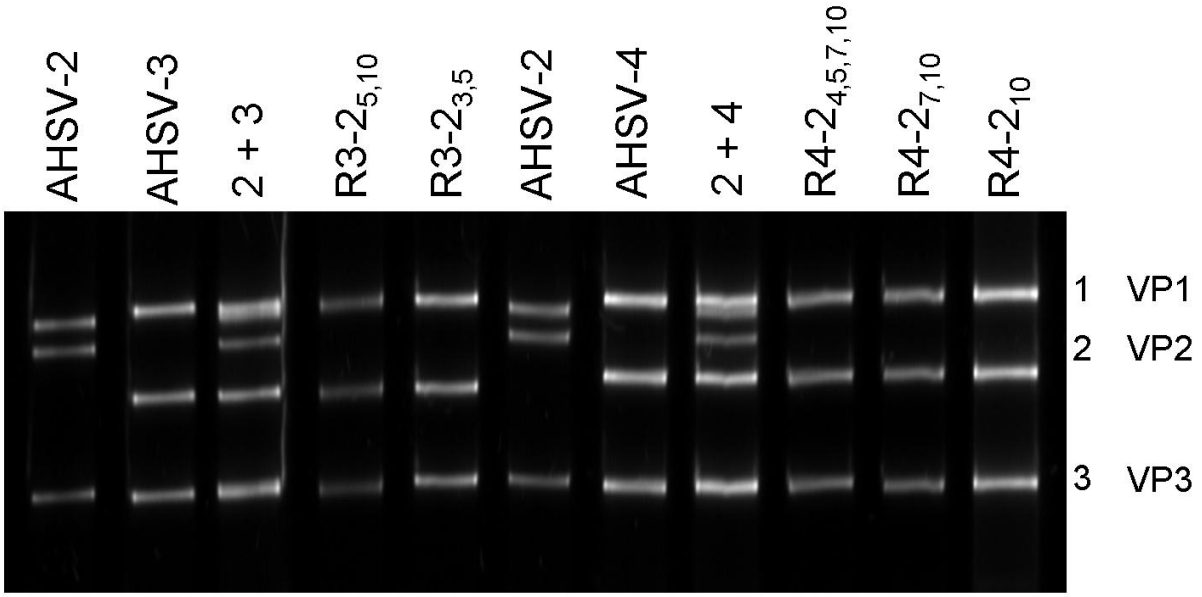

Fig. 2.2 Determination of the parental origin of segment 1 (encoding VP1) of the AHSV reassortants. The dsRNA was analysed on a 14% polyacrylamide gel stained with SYBR gold and visualised under UV transillumination. Lanes 3 and 8 were loaded with a mixture of the dsRNA from the respective parental strains. Numbers 1 to 3 on the right indicate the approximate positions of the dsRNA segments; the protein encoded by each segment is also shown.

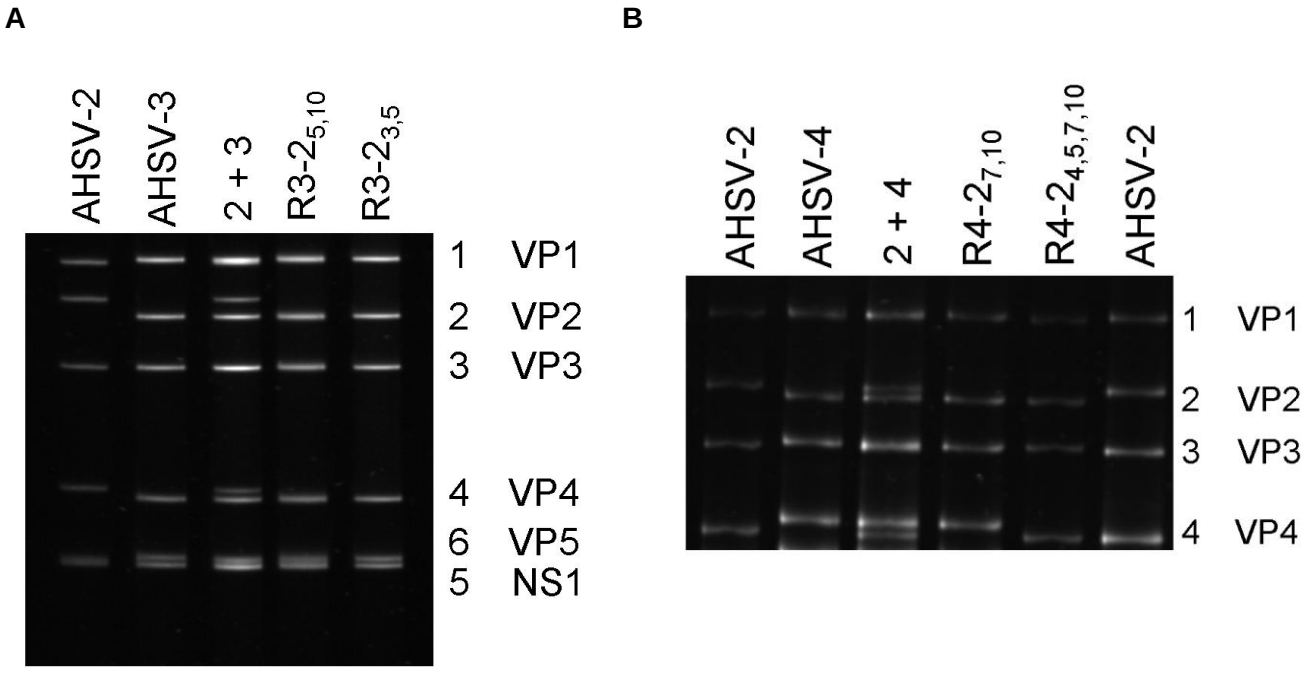

Fig. 2.3 Determination of the parental origin of segment 4 (encoding VP4) of the AHSV reassortants. Viral dsRNA was analysed on a 6% polyacrylamide gel (A) or the PCR products from the amplification of the complete viral cDNA were analysed on an 8% polyacrylamide gel (B) stained with SYBR gold and visualised under UV transillumination. Numbers on the right indicate the approximate positions of the dsRNA or cDNA segments; the protein encoded by each segment is also shown.

For sequencing, the parental and reassortant total dsRNA genomes were converted to cDNA, PCR amplified and the individual genes amplified and sequenced using gene-specific primers. Fig. 2.4 shows the PCR amplification of the genes of reassortant R4-$2_{4,5,7,10}$. Sequences for segments 2, 3, 5, 6, 7, 8, 9 and 10 were aligned and are given in Appendix A.

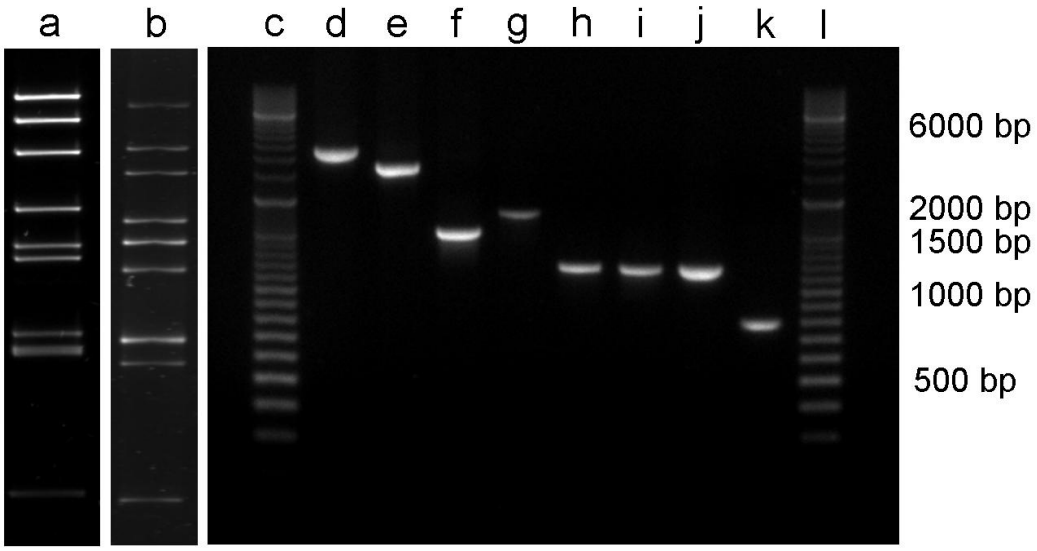

Fig. 2.4 PCR amplification of genes of R4-$2_{4,5,7,10}$ for sequencing. Total viral dsRNA (a) was converted to cDNA using a single-primer amplification sequence-independent method and PCR amplified (b). The genes encoding VP2 (d), VP3 (e), VP5 (f), NS1 (g), VP7 (h), NS2 (i), VP6 (j) and NS3 (k) were then amplified using the gene specific primers listed in Table 2.1. PCR products (d – k) were analysed by 0.8% agarose gel electrophoresis, stained with ethidium bromide (EtBr) and visualised under an UV illuminator. DNA size markers were included in lanes (c) and (l).

The parental origin of the genome segments of the reassortants is summarised in Table 2.3. The nomenclature used for the reassortant viruses (R) is as follows: the first number indicates the parent virus contributing the majority of segments, the second number indicates the parent virus from which the reassorted segments (in subscript) derives. Of the five reassortants that were identified four had the S10 genome segment exchanged. One was a monoreassortant with nine genome segments from AHSV-4 and the S10 genome segment encoding NS3 from AHSV-2 (R4-2_{10}). In addition to S10 the other reassortant viruses had segment 5 encoding NS1 (R3-$2_{5,10}$) or segment 7 encoding VP7 (R4-$2_{7,10}$) or segments 4, 5 and 7 encoding VP4, NS1 and VP7 respectively (R4-$2_{4,5,7,10}$) from AHSV-2. The reassortant R3-$2_{3,5}$ carried segments 3 and 5, encoding VP3 and NS1 respectively, from AHSV-2 in a genetic background of AHSV-3.

Table 2.3 Parental origin of the genome segments of the AHSV reassortants

Segment	Protein encoded	R3-$2_{5,10}$	R3-$2_{3,5}$	R4-$2_{4,5,7,10}$	R4-$2_{7,10}$	R4-2_{10}
1	VP1	3*	3	4	4	4
2	VP2	3	3	4	4	4
3	VP3	3	**2**	4	4	4
4	VP4	3	3	**2**	4	4
5	NS1	**2**	**2**	**2**	4	4
6	VP5	3	3	4	4	4
7	VP7	3	3	**2**	**2**	4
8	NS2	3	3	4	4	4
9	VP6	3	3	4	4	4
10	NS3	**2**	3	**2**	**2**	**2**

* The numbers 2, 3 and 4 in the five columns on the right indicate the parental strains AHSV-2, AHSV-3 and AHSV-4 respectively

No reassortants were identified where the majority of segments originated from AHSV-2 and S10 was contributed by AHSV-3 or AHSV-4. The reason for this phenomenon is not understood but several studies of co-infections with BTV report a similar under-representation of one of the parents, and segments from this parent, among progeny from mixed infections (Ramig *et al.*, 1989). Previous studies of AHSV and BTV reassortants have also shown that non-random segregation of S10 occurs, where the S10 is preferentially derived from one of the parents and may have a selective advantage (Ramig *et al.*, 1989; O'Hara *et al.*, 1998). Co-infections with the parental strains AHSV-3 and AHSV-4 were additionally performed but analysis of 30 progeny plaques revealed no reassortment of S10, indicating that there may be some constraints on the reassortment of the S10 genome segment between these viruses.

2.3.2. Virus yield and release

AHSV particles in both the cellular fractions and medium of infected Vero cells were titrated, and the values combined to represent the total virus yield (Fig. 2.5A) at 24 and 48 h p.i.. The three parental strains AHSV-2, AHSV-3 and AHSV-4 produced similar levels of total progeny virus of between 0.7 - 1.1 x 10^7 pfu/ml. This was important to establish, as it indicates that any phenotypic variations observed between these viruses was not a result of differences in the efficiency of virus production of the strains in Vero cells. Reassortant strains produced high levels of infectious virus, indicating that the exchange of the genome segments in these viruses did not

affect their ability to infect and replicate in Vero cells. Interestingly, reassortants R4-2_{10} and R4-$2_{7,10}$ with a background of AHSV-4 segments containing respectively the NS3 gene or a combination of both the NS3 and VP7 genes from AHSV-2 had titres of up to ten-fold higher than those of AHSV-2 or AHSV-4. Reassortant R4-$2_{4,5,7,10}$, which apart from the NS3 and VP7 genes of AHSV-2 also included the AHSV-2 NS1 and VP4 genes produced titres five-fold higher than those of AHSV-2 or AHSV-4. Reassortants with a background of AHSV-3 segments (R3-$2_{3,5}$ and R3-$2_{5,10}$) were much less affected by reassorting with AHSV-2 genes, showing a two-fold increase in titre over the parental serotype 2 and 3 strains.

As AHSV NS3 has been reported to play a role in virus release (Martin *et al.*, 1998), the relative levels of released virus in parental and reassortant strains was compared. Virus release was calculated by expressing the titres obtained from the culture medium as a percentage of the total titre. The results are shown in Fig. 2.5B**.** The largest proportion of the virus remained cell-associated in all cases, as typically observed with orbiviruses (Eaton *et al.*, 1990). A statistically significantly higher percentage of viruses were released from AHSV-2 infected Vero cells when compared to either AHSV-3 or AHSV-4 infected cells. For example, 32±0.9% of AHSV-2 was extracellular at 24 h p.i compared to 14±2.6% for AHSV-3 ($P < 0.001$) and 21±1.0% for AHSV-4 ($P < 0.001$). The levels of release of the reassortant viruses were similar to that of the parental strain from which their S10 genome segment was derived. Reassortants with S10 from AHSV-2 in a genetic background of either AHSV-3 (R3-$2_{5,10}$) or AHSV-4 (R4-$2_{4,5,7,10}$, R4-$2_{7,10}$ and R4-2_{10}) showed between 35 and 40% release of the total virus produced at 48 h p.i., which is closer to the levels observed for AHSV-2 (39±2.1%) than to either AHSV-3 (20±4.2%) or AHSV-4 (31±3.7%). At the same time point only 22±2.9% of reassortant R3-$2_{3,5}$ was released into the culture medium, which is similar to the AHSV-3 parental strain (20±4.2%, $P = 0.48$) from which the S10 segment derives and significantly different ($P = 0.0002$) from AHSV-2. The presence of the other reassorted segments 3, 4, 5 and 7 did not affect the amount of virus released. Therefore genome segment S10, encoding NS3, appears to be a major determinant in controlling the differences in the percentage virus released between AHSV-2, AHSV-3 and AHSV-4.

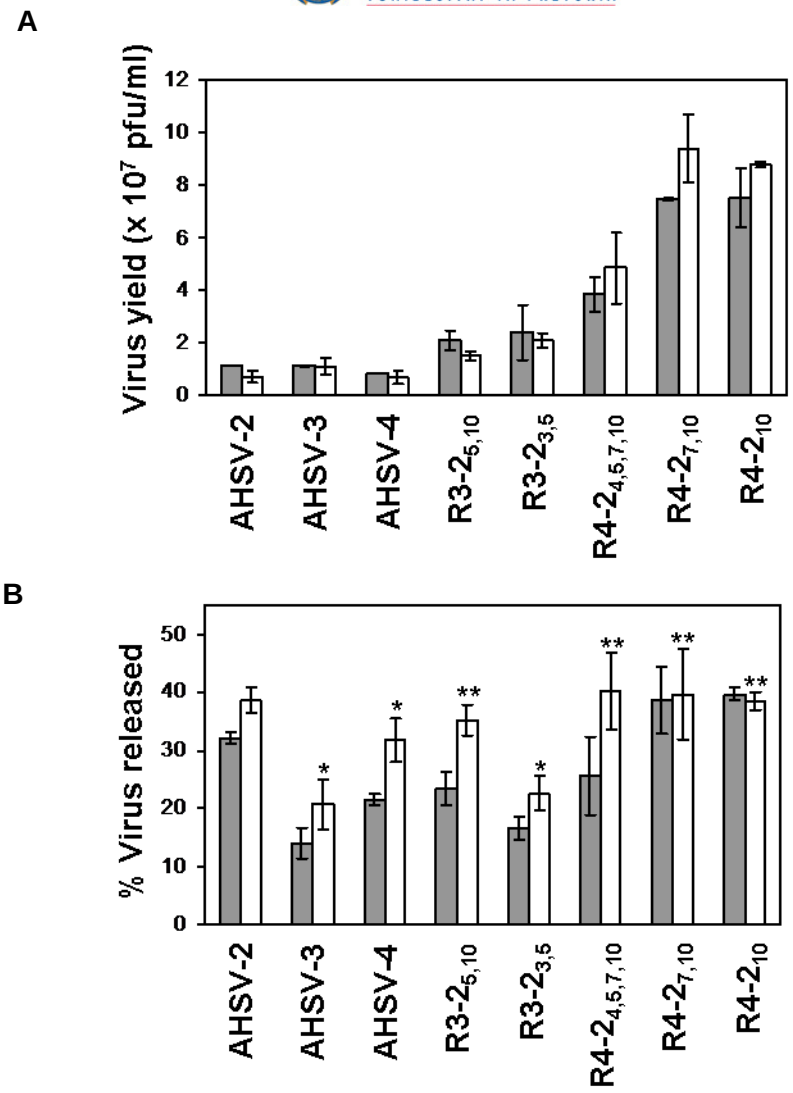

Fig. 2.5 Total infectious virus yield (A) and percentage virus released (B) of parental and reassortant viruses in Vero cells. Cells were infected with the indicated viruses at a MOI of 10 and cell-associated and released virus titrated at 24 h post infection (p.i.; grey columns) and 48 h p.i. (white columns). Values indicate the mean ±SD of two independent experiments with two repeats during each experiment. Values for the parental and reassortant viruses were compared to AHSV-2 by *t* test where * indicates statistically significant difference ($P < 0.01$) and ** indicates no statistically significant difference ($P > 0.05$).

2.3.3. Induction of CPE

The timing and severity of virally induced CPE was scored (Table 2.4) by observing changes in cell morphology, such as shrinking and rounding of cells, loss of contact between neighbouring cells and detachment from the culture plate. The results given in Fig. 2.6 illustrate the effects of the viruses on cell cultures at 48 h p.i. In the case of AHSV-2 CPE was observed at relatively early times post infection (24 h p.i., Table 2.4) with very few cells still attached to the cell culture plate at 48 h p.i. (Fig. 2.6). The development of CPE in AHSV-4 infected cells was a distinctly later event (36 h p.i., Table 2.4) with more cells remaining attached at 48 h p.i. (Fig. 2.6). AHSV-3 infected cells displayed an intermediate phenotype between these two viruses in terms of the

timing of onset of CPE (Table 2.4) but at late times post infection the induced CPE observed was closer to AHSV-2 than AHSV-4 (Fig. 2.6). The CPE of reassortant viruses R3-$2_{3,5}$, R4-$2_{7,10}$ and R4-2_{10} was less than either of the respective parental strains. Of these the monoreassortant R4-2_{10}, with just the NS3 gene of AHSV-2 in the AHSV-4 background, displayed no discernible CPE up to nearly 48h p.i.. In contrast to this, both the timing and severity of the CPE in cells infected with R3-$2_{5,10}$ and R4-$2_{4,5,7,10}$ was closer to that observed for AHSV-2 infected cells than AHSV-3 and AHSV-4 respectively. Based on these observations it can be postulated that simultaneously exchanging both segments 5 and 10 (encoding NS1 and NS3) confers the CPE characteristic of the parent contributing these segments (in this case AHSV-2), while an exchange of only one of the two segments results in reduced CPE. Additional reassortants are, however, required to confirm this.

Table 2.4 Cytopathic effect of AHSV strains on Vero cells infected at a MOI of 5 pfu/cell

Virus Strain	12 h	24 h	36 h	48 h
AHSV-2	-	++	+++	++++
AHSV-3	-	+	++	++++
AHSV-4	-	-	+	+++
R3-$2_{5,10}$	-	++	+++	++++
R3-$2_{3,5}$	-	+	+	+++
R4-$2_{4,5,7,10}$	-	+	+	++++
R4-$2_{7,10}$	-	-	+	++
R4-2_{10}	-	-	-	+

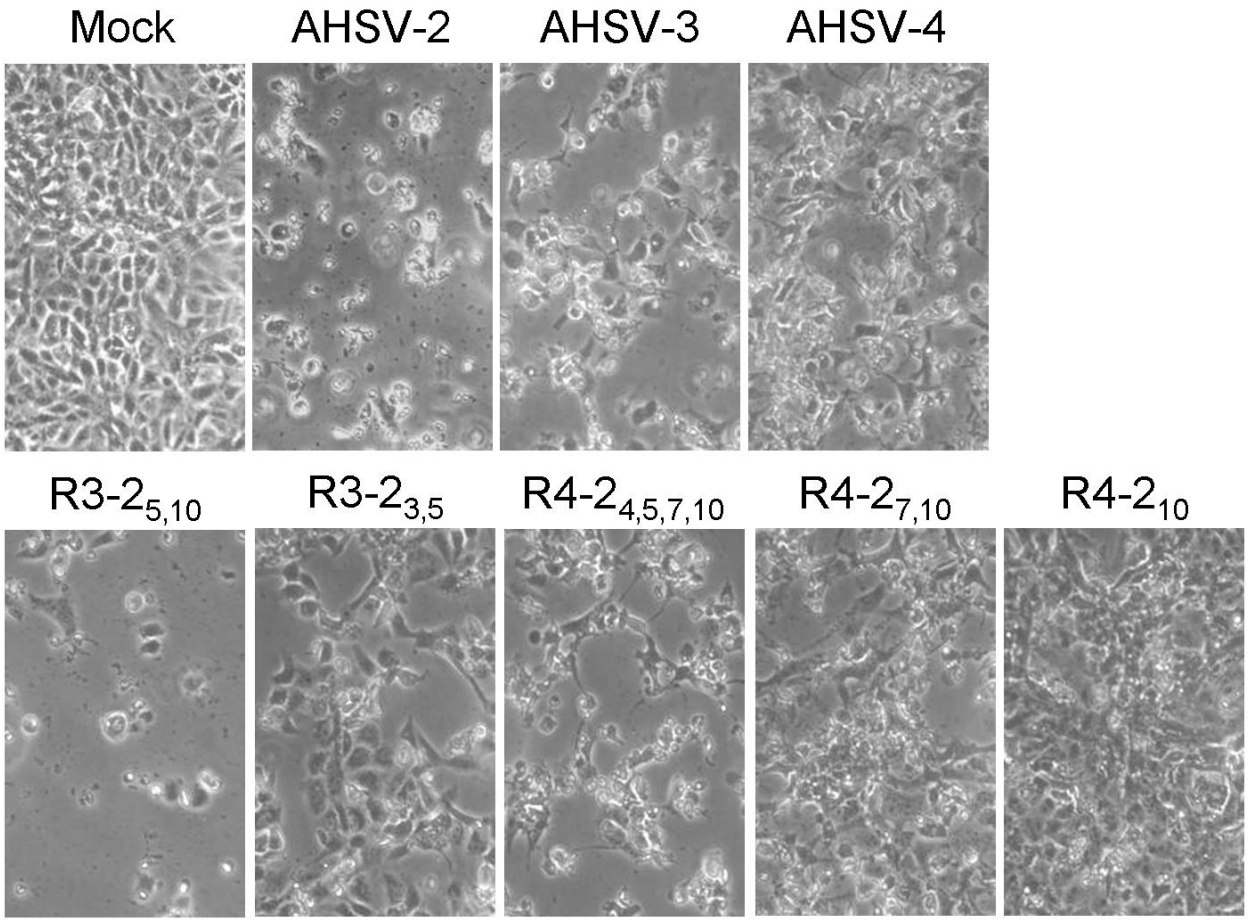

Fig. 2.6 Cytopathic effect of AHSV parental and reassortant strains on Vero cells. Cells were examined 48 h post infection with the indicated viruses (MOI 5 pfu/cell) under a phase contrast microscope.

2.3.4. Infected Vero cell viability and protein synthesis levels

As estimating CPE can be subjective, an additional quantitative measure of cell viability was obtained using the CellTiter-Blue™ cell viability assay (Promega). The results are shown in Fig. 2.7A. AHSV-2 induced rapid cell death, with only 51±1.1% viable cells remaining at 24 h p.i. compared to AHSV-3 (81±3.6%, $P < 0.01$) and AHSV-4 (93±1.2%, $P < 0.01$), these values declined further resulting in 15±0.5%, 22±4.4% ($P < 0.01$) and 36±4.9% ($P < 0.01$) cell viability respectively at 48 h p.i.. All the reassortants, except R4-2_{10}, displayed an intermediate phenotype between the respective parental strains. R4-2_{10} did not induce significant cell death, with 85±2.5% viable cells still remaining at 48 h p.i., which corresponded to the lack of CPE previously observed (Fig. 2.6). There was no clear link between the phenotypes of reassortant viruses and the origin of their NS3 proteins.

As an additional measure of the metabolic activity of infected cells, pulse-labelling with [^{35}S]-methionine was used to monitor total intracellular protein synthesis over an 18 h period as compared to uninfected cells (Fig. 2.7B), before cells started showing distinct CPE. Protein synthesis in AHSV-2 and AHSV-3 infected cells declined rapidly to 34.9±0.72% and 37.4±6.2% respectively of the uninfected control at 18 h p.i. In AHSV-4 infected cells protein synthesis fluctuated closer to that in uninfected Vero cells, at levels of 76.8±2.3% of the control. The values for four of the five reassortants were intermediary to those of the two parental strains. Protein synthesis levels in cells infected with R3-$2_{5,10}$ and R3-$2_{3,5}$ decreased to 35.8±0.12% and 37.9±3.4% compared to the control, and for R4-$2_{4,5,7,10}$ and R4-$2_{7,10}$ the corresponding values were 54.5±2.4% and 65±12.3%. Only in the case of R4-2_{10} did the exchange of the single segment apparently have no effect, resulting in a profile very similar to AHSV-4 with an endpoint value of 83.3±8.8% protein synthesis. Significant correlation was found between the percentage viable cells and percentage protein synthesis ($r = 0.76$, $p = 0.028$). For each of the AHSV strains the decrease in protein synthesis in the period up to 18 h p.i. (Fig. 2.7B) corresponded to the observed subsequent decrease in cell viability as measured by the CellTiter-Blue™ cell viability assay (Fig. 2.7A).

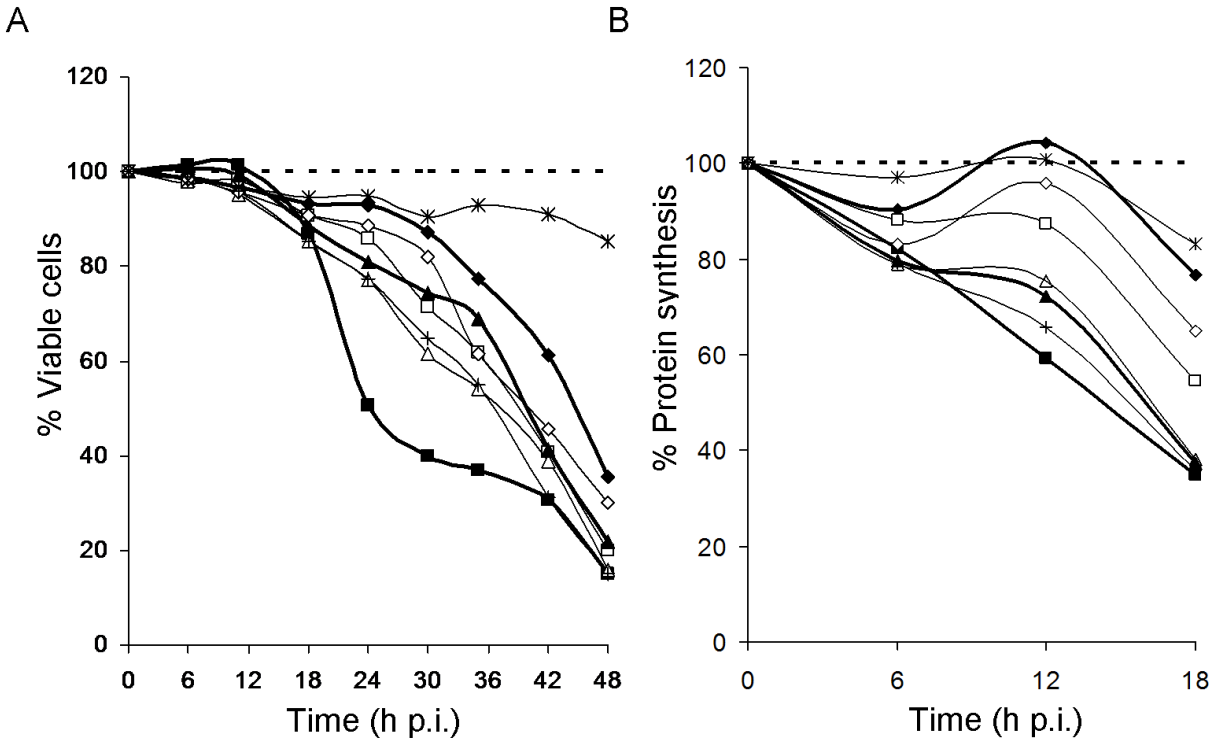

Fig. 2.7 Effect of parental and reassortant AHSV strains on cell viability (A) and total protein synthesis (B) in Vero cells. Cells were infected at a MOI of 10 pfu/cell with AHSV-2 (■), AHSV-3 (▲), AHSV-4 (◆), R3-$2_{5,10}$ (+), R3-$2_{3,5}$ (△), R4-$2_{4,5,7,10}$ (□), R4-$2_{7,10}$ (◇) and R4-2_{10} (✳). Viability was determined over a 48 h period using the CellTiter-Blue™ assay, and protein synthesis monitored by [^{35}S] L-methionine incorporation during a 30 min pulse at 6-hourly intervals up to 18 h p.i. The results in both cases are plotted as a percentage of mock-infected control cells (dashed line). Values indicate the mean of three independent experiments with three repeats during each experiment.

2.3.5. Membrane permeability of infected cells

A Hygromycin B (Hyg B) assay was used to monitor membrane permeability of infected cells. Hygromycin B is a protein synthesis inhibitor that can only penetrate and function in cells after the cell membrane has been permeabilised. Protein translation levels in infected cells, in the presence and absence of Hyg B, is monitored by the measurement of [^{35}S] L-methionine incorporation, see 2.2.6. Decreased levels of [^{35}S] L-methionine incorporation in the presence of Hyg B, in relation to that in the absence of Hyg B, would then indicate permeability of the membrane to Hyg B. The percentage permeabilised cells was calculated as described in 2.2.6. and the results are shown in Table 2.5. Vero cells infected with AHSV-2 consistently showed significantly higher levels of permeabilisation with 67.08±3.32% permeabilised cells compared to AHSV-3 (54.47±5.93%, $P < 0.05$) and AHSV-4 (3.67±3.32%, $P < 0.01$) at 24 h p.i. Cells infected with R4-$2_{4,5,7,10}$, R4-$2_{7,10}$, R4-2_{10} and R3-$2_{5,10}$ were permeabilised to a greater extent than those infected with AHSV-4 or -3 and were closer to that observed for infection with AHSV-2. For example, 67.39±4.33% of the cells infected with R3-$2_{5,10}$ were permeabilised which is significantly closer to the permeabilisation levels of AHSV-2 infected cells ($P = 0.93$) than AHSV-3 infected

cells (P = 0.038). Infection with R3-$2_{3,5}$, the only reassortant that does not contain S10 from AHSV-2, resulted in 54.7±1.38% permeabilisation. This is significantly closer to the effect of AHSV-3 (P = 0.95) than AHSV-2 (P < 0.01). Reassortant viruses therefore showed a tendency towards the levels of permeabilisation observed for the parental virus from which the S10 genome segment was derived. The percentage permeabilised cells was found not to correlate significantly to the percentage viable cells (r = -0.22, p = 0.54) or to the percentage virus released (r = 0.46, p = 0.25). A possible functional link can however not be excluded as sample sizes are relatively small.

Table 2.5 Membrane permeabilisation of Vero cells 24 h after infection with AHSV strains

Virus Strain	% permeabilised cells*
AHSV-2	67.08±3.32
AHSV-3	54.47±5.93
AHSV-4	3.67±3.32
R3-$2_{5,10}$	67.39±4.33
R3-$2_{3,5}$	54.7±1.38
R4-$2_{4,5,7,10}$	80.22±1.10
R4-$2_{7,10}$	76.57±1.35
R4-2_{10}	71.12±1.12

* Values represent mean (n = 3) ± SD

2.4. DISCUSSION

AHSV NS3 is the second most variable AHSV protein, with only outer capsid protein VP2 displaying more variation across all serotypes (Van Niekerk *et al.*, 2001b). This distinguishes it from the highly conserved cognate BTV NS3. The reason for this high level of variation and its impact are not yet clear. In this study three strains of AHSV were selected that each expressed a NS3 protein from one of the three phylogenetic groups, i.e. AHSV-2 (γ NS3), AHSV-3 (β NS3) and AHSV-4 (α NS3). The phenotypic effects of these viruses in mammalian cells was characterised and it was investigated whether this could be linked to the respective NS3 proteins.

Infection with AHSV-2 resulted in significantly higher amounts of membrane permeabilisation, virus release, cell death, morphological damage and cell detachment. AHSV-4 scored lowest in all of these traits and AHSV-3 displayed an intermediate phenotype (closer to AHSV-2). We hypothesised that, firstly, differences in the levels of membrane permeabilisation induced by these viruses could be linked to differences in the encoded α, β, or γ NS3 proteins, based on the finding that recombinant expression of NS3 is cytotoxic to cells possibly as a result of increased

membrane permeabilisation. Secondly, we postulated that in cells infected with AHSV-2, for example, the rapid cell death, high CPE and high amounts of virus release could be linked to the high levels of cell membrane permeabilisation leading to cell lysis. The converse argument would then be true for AHSV-4. As an initial investigation we randomly generated five reassortant viruses selecting for the exchange of the genome segment encoding NS3 to determine the effect on viral phenotype.

The incorporation of AHSV-2 NS3 into a genetic background of AHSV-3 or -4 resulted in an increase in both membrane permeability and the amount of virus released, matching or exceeding that of AHSV-2. These results suggest that the NS3 protein may be the primary determinant of two aspects in the viral life cycle: the amount of virus released from infected cells, and the degree of membrane permeabilisation. This finding confirms previous studies that have shown that the origin of the S10 gene, i.e. whether it groups into the α, β or γ clade, could contribute to the release characteristics of the virus (Martin *et al.*, 1998). Whether the percentage virus released is the direct result of the change in membrane permeability is not yet clear. AHSV and BTV can be released from infected cells either by budding, whereby a temporary lipid envelope is acquired, or by extrusion through a locally disrupted membrane (Eaton *et al.*, 1990; Stoltz *et al.*, 1996). The budding of BTV enveloped particles could result from the interaction of NS3 with components of the vacuolar sorting pathway. This may be the predominant mechanism in insect cells where no CPE is observed (Wirblich *et al.*, 2006). The viroporin activity of NS3 (Han & Harty, 2004) on the other hand could contribute to particle release due to cell lysis, which could be more important in mammalian cells (Wirblich *et al.*, 2006). An interesting preliminary observation (results not shown) was that in KC cells (a *Culicoides* cell line) the trend with respect to virus release was reversed. AHSV-4 displayed the highest percentage release (72.5%), followed by AHSV-3 (43.5%) and then AHSV-2 (35.6%) at 48 h p.i. This emphasises the important contribution of the host cells environment, e.g. proteins and membranes, on the viral release mechanisms.

Membrane permeabilisation, often mediated by a single viral protein or viroporin, can play numerous functions in the viral life cycle and have several consequences for the infected cell. The disorganisation of the cell membrane can facilitate virus budding (Carrasco, 1995; Gonzalez & Carrasco, 2003). Increased permeability to ions and low-molecular-weight compounds also changes the cellular homeostasis of the cell, often promoting viral protein synthesis and providing an ideal environment for virion assembly. Viroporins have furthermore been implicated in the development of CPE by membrane disorganisation and subsequent cell lysis and/or apoptosis (Carrasco, 1995; Gonzalez & Carrasco, 2003; Madan *et al.*, 2008).

Investigation of other aspects, such as cell viability and the development of CPE, showed that these could not be linked to NS3 alone. The incorporation of the NS3 from AHSV-2 into a genetic

background of AHSV-4 in the monoreassortant R4-2_{10}, for example, showed a dramatic increase in membrane permeability and virus release but little to no cell death and CPE. In terms of AHSV cytopathology our results suggest involvement of the non-structural protein NS1, encoded by segment 5, in conjunction with NS3. NS1 is expressed to high levels in infected cells where it forms characteristic tubules, with as yet unknown function. Reassortant viruses with a combination of segments 5 and 10 from AHSV-2 (R3-$2_{5,10}$ and R4-$2_{4,5,7,10}$) displayed a greater tendency towards the AHSV-2 phenotype, with severe CPE. However reassortants in which either AHSV-2 segment 5 (R3-$2_{3,5}$) or 10 (R4-$2_{7,10}$ and R4-2_{10}) were exchanged showed less CPE. In the case of BTV it has been proposed that NS1 is a major determinant of pathogenesis in the vertebrate host, and that modifying the ratio of NS1 to NS3 can shift the mechanism of viral release from a lytic process to one of non-lytic budding from the cell surface (Owens *et al.,* 2004). NS1 tubule formation in BTV-infected mammalian cells was abrogated by the expression of a monoclonal antibody specific to the C-terminal region of NS1 that is essential for tubule formation. This resulted in an increase in the amount of virus released, a shift from lytic release to budding and a dramatic decrease in cellular pathogenesis in these cells. NS1 tubules are found in abundance in BTV-infected insect cells yet there is little CPE in these cells and virus is released by budding. The authors therefore proposed that BTV cellular pathogenesis and release from cells may be a function of the relative ratios of NS1 to NS3 protein levels. In BTV-infected insect cells the levels of NS3 are high in comparison to NS1 so NS3-mediated non-lytic release may allow for the budding of virus without CPE. In mammalian cells, where NS3 levels are lower, NS1 increases virus retention in the cytoplasm, leading to cytolysis and cell death (Owens *et al.*, 2004). The results presented here corroborate the notion that a specific combination of NS1 and NS3 determines AHSV cytopathogenesis, although further investigation is required.

Increased membrane permeability could not, under the conditions used here, be related to increased cell death as proposed for some viroporins. Cell death following viral infection is the endpoint result of a complex interaction of multiple viral and host factors. It is currently unknown whether AHSV induces apoptosis, for example. Recent studies have shown that BTV induces apoptosis in both primary and continuous endothelial cell lines (DeMaula *et al.*, 2001; DeMaula *et al.*, 2002) and that apoptosis is triggered by the outer capsid VP2 and VP5 proteins (Mortola *et al.*, 2004). The mechanism of BTV-induced apoptosis occurs via both caspase-dependant extrinsic and intrinsic pathways (Nagaleekar *et al.*, 2007). Interestingly, BTV induces apoptosis in mammalian cells characterised by extensive CPE but not in insect cells that show no CPE (Mortola *et al.*, 2004). Several viroporins have also been shown to induce apoptosis (Madan *et al.*, 2008). Virus-induced apoptosis may therefore play a significant role in cytopathology.

Our investigation into the amount of infectious virus produced by the reassorted viruses gave surprising results, with an up to ten-fold increase in yield over the parental strains. This increase

in yield may be the result of a combination of factors including the decreased cytopathic effect of some of the reassorted viruses, which would allow for the sustained production of virus, and the increased membrane permeability, which alters the infected cell homeostasis. It would be interesting to investigate whether changes in cell membrane permeability induced by NS3 affects virus replication, protein synthesis and/or assembly. Some viroporins are not essential for viral progeny formation but their expression has been found to significantly increase the production of virus particles (Carrasco, 1995; Gonzalez & Carrasco, 2003; Madan *et al.*, 2008).

In summary, it was shown that non-structural protein NS3 can act in the AHSV life cycle as a viroporin by altering membrane permeability and facilitating virus release from infected cells. The extent of this however depends on which variant of NS3 (α, β, or γ) is carried by the specific virus strain or reassortant. This alteration of membrane permeability by NS3 may fulfil an important function in enhancing virus yield, possibly by altering the infected cell homeostasis. It is clear that NS3 is not the sole determinant of the cytopathic properties of the virus and other viral factors remain under investigation. The NS3 amino acid sequence variation between the isolates used in this study was 34.7% between AHSV-2 and AHSV-3 and 35.2% between AHSV-2 and AHSV-4. This high level of diversity makes it impossible to identify specific residues responsible for the observed phenotypic effects.

In chapter 3 the AHSV-2 NS3 protein was recombinantly expressed in bacterial cells. The cytolytic and membrane permeabilising activity of this protein in these cells was examined, and compared to that of the cognate proteins of BTV and EEV. The regions of AHSV-2 NS3 critical to its cytolytic and membrane permeabilising activity were also examined. In chapter 4 the NS3 proteins from AHSV-2, AHSV-3 and AHSV-4 were recombinantly expressed in insect cells and their exogenous effect on Vero cell membrane permeability compared, in the absence of other AHSV proteins. The cytotoxicity, membrane association and localisation of these proteins expressed in insect cells were also compared in chapter 4.

CHAPTER 3: COMPARISON OF THE CYTOTOXICITY AND MEMBRANE PERMEABILISING ACTIVITY OF AHSV, BTV AND EEV NS3 AND IDENTIFICATION OF DOMAINS IN AHSV NS3 THAT MEDIATE THESE ACTIVITIES

3.1. INTRODUCTION

Bluetongue virus (BTV), African horsesickness virus (AHSV) and equine encephalosis virus (EEV) are closely related members of the *Orbivirus* genus of the family *Reoviridae*. These viruses are similar in morphology and molecular constitution but differ greatly in their ability to cause disease. African horsesickness (AHS) is characterised, in its acute form, by pulmonary oedema, pleural effusion and haemorrhage, with a mortality rate of up to 90% in susceptible horses (reviewed in Mellor & Hamblin, 2004). Loss of endothelial cell barrier function is believed to be the cause of the characteristic pathological features in AHS (Laegreid *et al.*, 1993). Bluetongue disease exhibits similar vascular changes as AHS (Howerth & Tyler, 1988), with pulmonary oedema observed in infected sheep, but the mortality rate is much lower (0-50%). EEV causes a disease characterised by a high morbidity (60-70%) but a low mortality (5%). Clinical disease occurs infrequently and lesions are attributable to endothelial damage of certain blood vessels (Coetzer & Erasmus, 1994). Pathological features of orbiviral diseases therefore include oedema and haemorrhage which have been associated with permeability changes in endothelial cells.

In the preceding chapter it was shown that in tissue culture the NS3 protein contributes to cell membrane permeabilisation and virus release during the AHSV life cycle. AHSV NS3 is a small membrane-associated protein that has previously been implicated in virus release from infected cells (Stoltz *et al.*, 1996), and in virus virulence (O'Hara *et al.*, 1998). Expression of this protein in insect cells causes rapid cell death, that is dependant on the integrity of two hydrophobic domains (HDs) within the protein (Van Staden *et al.*, 1995; Van Staden *et al.*, 1998). Van Niekerk et al. (2001a) first proposed that AHSV NS3 has viroporin-like characteristics and may therefore contribute to pathogenesis.

BTV NS3 is essential for the release of virus-like particles from BTV-infected cells and is involved in the final stages of virus assembly (Hyatt *et al.*, 1991; Hyatt *et al.*, 1993). This protein interacts with the host-trafficking proteins, as well as VP2 and VP5 of progeny virions, to facilitate the release of viral particles (Beaton *et al.*, 2002; Wirblich *et al.*, 2006; Bhattacharya & Roy, 2008). Han & Harty (2004) demonstrated that BTV NS3 has viroporin-like activity as it localizes to the Golgi apparatus and plasma membrane of transfected cells where it causes an increase in membrane permeability, this may have important implications for the pathogenicity of BTV infection.

EEV NS3 gene and protein sequences from South African isolates have been studied and compared to other cognate orbivirus NS3 sequences. The protein was found to have conserved motifs similar to those in BTV and AHSV NS3 (Van Niekerk *et al.*, 2003). These include a second

in-phase AUG, a highly conserved region, a proline rich region and two hydrophobic domains. There is about 17% variation between different EEV proteins, which is more than the 10% of that between BTV NS3 proteins, but much less than the 37% variation observed between different AHSV NS3 proteins (Van Niekerk *et al.*, 2001b; Van Niekerk *et al.*, 2003). EEV NS3 is postulated to play a similar role in virus release and subsequent dispersion of EEV.

As the NS3 proteins of EEV, AHSV and BTV potentially contribute to pathogenesis it would be of interest to study the cytolytic properties of these proteins in the same cell system. This is particularly important in view of the large differences in the virulence of the different viruses and the differences in the pathogenicity of the bluetongue, African horsesickness and equine encephalosis diseases. To compare the cytotoxicity of AHSV, EEV and BTV NS3 these proteins were expressed in *Spodoptera frugiperda* (Sf9) insect and *Escherichia coli* (*E. coli*) cells. The domains within AHSV NS3 involved in cytotoxicity and membrane permeabilisation were additionally investigated through the construction and expression of several truncated mutants in *E. coli.*

3.2. MATERIALS AND METHODS

3.2.1. Expression of orbiviral NS3 proteins as recombinants in insect cells

3.2.1.1. Cells and baculoviruses

Spodoptera frugiperda (Sf9) insect cells were maintained in suspension cultures or as monolayers in Grace's or TC-100 Insect medium (Highveld Biological) supplemented with 10% FCS (Sigma), 0.8% pluronic F-68 (Sigma) and antibiotics (Highveld Biological).

Recombinant baculoviruses expressing NS3 of AHSV-2 or AHSV-4 were obtained from M. van Niekerk (Van Niekerk, 2001) and J. Korsman (UP). The recombinant baculovirus expressing the BTV-10 NS3 gene was a kind gift from Prof. P. Roy (London School of Hygiene and Tropical Medicine, UK). The recombinant baculovirus expressing EEV Bryanston NS3 was obtained from L. Teixeira (UP). As controls, recombinant baculoviruses expressing enhanced green fluorescent protein (eGFP) (M. Victor, UP) and AHSV NS2 (Uitenweerde *et al.*, 1995) were used.

3.2.1.2. Trypan blue cell viability assay

Suspension cultures (50 ml) of Sf9 cells at 1 x 10^6 cells/ml were pelleted at 1000 rpm for 20-30 min. Cells were gently resuspended in inoculum with recombinant baculoviruses at a MOI of 5-10 pfu/cell made up to a total volume of 5 ml with TC-100 medium. Cells were incubated with shaking at 27^{o}C for 1-2 h. The volume was subsequently increased to 50 ml with supplemented TC-100 and incubated with shaking at 27^{o}C. Aliquots were removed every 3 h for 48 h, stained in an equal volume 0.4% Trypan blue (Sigma) and counted using a haemacytometer.

3.2.1.3. CellTiter-Blue^{TM} Cell Viability Assay

Suspension cultures of Sf9 cells at 1 x 10^6 cells/ml were collected at 1000 rpm for 30 min. The cells were mock infected or resuspended in medium containing recombinant baculoviruses expressing AHSV-4 NS3, BTV-10 NS3, EEV-1 NS3 or eGFP at a MOI of 10 pfu/cell. Cells were infected for 3 h at 27^{o}C with shaking. Infected cells were then collected, resuspended in supplemented TC-100 at 4 x 10^5 cells/ml and 100 µl/well seeded on 96 well plates. Cells were incubated at 27^{o}C and viability monitored at 24 and 48 h p.i. using the CellTiter-Blue^{TM} Cell Viability Assay (Promega) according to the manufacturer's instructions. Briefly, a volume of 20 µl CellTiter-Blue^{TM} reagent was added per well and cells incubated at 27°C for a further 3 h. Fluorescence (530-570$_{Ex}$/580-620$_{Em}$) was recorded using a Thermo Labsystems Fluoroskan Ascent FL plate reader. Background fluorescence was corrected for by including wells with serum supplemented culture medium in the absence of cells. Fluorescence readings for these wells were subtracted from experimental wells. The percentage viable cells was calculated by expressing the fluorescence in wells containing insect cells infected with baculoviruses as a percentage of the fluorescence in wells containing uninfected (mock) cells.

3.2.2. Expression of orbiviral NS3 proteins, and truncated AHSV NS3 mutants, in *E. coli*

The pET-41a-c vector series (Novagen) was used for recombinant protein expression in bacteria. This vector is designed for the inducible high-level expression of proteins fused to the carboxyl terminal of a glutathione S-transferase (GST)-Tag protein in *E. coli* (Fig. 3.1).

pET-41a(+) sequence landmarks

T7 promoter	1167–1183
T7 transcription start	1166
GST• Tag coding sequence	436–1095
His• Tag coding sequence	397–414
S• Tag coding sequence	310–354
Multiple cloning sites (*Psh*AI-*Xho*I)	174–265
His• Tag coding sequence	150–173
T7 terminator	26–72
*lac*I coding sequence	1574–2656
pBR322 origin	3850
Kan coding sequence	4559–5374
F1 origin	5474–5921

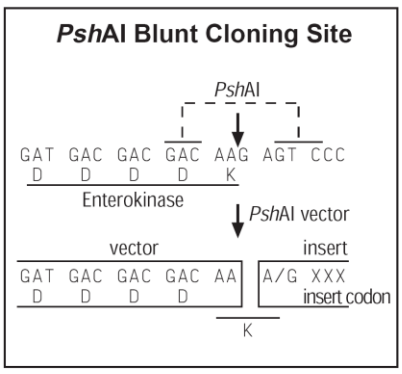

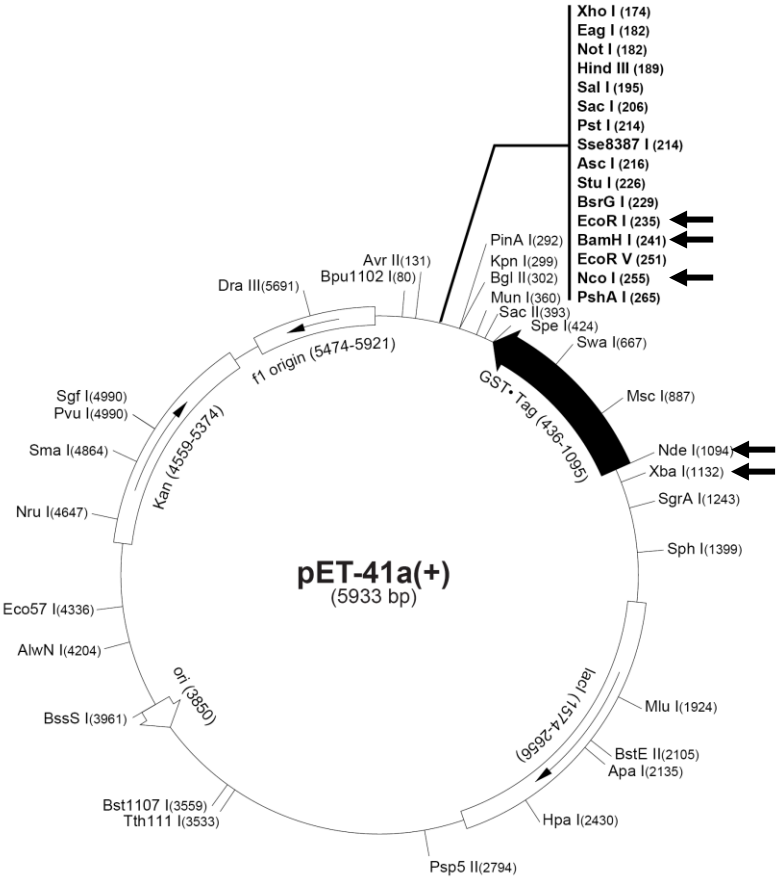

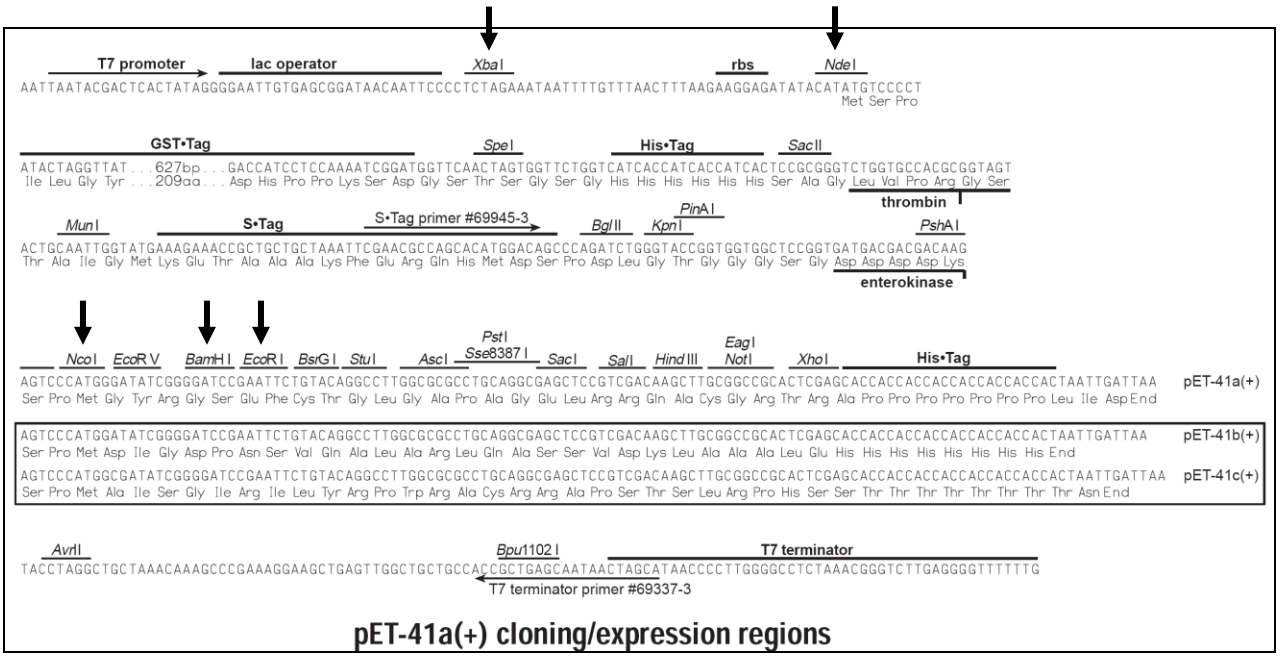

pET-41a(+) cloning/expression regions

Fig. 3.1 Vector map of the pET-41a-c plasmids (Novagen). Restriction enzyme sites used during construction and screening of recombinant pET-41 plasmids in this study are indicated with arrows.

3.2.2.1. PCR amplification of orbiviral S10 genes and truncated AHSV S10 mutants

Full length and truncated versions of the AHSV-2 S10 gene were PCR amplified for cloning into pET-41c using a recombinant pFastBac1 plasmid containing a cDNA copy of the AHSV-2 82/61 reference strain NS3 gene as template (kindly provided by Dr. M. van Niekerk, UP). The primers and PCR conditions used are listed in Table 3.1. The primers used during PCR were designed to include codons to initiate and stop translation where necessary, and to create both *Bam*HI and *Nde*I restriction sites on the 5' end of the gene and an *Eco*RI restriction site on the 3' end of the gene (Table 3.1). The *Bam*HI and *Eco*RI sites were included for directional cloning into the multiple cloning site (MCS) of pET-41c downstream of, and in frame with, the GST-Tag. This would allow for expression of recombinant proteins as GST-Tag fusions. For expression of recombinant proteins without this Tag protein the *Nde*I site was included in primer sequences to allow removal of the vector sequence coding for GST (an *Nde*I site is also present in the vector upstream of the GST-Tag sequence, see Fig. 3.1). PCR amplification with these primers therefore allowed cloning into the pET-41c vector and expression of recombinant proteins with and without the GST-Tag.

All truncated versions of the AHSV-2 NS3 gene were amplified as described above except the nucleotide region (526-657) encoding amino acids 176 to 218 of AHSV NS3 (C-terminal region). This region was amplified using the forward primer HS2NS3C-termNco (Table 3.1) with the AHSVNS3pEco reverse primer (Table 3.1). This created an *Nco*I restriction enzyme site on the 5' end of the insert and an *Eco*RI restriction site on the 3' end. This would allow for the insertion of this NS3 specific sequence into the MCS downstream of the GST-Tag in pET-41a and expression of this region of NS3 as a GST-Tag fusion protein.

For cloning of the BTV-4 NS3 gene into pET-41c BTV-4 dsRNA (Van Niekerk *et al.*, 2003) was reverse-transcribed into cDNA and PCR amplified as previously described (Van Niekerk *et al.*, 2001b) using the S10 specific BTV primers listed in Table 3.1. Briefly, approximately 250 ng of dsRNA was denatured in an equal volume 10 mM methylmercuric hydroxide (MMOH) for 10 min at room temperature. To this 2 µl 0.7 M β-mercaptoethanol was added per 10 µl reaction volume to reduce the MMOH and the reaction incubated for 5 min at room temperature in the presence of 40 U RNase inhibitor (recombinant RNasin, Promega). The denatured RNA was added to a cDNA reaction mix containing 100 pmol of each primer, 2.5 mM of each dNTP, reaction buffer and 10 U AMV reverse transcriptase (Promega) and incubated for 90 min at 42^{o}C. The cDNA was then amplified by PCR (2.2.3.2 and Table 3.1). The BTV S10 specific primers were designed to create *Bam*HI and *Nde*I restriction sites on the 5' end of the gene and an *Eco*RI restriction site on the 3' end of the gene.

All PCRs were carried out as described in section 2.2.3.2. and analysed by 1 or 2% agarose gel electrophoresis.

Table 3.1 Oligonucleotide primers and PCR conditions used for the cloning of orbiviral NS3 genes and NS3 mutants

Nucleotide (nt) region of S10 gene amplified (amino acid (aa) region encoded)	**Forward and Reverse primers (Storage code) 5' to 3' sequence* Restriction enzyme sites(/s)**	**PCR conditions**
Full length AHSV-2 NS3 gene (aa 1-218)	Forward primer CGGGATC**CAT**ATGAATCTTGCTAGCATCTCC *Bam*HI and ***Nde*I** Reverse primer (P11E4) CGGAATTCGTAAGTCGTTATCCCGG *Eco*RI	95°C 2min, (94°C 45 sec; 60°C 30 sec; 72°C 2 min) x 30, 72°C 5 min
Full length BTV-4 NS3 gene (aa 1-229)	Forward primer GCGGATC**CAT**ATGCTATCCGGGCTGATC *Bam*HI and ***Nde*I** Reverse primer CGGAATTCGTTAGTGTGTAGAGCCGCG *Eco*RI	95°C 2min, (94°C 45 sec; 60°C 30 sec; 72°C 2 min) x 30, 72°C 5 min
Nt **1-276**# of AHSV-2 S10 (aa **1-92)**	Forward primer CGGGATC**CAT**ATGAATCTTGCTAGCATCTCC *Bam*HI and ***Nde*I** Reverse primer (P11G3) CGGAATTCTCAACCTACTCGTCGCTTAATTTTTC *Eco*RI	96°C 2min, (96°C 30 sec; 59°C 30 sec; 72°C 1 min) x 35, 72°C 5 min
Nt **1-354** of AHSV-2 S10 (aa **1-118)**	Forward primer CGGGATC**CAT**ATGAATCTTGCTAGCATCTCC *Bam*HI and ***Nde*I** Reverse primer (P11G2) CGGAATTCTCAAAACATAATTATTTTCAAAATC *Eco*RI	96°C 2min, (96°C 30 sec; 54°C 30 sec; 72°C 1 min) x 35, 72°C 5 min
Nt **1-420** of AHSV-2 S10 (aa **1-140**)	Forward primer CGGGATC**CAT**ATGAATCTTGCTAGCATCTCC *Bam*HI and ***Nde*I** Reverse primer (P11G5) CGGAATTCTCAAATATCCTCATCAACGATAG *Eco*RI	96°C 2min, (96°C 30 sec; 59°C 30 sec; 72°C 1 min) x 35, 72°C 5 min
Nt **451-657** of AHSV-2 S10 (aa **151-218**)	Forward primer (P11G4) CGGGATC**CAT**ATGGATTGGGTGTCAAAAACGG *Bam*HI and ***Nde*I** Reverse primer (P11E4) CGGAATTCGTAAGTCGTTATCCCGG *Eco*RI	96°C 2min, (96°C 30 sec; 59°C 30 sec; 72°C 1 min) x 35, 72°C 5 min
Nt **337-657** of AHSV-2 S10 (aa **113-218**)	Forward primer (P11G7) CGGGATC**CAT**ATGTTGAAAATAATTATGTTTATTTGC *Bam*HI and ***Nde*I** Reverse primer (P11E4) CGGAATTCGTAAGTCGTTATCCCGG *Eco*RI	96°C 2min, (96°C 30 sec; 59°C 30 sec; 72°C 1 min) x 35, 72°C 5 min

Nucleotide (nt) region of S10 gene amplified (amino acid (aa) region encoded)	**Forward and Reverse primers (Storage code) 5' to 3' sequence* Restriction enzyme sites(/s)**	**PCR conditions**
Nt **277-657** of AHSV-2 S10 (aa **93-218**)	Forward primer (P11G6) CGGGATC**CAT**ATG**ATCCAAACTCTAAAAACATTG** *Bam*HI and ***Nde*I**	96°C 2min, (96°C 30 sec; 59°C 30 sec; 72°C 1 min) x 35, 72°C 5 min
	Reverse primer (P11E4) CGGAATTCGTAAGTCGTTATCCCGG *Eco*RI	
Nt **337-528** of AHSV-2 S10 (aa **113-176**)	Forward primer (P11G7) CGGGATC**CAT**ATG**TTGAAAATAATTATGTTTATTTGC** *Bam*HI and ***Nde*I**	96 °C 2min, (96 °C 30 sec; 59 °C 30 sec; 72 °C 1 min) x 35, 72 °C 5 min
	Reverse primer CGGAATTCTCATTCCGATATTTTATTCGC *Eco*RI	
Nt **526-657** of AHSV-2 S10 (aa **176-218**)	Forward primer TGTGG**CC**ATG**GT**CGAAAAGGTGAGAGAAGAG ***Nco*I**	96 °C 2min, (96 °C 30 sec; 59 °C 30 sec; 72 °C 1 min) x 35, 72 °C 5 min
	Reverse primer (P11E4) CGGAATTCGTAAGTCGTTATCCCGG *Eco*RI	

[#] Nucleotide numbering of AHSV S10 excludes the 5' non-coding region, with position 1 indicating the first nucleotide (A) in the initiation codon of the NS3 gene
* Initiation and termination codons are blocked

3.2.2.2. Cloning of S10 amplicons into pET-41 and screening recombinants

PCR products were purified from solution using the High pure PCR purification kit (Roche). Amplicons were digested with *Bam*HI and *Eco*RI, or *Nco*I and *Eco*RI, purified, and ligated to linearised pET-41a/c vector digested with the same restriction enzymes. Insertion at these sites places the sequence in the multiple cloning site downstream and in frame with the glutathione S-transferase (GST) gene in the pET-41 a/c vector (Fig. 3.1). Ligation mixtures were used to transform competent XL1 Blue or JM109 *E. coli* cells. Competent cells were prepared by treatment with $CaCl_2$ in the early log phase of growth and transformations performed by heat shock at 42ºC as described by Sambrook and Russell (2001). Possible recombinant colonies were grown overnight at 37ºC on agar plates containing 15 μg/ml kanamycin (kan) and 12.5 μg/ml tetracycline (tet) for XL1 Blue cells, and 15 μg/ml kan for JM109 cells. Possible recombinant plasmids were isolated by a conventional small scale alkaline-lysis plasmid isolation protocol (Sambrook & Russell, 2001).

Recombinant plasmids were verified by restriction enzyme digestion with *Bam*HI and *Eco*RI or *Xba*I and *Eco*RI. For sequencing recombinant plasmids were purified using a commercial purification kit (Roche) and sequenced using an ABI PRISM Big Dye Terminator Cycle Sequencing Ready Reaction kit with an S-Tag (5' CGAACGCCAGCACATGGACAG 3') forward primer and a T7 terminator (5' GCTAGTTATTGCTCAGCGG 3') reverse primer specific for the S-Tag and T7 terminator sequences respectively, on the pET-41 vector. Sequences were analysed on an ABI 377 automated sequencer (Perkin Elmer).

For expression of NS3 proteins without the GST-Tag protein, the region of the recombinant pET-41 plasmids encoding GST was removed by *Nde*I digestion as *Nde*I cleaves its recognition site on the pET-41c vector upstream of the GST coding sequence (Fig. 3.1) and at the *Nde*I site included in the primer sequences. Digested plasmids were then self ligated, transformed into

competent cells, the cells grown and possible recombinant plasmids isolated as described above. Removal of the vector sequence encoding GST was confirmed by digestion of recombinant plasmids with *Xba*I and *Eco*RI. The *Xba*I enzyme cleaves upstream of the *Nde*I site and the GST-Tag coding sequence on pET-41.

A recombinant pET-41a plasmid containing a cDNA copy of the EEV(Bryanston) NS3 gene (pET-EEV NS3) was obtained from L. Teixeira (UP). The sequence encoding the GST-Tag protein had been removed from this recombinant plasmid using a similar protocol (Teixeira, 2005).

3.2.2.3. Transformation of E. coli *with recombinant pET-41 plasmids*

The *E. coli* expression hosts BL21(DE3)pLysS or BL21(DE3) cells (Novagen) were used for the bacterial recombinant expression of full length and truncated NS3 proteins. Cells were grown to early log phase and made competent by treatment with $CaCl_2$. The recombinant pET-41 plasmids constructed in 3.2.2.1 were used to transform competent cells by heat shock (Sambrook & Russell, 2001). Transformed cells were selectively grown on agar plates containing 15 μg/ml kan for BL21(DE3) cells, and 15 μg/ml kan and 34 μg/ml chloramphenicol for BL21(DE3)pLysS cells.

3.2.2.4. Induction and analysis of recombinant protein expression in E. coli

Transformed expression hosts were grown and induced as recommended by the manufacturers (Novagen). Single transformed colonies were used to inoculate a small volume (2 to 3 ml) of Luria-Bertani medium (LB) supplemented with appropriate antibiotics. Cultures were grown with shaking at 37°C to an absorbance at 600 nm (OD_{600}) of 0.6–0.8 units. The cells were diluted 100-fold in fresh supplemented LB medium and grown at 37°C until an OD_{600} of 0.5-0.6 was reached. Recombinant protein expression was induced by the addition of isopropyl-β-D-thiogalactoside (IPTG) to a final concentration of 1 mM.

Protein expression in cells transformed with pET-41 plasmids expressing recombinant proteins without the GST-Tag was monitored by metabolic labelling of proteins. For this purpose aliquots of each induced culture were taken 10 min prior to labelling and incubated in the presence or absence of 200 μg/ml rifampicin (rif) at 37°C for 10 min. Samples were then labelled with 5 μCi/ml [^{35}S] L-methionine (Perkin Elmer) for 20 or 45 min. Cultures were collected (1 min at 13 200 rpm) and resuspended in 1 x protein solvent buffer (PSB). Protein samples were resolved by standard 15, 18 or 20% SDS-PAGE and soaked overnight in a 20% methanol, 3% glycerol solution. Gels containing 18 or 20% polyacrylamide were dried overnight using a BioRad GelAir Dryer. Gels containing 15% polyacrylamide were dried for 1 to 2 h at 80ºC under vacuum. Dried gels were exposed to an imaging screen-K (BioRad), and scanned using a Personal Molecular Imager FX (BioRad) or exposed to X-ray films in a cassette for 48 h following which they were developed and fixed for visualisation of labelled proteins using standard autoradiographic methods.

For the analysis of protein expression in cells transformed with pET-41 plasmids expressing recombinant GST-Tag fusion proteins, samples of induced cultures were taken every 30 min for 2 h, the cells harvested by centrifugation and resuspended in PBS. An equal volume of 2 x PSB was added and proteins analysed by 10 or 12% SDS-PAGE. Gels were stained with 0.05% w/v Coomassie blue and destained in a 5% v/v methanol and 5% v/v acetic acid solution.

3.2.2.5. E. coli *cell growth assays*

Cells transformed with non-recombinant or recombinant pET-41 plasmids were grown and IPTG induced as described above (3.3.2.3). Cell growth was then monitored by measuring the OD_{600} of cultures every hour for 4 h. All data represent the mean and standard deviation calculated from at least four independent experiments. For cell growth plots the mean OD_{600} values at each time point were expressed as a percentage of the mean OD_{600} value for that culture at induction. The

percentage growth of recombinant cultures was also calculated relative to that of the control culture (cells transformed with the non-recombinant pET-41 c) i.e. control culture growth was set at 100%. This calculated value was then subtracted from 100% to obtain the percentage inhibition of growth relative to the control culture.

3.2.2.6. Hygromycin B E. coli *membrane permeability assay*

For the Hyg B membrane permeability assay, recombinant cultures were IPTG induced for 30 min and incubated for a further 20 min in the absence or presence of 500 μg/ml Hyg B. Thereafter samples were labelled for 45 min with 5 μCi/ml [^{35}S] L-methionine (Perkin Elmer). Proteins were resolved and visualised as described (3.3.2.3). Translation levels were estimated by quantifying radiolabelled protein bands in each lane on SDS-PAGE gels using Quantity One 1-D Analysis Software (BioRad). The amount of protein in lanes representing samples metabolically labelled in the presence of Hyg B is then expressed as a percentage of the amount of protein in lanes representing the same culture metabolically labelled in the absence of Hyg B. This percentage is then representative of the percentage cells that where permeabilised to Hyg B, and is referred to as the percentage permeabilised cells.

3.2.2.7. β-galactosidase E. coli *membrane permeability assay*

Recombinant bacterial cultures were grown and induced as described above (3.3.2.3). At 4 h post induction the OD_{600} of each culture was measured. A volume of 0.5 ml culture was removed, the cells pelleted (1 min at 13 200 rpm) and resuspended in fresh medium. ONPG (*o*-nitrophenyl-*β*-D-galactopyranoside) was added to the resuspended pellets at a final concentration of 2 mM and incubated at 30ºC for 10 min. The reaction was stopped through the addition of 200 µl 1 M sodium carbonate buffer (pH 9.5). Cells were pelleted and the absorbance at 420 nm of the supernatant read to measure ONPG cleavage by β-galactosidase within permeabilised cells. OD_{420} readings were standardised to the bacterial growth (OD_{600}) of that culture.

3.2.2.8. Purification of N- and C-terminal regions of AHSV-2 NS3

3.2.2.8a Analysis of solubility of GST-NS3 Tag fusion proteins

BL21(DE3) cells containing recombinant pET-41 plasmids expressing truncated versions of NS3 as GST fusions were grown and induced as described in 3.3.2.3. Induced cultures were incubated at 37^{o}C for 3 h with agitation. Cells were collected by centrifugation at 4000 rpm for 15 min. Cell pellets were frozen and stored at -80^{o}C or used immediately. Cell pellets were resuspend in 4ml Lysis buffer (0.05% Tween 20; 50 mM EDTA; 1 mg/ml lysozyme; 0.7 µg/ml pepstatin; 1 mg/ml pefabloc SC in PBS) per 100 ml starting culture. Cells were incubated on ice for 1 h and sonicated 10 times at 50% duty cycle 3 output for 20 sec followed by 30 sec on ice each. Samples were centrifuged at 2500 g for 15 min. The supernatant (soluble fraction) was transferred to a clean tube and the pellet (particulate fraction) resuspended in an equal volume Lysis buffer. Proteins in the particulate and soluble fractions were analysed by SDS-PAGE and visualised by Coomassie staining.

3.2.2.8b Purification of fusion proteins and cleavage of GST from GST-NS3 fusion proteins

Lyophilised glutathione immobilized on cross-linked 4% beaded agarose (Sigma) was allowed to swell in 200 ml/g double distilled water overnight at 4^{o}C. The swelled resin was centrifuged at 500 g for 5 min, washed with ten bed volumes of cold PBS and recentrifuged. An equal volume of PBS was then added to make a 50% glutathione agarose slurry.

Soluble fractions of lysates from induced recombinant BL21(DE3) cells were prepared as described above (3.3.2.8a) except that cells were induced for 24 h at 20^{o}C. Soluble fractions were mixed with 50% glutathione agarose slurry (2 ml per 100 ml starting culture) and DTT (dithiothreitol) added to a final concentration of 1 mM. Samples were agitated at room temperature for 1 h and centrifuged at 500 g for 5 min. The resin was washed twice with ten bed

volumes cold PBS containing 1% v/v Triton X-100 and once with ten bed volumes of cold PBS, with each wash the sample was mixed by inverting and the resin collected by centrifugation at 500 g for 5 min at 4ºC. For each 1 ml bed volume 2U Thrombin (Boehringer Mannheim GmbH) and 1 ml cold sterile PBS was then added. Samples were incubated overnight at room temperature with gentle agitation and centrifuged at 500 g for 5 min at 4ºC. The supernatant, containing the purified protein, was freeze dried and resuspend in 100-200 µl sterile PBS. The resin was washed once with cold PBS and resuspended in an equal volume PBS. Proteins were analysed by SDS-PAGE and Coomassie staining. The quantification of protein bands was performed using Quantity One 1-D Analysis Software (BioRad).

3.3. RESULTS

This part of the study aimed to characterise and compare the cytolytic and membrane permeabilising properties of the AHSV, BTV and EEV NS3 proteins, and to identify the protein domains determining these properties. The orbiviral NS3 proteins were therefore recombinantly expressed and their effects compared in both insect and bacterial cells. The domains within AHSV NS3 responsible for these activities was subsequently investigated, through the construction, expression and analysis of truncated mutants of the protein in *E. coli*. The expression of these truncated mutants as GST-Tag fusion proteins in *E. coli* for purification purposes is also described here.

3.3.1. Comparison of the cytolytic properties of BTV, AHSV and EEV NS3 in Sf9 cells

It was of interest to investigate whether there are any differences in the cytolytic properties of the AHSV, BTV and EEV NS3 proteins. The proteins were therefore expressed in Sf9 cells using the recombinant baculovirus expression system. Recombinant baculoviruses had previously been generated and the expression kinetics of the NS3 proteins characterised (Van Niekerk, 2001; Teixeira, 2005).

To assess changes in the viability of Sf9 cultures expressing the recombinant orbiviral NS3 proteins a Trypan blue cell viability assay was used (Fig. 3.2). Sf9 cells were infected with wild-type baculovirus or recombinant baculoviruses expressing AHSV, BTV or EEV NS3 and AHSV NS2. Samples of infected cells were removed every three hours for 48 hours and Trypan blue added. The cytoplasm of non-viable or permeabilised Sf9 cells is stained blue by this vital exclusion dye, while viable and non-permeabilised cells remain unstained. The number of stained and unstained cells were therefore counted at each time point. The percentage viable cells was then calculated as the number of unstained cells over the total (stained and unstained) number of cells x 100.

At 18 h p.i. (Fig. 3.2) there was no difference in the percentage viable cells in cultures infected with wild-type or recombinant baculoviruses. Expression of recombinant proteins in the baculovirus expression system occurs under the control of a strong late polihedrin baculovirus promoter. Recombinant proteins are therefore expressed and detected between 18 and 24 h p.i. in this system. Control cultures infected with wild-type baculovirus then displayed only a slight decrease in viability with 84% viable cells still remaining at 48 h p.i.. Similarly, 76% of the cells infected with a recombinant baculoviruses that express the AHSV NS2 protein still remained viable at 48 h p.i.. Therefore, over-expression of a recombinant protein, in this case NS2, does not necessarily negatively impact on the viability of the cells. From 18 h p.i. the viability of cells

expressing AHSV, BTV and EEV NS3 decreased, with a dramatic decline in viability observed from approximately 27 h p.i. up to 48 h p.i. with only 8, 14 and 16% viable cells respectively remaining at this time.

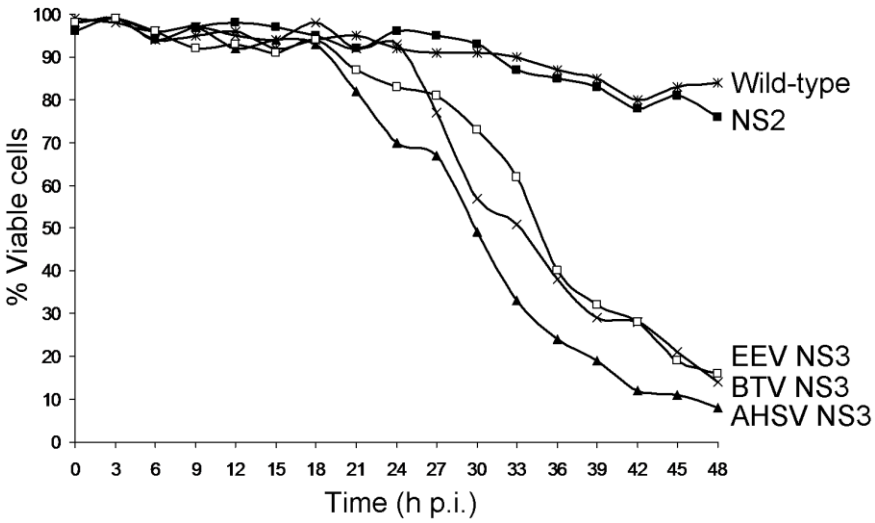

Fig. 3.2 Effect of orbiviral NS3 proteins on the viability of insect cells. Sf9 viability was monitored by staining with Trypan blue and counting viable and non-viable cells every 3 h for 48h. Wild-type baculovirus and a recombinant baculovirus expressing NS2 were included as non-cytotoxic controls.

To additionally assess changes in the viability of Sf9 cultures expressing the recombinant NS3 proteins a CellTiter-Blue™ Cell Viability Assay was used. In this assay the non-fluorescing resazurin substrate is added to the culture media of cells and the viability of cells estimated by quantifying the reduction of this substrate to a fluorescent product (resorufin) by metabolically active cells. Sf9 cells were mock infected or infected with recombinant baculoviruses expressing AHSV, BTV or EEV NS3 and eGFP. Viability of the infected cells was assayed at 24 and 48 h p.i. (Fig. 3.3). The percentage viable cells was calculated relative to uninfected cells (Mock) at each time point. Values represent the mean and standard deviation of three repeats. At 24 h p.i. no noteworthy differences in the viability of cells expressing eGFP or the AHSV, BTV and EEV NS3 proteins was observed with 94.0±4.8, 94.9±0.5, 96.8±2.2 and 91.8±3.3% viable cells, respectively. At 48 h p.i. control cultures expressing the non-cytotoxic eGFP were on average more than 81.7±10.4% viable. At the same time point the expression of AHSV, BTV and EEV NS3 in insect cells lead to a decrease in the number of viable cells with only 21.3±2.9, 13.3±0.8 and 20.1±1.1% viable cells remaining, respectively.

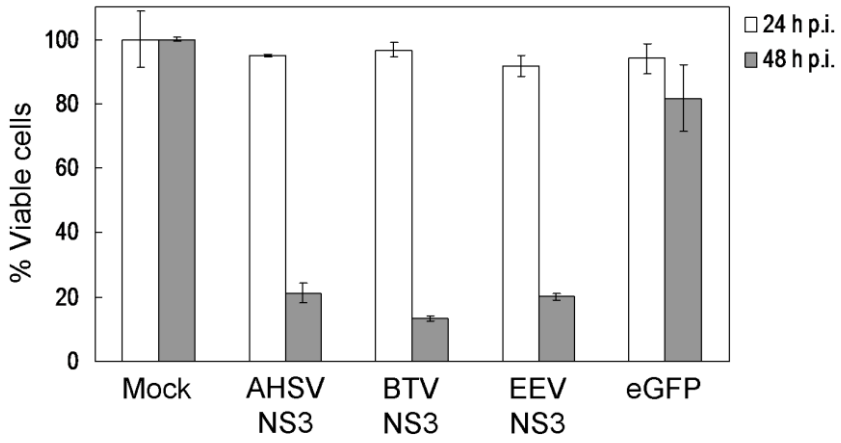

Fig. 3.3 Effect of orbiviral NS3 proteins on Sf9 insect cell viability. Sf9 cells were uninfected (Mock) or infected at a MOI of 10 pfu/cell with recombinant baculoviruses expressing AHSV NS3, BTV NS3, EEV NS3 and eGFP. Viability was monitored at 24 and 48 h p.i. using the CellTiter-Blue™ viability assay.

Both the CellTiter-Blue™ and Trypan blue assays therefore showed that AHSV, BTV and EEV NS3 were equivalently cytotoxic to Sf9 insect cells.

3.3.2. Expression of BTV, AHSV and EEV NS3 in *E. coli* cells

The effect of AHSV, BTV and EEV NS3 on bacterial cell viability and membrane permeability was subsequently investigated by means of an inducible pET prokaryotic expression system (Studier & Moffat, 1986). This system has been shown to be suitable for the identification of a number of virally encoded membrane-active proteins (Guinea & Carrasco, 1994; Aldabe *et al.*, 1996; Gonzalez & Carrasco, 2003). The membrane destabilising activity of proteins encoded by other members of the family Reoviridae including rotavirus NSP4 (Browne *et al.*, 2000) and avian reovirus p10 (Bodelón *et al.*, 2002) have also been studied using this system.

In the pET expression system target genes are placed under the control of a tightly regulated bacteriophage T7 promoter in the pET vector. Expression is initiated by providing a source of T7 RNA polymerase in the host cell. Target genes are initially cloned using bacterial hosts that do not express T7 RNA polymerase. Genes under the control of this promoter are therefore transcriptionally inactive in these host strains. This allows for the establishment of high plasmid copy numbers and possibly eliminates plasmid instability due to the production of potentially toxic proteins. Target gene expression is then initiated by transferring the plasmid into an expression host containing a chromosomal copy of the T7 RNA polymerase gene. Expression hosts are lysogens of the bacteriophage DE3, a lambda derivative that includes a DNA fragment with the *lacI* gene, the *lacUV5* promoter, and the gene for T7 RNA polymerase. When IPTG is added to expression hosts the *lacUV5* promoter is induced and in turn initiates the transcription of T7 RNA

polymerase. The T7 RNA polymerase then transcribes the target gene in the pET plasmid (Studier, 1991). T7 RNA polymerase is highly selective and when fully induced, the majority of the host cell's resources are directed towards target gene expression.

For expression of the orbiviral NS3 proteins in the pET system the pET-41a-c expression vector series was chosen. This vector was chosen for several reasons. This tightly regulated inducible system is ideal for the expression of potentially cytotoxic proteins, as described above. In this vector target genes inserted into the MCS are expressed fused to a 220 amino acid GST-Tag proteins, that may increase the solubility of fused peptides and facilitates affinity purification. The cloning of the orbiviral S10 genes into this vector is described in the following section.

3.3.2.1. Cloning AHSV and BTV S10 genes into pET-41c

The open reading frames of AHSV-2 and BTV-4 S10 were amplified by PCR with the primers specified in Table 3.1. PCR products were analysed by agarose gel electrophoresis (Fig. 3.4) and fragments of the expected sizes were obtained for the BTV (812 bp, Fig. 3.4 lane b) and AHSV (750 bp, Fig. 3.4 lane c) NS3 genes.

Fig. 3.4 Agarose gel showing PCR amplification of the S10 open reading frames of BTV and AHSV for cloning into pET-41c. The BTV and AHSV S10 amplicons are in lanes (b) and (c) respectively. Sizes of selected DNA fragments in the 100 bp DNA ladder (a; Promega) are as indicated on the left.

PCR products were cloned as *Bam*HI and *Eco*RI digested fragments into pET-41c vector digested with the same restriction enzymes as described in 3.2.2.1. Successful cloning was verified by digestion with *Bam*HI and *Eco*RI, and the orientation and identity of inserts confirmed by sequencing of recombinant plasmids (see 3.2.2.2). During cloning the non-expression host XL1 Blue strain was used. The region of the plasmid representing the GST ORF was then excised from these recombinant plasmids by *Nde*I digestion as described in 3.2.2.2. As the aim here was to compare the cytolytic and membrane permeabilising functions of the NS3 proteins the GST-Tag was removed as it may interfere with these activities. Removal of the GST-Tag coding sequence was confirmed by *Xba*I and *Eco*RI digestion of recombinant plasmids.

Recombinant pET-41 plasmids containing the orbiviral NS3 genes without the GST-Tag sequences were named pET-AHSV-2 NS3 and pET-BTV-4 NS3.

The EEV S10 ORF had previously been cloned in pET-41a and the GST coding sequence removed (Teixeira, 2005). The pET-AHSV-2 NS3, pET-BTV-4 NS3 and pET-EEV NS3 plasmids were transformed into the expression host BL21(DE3)pLysS as described in 3.2.2.3.

3.3.2.2. Analysis of expression of AHSV, BTV and EEV NS3 in E. coli

To analyse the expression of the orbiviral NS3 proteins, transformed *E. coli* BL21(DE3)pLysS cells were grown and induced (see 3.2.2.4). Expression of the NS3 proteins in BL21(DE3)pLysS cells was monitored at 15, 30 and 60 minutes (min) post induction by metabolic labelling at these times in the presence and absence of rifampicin. Rifampicin is an *E. coli* polymerase inhibitor. In the presence of this antibiotic *E. coli* protein synthesis is therefore inhibited, and the target gene product expressed from the T7 polymerase promoter in the pET vector is the major protein synthesised. Proteins in cell extracts were separated by SDS-PAGE and visualised by phosphorimaging (Fig. 3.5). Cells transformed with the parent pET-41c vector were included as a control and expressed the GST-Tag protein (35.6 kDa) to high levels (Fig. 3.1D). In the presence of rifampicin this was the major protein synthesised as expected (Fig. 3.1D, last three lanes). A novel protein was synthesized from the T7 promoter in cells transformed with pET-AHSV-2 NS3 (Fig. 3.5A), pET-BTV-4 NS3 (Fig. 3.5B) and pET-EEV-NS3 (Fig. 3.5C). In the presence of rifampicin these were the major proteins synthesised, although expression levels were significantly lower than that of the GST-Tag protein. The BTV NS3 protein (Fig. 3.5B, last three lanes) appeared to be expressed to slightly higher levels than the AHSV and EEV NS3 proteins (Fig. 3.5A and B, last three lanes, respectively).

To compare the relative sizes of the recombinant proteins, proteins from induced cultures were metabolically labelled in the presence and absence of rifampicin, separated on a 15% SDS-PAGE gel and visualised by autoradiography (Fig. 3.6). For each recombinant a novel band of the expected sizes of 23.5 kDa for AHSV NS3, 25 kDa for BTV NS3, 27.2 kDa for EEV NS3 and 35.6 kDa for the GST-Tag protein (indicated by the arrows in Fig. 3.6) was observed. As equivalent amounts of cell extracts were not loaded on the gel in Fig. 3.6 comparisons of the relative expression levels of the proteins cannot be made here. The identity of the AHSV and EEV NS3 proteins was furthermore confirmed by immunoblot with monospecific polyclonal antibodies (results not shown).

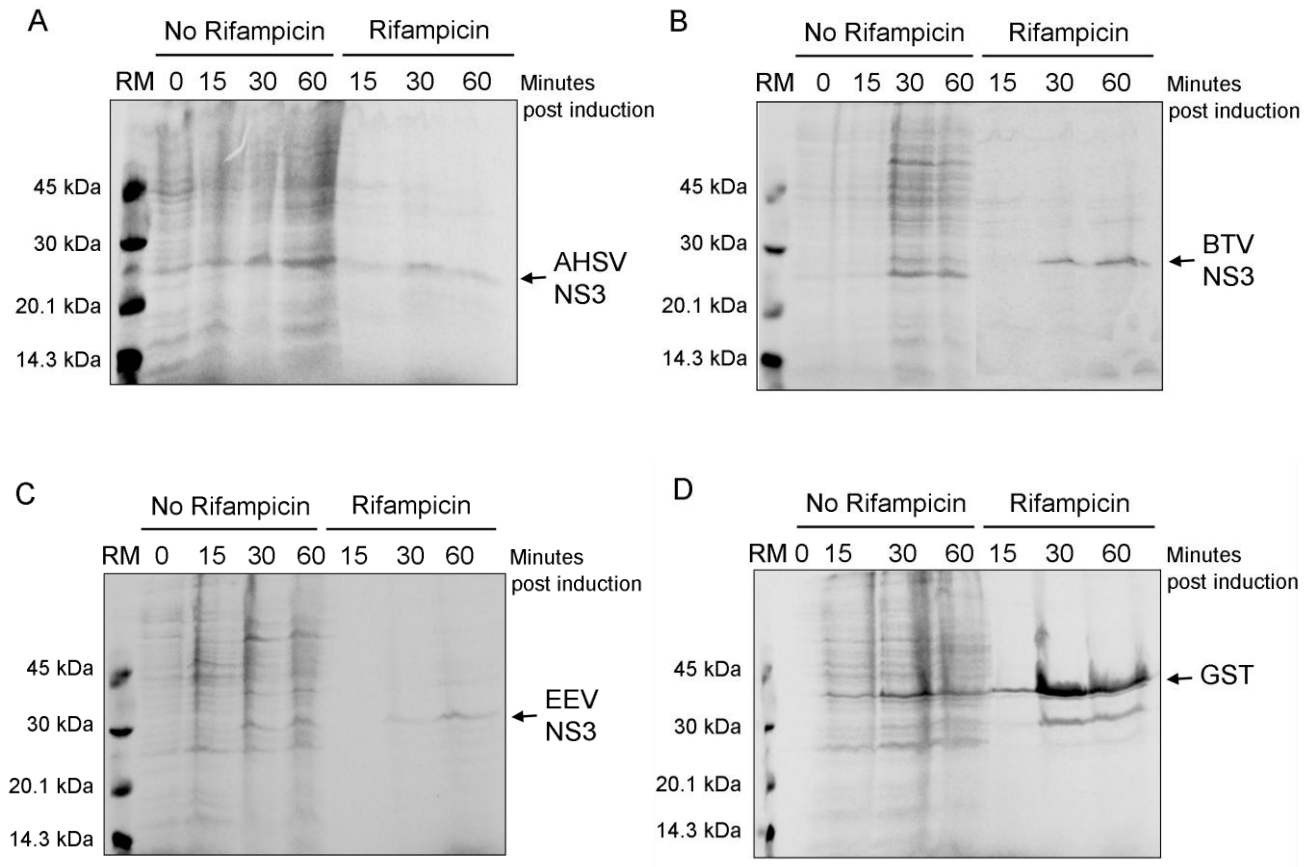

Fig. 3.5 Expression of three different orbiviral NS3 proteins in BL21(DE3)pLysS cells. Cultures transformed with recombinant pET-41 plasmids expressing AHSV (A), BTV (B) or EEV (C) NS3 or non-recombinant pET-41c (D) were induced and at the indicated times post induction proteins labelled for 20 min with [^{35}S] L-methionine. Where indicated rifampicin was added to the bacterial cells 10 min prior to labelling. Proteins were separated by 15% SDS-PAGE and detected by phosphorimaging. The positions of the orbiviral NS3 proteins and the GST-Tag protein expressed from the pET-41c plasmid are indicated. The sizes of the molecular weight marker (Rainbow Marker, RM) are as indicated on the left.

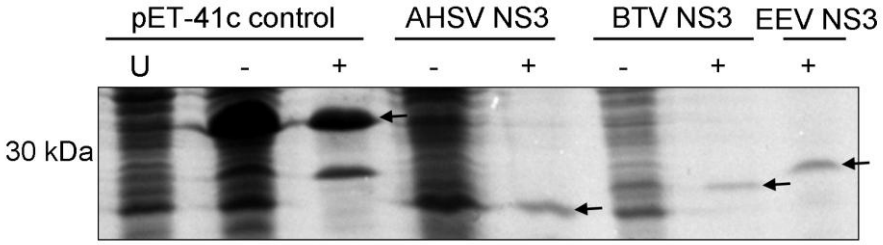

Fig. 3.6 Comparative expression of orbiviral NS3 proteins in BL21(DE3)pLysS cells. Bacterial cultures transformed with pET-41c or recombinant plasmids containing the NS3 genes from AHSV, BTV or EEV were induced. At 10 min post induction rifampicin was added (+) or not added (-) and incubated for a further 10 min. Labelling with [^{35}S] L-methionine was allowed to occur for 45 minutes. Proteins were separated by 15% SDS-PAGE and detected by autoradiography. The arrows indicate the position of AHSV NS3, BTV NS3 and EEV NS3 in their respective lanes or the GST-Tag protein expressed from the non-recombinant pET-41c plasmid. U is an uninduced BL21(DE3)pLysS culture transformed with pET-41c. The position of the 30 kDa molecular weight marker is indicated on the left.

3.3.2.3. Viability of E. coli *expressing AHSV, BTV and EEV NS3*

To compare the effect of the orbiviral NS3 proteins on *E. coli* cell growth and viability, growth rates of BL21(DE3)pLysS cells expressing these proteins were monitored. Following induction of recombinant protein expression in transformed cells, cell density was monitored every hour for four hours by measurement of the OD_{600} of cultures. The OD_{600} values at each time point were then expressed as a percentage of the OD_{600} value for that culture at induction. The results are shown in Fig. 3.7 and represent the mean and standard deviation of at least four independent measurements. Bacteria transformed with pET-41c, expressing the non-cytotoxic GST-Tag, were used as a control and grew exponentially over the 240 min period following induction. The expression of BTV NS3 had little effect on the growth rates of BL21(DE3)pLysS cells as cultures grew to almost the same levels as the control cells. Cells expressing AHSV and EEV NS3, however, showed a decrease in cell growth relative to the control. As a measure of these differences in cell growth the values at 4 hours post induction were calculated as a percentage of the control cell growth (100%) at this time. Percentage growth inhibition relative to the control was then calculated by subtracting these values from 100%. Bacteria expressing BTV NS3 showed a slight inhibition of 10% (±1.3) in cell growth relative to the growth of control cells at 4 hours post induction. Expression of AHSV NS3 was clearly inhibitory to cell growth with growth inhibited by 35% (±2.1). The effect of EEV NS3 was more profound, with cells expressing this protein displaying a decrease in growth of 71% (±1.9).

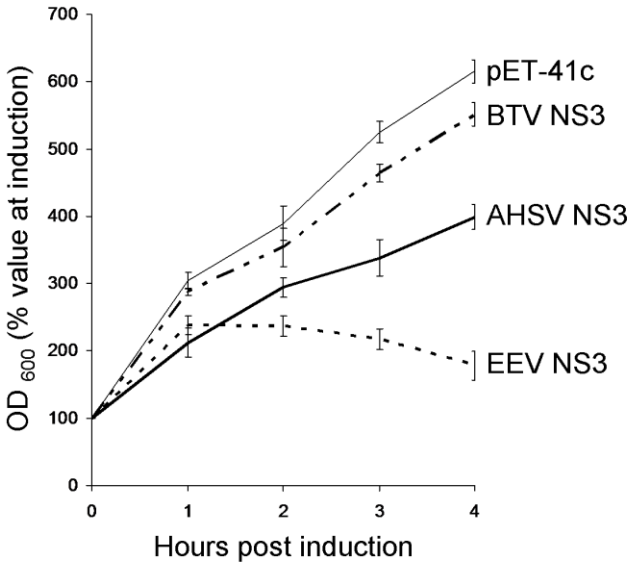

Fig. 3.7 Growth curves of bacterial cells transformed with pET-41 recombinants expressing orbiviral NS3 proteins. *E. coli* BL21(DE3)pLysS cells transformed with pET-41c (control) or recombinant pET-41 plasmids expressing AHSV NS3, BTV NS3 and EEV NS3 were IPTG induced. The OD_{600} of each culture was measured at the indicated times and expressed as a percentage of the value of that culture at induction.

In the BL21(DE3)pLysS strain disruption of the bacterial inner cell membrane results in release of T7 lysozyme by the cell and subsequent cell lysis. These cells contain an IPTG-inducible T7 RNA polymerase gene as well as the pLysS plasmid that constitutively expresses T7 phage lysozyme (Studier & Moffat, 1986; Studier, 1991). This intracellular lysozyme cannot degrade the cell wall peptidoglycan, as the bacterial membrane forms an impermeable barrier. If however the membrane is destabilised by recombinant proteins expressed in the cell, the lysozyme can pass into the periplasmic space and exert its lytic activity on the bacterial cell wall. It was therefore postulated that the expression of AHSV and EEV NS3 had a membrane destabilising effect on the *E. coli* cells, leading to cell lysis that was observed as decreased optical density of cultures.

3.3.2.4. Membrane permeability of E. coli *expressing AHSV, BTV and EEV NS3*

To determine if the observed cell growth arrest was actually the result of an increase in permeability of the bacterial inner membrane, a Hyg B membrane permeability assay was performed. Here protein translation in induced cultures is monitored by metabolic labelling in the presence and absence of Hyg B, a membrane impermeable translation inhibitor. BL21(DE3)pLysS cells transformed with recombinant pET-41 plasmids were therefore grown and induced for 30 min (see 3.2.2.6) then incubated in the presence or absence of Hyg B for a further 20 min and proteins synthesis in these cells monitored by metabolic labelling with [^{35}S] L-methionine for 45 min. Labelled proteins were then analysed by SDS-PAGE and phosphorimaging (Fig. 3.8). The amount of protein in each lane was estimated using Quantity One (BioRad) and the percentage permeabilised cells calculated as the protein expression levels in the presence of Hyg B over protein expression levels in absence of Hyg B x 100.

E. coli cells expressing GST (from the parent pET-41c vector) or BTV NS3 showed equivalent levels of protein translation in both the presence and absence of Hyg B (Fig. 3.8), with approximately 0% permeabilised cells. BTV NS3 expression in these cells did not, therefore, cause an increase in membrane permeability. This is in contrast to cells expressing AHSV NS3 and EEV NS3, in which a marked decrease in translation was observed in the presence of the membrane impermeable translation inhibitor (Fig. 3.8), and the percentage permeabilised cells was calculated to be 41% and 69%, respectively.

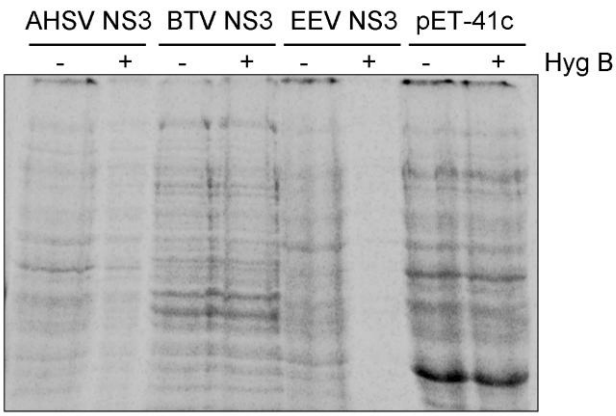

Fig. 3.8 Effects of orbiviral NS3 proteins on bacterial cell membrane permeability. *E. coli* BL21(DE3)pLysS cells transformed with pET-41c (control) or recombinant pET-41 plasmids expressing AHSV NS3, BTV NS3 and EEV NS3 were induced with IPTG. Cultures were then incubated in the presence (+) or absence (-) of Hyg B and proteins radiolabelled. Proteins were resolved by 12% SDS-PAGE and visualised by phosphorimaging.

The cytolytic effect of the AHSV and EEV NS3 proteins appeared therefore to be a consequence of increased membrane permeability. As the pET expression system proved to be a simple and rapid means of assessing the cytolytic and membrane permeabilising properties of proteins, we then used this system to clone and express a variety of truncated forms of AHSV NS3 to determine which domains within this protein are involved in these activities.

3.3.2. Expression of AHSV NS3 truncated mutants in *E. coli* cells

Previous studies of membrane permeabilising proteins have implicated a variety of domains within these proteins as being involved in this activity, directly or indirectly. Of particular importance are hydrophobic stretches within proteins that may form membrane-spanning domains that destabilise the membrane. In proteins with more than one hydrophobic domain, one or more of these regions may be critical for membrane permeabilisation. Other hydrophobic domains may not be directly involved in membrane destabilisation but necessary for membrane targeting of the protein. Amino acids adjacent to or outside of these regions may also be involved, and regions involved in oligomerisation, such as coiled-coil domains, may enhance permeabilisation activity (Arroyo *et al.*, 1995; Browne *et al.*, 2000; Ciccaglione *et al.*, 2001; Gonzalez & Carrasco, 2003). In this study a series of truncated versions of AHSV NS3 were therefore designed to target conserved regions within the protein that may have structural or functional importance (Fig. 3.9). Several conserved regions have been identified within AHSV NS3. These are illustrated, and their respective positions in the amino acid sequence indicated, in the schematic representation of AHSV NS3 in Fig. 3.9. The conserved regions include (i) an initiation codon (AUG) for NS3A, (ii) a proline-rich region (PRR), (iii) a highly conserved region (CR) that shows little sequence diversity across all serotypes of AHSV, and (iv) two hydrophobic domains HDI and HDII (Van Staden *et al.*, 1995; Van Niekerk *et al.*, 2001b; Quan *et al.*, 2008). A

putative coiled-coil (C-C) region (amino acids 93 to 115) that may mediate oligomerisation was also identified by Smit (1999).

The truncated mutants to be cloned and expressed in this study represented (i) the N-terminal region up to and including the CR (termed mutant A_{1-92}), (ii) the N-terminal region up to and including the C-C domain (A_{1-118}), (iii) the N-terminal region up to and including the HDI (A_{1-140}), (iv) the C-terminal region from HDII ($A_{151-218}$), (v) the C-terminal region including HDI and HDII ($A_{113-218}$), (vi) the C-terminal region from the C-C domain including HDI and HDII (A_{93-218}), (vii) the region spanning HDI and HDII ($A_{113-176}$) and (viii) the C-terminal from but not including HDII ($A_{176-218}$) (Fig. 3.9). Mutant proteins were named A_{x-y}, where A represents AHSV NS3 and x-y represents the amino acid region of AHSV NS3 present in the mutant. The following section describes the PCR amplification and cloning of the nucleotide regions of AHSV-2 NS3 gene coding for these truncated proteins for expression in *E. coli*.

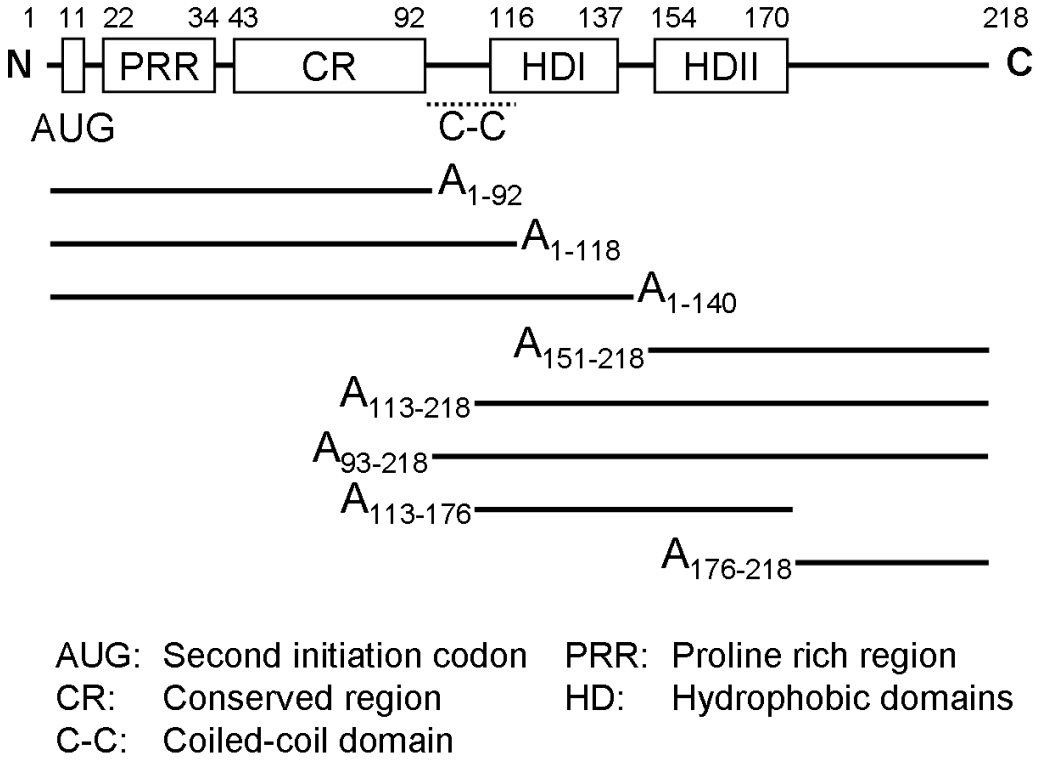

Fig. 3.9 Schematic representation of the AHSV NS3 and the AHSV NS3 truncated proteins designed for expression and analysis in *E. coli*.

3.3.2.1. Cloning of truncated mutants of the AHSV S10 gene into pET-41c

The regions of the AHSV-2 S10 gene encoding the various truncated mutants to be expressed in *E. coli* were amplified using the PCR conditions and primers given in section 3.2.2.1 and Table 3.1. PCR products were analysed by 2% agarose gel electrophoresis (Fig. 3.10). Amplicons were of the expected size. For the expression of amino acids 1-92 of AHSV NS3 (A_{1-92}) the

region from nucleotides 1 (start codon) to 276 of the AHSV S10 gene (nt 1-276) were amplified and a PCR product of the expected size of 299 bp obtained (Fig. 3.10 lane a). Similarly PCR products of the expected sizes of 375 bp for nt 1-354 (Fig. 3.10 lane b), 441 bp for nt 1-420 (Fig. 3.10 lane c), 216 bp for nt 337-528 (Fig. 3.10 lane d), 490 bp for nt 277-657 (Fig. 3.10 lane e), 430 bp for nt 337-657 (Fig. 3.10 lane f), 316 bp for nt 451-657 (Fig. 3.10 lane g) and 239 bp nt 526-657 (Fig. 3.10 lane j) were obtained. Amplicons include restriction enzyme sites from the primer sequences and, in the case of those amplified with the NS3pEco reverse primer, the 3' untranslated region of S10 and are therefore larger than the region they represent of the AHSV-2 S10 ORF. The amplification of nt 1-354 of AHSV-2 S10 yielded low amounts of product (Fig. 3.10 lane b) and the PCR was subsequently repeated with a lower primer annealing temperature which resulted in increased yields (results not shown). The final PCR conditions used for amplification are given in Table 3.1.

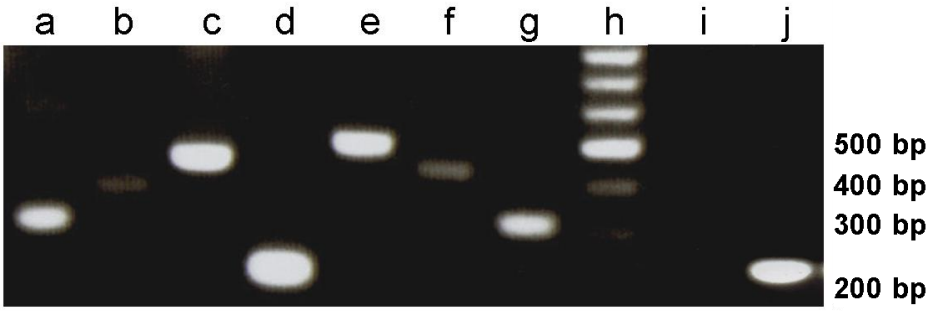

Fig. 3.10 Agarose gel electrophoretic analysis of the PCR amplification of various regions of the AHSV NS3 gene for cloning into pET-41. The following nucleotide regions of AHSV NS3 gene were amplified: 1-276 (a), 1-354 (b), 1-420 (c), 337-528 (d), 277-657 (e), 337-657 (f), 451-657 (g) and 526-657 (j). PCR products were analysed by 2% agarose gel electrophoresis, stained with ethidium bromide (EtBr) and visualised under an UV illuminator. Sizes of selected DNA fragments in the Promega 100 bp DNA ladder (h) are as indicated on the right. A negative control was included in which no template was added to the PCR reaction (i).

*Bam*HI and *Eco*RI, or *Nco*I and *Eco*RI, recognition sites were included in primers for cloning into these sites in the MCS of pET-41. After purification, PCR products were therefore ligated as *Bam*HI-*Eco*RI or *Nco*I-*Eco*RI inserts into appropriately digested pET-41a/c. Ligated plasmids were transformed into the non-expression hosts XL1 Blue or JM109. Insertion of the NS3 specific sequences was analysed by restriction digestion of recombinant plasmids with *Bam*HI and *Eco*RI or *Xba*I and *Eco*RI. Fig. 3.11 shows the *Xba*I and *Eco*RI double digestion of a putative pET-41 recombinant plasmid with nt 526-657 of S10 as an example of recombinant plasmid screening. Digestion of the non-recombinant parent pET-41a vector with these enzymes results in two linear DNA fragments of approximately 5036 bp (Fig. 3.11 lane b, upper band) and 897 bp (Fig. 3.11 lane b, lower band). Digestion of the putative pET-41 recombinant plasmid resulted in two DNA fragments of approximately 5036 bp (Fig. 3.11 lane c, upper band) and approximately 1130 bp (Fig. 3.11 lane c, lower band) as expected for a recombinant. The identity of the inserted sequences were confirmed by sequencing as described in 3.2.2.2. The recombinant pET-41

plasmids generated here contain the truncated versions of the S10 ORF downstream, and in-frame with, the GST-Tag encoding sequence and were named pET-GST-A_{x-y}, where A represents AHSV NS3 and x-y represents the amino acid region of AHSV NS3 encoded by the plasmid. These recombinant plasmids were used for the affinity purification of the N- and C-terminal regions of AHSV NS3 described later in this chapter.

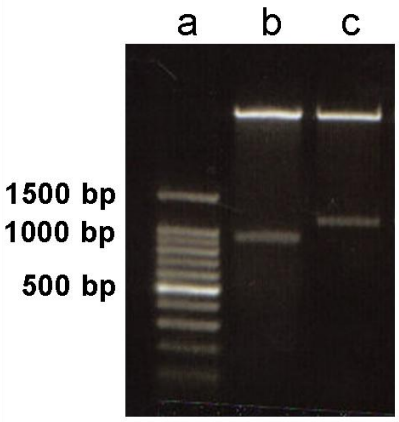

Fig. 3.11 Agarose gel electrophoretic analysis of *Xba*I and *Eco*RI digestion of pET-GST-$A_{176-218}$. pET-41c (b) and a putative pET-41-GST-$A_{176-218}$ recombinant plasmid (c) were digested with *Xba*I and *Eco*RI. Digestion products were analysed by 1% agarose gel electrophoresis, stained with ethidium bromide (EtBr) and visualised under an UV illuminator. DNA size marker was included in lane (a) and sizes of selected fragments are as indicated on the left.

Recombinant pET-41 plasmids expressing the same truncated versions of AHSV NS3 but without the GST-Tag were also generated. This was achieved by removing the GST-Tag coding sequence from the recombinant plasmids generated above by digestion with *Nde*I and religation as described in 3.2.2.2. Removal of the GST-Tag coding sequence in the resulting plasmids was confirmed by restriction digestion with *Xba*I and *Eco*RI. Recombinant plasmids that would express the truncated mutants of AHSV NS3 without the GST-Tag were named pET-A_{x-y}. Table 3.2 lists the pET-41 recombinant plasmids expressing truncated versions of AHSV-2 NS3 that were generated during this study.

Table 3.2 Recombinant pET-41 plasmids expressing truncated versions of AHSV-2 NS3

Recombinant plasmid name	**Region of S10 gene cloned (nt)***	**Region of NS3 protein encoded (aa)**	**NS3 domains[#]**
pET-A_{1-92}	1-276	1-92	N-PRR-CR
pET-A_{1-118}	1-354	1-118	N-PRR-CR-CC
pET-A_{1-140}	1-420	1-140	N-PRR-CR-CC-HDI
pET-A_{93-218}	277-657	93-218	CC-HDI-HDII-C
pET-$A_{113-218}$	337-657	113-218	HDI-HDII-C
pET-$A_{151-218}$	451-657	151-218	HDII-C
pET-$A_{113-176}$	337-528	113-176	HDI-HDII
pET-GST- A_{1-92}	1-276	1-92	N-PRR-CR
pET-GST-A_{1-118}	1-354	1-118	N-PRR-CR-CC
pET-GST-A_{1-140}	1-420	1-140	N-PRR-CR-CC-HDI
pET-GST-A_{93-218}	277-657	93-218	CC-HDI-HDII-C
pET-GST-$A_{113-218}$	337-657	113-218	HDI-HDII-C
pET-GST-$A_{151-218}$	451-657	151-218	HDII-C
pET-GST-$A_{113-176}$	337-528	113-176	HDI-HDII
pET-GST-$A_{176-218}$	526-657	176-218	C

* nucleotide numbering excludes the 5' untranslated region of S10, with position 1 indicating the first nucleotide (A) in the start codon of the NS3 gene
[#]N, N-terminal region; PRR, proline rich region; CR, conserved region; CC, coiled-coil domain; HDI, hydrophobic domain I; HDII, hydrophobic domain II; C, C-terminal region

3.3.2.2. Viability and membrane permeability of E. coli *expressing truncated AHSV NS3 variants*

As the full length AHSV NS3 protein was found to inhibit *E. coli* cell growth and to increase membrane permeability the analysis of truncated mutants of this protein would allow for the determination of regions critical to these effects. To compare the cytolytic and membrane permeabilising activities of the truncated AHSV NS3 proteins, these proteins were expressed, without the GST-Tag, in the expression host BL21(DE3)pLysS. For this purpose cultures of these cells were transformed with the recombinant plasmids (pET-A_{x-y}) generated above, grown and induced as described (3.2.2.4). Expression was then monitored by metabolic labelling in the presence of rifampicin as previously described for the full length orbiviral NS3 protein. Whole cell lysates were subjected to SDS-PAGE and labelled proteins detected by phosphorimaging (Fig. 3.12). Expression levels varied considerably, with NS3 variants lacking the HDs (A_{1-92} (9.8 kDa) and A_{1-118} (12.7 kDa)) expressed to much higher levels than the full length NS3 proteins or other truncated mutants that contained either one or both of the HDs of NS3. Low level expression was observed for mutants A_{1-140} (14.9 kDa), $A_{151-218}$ (7.3 kDa) and A_{93-218} (13.9 kDa), while expression of mutants $A_{113-218}$ (11 kDa) and $A_{113-176}$ (6.6 kDa) could not be detected at all.

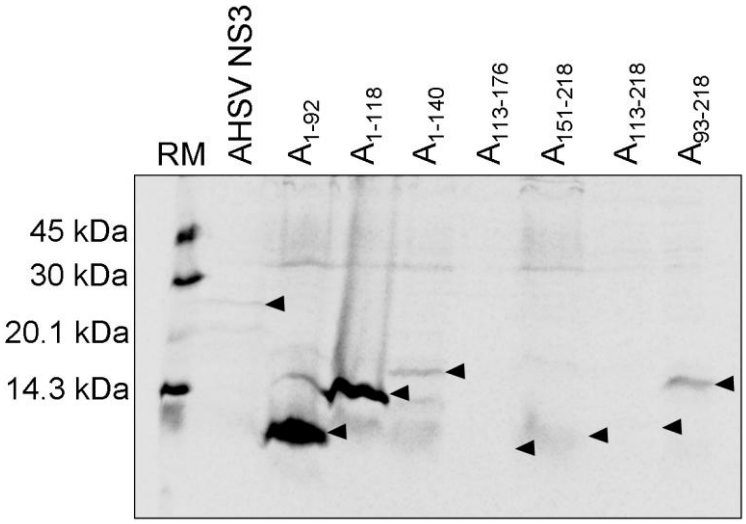

Fig. 3.12 Expression of AHSV NS3 and truncated mutants in *E. coli*. Bacterial cultures were induced with IPTG and radiolabelled in the presence of Rifampicin. Proteins were separated by 20% SDS-PAGE and detected by phosphorimaging. The arrows indicate the expected positions of the full length NS3 protein or truncated mutants in their respective lanes. Sizes of molecular weight markers are as indicated on the left.

The cytotoxicity of the truncated NS3 proteins was then analysed by monitoring cell density of induced recombinant cultures at OD_{600} at various times post-induction (Fig. 3.13). The expression of mutants A_{1-92} and A_{1-118} did not inhibit cellular growth relative to the pET-41 control. Mutants A_{1-140} and $A_{151-218}$, which contained either HDI or HDII respectively, also had little to no effect on cell growth. In contrast, expression of mutants A_{93-218}, $A_{113-218}$ and $A_{113-176}$, which contain both HDs of AHSV NS3, caused a rapid decline in cell growth (Fig. 3.13). The inhibitory effect of these mutants on cell growth (71±3.1, 92±2.5 and 83±3.5%, respectively) was greater than that

observed for the full length AHSV NS3 protein (35±2.1%). The difference in toxicity of $A_{113-218}$ and $A_{113-176}$ also suggests that the C-terminal region indirectly enhances the lytic effect. Nonetheless, it is clear from these results that the two hydrophobic domains of AHSV NS3 are responsible for cytotoxicity.

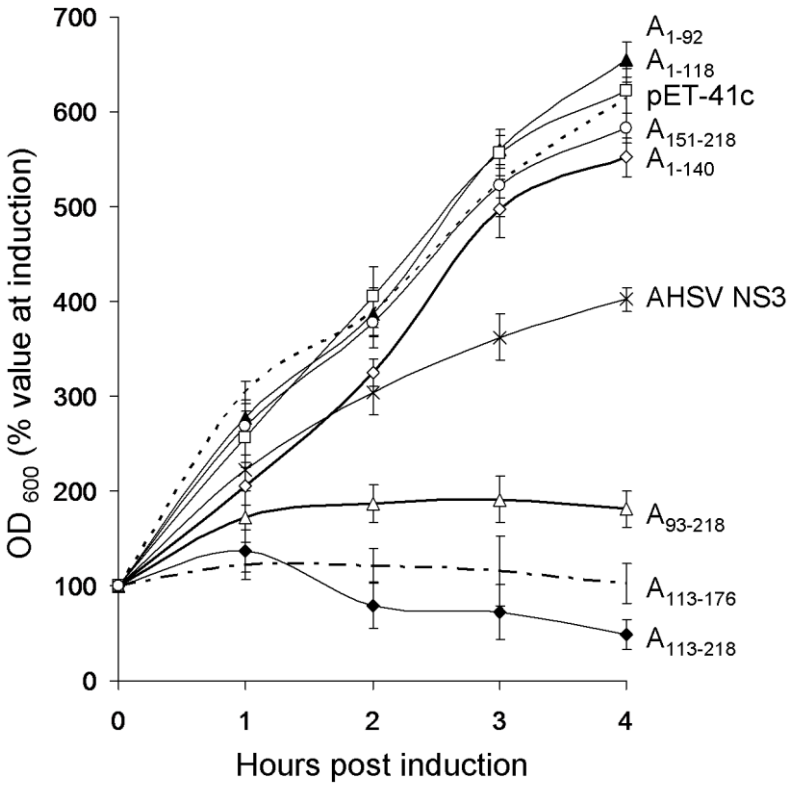

Fig. 3.13 Effect of AHSV truncated mutants on bacterial cell growth. *E. coli* BL21(DE3)pLysS cells transformed with pET-41c (control) or recombinant pET-41 plasmids expressing full length or truncated AHSV NS3 proteins were induced with IPTG. The OD_{600} of each culture was then measured at the indicated times and expressed as a percentage of the value of that culture at induction.

Hyg B assays were again used to confirm whether the lytic or non-lytic activity of the truncated mutants was related to their ability to increase membrane permeability. The results for selected truncated mutants are shown in Fig. 3.14. Expression of the noncytotoxic proteins or peptides GST (not shown) and A_{1-118} did not adversely affect translation in the presence of Hyg B, with similar translation levels in the presence and absence of the membrane impermeant antibiotic. In contrast, translation in *E. coli* cells expressing the cytotoxic peptides $A_{113-218}$ and A_{93-218} was almost completely inhibited in the presence of Hyg B. The percentage permeabilised cells was calculated to be 82% and 62%, respectively.

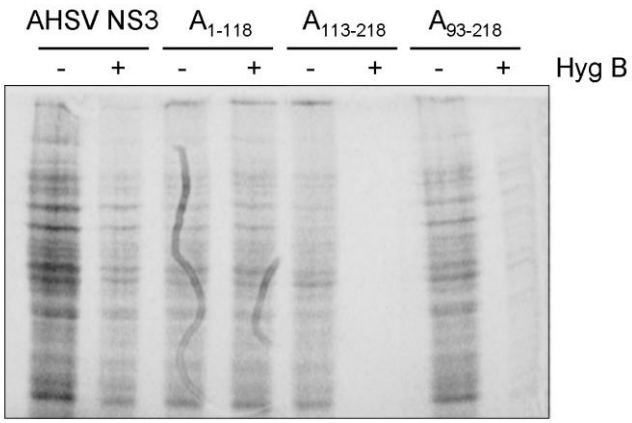

Fig. 3.14 Effect of AHSV-2 NS3 and truncated mutants on bacterial membrane permeability. BL21(DE3)pLysS cells carrying recombinant pET-41 plasmids expressing AHSV-2 NS3 or the indicated truncated versions were induced. Proteins were metabolically labelled with [^{35}S] L-methionine in the absence (-) or presence (+) of Hyg B. Proteins were resolved by 12% SDS-PAGE and visualised by phosphorimaging.

A summary of the results obtained from the analysis of the expression, cytotoxicity and membrane permeabilising activity of full length and truncated NS3 proteins is given in Table 3.3.

As an additional measure of *E. coli* cell membrane permeability, a β-galactosidase membrane permeability assay was performed. This assay has been extensively used to monitor the membrane permeabilisation activity of viral proteins expressed in *E. coli* (Guinea & Carrasco, 1994; Lama & Carrasco, 1995; Ciccaglione *et al.*, 1998; Dowling *et al.*, 2000). ONPG is a substrate of β-galactosidase and in the presence of this enzyme is hydrolysed to free *o*-nitrophenol, a coloured product that absorbs light at 420nm wavelength (Sambrook & Russell, 2001). ONPG is normally excluded by the membranes of intact cells. ONPG hydrolysis to *o*-nitrophenol by *E. coli* β-galactosidase therefore only occurs in permeabilised cells. The appearance of *o*-nitrophenol at OD_{420} is therefore a measure of membrane permeabilisation. BL21(DE3)pLyS cells expressing the full length orbiviral NS3 proteins and the truncated AHSV NS3 proteins were induced. At 4 h post induction samples were removed, the cells resuspended in fresh medium and incubated in the presence of ONPG (3.2.2.7). The appearance of ONPG cleavage product was then quantified by measuring the OD_{420}. These values were then expressed relative to cell density for each culture (OD_{600}). The ratio of ONPG cleavage (OD_{420}) to the optical density of cultures (OD_{600}) for each recombinant is shown in Table 3.2. Expression of BTV NS3 and the truncated AHSV NS3 mutants A_{1-92}, A_{1-118}, A_{1-140} and $A_{151-218}$ did not increase ONPG entry into cells (with values of 0.12±0.03, 0.18±0.03, 0.07±0.04 and 0.08±0.05, respectively) indicating that these proteins are not permeabilising to the bacterial membrane. Expression of full length EEV and AHSV NS3, as well as the truncated AHSV NS3 mutants A_{93-218}, $A_{113-218}$ and $A_{113-176}$, resulted in a clear increase in the level of ONPG entry into cells (with values of 0.54±0.04, 0.36±0.04, 0.73±0.04, 1.4 ±0.16 and 1.13±0.06, respectively). Therefore the

influx of ONPG through the membrane agrees well with the uptake of Hyg B observed previously; with cultures expressing cytolytic proteins or peptides showing an increased uptake of these compounds in comparison to non-cytolytic proteins. This confirms our finding that the cytolytic activity of these proteins is a result of increased membrane permeability, and that the presence of both HDs is required for this activity.

Table 3.3 Summary of results from the expression of orbiviral NS3 proteins and mutants in *E. coli*

	NS3 domains	**Expression levels***	**% Growth inhibition (SD)**	**% Permeabilised cells**	**ONPG cleavage/OD_{600} (SD)**
AHSV NS3	Full length	+	35 (±2.1)	41	0.36 (±0.04)
A_{1-92}	N-PRR-CR	+++	0 (±3.0)	ND	0.12 (±0.03)
A_{1-118}	N-PRR-CR-CC	+++	0 (±3.8)	6	0.18 (±0.03)
A_{1-140}	N-PRR-CR-CC-HDI	+	10 (±3.2)	ND	0.07 (±0.04)
A_{93-218}	CC-HDI-HDII-C	+	71 (±3.1)	62	0.73 (± 0.04)
$A_{113-218}$	HDI-HDII-C	-	92 (±2.5)	82	1.4 (±0.16)
$A_{151-218}$	HDII-C	+	5 (±2.5)	ND	0.08 (±0.05)
$A_{113-176}$	HDI-HDII	-	83 (±3.5)	ND	1.13 (±0.06)
EEV NS3	Full length	+	71 (±1.9)	69	0.54 (±0.04)
BTV NS3	Full length	+	10 (± 1.3)	0	0.0 (±0.04)

* +++ indicates proteins expressed to high levels, + low level expression, and – expression at undetectable levels
ND, Not determined
SD, Standard deviation

3.3.2.3. Expression and purification of N- and C-terminal regions of AHSV-2 NS3

In the following section the pET recombinants expressing AHSV NS3 truncated mutants as GST-Tag fusions were investigated as to their suitability for the purification of domains of AHSV NS3. In particular, proteins representing the N- and C-terminal regions of NS3 were required for their use in the production of monospecific antibodies in chapter 4.

Investigations of membrane proteins are often hindered by the difficulties encountered during purification of these proteins, including their insolubility in aqueous buffers and their instability in the absence of lipid bilayers, which are probably due to their hydrophobic nature. Sufficient quantities of protein are therefore not generally obtained for further characterisation (Bechinger, 2008). These problems are further compounded when dealing with a cytotoxic membrane protein that is expressed to low levels. It was therefore argued that removal of the hydrophobic domains of AHSV NS3 would result in soluble non-cytotoxic proteins that would be expressed to high levels and therefore suitable for purification.

Four proteins (GST-A_{1-92}, GST-A_{1-118}, GST-$A_{151-218}$, GST-$A_{176-218}$) representing the terminal regions of AHSV-2 NS3 fused to GST were expressed and analysed in terms of their suitability for purification, i.e. expression levels and solubility. BL21(DE3) cells were transformed with pET-41 recombinant plasmids expressing these fusion proteins (see Table 3.2), induced and culture samples taken every 30 min for 2 h. Proteins were separated by denaturing SDS-PAGE and stained with Coomassie blue (Fig. 3.15).

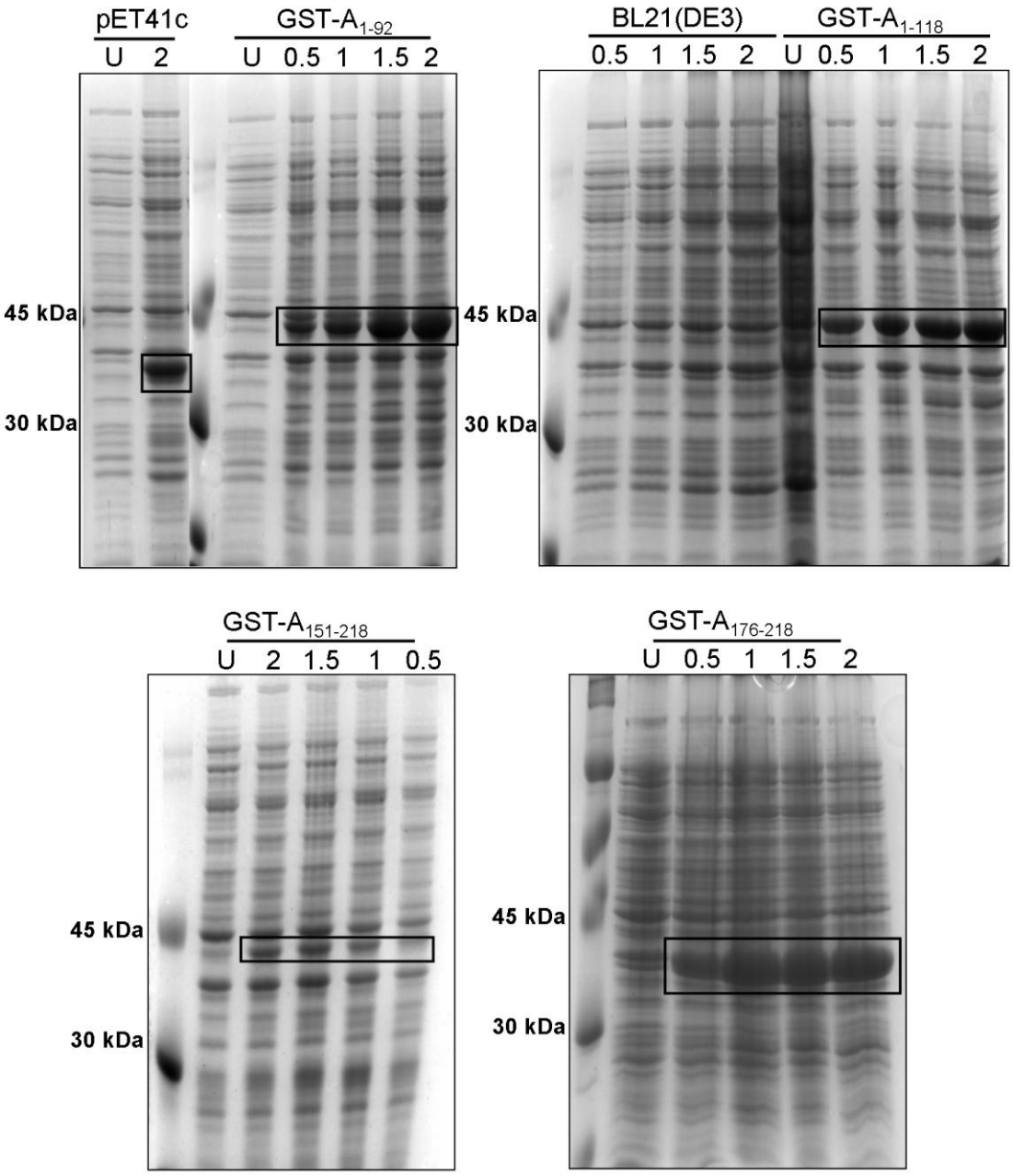

Fig. 3.15 SDS-PAGE analysis of the expression of the N- and C-terminal regions of AHSV-2 NS3 as GST fusion proteins. Samples of untransformed BL21(DE3) cultures, or cultures transformed with non-recombinant pET-41c expressing GST or recombinant pET-41c expressing GST-NS3 fusion proteins were removed at 0.5, 1, 1.5 and 2 h post induction. Proteins were separated by 12% SDS-PAGE and stained with Coomassie blue. U (uninduced) represents samples taken prior to induction and were included as negative controls. The GST protein and GST-NS3 fusion proteins are indicated by blocks in their respective lanes. Sizes of molecular weight markers are as indicated on the left.

A unique protein band of the expected sizes of 35.6 kDa for the GST-Tag (expressed from pET-41c), 45.4 kDa for GST A_{1-92}, 48.3 kDa for GST-A_{1-118}, 42.9 for GST-$A_{151-218}$ and 40.6 kDa for GST-$A_{176-218}$, was observed from 30 min post induction (Fig. 3.15). As previously observed (3.3.2.2) proteins without HDs (GST A_{1-92}, GST A_{1-118} and GST $A_{176-218}$) were expressed to high levels, while proteins containing hydrophobic stretches (GST $A_{151-218}$) were expressed to low levels.

The solubility of the GST-NS3 fusion proteins was analysed by separating total cell lysates (T) of induced cultures into soluble (S) and particulate (P) components by centrifugation (Fig. 3.16). Under the conditions used (3.2.2.8a), GST-A_{1-92} and GST-$A_{176-218}$ were found to be present in approximately equivalent amounts in the soluble and particulate fractions (50% soluble). GST-A_{1-118} and GST-$A_{151-218}$ were present almost exclusively in the particulate fractions. The insolubility of these proteins may be due to the presence of the coiled-coil domain in GST-A_{1-118} and HDII in GST-$A_{151-218}$. The fusion proteins GST-A_{1-92} and GST-$A_{176-218}$ were therefore expressed to high levels in soluble forms and were suitable for use in affinity purification.

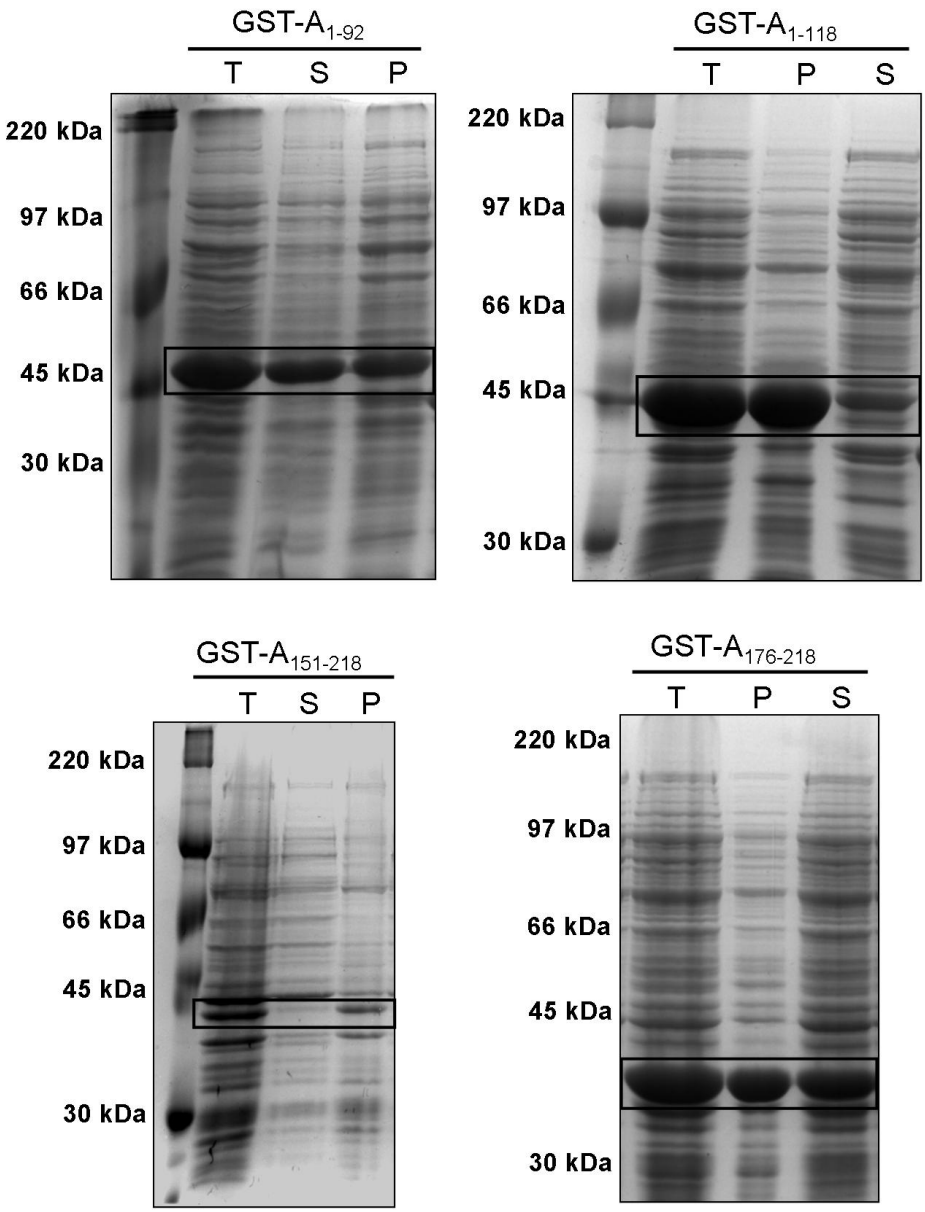

Fig. 3.16 PAGE analysis of the solubility of the GST-NS3 fusion proteins expressed in *E. coli*. Induced BL21(DE3) cultures transformed with recombinant pET-41c plasmids expressing GST-NS3 fusion proteins were lysed (Total fraction, T) and separated into soluble (S) and particulate (P) fractions by centrifugation. Proteins in the fractions were separated by SDS-PAGE and stained with Coomassie blue. The GST fusion proteins are indicated by blocks in their respective lanes. Sizes of molecular weight markers are as indicated on the left.

BL21(DE3) cells transformed with pET-41 recombinants expressing GST-A_{1-92} and GST-$A_{176-218}$ were induced, lysed and separated into soluble and particulate fractions. The soluble fractions were mixed with glutathione-coupled agarose and proteins purified as described in 3.2.2.8b. The GST-Tag in these fusion proteins was allowed to bind to its substrate, glutathione, and unbound proteins removed by washing. The NS3 N-terminal (A_{1-92}; 15 kDa), and C-terminal ($A_{176-218}$; 11 kDa) peptides were then cleaved from the GST-Tag by digestion with thrombin, which has a cleavage site between the GST and NS3 proteins (see Fig. 3.1). Cleavage released the truncated soluble NS3 proteins into the supernatant (Fig. 3.17A lanes b and c; Fig. 3.17B lanes b and d), while the GST protein remained bound to the glutathione agarose (Fig. 3.17A lane e).

Thrombin remained in the supernatant and is indicated in Fig. 3.17A. The amount of purified protein was estimated by comparison to standard molecular weight markers and sufficient protein was produced for eliciting an immune response against the terminal regions of AHSV-2 NS3 in the following chapter. Note that in addition to a GST-Tag the pET-41 vector encodes a S-tag (see Fig. 3.1) that was not cleaved from the NS3 proteins by thrombin.

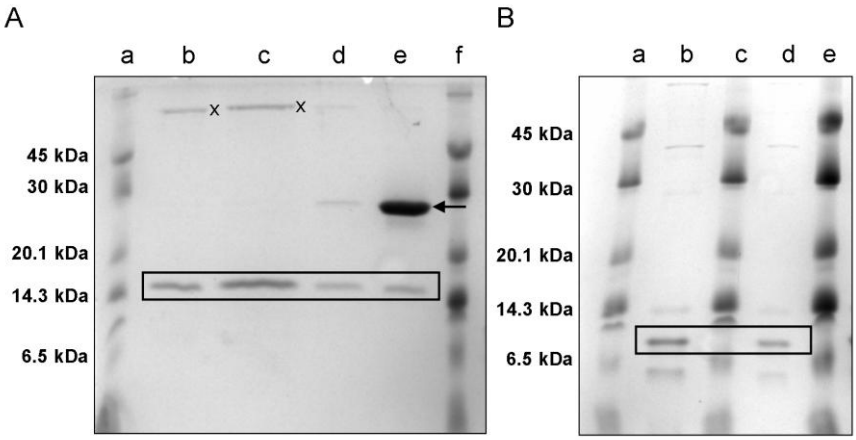

Fig. 3.17 Analysis of the purified N-terminal (A_{1-92}) (A) and C-terminal ($A_{176-218}$) regions (B) of AHSV-2 NS3. In (A) 1/100 (b) and 1/50 (c) of the purified N-terminal NS3 sample was compared to 0.5 µl (a) and 1.0 µl (f) molecular weight marker (1 µg/µl). Lane (d) represents the wash step following thrombin digestion and (e) the glutathione agarose resin to which the GST protein remains bound following thrombin cleavage. In (B) 0.5 (a), 1.0 (c) and 2.0 (e) µl of molecular weight marker (1 µg/µl) were compared to 1/100 (b) and 1/200 (d) of the purified C-terminal NS3 protein sample. Proteins were separated by 18% SDS-PAGE at 80-90V and stained with Coomassie blue. The positions of the truncated NS3 (blocks), thrombin (x) and GST (arrow) proteins are indicated. Sizes of molecular weight markers are as indicated on the left.

3.4. DISCUSSION

The pathogenesis of BTV, AHSV and EEV has been well characterised on a clinical level (Burrage & Laegried, 1994; MacLachlan, 1994; Skowronek *et al.*, 1995), yet the molecular basis of orbivirus virulence and pathogenesis is not well understood and thought to be complex and multifactorial (Laegreid *et al.*, 1993; O'Hara *et al.*, 1998). Prominent pathological features of orbiviral diseases include oedema, effusion and haemorrhage, indicative of a loss in endothelial cell barrier function. Alteration of membrane permeability is a common feature of infection by cytolytic animal viruses (Carrasco, 1995) resulting in drastic changes in the metabolism of infected cells and contributing to the development of the cytopathic effect. Proteins that affect membrane permeability are therefore of particular importance in determining virus virulence.

In this chapter the cytolytic and membrane permeabilising activities of the NS3 proteins of three different orbiviruses were compared in both insect (Sf9) and *E. coli* cells. In addition to this, the regions within AHSV NS3 responsible for membrane destabilisation in *E. coli* were identified.

Expression of AHSV, EEV and BTV NS3 as baculovirus recombinants in insect cells caused a marked decline in cell viability, with all three proteins causing similar levels of cytotoxicity at 48 h p.i. This confirms previous reports of viroporin-like activity for AHSV and BTV NS3 (Van Niekerk *et al.*, 2001a; Han & Harty, 2004). The EEV NS3 protein, furthermore, has many of the shared characteristics found in viroporins, in that it is a small virally encoded membrane-associated protein with two hydrophobic domains. This suggests that EEV NS3 has viroporin-like activity. This activity is thought to result in not only the efficient release of viral particles from infected cells but may also contribute to viral pathogenesis and cytopathic effects in infected cells.

Expression of the orbivirus NS3 proteins in bacterial cells showed significant differences in their cytolytic and membrane permeabilising activity. Both AHSV and EEV NS3 inhibited cell growth in *E. coli,* with EEV NS3 having the greatest inhibitory effect on these cells. Expression of these proteins permeabilised the membrane to Hyg B and ONPG. Both EEV NS3 and AHSV NS3 are therefore cytotoxic to *E. coli*, and this lytic effect is a result of increased membrane permeability. BTV NS3 had little to no effect on *E. coli* cell growth and membrane permeability. This appears to be in contrast to our finding that the protein is cytotoxic to insect cells, and previous reports where BTV NS3 was shown to increase the permeability of COS-1 cells to Hyg B (Han & Harty, 2004). There are a number of factors that may affect the outcome of studies of the cytolytic properties of proteins in different cell systems, including the membrane composition of the cells, stability of the membrane-association of the protein in that system, and post-translation modifications. Many viroporins have been shown to permeabilise both bacterial and mammalian cells, while other viroporins such as picornavirus 3A perturbs bacterial but not BHK-21 or HeLa cell membranes

(Madan *et al.*, 2008). The lipid composition of the bacterial inner membrane differs significantly from the plasma membrane of mammalian and insect cells, for example very low levels of cholesterol are found in the bacterial and ER membrane whereas this is a major component of the membrane of mammalian cells. It is therefore not surprising that the results from cytotoxicity and permeability studies in different cell lines may vary. NSP4 of rotavirus, for example, preferentially interacts with membranes that are rich in both cholesterol and negatively charged phospholipids (Huang *et al.*, 2001). BTV NS3 is furthermore a glycosylated protein (Wu *et al.*, 1992), where glycosylation may prevent the protein from being degraded (Bansal *et al.*, 1998). The absence of this glycosylation in *E. coli* may therefore lead to decreased stability and functionality of BTV NS3 in *E. coli* cells. There is no evidence that either AHSV or EEV NS3 exist in a glycosylated form and indeed NS3 from some serotypes of AHSV lack glycosylation sequence motifs (Van Niekerk *et al.*, 2001a). As both EEV and AHSV NS3 were cytotoxic in *E. coli*, glycosylation does not appear to play any role in the activity and stability of these proteins.

Using the pET prokaryotic expression system, there are therefore distinct differences between the effects of NS3 from BTV, AHSV and EEV. Although these effects can not be directly extrapolated or linked to the effect these proteins have on eukaryotic cells or to the diseases caused by the respective viruses, it provides evidence for structural and/or functional differences between these proteins.

To investigate the regions of AHSV NS3 that directly mediate cytotoxicity, and that play a role in structural stability, we constructed a variety of truncated mutants of the protein. These truncated mutants were also expressed and analysed in the pET expression system.

Expression levels of truncated mutants varied considerably, with peptides lacking the hydrophobic domains ($A_{1\text{-}92}$ and $A_{1\text{-}118}$) expressed to much higher levels than the full length NS3 and other truncated mutants. Truncated mutants without the HDs, representing the N- and C-termini of NS3, were therefore expressed as GST-Tag fusion proteins (GST-$A_{1\text{-}92}$ and GST-$A_{176\text{-}218}$) and found to be expressed to high levels in soluble forms. This facilitated the affinity purification of these peptides for later use in the production of monospecific antibodies to these regions of NS3. Low expression levels were observed for the peptides that contain only one of the AHSV hydrophobic domains, $A_{1\text{-}140}$ and $A_{151\text{-}218}$. As these proteins were found not to be lytic to cells, the explanation for the low levels of synthesis of these peptides is unclear. Expression of the $A_{151\text{-}218}$ truncated mutant as a GST-Tag fusion protein also showed low levels of synthesis of the recombinant protein. Similar inexplicably low level expression was observed for non-lytic fragments of HIV gp41 (Arroyo *et al.*, 1995) and rotavirus NSP4 (Browne *et al.*, 2000) in *E. coli*. In the case of rotavirus NSP4, peptides representing the soluble regions of the cytoplasmic domains were expressed to high levels, and those containing hydrophobic domains expressed to

low levels (Browne *et al.*, 2000). In our case, low level expression was also observed for $A_{93\text{-}218}$, while no expression of the $A_{113\text{-}218}$ and $A_{113\text{-}176}$ proteins could be observed. This was probably linked to the highly lytic effect of these proteins.

AHSV mutants lacking both HDs, or containing either HDI or HDII, did not inhibit cell growth and did not increase the uptake of Hyg B or ONPG. These truncated mutants were therefore not cytotoxic and had no membrane permeabilising activity. In contrast, truncated mutants containing both HDs had a severe negative effect on cell viability and greatly increased the uptake of the membrane impermeant Hyg B and ONPG. These proteins were therefore highly toxic to *E. coli* and this is probably linked to their ability to permeabilise the membrane of these cells. Interestingly, the cytolytic and membrane permeabilising effects of these mutants was greater than that observed for the full length protein. Browne and coworkers (2000) report a similar finding when expressing truncated peptides of rotavirus NSP4 in *E. coli*, with cytolytic truncated peptides displaying a more potent lytic and membrane destabilising effect than the full length protein.

Previous studies of AHSV NS3 in insect cells have implicated both HDs within the protein as mediating cytotoxicity while studies of BTV NS3 found only one of the HDs to be critical. Substitution mutational analysis of AHSV NS3 indicated that the cytolytic activity was dependant on the integrity of the two hydrophobic domains within the protein (Van Niekerk *et al.*, 2001a). Disruption of either hydrophobic domain prevented the membrane anchoring of NS3 in an *in vitro* system, suggesting that the cytotoxicity of AHSV NS3 was dependant on the correct membrane insertion and topography. In contrast, in a study by Han & Harty (2004), mutation of HDI of BTV NS3 abolished the protein's membrane permeabilising activity, while mutation of HDII had no effect. Predictions of transmembrane (TM) regions using the TMHMM (TransMembrane prediction using a Hidden Markov Model) program (Krogh *et al.*, 2001) indicated that that both HDs within BTV-4, AHSV-2 and EEV-1 NS3 would form TM regions. For EEV NS3, both HDI and HDII have a high probability (1.0) of forming TM regions. In AHSV and BTV NS3, HDI has a probability of 1.0 to form a TM region, whereas HDII has a probability of only 0.3 and 0.8 respectively. This may suggest that there are different conformational constraints within these proteins that may affect membrane insertion and stability within the membrane.

In a mutagenesis study of the 2B viroporin of coxsackievirus it was shown that either of the two predicted transmembrane domains within this protein could mediate membrane binding, but that the presence of both these domains was necessary for membrane permeabilising activity in mammalian cells (De Jong *et al.*, 2003). In a follow up study a library of soluble overlapping peptides that spanned the complete 2B sequence were synthesised and assayed for their ability to permeabilise cultured cells following extracellular addition. Here it was shown that a peptide

corresponding to only one of the transmembrane domains (TM1) could effectively permeabilise the cell membrane of BHK-21 cells but its addition to bacteria did not affect growth of these cells (Madan *et al.*, 2007). In a similar peptide-based assay it was shown that the 2B viroporin requires the cooperation of both transmembrane domains for insertion into, and destabilisation of, bacterial membranes (Sánchez-Martínez *et al.*, 2008). They suggest that differences could be due to the differences in charge and phospholipids content of the target membranes used in the various assays. In bacterial membranes, and the lipid bilayers surrounding organelles, the cytolytic activity of TM1 requires the cooperation of the second transmembrane domain, possibly for translocation of TM1 across the bilayer.

In this study cytotoxicity was also found to be affected by other regions within the AHSV NS3 protein not directly involved in or responsible for this activity. Truncation of the C-terminal region of AHSV NS3 was found to cause a decrease in the membrane permeabilising activity, suggesting that this region may have a stabilising effect. Removal of the N-terminal region, in contrast, resulted in enhanced cytotoxicity and membrane permeabilisation. Destabilisation of the membrane therefore involves both disruption of the lipid bilayer and maintaining a stable integration into the membrane.

The different orbiviral NS3 primary sequences have a similar predicted secondary structure with two hydrophobic domains, proposed to oligomerise and span the membrane twice with the N- and C- termini in the cytoplasm. We have demonstrated here that these proteins do however vary in terms of which regions are important in interactions with and destabilisation of membranes from different cell lines. From our data we propose that the mechanisms used by the NS3 proteins to fulfil these functions are not necessarily exactly the same for the orbiviruses studied.

In chapter 2 it was shown that the NS3 protein plays a central role in determining the membrane permeabilising and release characteristics of the virus. In this chapter it was shown that AHSV NS3 when expressed as a recombinant has membrane permeabilising activity. Differences in the membrane permeabilising and release characteristics of the AHSV-2, -3 and -4 viruses may depend on the variation within their encoded NS3 proteins. In the following chapter AHSV-2, AHSV-3 and AHSV-4 NS3 were therefore recombinantly expressed and compared.

CHAPTER 4: COMPARISON OF THE NS3 PROTEINS OF AHSV-2, AHSV-3 AND AHSV-4

4.1. INTRODUCTION

In chapter 2 it was shown that viruses (AHSV-2, AHSV-3 and AHSV-4) encoding NS3 proteins from the three different phylogenetic clades (γ, β, and α, respectively) permeabilised Vero cell membranes to Hygromycin B to different extents. These viruses also differed in their release and cytopathic effect on cells. AHSV-2 infection of Vero cells resulted in the most severe cytopathic effect, with the highest amounts of membrane permeabilisation and viral release when compared to the other viruses. Using reassortants, it was shown that while NS3 was not the exclusive determinant of the cytopathic effects of the virus, it was possibly involved in this together with the non-structural NS1 protein. The membrane permeabilising and release properties of AHSV-2 however showed clear segregation to reassortants encoding the AHSV-2 NS3 protein. The membrane permeabilising effect of the virus could therefore be related to the encoded NS3 protein.

Sequence variation between NS3 of AHSV-2, AHSV-3 and AHSV-4, that impacts on the structure and functioning of these proteins, may therefore be important in determining the differences observed in the parental viruses. As the amino acid sequence variation between the α, β and γ NS3 proteins is high (34.7% between AHSV-2 and AHSV-3 and 35.2% between AHSV-2 and AHSV-4, for example) it was impossible to identify specific amino acid differences that may impact on this. We therefore set out to firstly determine if NS3 had membrane permeabilising activity when expressed alone as a recombinant protein and, secondly to identify domains within the protein that mediated this activity. For this purpose the inducible prokaryotic pET expression system was used and recombinant expression of AHSV-2 NS3 in *E. coli* showed that this protein had membrane destabilising activity (see chapter 3). This is then probably the basis for the cytotoxicity observed when NS3 was expressed in insect cells (Van Staden *et al.*, 1995; Van Niekerk *et al.*, 2001a).

In a study by van Niekerk *et al.* (2001a) substitution mutation of the HDs of NS3, in which the hydrophobic nature was altered by replacement of nonpolar residues with charged residues, significantly reduced the cytotoxic effect of the protein and prevented localisation to the outer plasma membrane of Sf9 cells. The ability of these mutants to associate with membranes was then analysed using *in vitro* translation in the presence of microsomal membranes, followed by treatment with a variety of buffers. Mutants were shown not to be stably integrated or anchored in these membranes. The cytotoxicity of NS3 was therefore shown to be dependant on membrane association of the protein, mediated by the two hydrophobic domains. This study did not exclude the possibility that, following correct membrane association and targeting to the outer membrane, other regions within the protein could mediate the cytotoxic effect. In chapter 3 a panel of truncated mutants of AHSV-2 NS3 was therefore constructed and expressed in bacterial

cells. The membrane permeabilising activity of NS3 could be directly linked to the two hydrophobic domains within the protein, and both domains were required for this activity. Differences in the hydrophobic domains between AHSV-2, AHSV-3 and AHSV-4 NS3, that impact on their association with membranes, membrane topology and subcellular localisation, may therefore directly or indirectly impact on their membrane permeabilising effect and cytotoxicity.

In this chapter we therefore set out to compare the AHSV-2, AHSV-3 and AHSV-4 (or α, β and γ) NS3 proteins. The proteins were initially analysed using several computer programs to predict whether amino acid sequence variation potentially impacted on various properties of the protein, such as the ability of the HDs to form transmembrane regions, the topology of the proteins in the membrane and the localisation of the proteins within the cell. The proteins were then recombinantly expressed in insect cells, using the baculovirus expression system, as both wild-type recombinant proteins and as eGFP fusion proteins. The membrane permeabilising activity, cytotoxicity, membrane association, membrane topology and localisation of these proteins was then examined for potential differences.

4.2. MATERIALS AND METHODS

4.2.1. AHSV-2, AHSV-3 and AHSV-4 NS3 sequence analysis and computational comparison

The AHSV-2 (82/61), AHSV-3 (M322/97) and AHSV-4 (HS39/97) NS3 amino acid sequences were aligned using AlignX (Vector NTi, Invitrogen) and the percentage sequence identity for conserved regions calculated. Transmembrane regions were predicted using a TMHMM (TransMembrane prediction using a Hidden Markov Model) transmembrane prediction program (http://www.cbs.dtu.dk/services/TMHMM-2.0/ (Krogh *et al.*, 2001)). The presence of potential nuclear localisation signals (NLS) was analysed using PredictNLS online (http://cubic.bioc.columbia.edu/predictNLS/ (Cokol *et al.*, 2000)).

4.2.2. Expression of AHSV-2, AHSV-3 and AHSV-4 NS3 in Sf9 cells

Recombinant baculoviruses expressing NS3 of AHSV-2, AHSV-3 or AHSV-4 were available and have been described previously (3.2.1.1.). Recombinant baculoviruses expressing NS3 of AHSV-3 (Van Staden *et al.*, 1995) and NS3 of AHSV-3 fused to the amino terminal of eGFP (Hatherell, 2007) were available. For the expression of AHSV-2 and AHSV-4 NS3 as eGFP fusion proteins the NS3 genes were cloned into a pFastBac1 baculovirus expression vector containing the eGFP coding sequence and recombinant baculoviruses generated as described in the following section.

4.2.2.1. Cloning of AHSV-2 and AHSV-4 NS3 as eGFP fusions in the BAC-TO-BAC™ expression system

4.2.2.1a. Cloning S10 of AHSV-2 and AHSV-4 into pFastBac1-eGFP

The AHSV-2 and -4 NS3 genes were PCR amplified from cDNA copies cloned into pCMVScript (from J. Korsman and M. van Niekerk, UP, respectively). In both cases the forward primer NS3pBam (5' CGGGATCCGTTTAAATTATCCCTTG) was used and included a *Bam*HI restriction site. The reverse primers P11G9 (5' CGGAATTCGTCTCCATATTTTACATC3') and P11G8 (5' CGGAATTCGCTCTCGCCATACTTAATTC3') specific to the 3' end of the NS3 genes of AHSV-2 and AHSV-4, respectively, included an *Eco*RI restriction site and were designed to remove the stop codon, as the NS3 genes were to be cloned upstream of an eGFP gene. PCR reactions were setup as described in 2.2.3.2. and reaction conditions were: one cycle of 2 min at 94°C, followed by 35 cycles of 30 sec at 94°C, 30 sec at 59°C and 60 sec at 72°C, followed by a final cycle at 72°C for 5 min. PCR products were resolved by 1% gel electrophoresis and purified using a High pure PCR purification kit (Roche).

Purified PCR products were digested with *Bam*HI and *Eco*RI and ligated to a pFastBac1 donor vector containing a cloned copy of the gene encoding eGFP (obtained from M. Victor, UP) digested with the same enzymes. Ligated plasmids were transformed by heat shock into $CaCl_2$ competent XL1 Blue cells. Possible recombinant colonies were grown overnight at 37ºC on agar plates containing 100 μg/ml ampicillin and 12.5 μg/ml tetracyclin.

Possible recombinant plasmids were isolated by a conventional small scale alkaline-lysis plasmid isolation protocol (Sambrook & Russell, 2001) and possible recombinants were screened by digestion with *Bam*HI and *Eco*RI. For sequencing, recombinant plasmids were purified using a commercial purification kit (Roche) and sequenced using an ABI PRISM Big Dye Terminator Cycle Sequencing Ready Reaction kit with a pPolhFw (5'TTCCGGATTATTCATACC3') forward primer specific to the pFastBac vector or an eGFPinternal reverse primer (5'GGGCATGGCGGACTTGAAGAAG3') specific to the eGFP gene. Sequences were analysed on an ABI PRISM 3130xl Genetic Analyzer (Perkin Elmer). Recombinant plasmids were named pFastBac-AHSV-2-NS3-eGFP and pFastBac-AHSV-4-NS3-eGFP.

4.2.2.1b. Transposition and isolation of recombinant bacmid DNA

Recombinant pFastBac plasmids were transformed into DH10Bac™ *E. coli* cells according to the BAC-to-BAC™ Baculovirus expression system manual (Invitrogen Life Technologies, Gaithersburg, MD). Briefly, approximately 10 ng of plasmid was mixed with 100 µl of DMSO competent DH10Bac™ cells and incubated on ice for 30 min. The cells were exposed to a heat shock for 90 sec at 42°C and cooled on ice for 2 min. To this 900 µl S.O.C. medium (LB medium containing 250 mM KCl, 10 mM $MgCl_2$ and 20 mM glucose) was added and the cells grown for 4 h at 37°C with agitation. Of this transformation mixture 100 µl was plated onto LB plates containing kan (50 µg/ml), gentamycin (7 µg/ml), tetracyclin (10 µg/ml), X-gal (100 µg/ml) and IPTG (40 µg/ml). Plates were incubated at 37°C for at least 24 h. White colonies were picked, streaked onto fresh LB plates (supplemented as above) and grown overnight to confirm the white phenotype.

White colonies were grown overnight in LB medium (supplemented as above) and used for the isolation of bacmid DNA. Bacmid DNA was isolated using a protocol adapted for isolating plasmids greater than 100 kb as outlined in the BAC-to-BAC™ Baculovirus expression system manual (Invitrogen Life Technologies, Gaithersburg, MD). DNA pellets were air dried in a sterile laminar flow, dissolved in 40 µl UHQ and used to transfect Sf9 cells.

4.2.2.1c. Transfection of Sf9 cells with recombinant bacmid DNA and amplification of recombinant baculoviruses

Sf9 cells were seeded at 1 x 10^6 cells/well on 6-well plates and allowed to attach for 1 - 2 h. A volume of 6 µl of isolated recombinant bacmid DNA was mixed with 100 µl of non-supplemented TC-100. A 6 µl sample of CELLFECTIN™ reagent (Invitrogen Life Technologies) was diluted in 100 µl non-supplemented TC-100. The diluted DNA and lipids were gently mixed, incubated for 45 min at room temperature and the volume increased to 1 ml with non-supplemented TC-100. Cells were rinsed twice with TC-100 and overlaid with the lipid DNA mixture. Transfection was allowed to occur for 5 h at 27°C, after which time the mixture was removed from the cells and replaced with supplemented TC-100. Cells were incubated for a further 91 h and the supernatant stored at 4°C as the primary transfection mixture.

Baculoviruses in the primary transfection mixture were amplified on 75 cm^2 monolayers of 1 x 10^7 Sf9 cells in a total volume of 5 ml supplemented TC-100 and incubated overnight at 27°C. The volume was then increased to 12 ml and plates incubated for a total of 4 days. The titre of virus in these stocks was then determined.

4.2.2.1d. Baculovirus titrations

Six-well plates were seeded with 8.5 x 10^5 Sf9 cells/well (approximately 55% confluency) and the cells allowed to attach for 2 h. Dilution series of the amplified recombinant baculoviruses were prepared in supplemented TC-100. Of each dilution 0.5 ml (in duplicate) was added per well and kept at room temperature for 1 h, with agitation every 12 min. A 2% w/v Agarose, Type VII (Sigma) solution was prepared in ultra high quality water (UHQ), boiled and cooled to about 50°C. A 1% agarose working stock was prepared by the addition of an equal volume double strength Grace's medium (Highveld Biological), pre-warmed to 38°C. Inoculums were gently aspirated and replaced with 2 ml/well 1% agarose. Plates were incubated at 27°C for 7 days until plaques were visible. Cells were then stained with 0.5 ml/well 0.1% w/v Thiazolyl Blue Tetrazodium Bromide (Sigma) in PBS and left for 24 h at 27°C. The titre (pfu/ml) was calculated as 2 x number of plaques x dilution factor.

4.2.2.2 Western blot analysis of recombinant NS3 expression in Sf9 cells

Protein samples were separated by SDS-PAGE and transferred to nitrocellulose membranes (Hybond-C+, Amersham Biosciences) in a submerged EC 140 mini blot apparatus (E-C Apparatus Corporation) at 16-20 V for 1 h in Transfer buffer (25 mM Tris, 192 mM Glycine).

Membranes were rinsed for 5 min in PBS and blocked for 30 min in 5% blocking solution (5% w/v low fat milk powder in PBS) with gentle shaking at room temperature. Blocked membranes were incubated with the primary antibody (diluted in 1% blocking solution) overnight at room temperature with gentle agitation. Membranes were washed three times for 5 min each with wash buffer (0.05% v/v Tween-20 in PBS) and reacted with the secondary antibody diluted in 1% blocking solution for 1 h at room temperature with gentle shaking. Membranes were washed as described above followed by a final wash in PBS for 5 min. Detection of bound peroxidase enzyme conjugate was carried out by incubating the membrane in enzyme substrate (60 mg 4-chloro-1-naphtol (Sigma) in 20 ml ice-cold methanol mixed with 60 µl hydrogen peroxide in 100 ml PBS) at room temperature until bands were visible. Membranes were then removed from the enzyme substrate, rinsed with H_20 and dried.

For identification of eGFP, anti-GFP N-terminal antibodies (Sigma) were used as primary antibody (diluted 1:1000). For identification of AHSV-2 and AHSV-3 NS3, rabbit anti-β-galactosidase(gal)-AHSV-2 and anti-β-gal-AHSV-3 NS3 sera (obtained from M. van Niekerk and V. van Staden, UP respectively; diluted 1:100) were used as primary antibodies. For identification of EEV NS3 guinea pig anti-β-gal-EEV NS3 serum (L. Teixeira, UP; diluted 1:100) was used. The above antibodies were detected with Protein A peroxidase conjugate (Calbiochem; 1:1000 dilution). For identification of AHSV-4 NS3, chicken anti-β-gal-AHSV-4 NS3 antibodies (obtained from J. Korsman; 1:50 dilution) were used and detected with a 1:250 dilution of anti-chicken IgY peroxidase conjugate (Sigma). All antibodies were diluted in 1% blocking solution. All the primary antibodies used were polyclonal monospecific antibodies raised against denatured and gel purified NS3 fused to the C-terminus of β-gal.

4.2.3. Exogenous addition of baculovirus expressed NS3 to Vero cells

Sf9 cell monolayers seeded at 1 x 10^7 cells in 75 cm^2 flasks were infected with wild-type baculovirus or with recombinant baculoviruses expressing NS3 of AHSV-2, AHSV-3 or AHSV-4 at a MOI of 5 pfu/cell. Cells were harvested 30 h p.i. and resuspended in lysis buffer without detergent (300mM NaCl; 50mM Tris-HCl, pH 7.5; 1 mM EDTA; 1mM PMSF, 1mM 2-mercaptoethanol) at 2 x 10^7 cells/ml. Cells were mechanically lysed by dounce homogenisation. Cell lysates were placed on ice and used immediately. Duplicate samples were prepared and used to confirm NS3 protein expression by SDS-PAGE and Western blot. Sf9 cell lysates were mixed with an equal volume of supplemented MEM and added to confluent Vero cells from which the growth medium had been removed. Cells were incubated at room temperature for 180 min, after which time the lysates were removed and the membrane permeability of the Vero cells determined using the Hyg B assay as described in 2.2.6.

4.2.4. Trypan Blue cell viability assay

The viability of Sf9 cells infected with recombinant baculoviruses was monitored by Trypan blue staining as described in section 3.2.1.2.

4.2.5. Subcellular fractionation and membrane flotation assay

Sf9 cells were seeded on 75 cm^3 flasks at 1 x 10^7 cells/flask and infected with recombinant baculoviruses at a MOI of 2 to 5 pfu/cell. At 48 h p.i. the cells were harvested and washed twice with cold PBS. The membrane flotation assay was based on the method described by Brignati and coworkers (2003). The cells were resuspended in 300 or 500 µl hypotonic buffer (10 mM Tris, 0.2 mM $MgCl_2$ [pH 7.4]) to which protease inhibitors had been added (1 mg/ml pefabloc SC, 0.7 µg/ml pepstatin, 1 mM PMSF) and incubated on ice for 30 min. Cells were mechanically lysed by passage through a 29G needle or by douncing 30 times. The nuclei, unlysed cells and debris were collected by low speed centrifugation at 1000 g for 10 min at 4°C.

For subcellular fractionations 125 µl of the supernatant following low speed centrifugation was made up to a total volume of 5 ml with hypotonic buffer. This was then separated into soluble and particulate fractions through centrifugation at 100 000 g for 90 min at 4°C. The supernatant was

transferred to a clean tube and the particulate fraction resuspended in 5 ml hypotonic buffer. Fluorescence ($485_{Ex}/538_{Em}$) in each of the fractions was recorded using a Thermo Labsystems Fluoroskan Ascent FL plate reader.

For membrane flotation 125 µl of the supernatant, obtained following low speed centrifugation, was combined with 670 µl of 85% sucrose in NTE (100 mM NaCl, 10 mM Tris, 1 mM EDTA [pH 7.4]) to make a final concentration of 71% sucrose. This sample was overlaid with 2920 µl 65% sucrose in NTE and 1290 µl 10% sucrose in NTE in a 5 ml polyallomer tube (Beckman). The gradient was centrifuged at 100 000 g for 18 h at 4°C and fractions collected either from the top using a micropipette or from the bottom of the tube using a needle. The pellet was resuspended in a volume equal to that of the fractions collected.

Fractions, from membrane flotation gradients of the wild-type NS3 proteins, were diluted with 2 volumes NTE and mixed. Four volumes of ice cold acetone were then added, the sample mixed well and proteins precipitated at -80ºC for 1 h. Proteins were collected by centrifugation in a tabletop centrifuge at maximum speed for 20 min at 4ºC and resuspended in 30 µl 1 x PSB. Proteins were analysed by standard SDS-PAGE and Western blot. The NS3-eGFP fusion proteins in membrane flotation gradient fractions were detected by measuring fluorescence ($485_{Ex}/538_{Em}$) using a Thermo Labsystems Fluoroskan Ascent FL plate reader.

4.2.6. Analysis of the membrane topology of AHSV-2 NS3

4.2.6.1. Production of antibodies against N- and C-terminal of AHSV-2 NS3

4.2.6.1a. Immunisation schedule

A hen was used for the production of antibodies against the C-terminal region of NS3 and a cock for that against the N-terminal region of NS3. The hen and cock were injected intramuscularly (pectoral muscle) with 150-300 µg antigen in an equal volume of ISA70 (Seppic) oil adjuvant. Antigens ($A_{1\text{-}92}$ and $A_{176\text{-}218}$) were obtained, purified and quantified as described in 3.3.2.3. The hen and cock were injected by Dr M Romito (OVI) and eggs collected in the case of the hen and the cock bled for serum. Following the first inoculations the IgY response was developed by four booster inoculations with the same quantity of antigen at 4 week intervals. Serum was termed anti-N-terminal NS3.

4.2.6.1b. IgY purification

A chloroform/PEG 6000 method was used for the purification of IgY from chicken eggs (Tini *et al.*, 2002). Briefly, the egg yolk was separated from the egg white, washed with dH_2O, made up to 25 ml with 100 mM Sodium Phosphate buffer (pH 7.6) and mixed vigorously. 20 ml chloroform was then added to the yolk and shaken until the formation of a semisolid phase after which the mixture was centrifuged at 1200 g for 30 min. PEG 6000 was added to the supernatant to a final concentration of 12% w/v and mixed well. Precipitated IgY was collected by centrifugation at 15 800 g for 10 min and resuspended in 1 ml PBS and termed anti-C-terminal NS3.

4.2.6.2. Immunofluorescence assays

4.2.6.2a. Pre-absorption of antibodies

The antibodies produced against the terminal regions of AHSV-2 NS3 (4.2.6.1) and anti-β-gal-AHSV-2 NS3 serum (Van Niekerk, 2001) were pre-absorbed prior to their use in immunofluorescence assays. Sf9 cells were seeded on 75 cm^3 flasks at a density of 1 x 10^7 cells per flask, allowed to attach for 1 h and washed with serum free TC-100 medium. Cells were infected with wild type baculovirus at a MOI of 1 pfu/cell in 5 ml medium. At 1-2 h p.i the total volume was increased to 12 ml with medium. Infected cells were harvested 3-4 days p.i. and collected by centrifugation at 2000 g for 10 min. The cells were resuspended in 3 ml 1% blocking solution (1% w/v low fat milk powder in PBS) and lysed by passing the suspension through a 29G

needle. Antibodies were added (1:50 dilution for anti-β-gal-AHSV-2 NS3 and anti-C-terminal NS3; 1:25 dilution for anti-N-terminal NS3) to the lysed cells. A volume of 100 µl of the glutathione agarose resin bound to GST, which was retained during the purification of the GST recombinants (3.2.2.8b), was added to bind antibodies against GST. The suspension was incubated for 2 h at room temperature with gentle agitation and bound antibodies removed by centrifugation at 2000 g for 10 min. The supernatant was used in Western blots and immunofluorescent assays.

4.2.6.2b. Immunofluorescence assays

Sf9 cells were seeded at a density of 2.5 x 10^5 cells per well on 24-well tissue culture plates and allowed to attach for 1 h. Cells were infected with wild type baculovirus or recombinant baculovirus expressing AHSV-2 NS3 (Van Niekerk, 2001) at a MOI of 5 pfu/cell. 1 h p.i. the virus inoculums were replaced with 500 µl supplemented TC-100 per well and the infected cells incubated at 27^{o}C. At 27 h p.i. the cells were rinsed with sterile PBS and methanol:acetone (50:50 v/v) added for 30 sec to fixed samples. Cells were then pre-blocked for 30 min with 5% blocking solution (5% w/v low fat milk powder in sterile PBS) and incubated with the pre-absorbed antibodies (4.2.6.2a.) for 1 h at room temperature. Cells were rinsed three times for 5 min each with 0.5% v/v Tween-20 in sterile PBS. Bound anti-β-gal-AHSV-2 NS3 antibodies were detected by incubation with goat anti-rabbit IgG FITC (fluoroscein isothiocyanate) conjugate (Sigma, diluted 1:250 in 1% blocking solution) for 45 min. Bound chicken anti-N-terminal NS3 and anti-C-terminal NS3 antibodies were detected using anti-chicken IgY-FITC conjugate (Sigma, diluted 1:500 in 1% blocking solution). Cells were washed as above and overlaid with PBS until viewed under a Zeiss fluorescent microscope.

4.2.7. Confocal Microscopy

Sf9 cells were seeded on sterile coverslips in 6-well plates at 1 x 10^6 cells/well and infected with recombinant baculoviruses at a MOI of 5 pfu/cell. Unfixed cells were viewed directly at 30 h p.i. using a Zeiss LSM 510 META Laser Scanning Microscope at 489 nm. Images were analysed using Zeiss LSM Image Browser Version 4,0,0,157.

4.3. RESULTS

As the aim here was to compare the NS3 proteins from AHSV-2, AHSV-3 and AHSV-4, initially computational analysis of the protein sequences was used to identify any potential differences. The proteins were then expressed, as both wild-type and eGFP fusion proteins, in the recombinant baculovirus expression system. The cytotoxicity, membrane association and subcellular localisations of the proteins in insect cells were then compared.

4.3.1. Comparison of AHSV-2, AHSV-3 and AHSV-4 NS3 sequences

The high levels of sequence variation between AHSV-2, AHSV-3 and AHSV-4 NS3 make it difficult to identify specific residues that may impact on the observed differences attributed to these proteins. The amino acid sequences were therefore aligned (Appendix B) and the percentage identity for the domains within the proteins calculated to identify regions of high variability. As shown in Fig. 4.1 the variation in the NS3 sequences is not equally distributed over the length of the different proteins. The percentage identity is lowest in the intermediate region between HDI and HDII (variable domain), and in HDI. This variation may be important in determining structural and/or functional differences in the proteins.

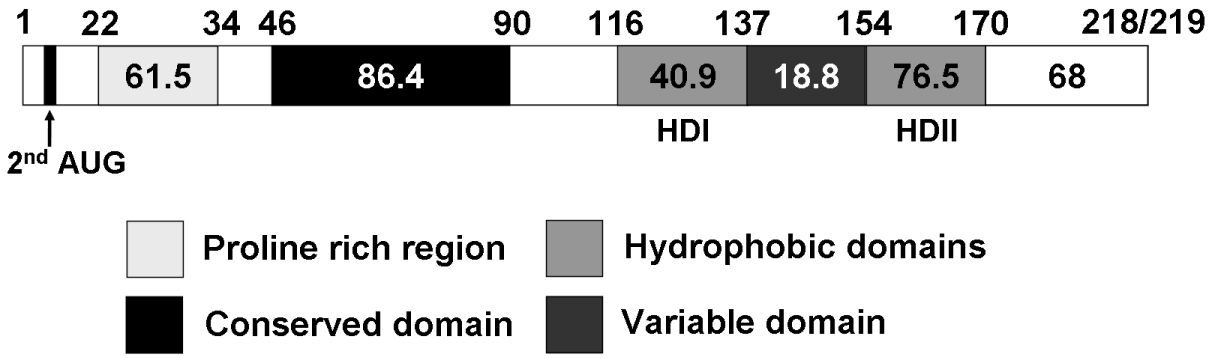

Fig. 4.1 Comparison of the conserved amino acid sequence elements in the NS3 proteins of AHSV-2 (82/61), AHSV-3 (M322/97) and AHSV-4 (HS39/97). Numbers within the sections indicate the percentage sequence identity for that region.

The AHSV-2, AHSV-3 and AHSV-4 NS3 sequences were then analysed using a variety of programs to identify any potential differences in membrane association or subcellular localisation.

The TMHMM program developed by Krogh and coworkers (2001) was used to predict both transmembrane regions within the NS3 proteins and the membrane topology. In this program hydrophobic stretches of approximately 20 amino acids are initially identified. Hydrophobicity is an important defining feature of transmembrane regions, and essential for insertion into the lipid bilayer. Stretches of about 20 hydrophobic residues are generally capable of spanning the bilayer

in a helical conformation. The orientation of this hydrophobic stretch in the bilayer is then predicted using the 'positive-inside rule'. This rule was based on the discovery of an asymmetric distribution of positively charged residues on the cytoplasmic side of membrane proteins. This asymmetric distribution may be the result of electrostatic potential differences on either side of the membrane and/or differences in the lipid composition between the lipids on either side of the lipid bilayer (Von Heijne, 1996; Krogh *et al.*, 2001). Other factors may however contribute to the determination of the topology of membrane proteins including the rate of synthesis and the length of the hydrophobic stretches (Bowie, 2005).

Predictions of transmembrane helices in the AHSV NS3 proteins using TMHMM indicate that the HDs form transmembrane (TM) regions (Fig. 4.2) although with different probabilities. In AHSV-4 NS3 both HDI and HDII have a high probability (0.8 – 1.0) of forming TM regions. In the topological model implicated by this prediction both the N- and C-terminus of the protein would be intracellular. In AHSV-2 and AHSV-3 NS3 HDI has a probability of 1.0 of forming a TM domain whereas HDII has a probability of only 0.3 and 0.45 respectively. HDII in these proteins is therefore predicted as not spanning the membrane. The predicted topology of AHSV-2 and AHSV-3 NS3 therefore differs from the AHSV-4 NS3 protein, with the N-terminus being inside and the C-terminus outside the cell.

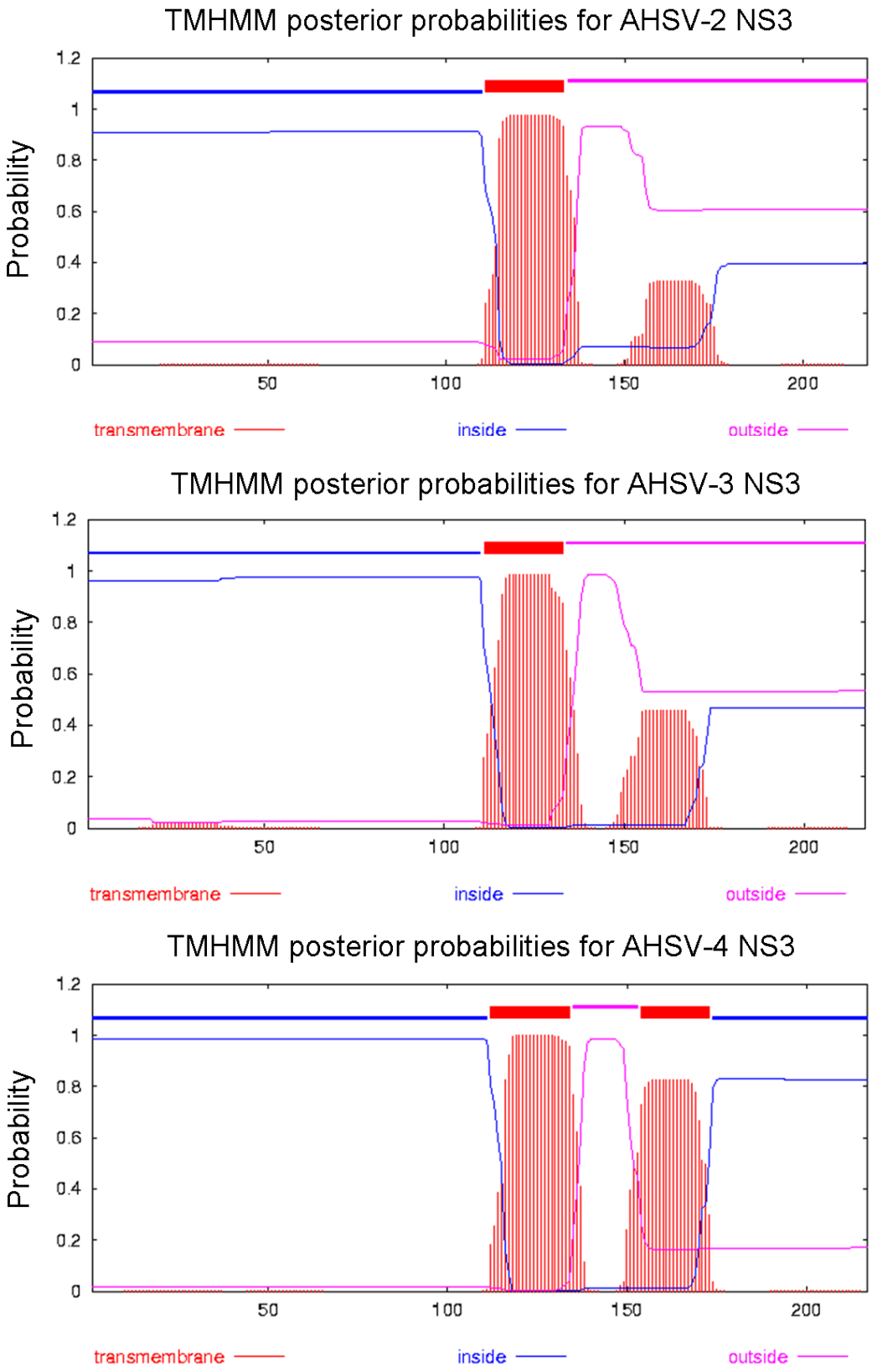

Fig. 4.2 Transmembrane helix predictions for AHSV-2, AHSV-3 and AHSV-4 NS3 proteins based on hidden Markov Model (TMHMM) (Krogh *et al.*, 2001). The 218/219 amino acid residues of NS3 are indicated on the x axis. The red line describes the probability of that part of the protein being a transmembrane domain, the blue line describes the probability of being inside the membrane (cytoplasmic) and the pink line describes the probability of being outside the membrane (lumenal).

The NS3 sequences were also scanned for nuclear localisation signals (NLS) using PredictNLS online (Cokol *et al.*, 2000). A NLS was predicted for AHSV-2 82/61 NS3 and the signal is underlined in Fig. 4.3. The NLS is positioned from residues 88-110 between the CR (bold italics) and HDI (bold). The generalised notation for this localisation signal is ***[RK](3,)?x(8,16)[RK](4,)?*** and the sequence is present in 197 proteins listed in the protein database Swiss-Prot. Of these, 97.92% are localised to the nucleus and the remaining 2.02% are non-nuclear. A NLS was not predicted for any of the other AHSV NS3 proteins listed in GenBank, or for BTV or EEV NS3.

MNLASISQSYMSHNENERSIVPYIPPPYHPTAPALAVSA***SQMETMSLGILN***
QAMSSSAGASGALKDEKAAFGAVAEALRDPEPIRKI<u>***KRRVG***</u>IQTLKTLKVE
<u>LSGMRRKK</u>LILK**IIMFICANVTMATSLVGGMSIVD**EDIAKHLAFDGKGDWV
SKTVHGLNLLCTTMLLAANKISEKVREEIARTKRDIAKRQSYVSAATMSWD
GDSVTLLRDVKYGD

Fig. 4.3 Nuclear localisation signal (underlined) present in AHSV-2 (82/61) NS3 as predicted by PredictNLS online (Cokol *et al.*, 2000). The CR is indicated in bold italics and HDI in bold.

4.3.2. Expression of AHSV-2, AHSV-3 and AHSV-4 in Sf9 cells

For the comparison of AHSV-2, AHSV-3 and AHSV-4 NS3 expression in insect cells, the proteins were expressed both as wild-type proteins and as eGFP fusion proteins. Recombinant baculoviruses expressing AHSV-2, AHSV-3, AHSV-4 NS3 or an AHSV-3-NS3-eGFP fusion protein were available. The following section describes the production of recombinant baculoviruses expressing AHSV-2 and AHSV-4 NS3 as eGFP fusion proteins.

4.3.2.1. Cloning AHSV-2 and AHSV-4 NS3 into pFastBac-eGFP

The NS3 genes of AHSV-2 and AHSV-4 were PCR amplified with primers that included *Bam*HI and *Eco*RI sites for cloning and that removed the stop codon from the NS3 coding sequence. The NS3 amplicons were inserted into a recombinant pFastBac1 plasmid containing the coding sequence for eGFP (pFastBac-eGFP). Insertion at the *Bam*HI and *Eco*RI sites placed the NS3 sequences upstream of and in-frame with the eGFP gene. Recombinant plasmids were confirmed by restriction digests with *Bam*HI and *Eco*RI and digestion products analysed by agarose gel electrophoresis (Fig. 4.4). Digestion of the non-recombinant pFastBac-eGFP vector resulted in linearization of the plasmid and a single fragment of the expected size of 5495 bp was observed (Fig. 4.4 lane a). Digestion of recombinant plasmids pFastBac-AHSV-2-NS3-eGFP and pFastBac-AHSV-4-NS3-eGFP resulted in two linear DNA fragments. These were of the expected sizes of 5495 bp representing the vector (pFastBac-eGFP) and approximately 678 bp for the AHSV-2 NS3 insert and 681 bp representing the inserted NS3 gene of AHSV-4.

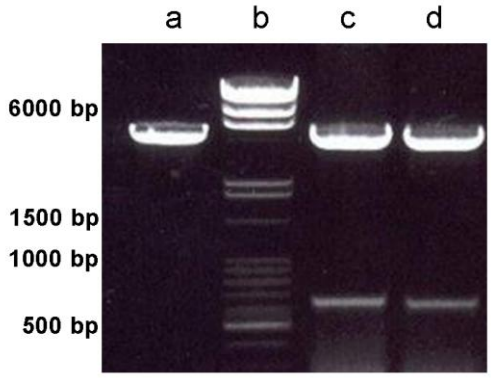

Fig. 4.4 Agarose gel electrophoretic analysis of restriction digestion of pFastBac-eGFP vector and possible recombinant plasmids. pFastBac-eGFP (a), pFastBac-AHSV2-NS3-eGFP (c) and pFastBac-AHSV4-NS3-eGFP (d) were digested with *Bam*HI and *Eco*RI. Digestion products were analysed by 1% agarose gel electrophoresis, stained with ethidium bromide (EtBr) and visualised under an UV illuminator. DNA size marker was included (b) and sizes of selected fragments are as indicated on the left.

Recombinant plasmids were then sequenced as described in 4.2.2.1a. Sequencing confirmed the insertion of the NS3 genes in the correct reading frame for expression as eGFP fusion proteins. Sequencing of the AHSV-2 NS3 gene in the pFastBac-AHSV-2-NS3-eGFP plasmid revealed the presence of two nucleotide changes (T to C at nt 347 and nt 458) that would result in amino acid changes in the encoded protein (I to T (aa116) and V to A (aa153)). Although a high fidelity Taq polymerase was used, these nucleotide changes probably occurred during PCR amplification of this gene. As these amino acid changes did not alter the membrane spanning potential of the AHSV-2 NS3 protein, as predicted by TMHMM analyses (results not shown), this construct was used for further studies.

Recombinant baculoviruses expressing AHSV-2-NS3-eGFP and AHSV-4-NS3-eGFP were then generated using standard procedures (4.2.2.1b to 4.2.2.1d). Briefly, the pFastBac-AHSV-2-NS3-eGFP and pFastBac-AHSV-4-NS3-eGFP plasmids were used to transform DH10Bac^{TM} cells for transposition of the NS3-eGFP inserts into the bacmid DNA present in these cells. Bacmid DNA was then isolated and used to transfect Sf9 cells to produce recombinant baculoviruses (Bac-AHSV-2-NS3-eGFP and Bac-AHSV-4-NS3-eGFP). Baculoviruses from these transfections were then amplified, titrated and used to infect Sf9 cells for analysis of recombinant protein expression.

4.3.2.2. Analysis of expression of AHSV NS3 and NS3-eGFP fusion proteins

To confirm expression of the NS3 and NS3-eGFP fusion proteins, Sf9 cells were infected with recombinant baculoviruses expressing eGFP, AHSV-2 NS3, AHSV-3 NS3, AHSV-4 NS3, AHSV2-NS3-eGFP, AHSV-3-NS3-eGFP and AHSV-4-NS3-eGFP. Proteins from infected cells were separated by 12% denaturing SDS-PAGE, transferred to nitrocellulose membranes and reacted with antibodies against eGFP (Fig. 4.5A), AHSV-2 NS3 (Fig. 4.5B), AHSV-3 NS3 (Fig. 4.5C) and

AHSV-4 NS3 (Fig. 4.5D). The eGFP antibodies detected eGFP (Fig. 4.5A lane a) and all three AHSV NS3 eGFP fusion proteins (Fig. 4.5A lanes e, f and g). Protein bands were of the expected sizes of approximately 27 kDa for eGFP and 51 kDa for the NS3-eGFP fusion proteins. AHSV-2 NS3 antibodies detected the 24 kDa AHSV-2 NS3 protein (Fig. 4.5B lane b) and the AHSV-2-NS3-eGFP fusion protein (Fig. 4.5B lane e). AHSV-3 NS3 antibodies detected AHSV-3 NS3 (Fig. 4.5C lane c) and AHSV-3-NS3-eGFP (Fig. 4.5C lane f). The polyclonal antibodies raised against AHSV-4 NS3 detected NS3 of all three serotypes (Fig. 4.5D lanes b, c and d) and reacted with all three NS3-eGFP fusion proteins (Fig. 4.5D lanes e, f and g).

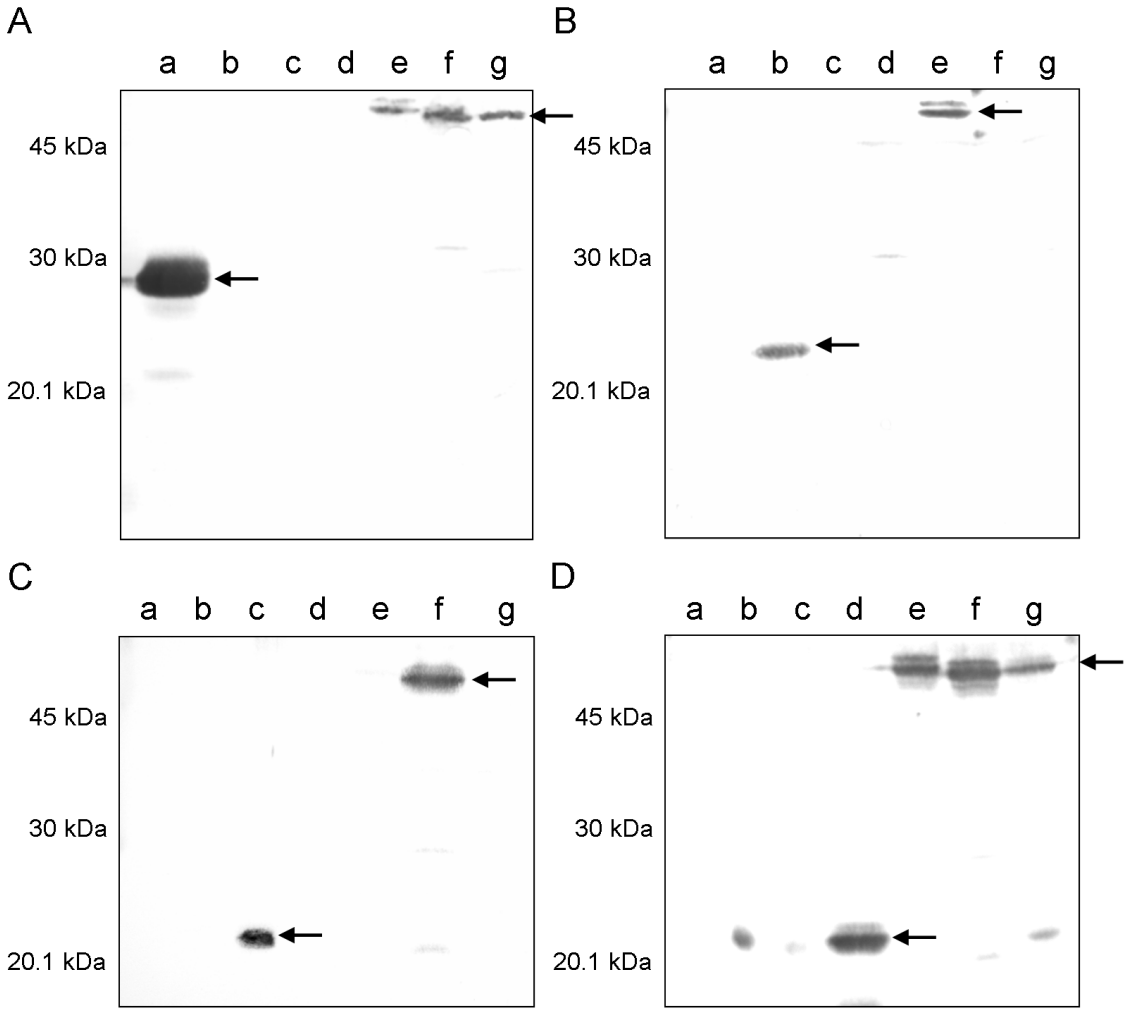

Fig. 4.5 Western blot analysis of NS3 and NS3-eGFP fusion proteins expressed in insect cells. Sf9 cells were infected with recombinant baculoviruses expressing eGFP (a), AHSV-2 NS3 (b), AHSV-3 NS3 (c), AHSV-4 NS3 (d), AHSV-2-NS3-eGFP (e), AHSV-3-NS3-eGFP (f) and AHSV-4-NS3-eGFP (g). Proteins from infected cells were separated by 12% SDS-PAGE, transferred to membranes and reacted with anti-eGFP (A), anti-β-gal-AHSV-2 NS3 (B) anti-β-gal-AHSV-3 NS3 (C) or anti-β-gal-AHSV-4 NS3 (D) antibodies. Arrows indicate the positions of the respective recombinantly expressed proteins. Molecular weight marker sizes are indicated on the left.

Following confirmation of expression, a number of assays were carried out to compare the AHSV NS3 proteins in terms of membrane permeabilising activity, cytotoxicity, membrane association and localisation.

4.3.3. Effect of exogenously added NS3 on Vero cell membrane permeability

To substantiate the finding in chapter 2 that NS3 is the primary AHSV protein involved in determining the membrane permeabilising effect of the virus, the effect of recombinantly expressed NS3 on cell membrane permeability was assayed. The NS3 proteins from the different AHSV strains were expressed in the baculovirus expression system, added externally to Vero cells and any differential impact on the permeability of the mammalian cell membranes monitored.

Recombinant baculoviruses expressing NS3 of AHSV-2, AHSV-3 or AHSV-4 were used to infect Sf9 insect cells. After confirmation that the NS3 proteins were expressed to similar levels (results not shown), crude cell lysates containing NS3 were prepared and equivalent amounts added to healthy Vero cells. Crude lysates containing NS3 were used here as a rapid and initial analysis of the effect of NS3, as attempts to purify NS3 had been unsuccessful due to the low levels of expression and insolubility of this cytotoxic membrane protein. The lysates were removed and membrane permeability monitored by a Hyg B assay (Fig. 4.6). Lysates from Sf9 cells infected with recombinant baculoviruses expressing NS3 were found to permeabilise the cell membrane to a greater extent than lysates of cells infected with wild-type baculoviruses. Theoretically the only difference between these lysates, although they are complex mixtures, is the presence of NS3. The control lysate of wild-type baculovirus infected cells caused only 15±2.6% permeabilisation. Incubation in the presence of AHSV-2 NS3 resulted in 72±0.5% membrane permeability, followed by AHSV-3 NS3 at 62±3.8% and AHSV-4 NS3 at 48±5.8%. This trend correlates with that observed for Vero cells infected with AHSV, where AHSV-2 (or reassortants containing NS3 originating from AHSV-2) caused more permeabilisation than AHSV-3, and AHSV-4 had the least severe effect (see 2.3.5. and Table 2.5).

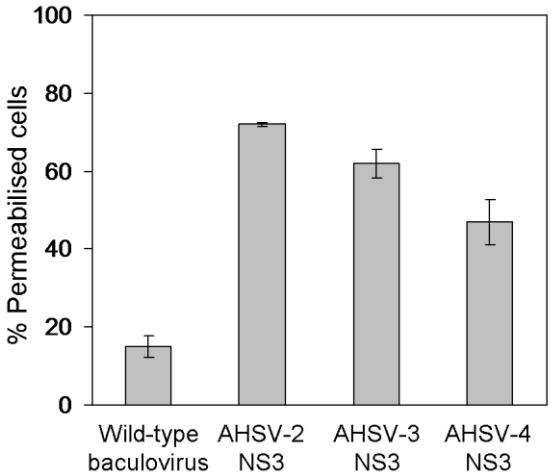

Fig. 4.6 Cell membrane permeabilisation assay of uninfected Vero cells following external addition of AHSV NS3. Lysates of Sf9 cells infected with wild-type baculovirus or recombinant baculoviruses expressing AHSV-2, AHSV-3 or AHSV-4 NS3 were added to Vero cells. Membrane permeability was determined 180 min later using a Hyg B assay.

4.3.4. Effect of *in vivo* expression of AHSV-2, AHSV-3 and AHSV-4 NS3 on insect cell viability

Computational analysis of AHSV-2, AHSV-3 and AHSV-4 NS3 revealed potential differences in the membrane association and localisation of these proteins. As this may impact on the functioning of the proteins, their cytotoxicity was compared following recombinant expression in insect cells.

The effect of the three AHSV NS3 proteins on the viability of insect cells was monitored using a Trypan blue assay (Fig. 4.7). Cultures infected with wild-type or recombinant baculoviruses expressing the non-cytotoxic AHSV NS2 displayed only a slight decrease in viability with more than 80% viable cells remaining at 48 h p.i.. Expression of AHSV-2, AHSV-3 and AHSV-4 NS3 in Sf9 cells caused a dramatic decrease in viability from 27 h p.i. with only 5 to 6% viable cells remaining at 48 h p.i. in all cases. The AHSV-2, -3 and -4 NS3 proteins were therefore equivalently cytotoxic when expressed in insect cells under the control of the strong polihedrin promoter.

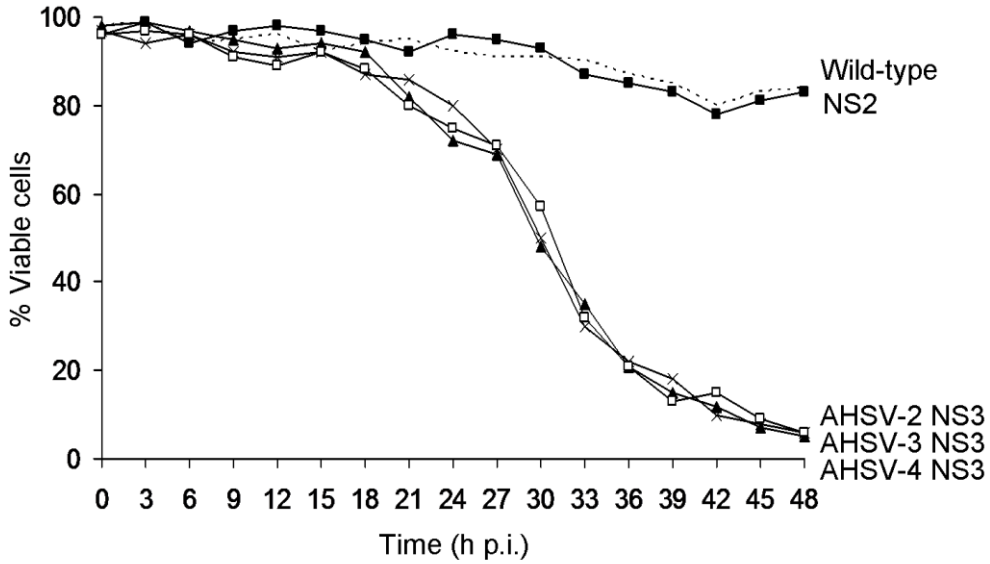

Fig. 4.7 Cytotoxic effect of AHSV-2, AHSV-3 and AHSV-4 NS3 on insect cells. Sf9 cells were infected with wild-type (dotted line) baculovirus or recombinant baculoviruses expressing AHSV NS2 (■) AHSV-2 NS3 (▲) AHSV-3 NS3 (x) and AHSV-4 NS3 (□). Viability was monitored every 3 h for 48h by staining with Trypan blue and counting viable and non-viable cells.

4.3.5. Membrane association of AHSV-2, AHSV-3 and AHSV-4 NS3

A membrane flotation assay was carried out to analyse the association of AHSV-2, AHSV-3 and AHSV-4 NS3 with the membranous components of the cell. Detergent-free lysates of Sf9 cells infected with recombinant baculoviruses expressing AHSV-2, AHSV-3 and AHSV-4 NS3 were loaded at the bottom of discontinuous sucrose gradients, with decreasing density towards the top

of the gradients, as described in 4.2.5. Following centrifugation fractions were collected from gradients, proteins precipitated with acetone and analysed by Western blot with appropriate antibodies. The results are shown in Fig. 4.8. In this assay the membranes, and any associated proteins, should migrate to the upper interface between the 65% and 10% sucrose during centrifugation due to the buoyant nature of the lipids. Membrane-associated proteins are therefore expected to be present in the top low density fractions of the gradient while non-membrane associated proteins remain in the bottom high density fractions (Brignati *et al.*, 2003). The soluble non-membrane associated protein eGFP was included as a control. As can be seen in Fig. 4.8 this protein remains in the bottom, or high density, fractions of the gradient. AHSV-2, -3 and -4 NS3 however migrated to the top, or low density, fractions of the gradient, indicating that all three proteins are membrane-associated. The greater intensity of the AHSV-4 NS4 protein band in Fig. 4.8 is probably due to the lower dilution of antibodies used to detect this protein. EEV NS3 was also included in this assay and as can be seen in Fig. 4.8 migrates upwards to the lower density fractions of a membrane flotation gradient and is similarly associated with the membranous components of the cell.

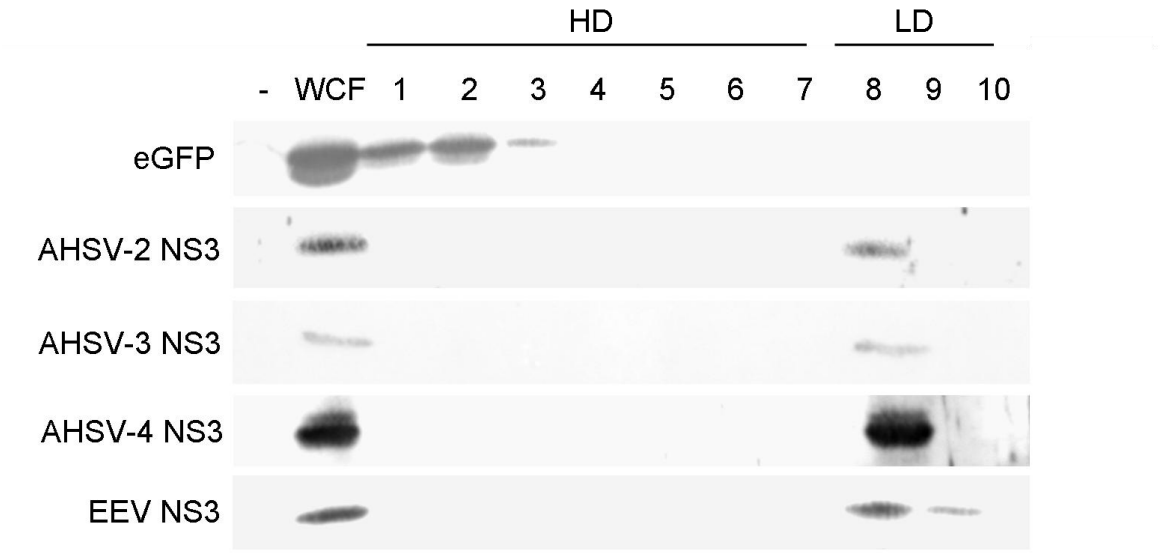

Fig. 4.8 Western blot analysis of proteins in high density (HD, 1-7) and low density (LD, 8-10) fractions from membrane flotation gradients. The negative control (-) for the Western blot of eGFP was the total lysate or whole cell fractions (WCF) of Sf9 cells infected with recombinant baculoviruses expressing EEV NS3. WCF of Sf9 cells expressing eGFP were used as a negative (-) control in all other cases.

The association of the NS3-eGFP proteins with membranous components of the cell was additionally investigated here by subcellular fractionation and membrane flotation assays.

The addition of the eGFP protein to the C-terminus of NS3 would enable easy visualisation but may however affect the localisation and membrane association of NS3. As an initial comparison of the localisation of the NS3-eGFP fusion proteins, Sf9 cell expressing the proteins were

fractionated into crude subcellular components (Fig. 4.9). Cells were mechanically lysed by dounce homogenisation, and unlysed cells and nuclei pelleted by low speed centrifugation (Nuclei, Fig. 4.9). Fluorescent readings were taken of the nuclear fraction and post-nuclear supernatant (Supernatant, Fig. 4.9) and the sum of these two values used as total fluorescence. The fluorescence of each of the subcellular fractions was then expressed as a percentage of this total fluorescence. 95.4% of the eGFP protein was present in the post-nuclear supernatant, with 4.6% of the protein present in the pelleted nuclear fraction. The bulk of this soluble protein therefore remained in the supernatant indicating that the majority of the cells were lysed. Approximately equivalent amounts of both AHSV-3 and AHSV-4-NS3-eGFP pelleted with the nuclei (50.9 and 52.3%, respectively) and remained in the supernatant (49.1 and 47.7%, respectively). In contrast to this, 83.6% of the AHSV-2-NS3-eGFP protein pelleted with the nuclei and unlysed cells, with only 16.4% of the protein remaining in the supernatant. The high amount of the NS3-eGFP proteins in the nuclear fractions is probably principally as a result of the association of NS3 with cell membranes that form highly insoluble aggregates which pellet together with the nuclei. The higher amount of AHSV-2-NS3-eGFP in the nuclear fraction, relative to that in AHSV-3- and AHSV-4-NS3-eGFP, may be a result of specific targeting to the nucleus.

The post-nuclear supernatant was then further separated into particulate and soluble fractions by high speed centrifugation (Fig. 4.9). The bulk of the eGFP was present in the soluble fraction (93%), while the majority of the NS3-eGFP proteins did not remain in solution and were pelleted to the particulate fractions. The association of the NS3-eGFP proteins with particulate fractions is probably as a result of their interaction with insoluble membrane components of the cell. To investigate this a membrane flotation assay was performed.

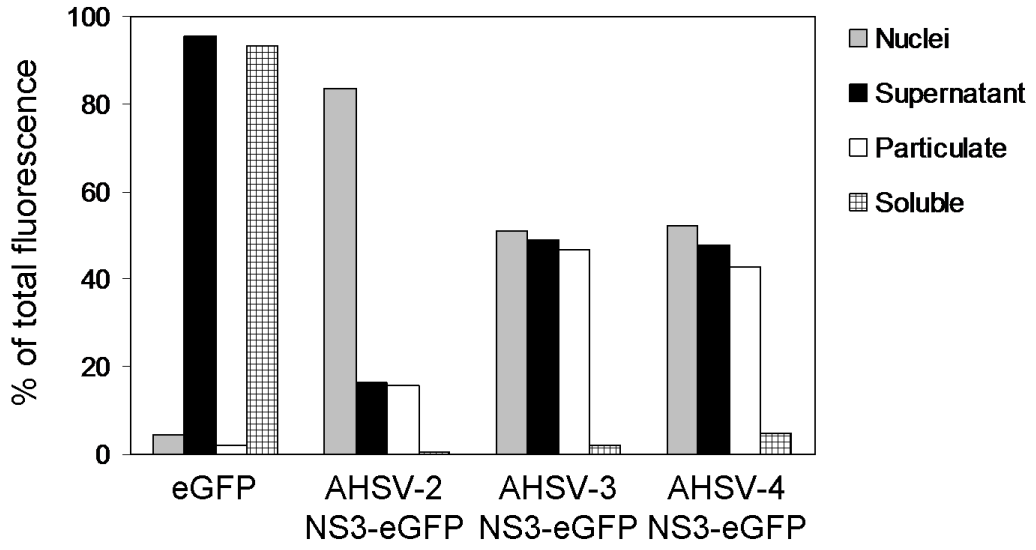

Fig. 4.9 Subcellular fractionation of Sf9 cells infected with recombinant baculoviruses expressing eGFP and the NS3-eGFP fusion proteins. Infected cells were harvested at 48 h p.i., lysed and nuclei pelleted by low speed centrifugation (Nuclei). The post-nuclear supernatant (Supernatant) was then fractionated by high speed centrifugation into insoluble (Particulate) and soluble (Soluble) components. Fluorescent readings for each of the subcellular fractions are expressed as a percentage of the total fluorescence.

To compare the intracellular membrane association of the NS3-eGFP fusion proteins membrane flotation assays were performed as described previously. Detergent-free lysates of Sf9 cells expressing eGFP and the NS3-eGFP fusion proteins were loaded at the bottom of membrane flotation sucrose gradients and following equilibrium density centrifugation fractions were collected. Fluorescence in each fraction was measured and expressed as a percentage of the total fluorescence (sum of fluorescence of all fractions). The results obtained for eGFP and AHSV-4-NS3-eGFP are shown in Fig. 4.10. The control eGFP protein was present at the bottom of the gradient in the high density fractions 1 to 5 as expected for a soluble non-membrane associated protein. The AHSV-4-NS3-eGFP fusion proteins migrated towards the top low density fractions of the gradient with a peak of fluorescence in fractions 14 to 16. Similar results were obtained for AHSV-2-NS3-eGFP (results not shown) and AHSV-3-NS3-eGFP (Hatherell, 2007). All three NS3-eGFP proteins were therefore deemed to be associated with the membranous components of the cell. The addition of the eGFP protein to the C-terminus of the NS3 proteins appeared therefore not to affect the membrane association of these proteins.

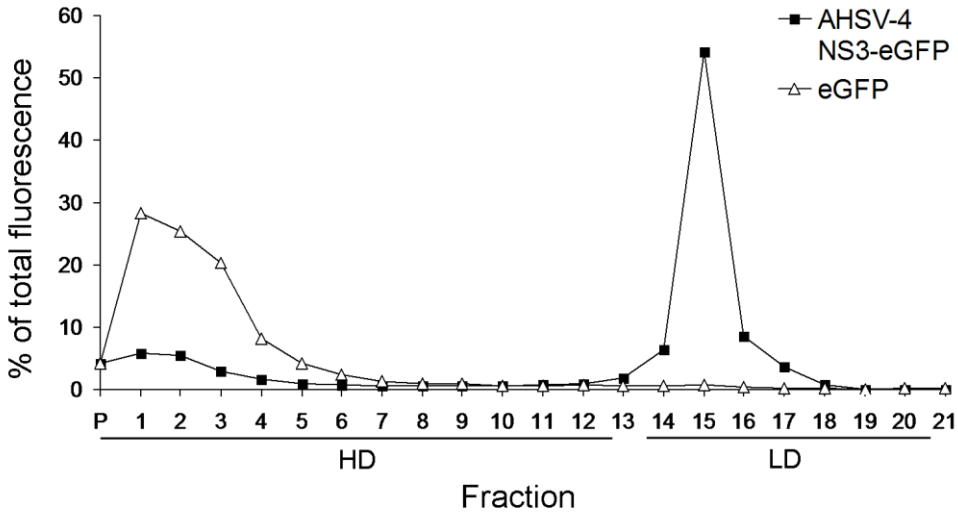

Fig. 4.10 Percentage of total fluorescence in fractions from membrane flotation sucrose gradients of lysates of Sf9 cell infected with recombinant baculoviruses expressing eGFP or AHSV-4-NS3-eGFP. The high density (HD) sucrose fractions at the bottom of the gradient and the low density sucrose fractions (LD) at the top of the gradient are indicated. P is the pellet fraction.

4.3.4. Membrane topology of AHSV-2 NS3

TMHMM analysis of the AHSV-2 and AHSV-3 NS3 proteins predicted a different membrane topology to that of AHSV-4 NS3, with the N-terminus being inside and the C-terminus outside the cell (Fig. 4.1). The membrane topology of AHSV-2 NS3 was therefore experimentally investigated here. In a previous study it was shown that antibodies to NS3 were not able to penetrate the cell membrane of unfixed Sf9 cells and react with intracellular recombinantly expressed NS3 up to 27 h p.i.(Smit, 1999). Van Niekerk *et al.* (2001a) demonstrated that unfixed Sf9 cells expressing NS3 showed fluorescence of the entire cell surface when reacted with antibodies against full length NS3 in indirect immunofluorescence assays. This indicated that the NS3 protein was localised to the outer plasma membrane. It was therefore argued that in unfixed cells antibodies specific to the N- and C-terminal regions of NS3 would bind only if these regions were exposed on the cell surface. The following section describes the production of site-specific antibodies against the N- and C-terminal regions of AHSV-2 NS3 for immunofluorescent analysis of membrane topology.

4.3.4.1. Production of anti-N-terminal and anti- C-terminal NS3 antibodies

In chapter 3 the N- and C-terminal regions of AHSV-2 NS3 were expressed to high levels in soluble forms as GST fusion proteins (GST-$A_{1\text{-}92}$ and GST-$A_{176\text{-}218}$, respectively) in *E. coli* and affinity purified. Following affinity binding to glutathione agarose resin the NS3 specific sequences ($A_{1\text{-}92}$ and $A_{176\text{-}218}$) were cleaved from the GST-Tag by thrombin digestion (see 3.3.2.3). Sufficient quantities of the N- and C-terminal NS3 proteins were obtained for their use

as antigens for the production of polyclonal antibodies in chickens as described in 4.2.6.1. Prior to inoculation, serum from the cock and IgY isolated from an egg from the hen were tested for response to Sf9 proteins in a Western blot. No reaction with Sf9 proteins was detected (results not shown).

Chickens were administered a primary and four booster injections of 150 – 300 µg of antigen each at four weekly intervals. Serum from the cock and IgY isolated from the hen's eggs were evaluated by Western blot for reaction with AHSV-2 NS3. The antibodies reacted with AHSV-2 NS3 expressed both in *E. coli* and Sf9 cells, although a high amount of non-specific reaction with bacterial proteins was also evident (results not shown). Following confirmation of reaction with AHSV-2 NS3 the antibody samples were pre-absorbed with Sf9 cell lysates infected with wild-type baculovirus. Pre-absorbed antibodies were again tested by Western blot (Fig. 4.11). Cell extracts from wild-type and AHSV-2 NS3 expressing recombinant baculovirus infections of Sf9 cells were separated by SDS-PAGE, proteins transferred onto nitrocellulose membranes and reacted with the pre-absorbed antibodies as the primary antibodies in Western blots. The pre-absorbed antibodies showed no reaction with Sf9 cellular or wild-type baculovirus proteins and a specific reaction with the 24 kDa AHSV-2 NS3. The pre-absorbed antibodies were therefore used in immunofluorescence assays. Antibodies against the full length AHSV-2 NS3 protein (anti-β-gal-AHSV-2-NS3) were additionally pre-absorbed with wild-type baculovirus infected Sf9 cell extracts.

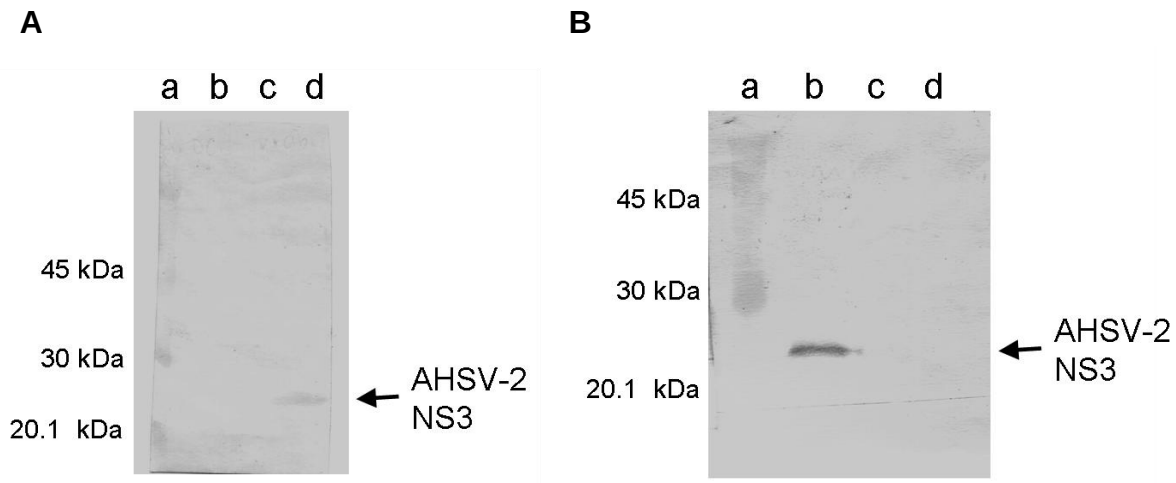

Fig. 4.11 Western blot analysis of chicken anti-N-terminal (A) and anti-C-terminal (B) NS3 antibodies. Uninfected Sf9 cell lysates (lane b in A and lane c in B) or lysates from cells infected with wild-type baculovirus (lane c in A, and lane d in B) or recombinant baculovirus expressing AHSV-2 NS3 (lane d in A and lane b in B) were separated by 12% SDS-PAGE. Protein were transferred to nitrocellulose membranes for reaction with antibodies raised against the N- and C-terminal regions of AHSV-2 NS3. The position of NS3 is indicated. The sizes of the molecular weight markers (a) are indicated on the left.

4.3.4.2. Immunofluorescent analysis of membrane topology of AHSV-2 NS3

To investigate the topology of AHSV-2 NS3 in the cell membrane, cells were analysed by indirect immunofluorescence with the antibodies produced against the N- and C-terminus of NS3.

Sf9 cells were infected with either wild-type baculovirus or recombinant baculovirus expressing AHSV-2 NS3. Fixed and unfixed cells were blocked and reacted with pre-absorbed NS3-specific antibodies, anti-β-gal-AHSV-2 NS3, anti-N-terminal NS3 and anti-C-terminal NS3. Binding of these antibodies was detected with fluoroscein labelled secondary antibodies and cells viewed under a Zeiss fluorescent microscope (Fig. 4.12).

Fixed and unfixed wild-type infected cells showed a low background fluorescent signal following immunofluorescent labelling (Fig. 4.12). Numerous repeats of the experiment yielded similar results. In a study by Stoltz and co-workers (1996) Sf9 cells infected with recombinant baculoviruses expressing AHSV NS3 were immunogold labelled with anti-NS3 and anti-NS2 monospecific antisera, as well as a pre-bled antiserum, and examined by electron microscopy. An intense, non-NS3-specific, labelling of baculoviruses with all three antibodies was observed and could not be explained. A similar non-specific labelling of baculoviruses may explain the background signal observed here. Nonetheless, fixed, permeabilised, Sf9 cells expressing AHSV-2 NS3 (Fig. 4.13) displayed a significantly brighter fluorescence for all the antibodies tested confirming both expression of NS3 and reaction of the antibodies to NS3. In unfixed NS3 expressing cells the antibodies against full length NS3 showed fluorescence of the cell surface. Unfixed NS3 expressing cells showed no reaction to the antibodies against either the N- or C-terminal regions of NS3. The N- and C-terminal regions of AHSV-2 NS3 appear therefore, under these conditions, not to be exposed on the cell surface. This would imply a topological model for membrane insertion of NS3 in which both the N- and C-terminus are located within the cytoplasm and only the stretch of amino acids between the two HDs is exposed to the extracellular environment. Reaction of the antibodies raised against β-gal-AHSV-2-NS3 with the surface of unfixed cells expressing NS3 then implies that antibodies specific to the extracellular region between the HDs are present in this polyclonal antiserum.

Immunolabelled fixed cells expressing AHSV-2 NS3 (Fig. 4.13) showed fluorescence of the outer membrane and throughout the interior of the cells possibly including the nucleus. Furthermore, both subcellular fractionations of cells expressing AHSV-2-NS3-eGFP and computational analysis of AHSV-2 NS3 indicated potential localisation to the nucleus. The subcellular localisation of AHSV-2 NS3 was therefore investigated in the following section by confocal fluorescent microscopy, and compared to AHSV-3 and AHSV-4 NS3.

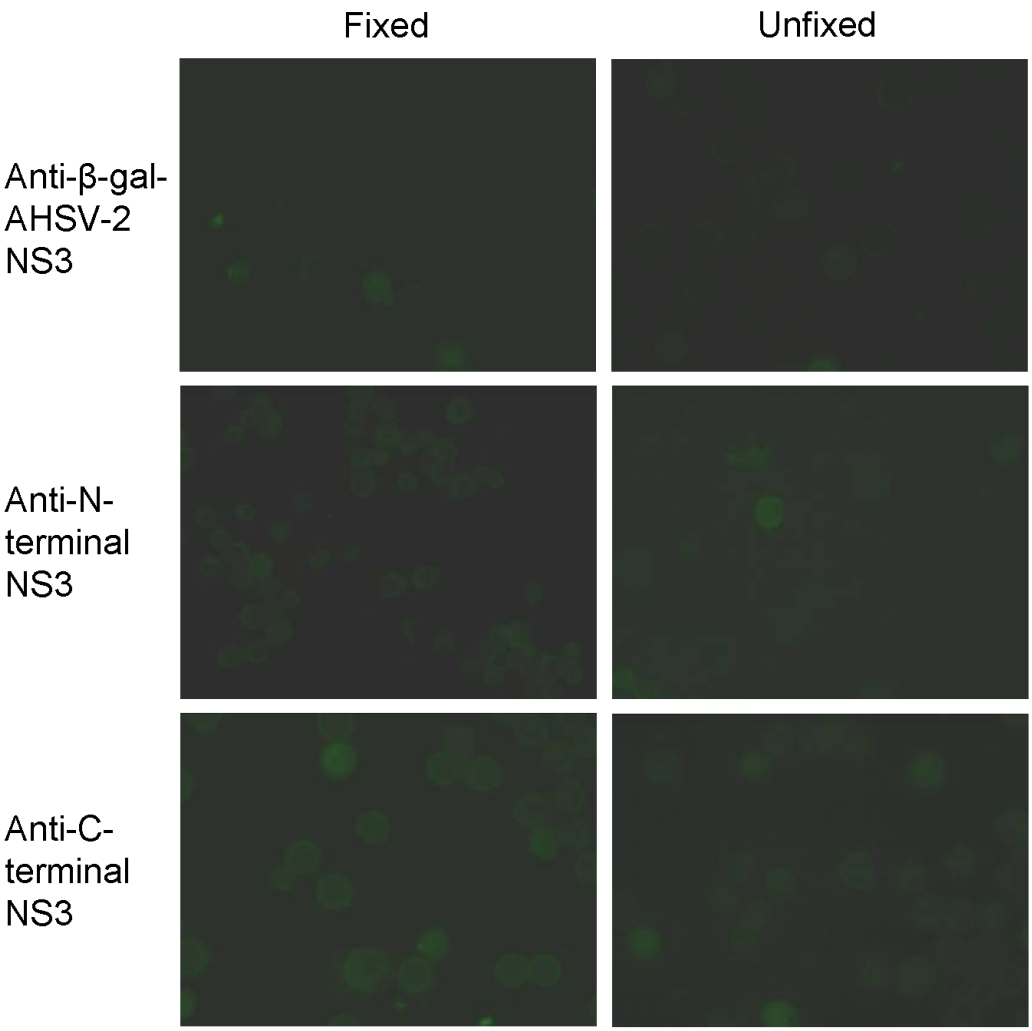

Fig. 4.12 Indirect immunofluorescence of wild-type baculovirus infected Sf9 cells. Unfixed or fixed cells were blocked and reacted with polyclonal NS3-specific antibodies at 27 h .p.i. followed by a fluorescent conjugated secondary antibody. Cells were viewed under a Zeiss fluorescent microscope at 20 or 40 x magnification.

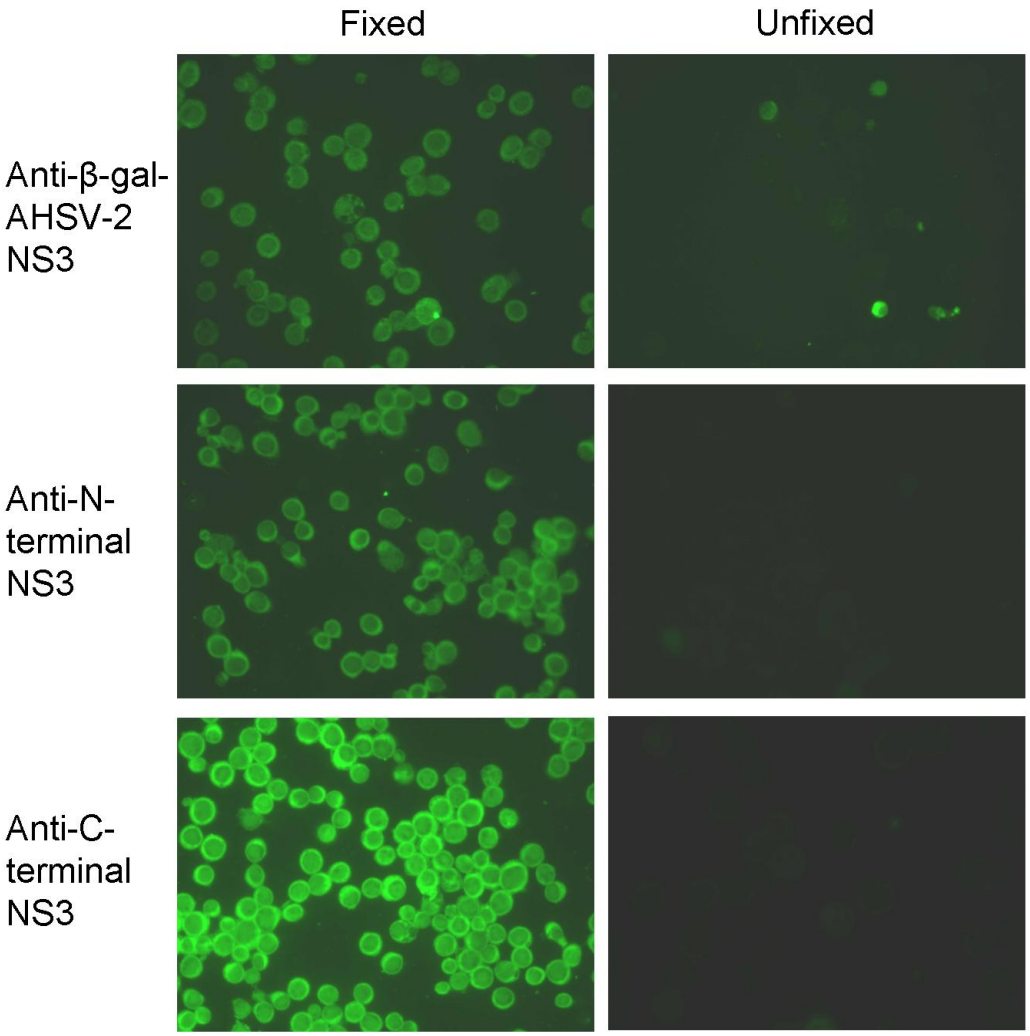

Fig. 4.13 Indirect immunofluorescence of Sf9 cells infected with recombinant baculoviruses expressing AHSV-2 NS3. Unfixed or fixed cells were blocked and reacted with polyclonal NS3-specific antibodies at 27 h .p.i. followed by a fluorescent conjugated secondary antibody. Cells were viewed under a Zeiss fluorescent microscope at 20 or 40 x magnification.

4.3.5. Confocal microscopy analysis of AHSV-NS3-eGFP fusion protein localisation

The intracellular localisation of the NS3-eGFP fusion proteins was examined by scanning confocal fluorescent microscopy. Sf9 cells were infected on sterile coverslips with recombinant baculoviruses expressing eGFP, AHSV-2-NS3-eGFP, AHSV-3-NS3-eGFP or AHSV-4-NS3-eGFP. Unfixed infected cells were then viewed at 30 h p.i. Representative results are given for eGFP in Fig. 4.14, AHSV-2-NS3-eGFP in Fig. 4.15, AHSV-3-NS3-eGFP in Fig. 4.16 and AHSV-4-NS3-eGFP in Fig. 4.17.

Sf9 cells infected with recombinant baculoviruses displayed the characteristic enlarged nuclei typically observed following infection with this nuclear polyhedrosis virus (Fig. 4.14 to 4.17). Sf9 cells infected with recombinant baculoviruses expressing eGFP show a uniform distribution of fluorescence across the cell, in both the cytoplasm and nucleus (Fig. 4.14A and B). eGFP is known to be found ubiquitously throughout the cell, and in previous studies the same distribution of eGFP in Sf9 cells was observed (Matsumoto *et al.*, 2004).

Sf9 cells infected with recombinant baculoviruses expressing AHSV-2-NS3-eGFP displayed a distinctly different fluorescence pattern. In these cells fluorescence was typically observed at the plasma membrane as well as within and around the nucleus as can be seen from the images taken of a field of cells in Fig. 4.15A and B. This is clearly illustrated in the cross-section through the centre of a cell (Fig. 4.15C) and the outer surface of the same cell (Fig. 4.15E). This localisation pattern is also demonstrated by the intensity plots generated of these images using the Zeiss LSM Image Browser software (Fig. 4.15D and F, respectively). Interestingly, the fluorescence observed was not uniform and appeared as discrete spots on the outer membrane and within the cell.

AHSV-3 and AHSV-4-NS3-eGFP displayed a similar localisation pattern to one another. A distinct punctuate fluorescence was observed in the perinuclear region of the cytoplasm (Fig. 4.16C and 4.17C) and in the plasma cell membrane (Fig. 4.16E and 4.17E). No fluorescence was observed within the nucleus. The intensity plots of these images are also shown (Fig. 4.16 and 4.17, D and F).

The AHSV-2-NS3-eGFP protein appeared therefore to differ in its subcellular localisation to that of serotypes 3 and 4. While all three proteins were associated with the membranous components of the cell the AHSV-2-NS3-eGFP was additionally localised to the nucleus. The punctuate perinuclear and outer membrane fluorescence observed in all three cases is illustrated in the three dimensional image generated from cross-sections through a Sf9 cell infected with a recombinant baculovirus expressing AHSV-4-NS3-eGFP in Fig. 4.18. The perinuclear distribution

may represent localisation to the ER and/or Golgi, this would, however, have to be confirmed with stains and cellular markers for various cellular compartments or organelles.

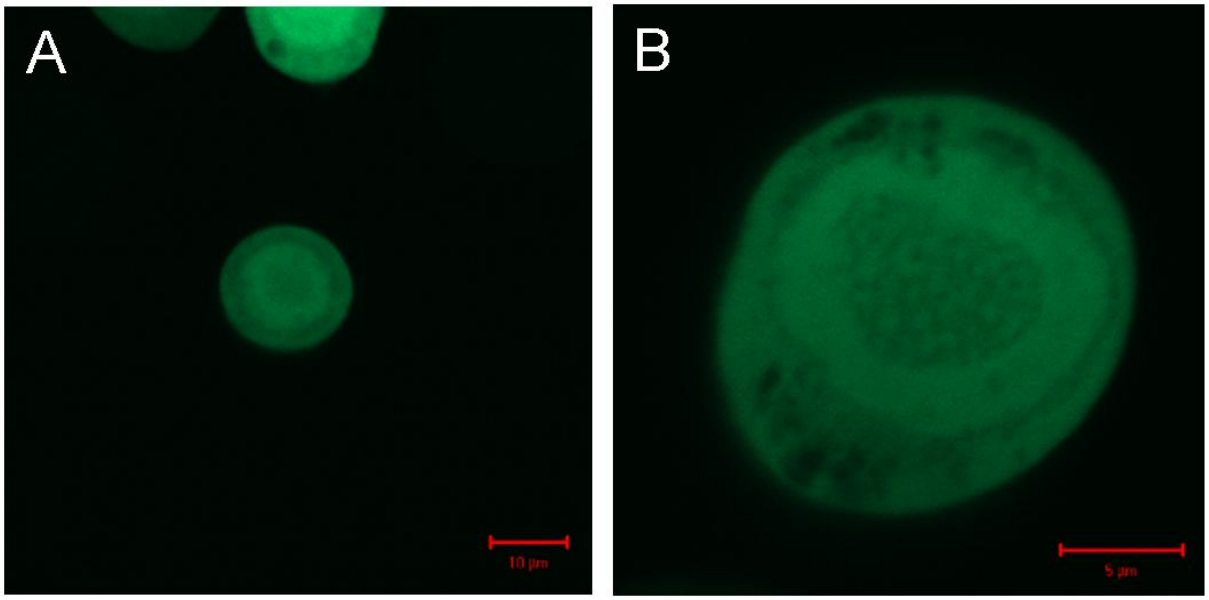

Fig. 4.14 Localisation of eGFP in Sf9 cells. Sf9 cells were infected with recombinant baculoviruses expressing eGFP and fluorescence visualised by live-cell confocal laser scanning microscopy at 30 h p.i. Cells were examined at 20x (A) and 63x (B) magnification. Size bars are included.

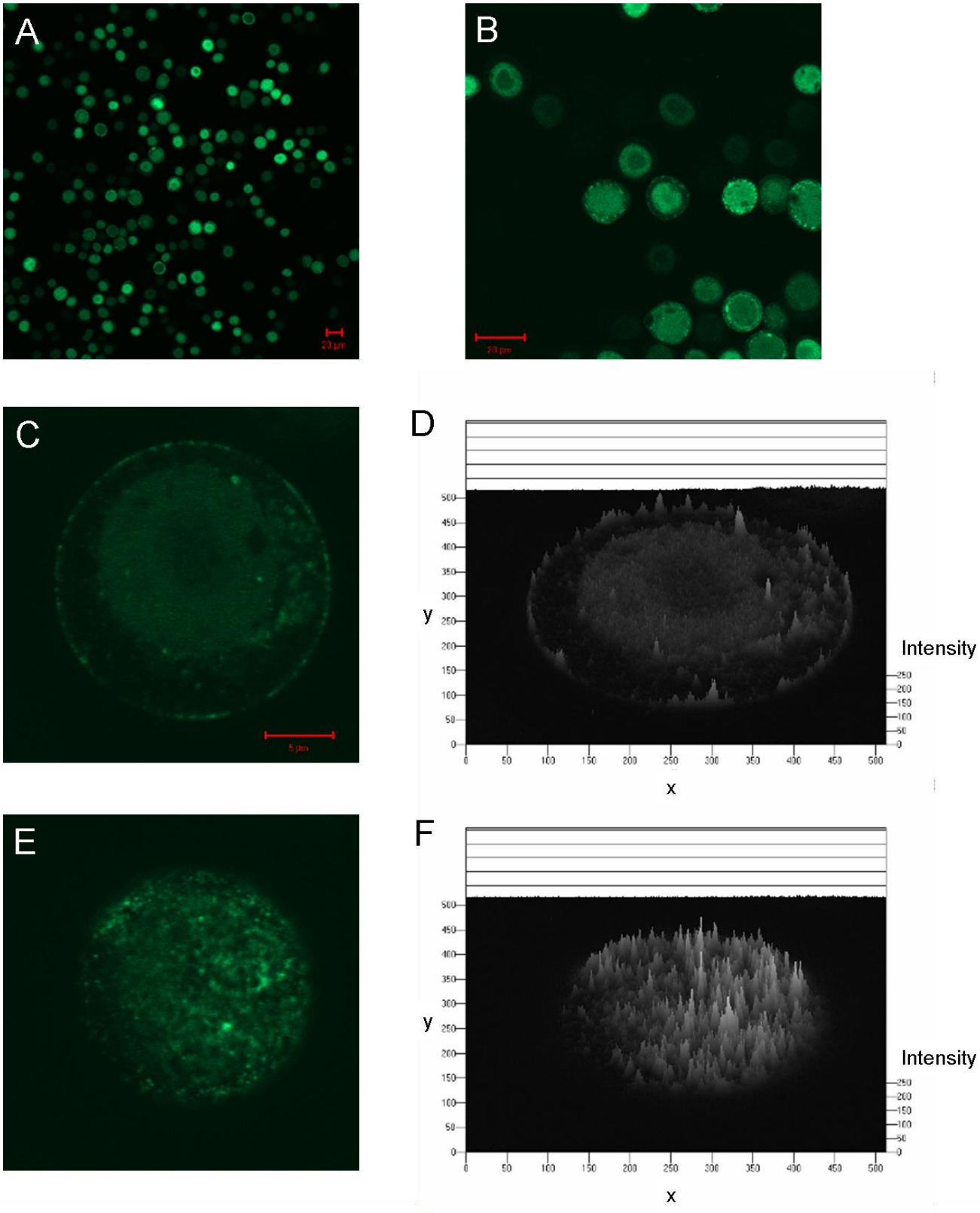

Fig. 4.15 Localisation of AHSV-2-NS3-eGFP in Sf9 cells. Sf9 cells were infected with recombinant baculoviruses expressing AHSV-2-NS3-eGFP and fluorescence visualised by live-cell confocal laser scanning microscopy at 30 h p.i. A cell was chosen that was representative of the localisation pattern observed at lower magnifications (A) and (B) and cross-sections scanned where (C) is a cross-section through the centre and (E) the outer surface of the cell. (D) and (F) are intensity plots of the images in (C) and (E) respectively. Size bars are included.

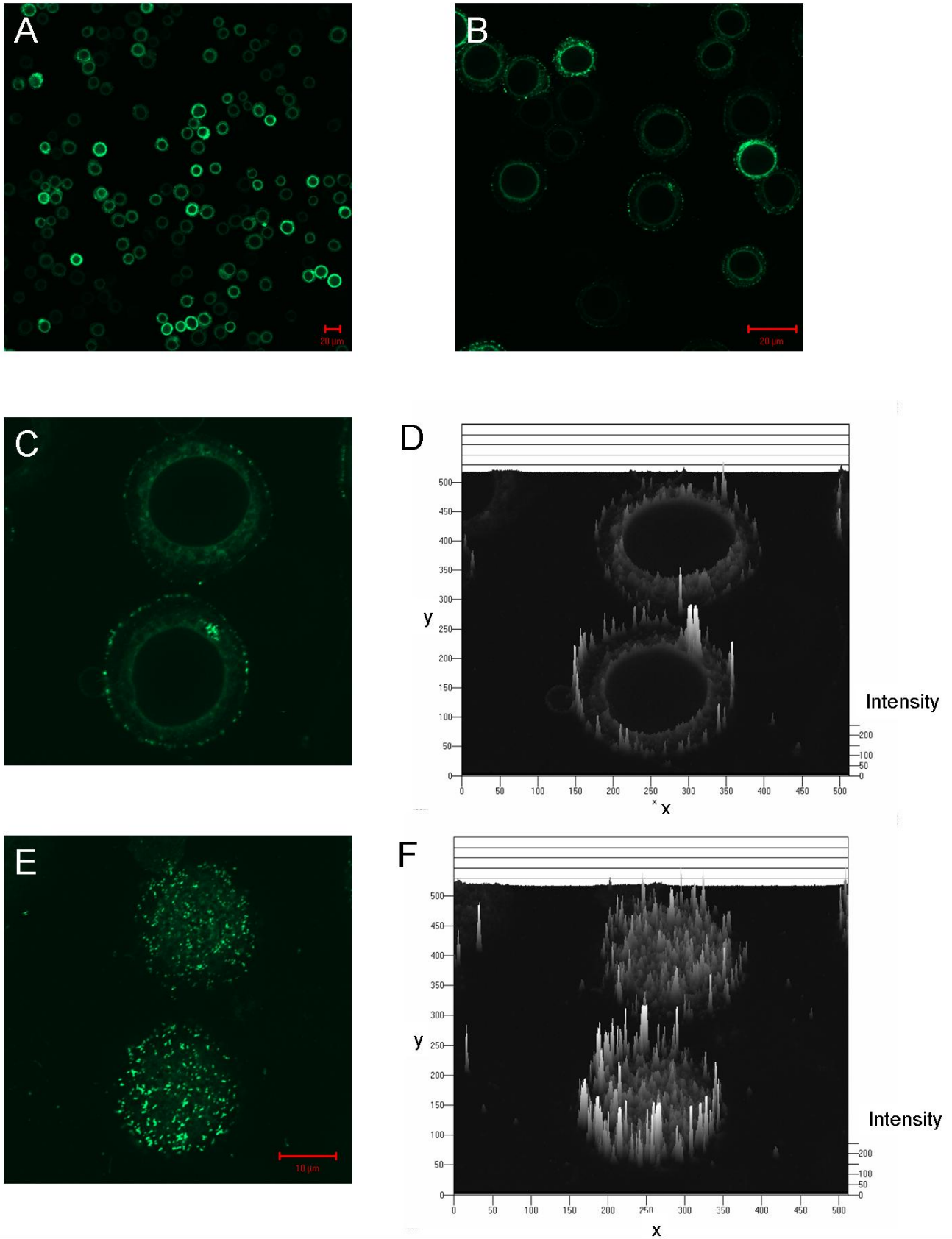

Fig. 4.16 Localisation of AHSV-3-NS3-eGFP in Sf9 cells. Sf9 cells were infected with recombinant baculoviruses expressing AHSV-3-NS3-eGFP and fluorescence visualised by live-cell confocal laser scanning microscopy at 30 h p.i. Cells that were representative of the localisation pattern observed at lower magnifications (A) and (B) were scanned and the cross-sections shown here are through the centre (C) and the outer surface (E) of the cells. (D) and (F) are intensity plots of the images in (C) and (E) respectively. Size bars are included.

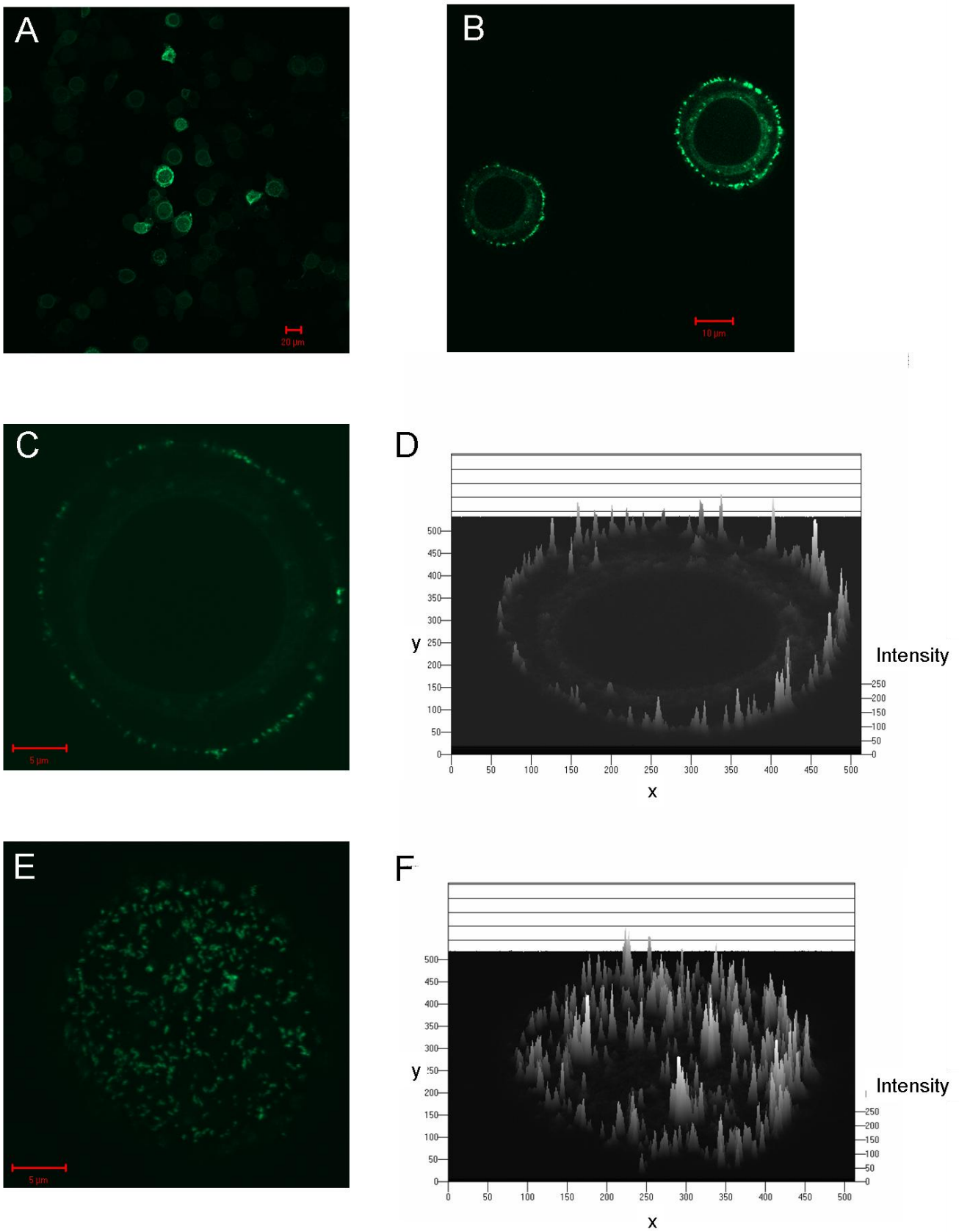

Fig. 4.17 Localisation of AHSV-4-NS3-eGFP in Sf9 cells. Sf9 cells were infected with recombinant baculoviruses expressing AHSV-4-NS3-eGFP and at 30 h p.i. fluorescence visualised by live-cell confocal laser scanning microscopy at 489 nm. A cell was chosen that was representative of the localisation pattern observed at lower magnifications (A) and (B) and cross-sections scanned, where (C) is the centre and (E) the outer surface of the cell. (D) and (F) are intensity plots of the images in (C) and (E) respectively. Size bars are included.

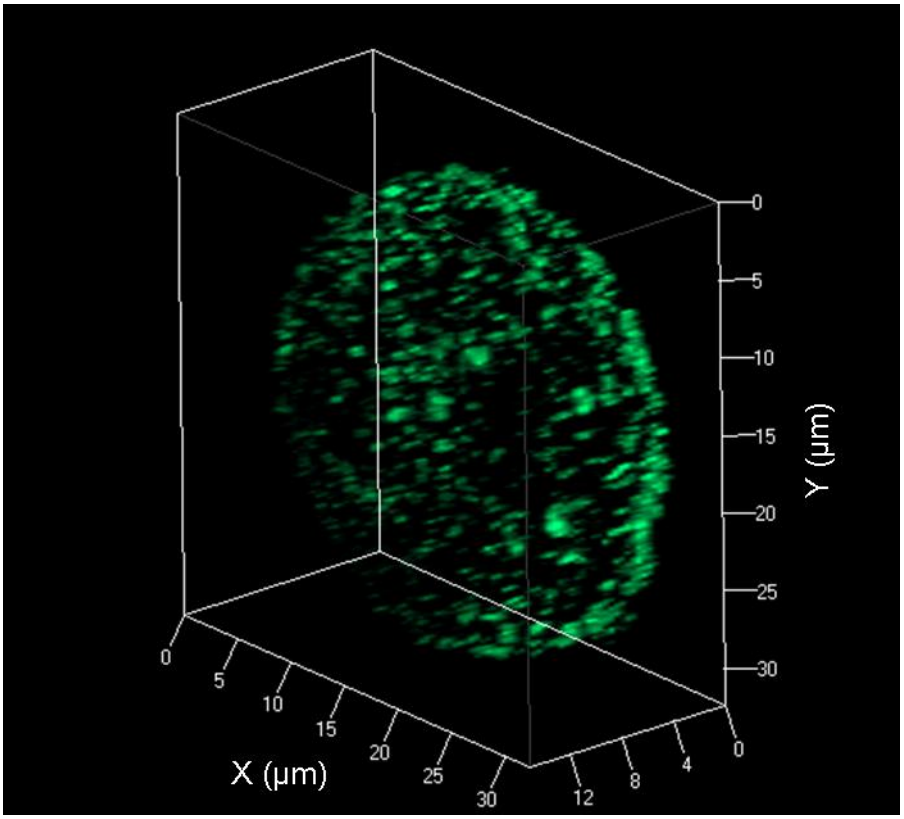

Fig. 4.18 Three dimensional image generated by the Zeiss LSM Image Browser software from cross-sections through a Sf9 cell infected with a recombinant baculovirus expressing AHSV-4-NS3-eGFP. Cross-sections were produced by confocal microscope laser scanning at 489 nm.

4.4. DISCUSSION

The central aim of this part of the study was to compare the γ, β, and α NS3 proteins encoded by AHSV-2, AHSV-3 and AHSV-4, respectively. This was done to ascertain whether the high level of variation in sequence between these NS3 proteins affected their structure or function in any way. Differences may then relate to the phenotypic differences observed in the viruses encoding these proteins in chapter 2.

As an initial means of comparing the NS3 proteins, amino acid sequence alignments were used to determine the percentage identity within conserved regions. Two regions of low identity were identified. The region between the first and second hydrophobic domains was found to have the lowest percentage identity between the NS3 proteins (18.8%). Quan and co-workers (2008) identified this region as being a highly variable hydrophilic region, under positive-selective pressure. This may be explained by the fact that this region is extracellular and therefore under immunological pressure. This variation is probably not significant in terms of structural and functional differences between the proteins. The first hydrophobic domain (HDI) was found to have the next lowest percentage identity (40.9%) between NS3 of the different serotypes. This domain is predicted to be membrane-spanning in AHSV-3 NS3 (Van Staden *et al.*, 1995) and mutations in this region abolished both the outer membrane targeting and cytotoxicity of NS3 in insect cells (Van Niekerk *et al.*, 2001a). In this study it was shown that this hydrophobic domain, together with HDII, is critical for membrane permeabilisation in *E. coli*. This variation may then potentially be significant in determining structural and functional differences, by impacting, for example, on the ability of this region to span the membrane. The amino acid sequences of the NS3 proteins were therefore compared using predictive algorithms (such as TMHMM) to determine the probability of the HDs forming transmembrane (TM) regions and the orientation of the predicted TM regions in lipid bilayers.

TMHMM analysis of the NS3 amino acid sequences of AHSV-2, AHSV-3 and AHSV-4 revealed interesting differences in both the membrane-spanning potential of the HDs and the orientation of these regions in the membrane. HDI in all three amino acid sequences had a high probability of spanning the membrane (approximately 1.0), while the probability of HDII forming TM regions was variable (ranging from 0.3 to 0.8). In all three cases HDI was orientated in the lipid bilayer such that the N-termini of the proteins would be cytoplasmically localised. Sequence differences in HDI of the three serotypes of NS3 therefore probably do not impact on the ability to span the membrane, and despite the variation, the overall nature of this region is hydrophobic in all three cases. Predictions for HDII were both non-membrane and membrane spanning. Other predictive algorithms, such as Phobius (http://www.cbs.dtu.dk/services/TMHMM-2.0/) or TMMOD (liao.cis.udel.edu/website/servers/TMMOD/) give similar variable probabilities for the formation of

a TM region by HDII. The variation in the probability of this region spanning the membrane impacted on the predicted orientation of this domain in the membrane. For the TMHMM analysis performed here the AHSV-2 and AHSV-3 NS3 HDII domains were not predicted to span the membrane with the result that the C-termini were located extracellularly. As the different predictive algorithms use different cut-off points for the probabilities, other programs predict a cytoplasmic localisation of the C-termini. These differences nonetheless raised several questions with regard to the membrane association and topology of the three NS3 proteins, and the impact this may have on the functions of the proteins, such as cytotoxicity. Several lines of investigation were therefore used here to examine the membrane association, membrane topology and cytotoxicity of the proteins as will be discussed later.

Further computational analysis of the NS3 proteins yielded an unexpected result. In the AHSV-2 (82/61) NS3 protein, used here as representative of the γ NS3 clade, a nuclear localisation signal was identified. The presence of this NLS was unique to AHSV-2 (82/61) NS3 and was not identified in other AHSV NS3 proteins, including that from other AHSV-2 strains. This prompted investigations into the subcellular localisations of the NS3 proteins, the results of which are outlined later in this discussion.

To investigate the significance, if any, of the potential differences revealed by computational analyses of the α, β, and γ NS3 proteins, the proteins were expressed and compared in the recombinant baculovirus expression system. As properties such as cytotoxicity and localisation were to be investigated the proteins were expressed as both wild-type recombinants and as eGFP fusions. Wild-type NS3 expressing recombinant baculoviruses were available and were used to examine differences in membrane permeabilisation, cytotoxicity, membrane association and membrane topology. Recombinant baculoviruses expressing AHSV-2 and AHSV-4 NS3 with C-terminal eGFP fusions (a recombinant expressing AHSV-3 NS3 as an eGFP fusion was available) were generated here and were used to examine the subcellular localisation of NS3. The expression of the NS3 proteins in the baculovirus system was confirmed by Western blot with antibodies specific to the AHSV-2, AHSV-3 and AHSV-4 NS3 proteins.

In chapter 2 it was shown that the membrane permeability of Vero cells infected with the parental viruses encoding AHSV-2, AHSV-3 and AHSV-4 NS3 differed. As the membrane permeabilising phenotype segregated with NS3 in reassortants, the effect of the AHSV-2, AHSV-3 and AHSV-4 NS3 proteins on Vero cell membrane permeability, in the absence of other AHSV proteins, was investigated here. Ideally to investigate this the proteins would have to be expressed as recombinants in these cells using a mammalian expression system. We however decided that for initial comparisons the NS3 proteins expressed in insect cells would be added to the extracellular media of healthy Vero cells and their effect on membrane permeability monitored. Similar

experiments using the exogenous addition of proteins to cells to study their membrane permeabilising capabilities are reported in the literature. For example, in a study by Madan et al. (2007) a synthetic soluble peptide representing the amino-terminal TM region of the picornavirus viroporin 2B was shown to produce the same permeabilisation effect when added exogenously to BHK cell monolayers as is observed during infection with picornavirus. This peptide, termed P3, was shown to insert into lipid bilayers and was located at the cell plasma membrane. In a similar peptide-based approach it was shown that extracellular 2B peptides had antimicrobial and antihaemolytic activities (Sánchez-Martínez *et al.*, 2008).

In this study the NS3 proteins were expressed in insect cells, crude lysates prepared and added exogenously to Vero cell monolayers. Membrane permeability was then monitored using a Hyg B assay and compared to cells treated with lysates from Sf9 cells infected with wild-type recombinant baculovirus. AHSV NS3, in the absence of other AHSV proteins, was shown to increase the permeability of Vero cell membranes, relative to wild-type lysate treated cells. Incubation in the presence of AHSV-2 NS3 resulted in the highest levels of membrane permeabilisation followed by AHSV-3, and then AHSV-4 NS3. This shows some similarity to the relative membrane permeabilisation levels of Vero cells infected with the different strains of AHSV, where AHSV-2 (or reassortants containing NS3 originating from AHSV-2) caused the greatest increase in permeability, followed by AHSV-3, and AHSV-4 had the least effect (see Table 2.5). This lends support to our hypothesis that different forms of AHSV NS3, originating from either the α, β or γ phylogenetic group, can differentially influence the membrane permeability of host cells. These differences may potentially be due to a variety of factors that affect the membrane association, stability within the membrane and levels of permeabilisation activity of the proteins, for example variation in the TM regions, degree of myristylation and stretches of positively charged amino acids. Crude lysates were used here as the AHSV NS3 proteins have never successfully been purified in a biologically active and soluble form. Further studies of the extracellular permeabilising effect of AHSV NS3 are complicated by the difficulties in purifying this protein as it is cytotoxic, expressed to low levels and highly insoluble. A similar peptide based approach as that discussed above for picornavirus 2B (Madan *et al.*, 2007; Sánchez-Martínez *et al.*, 2008), would therefore have to be used.

This assay also raises the question as to whether there is a soluble form of NS3 in the cell lysates that mediates the membrane permeabilising effect on Vero cells. In studies of rotavirus NSP4 two secreted forms of the protein have been identified, one is a soluble form of the protein which results from posttranslational modifications of NSP4 (Bugarcic & Taylor, 2006) and the other a small cleavage product of NSP4 (Zhang *et al.*, 2000). The 66 amino acid cleavage product of NSP4 has been shown to have enterotoxigenic properties (Zhang *et al.*, 2000). These forms are

proposed to mediate the diarrhoea inducing enterotoxic effect of NSP4 (Bugarcic & Taylor, 2006). The possibility of secreted and/or soluble forms of AHSV NS3 remains to be investigated.

As the α, β and γ NS3 proteins differed in their membrane permeabilising effect on Vero cells, we then examined the endogenous cytotoxic effect on insect cells expressing AHSV-2, AHSV-3 and AHSV-4 NS3 for differences. The viability of infected cells was monitored using a Trypan blue assay and all three proteins were found to cause an equivalently rapid and significant decline in cell viability. This cytotoxicity implies that all three proteins are membrane associated. This was investigated by discontinuous sucrose gradient centrifugation (or membrane flotation gradients) of lysates from cells infected with the recombinant baculoviruses. This method has been used to confirm the membrane association of a number of viral proteins including Dengue virus NS4B (Miller *et al.*, 2006) and influenza B virus BM2 protein (Paterson *et al.*, 2003). All three AHSV NS3 proteins were shown to be associated with the membranous components of the cell. The EEV NS3 protein was included in these assays and also shown to be membrane associated. This substantiates computer predictions of transmembrane regions within the protein and the finding that this protein has membrane permeabilising activity in bacterial cells (see chapter 3).

The finding that the NS3 proteins differed in their permeabilising effect on Vero cells but not in Sf9 cells highlights the importance of the target membrane in different assays. A similar finding was discussed in chapter 3 when comparing results from bacterial and insect cells. When compared to mammalian cells Sf9 cells have lower levels of sphingomyelin, higher levels of phosphatidylethanolamine and a lower cholesterol to phospholipid ratio (Marheineke *et al.*, 1998). The high cytotoxicity of NS3 in Sf9 cells may also be due to the higher level of expression of the protein (compared to levels observed in AHSV infected cells) under the control of the strong baculovirus polihedrin promoter. Studies of rotavirus NSP4 indicate that both cell type and context of expression affect the distribution of NSP4 (Bugarcic & Taylor, 2006). Extrapolations of findings in different cell systems should therefore be made with caution. It would be of interest to study the effect of endogenously expressed recombinant AHSV-2, AHSV-3 and AHSV-4 NS3 in mammalian cells.

TMHMM analyses of AHSV-4 NS3 predicted a double membrane-spanning topology, with both the N- and C-terminal regions of the protein located within the cytoplasm. In AHSV-2 and -3 NS3, however, only HDI was predicted to transverse the membrane with the result that the N-terminal is intracellular while the C-terminal is exposed on the surface of the cell. The N terminus of HCV NS4B has been reported to assume dual TM topology, with distinct functions on each side of the ER membrane (Lundin *et al.*, 2003). The hepatitis B virus surface L glycoprotein can act in virus assembly as a matrix-like protein and in virus entry as a receptor-binding protein by adopting different membrane topologies (Lambert & Prange, 2001). The Newcastle disease fusion protein

exists in two topological forms with respect to membranes, one of which has been proposed to be involved in cell-to-cell fusion (McGinnes *et al.*, 2003).

In this study we experimentally elucidated the membrane topology of NS3 using antibodies specific to the N- and C-terminus of the protein and examining the binding to fixed and unfixed (i.e. permeabilised and unpermeabilised) cells expressing NS3. Similar antibody based approaches have been used in to determine the topology of a number of viral membrane proteins, such as the E2p7 protein of hepatitis C virus (Isherwood & Patel, 2005), the BM2 protein of Influenza B virus (Paterson *et al.*, 2003) and gp41 of HIV-1 (Cheung *et al.*, 2005), and non-viral membrane proteins such as Nox 2 (Paclet *et al.*, 2004). In HIV-1 infected C8 166 cells and HeLa cells expressing recombinant gp41 it was shown, using an array of antibodies, that the C-terminal tail of gp41 is exposed on the cell surface (Cheung *et al.*, 2005). Antibodies to the N-terminal region of Nox 2 were shown to bind differentiated cell HL60 cells only after permeabilisation, indicating that the N-terminus of Nox 2 is cytoplasmically orientated (Paclet *et al.*, 2004).

For the production of site-specific antibodies, the N- and C-terminal regions of AHSV-2 NS3 were expressed as Glutathione S-tranferase (GST) fusion proteins in an inducible prokaryotic expression system (see chapter 3, 3.3.2.3.). Both the N- terminal and C-terminus fusion proteins were found to be expressed to high levels in a soluble form and were therefore suitable for affinity purification. Following binding of the GST-Tag to its substrate (glutathione bound to agarose resin) the NS3 peptides were cleaved from the GST-Tag using thrombin. Antibodies against these peptides were raised in chickens and shown to react with AHSV-2 NS3 in Western blots. These antibodies were then used in indirect immunofluorescent studies of fixed and unfixed Sf9 cells expressing AHSV-2 NS3. Polyclonal antibodies against full length NS3 were used as a positive control. Binding was detected with a FITC conjugated secondary antibody and cells viewed under a fluorescent microscope. In fixed cells binding of both the NS3 N- and C-terminal specific antibodies, as well as those directed against full length NS3, was observed. This confirmed both the expression of NS3 in these cells and the binding of the antibodies to NS3. In unfixed cells neither the NS3 N-terminal nor C-terminal specific antibodies bound, while antibodies against full length NS3 were detected on the cellular membrane. Neither the N- or C-terminal regions of AHSV-2 NS3 appeared therefore to be exposed on the surface of these cells.

This finding supports the computer-based topology predicted for AHSV NS3 by van Staden and coworkers (1995) with both hydrophobic domains forming transmembrane regions with the N- and C-termini cytoplasmically orientated. This model of NS3 should further our understanding of the mechanism of AHSV NS3-mediated virus release. The location of the N- and C-terminal regions in the cytoplasm may allow for their interaction with proteins in the cytoplasm, such as membrane trafficking proteins and proteins within the virus particle. A similar model has been experimentally

substantiated for BTV NS3 (Bansal *et al.*, 1998). In BTV NS3 it has been shown that the N-terminal region interacts with the cellular release factors, p11 and Tsg101 (Beaton *et al.*, 2002; Wirblich *et al.*, 2006), while the C-terminal region interacts with the outer capsid protein VP2 (Beaton *et al.*, 2002). BTV NS3 additionally binds to VP5, although the domain responsible has not been elucidated (Bhattacharya & Roy, 2008). The interactions between NS3 and these proteins form the basis for the model proposed of the NS3 mediated release of BTV from infected cells (Roy, 2008).

The subcellular localisation of the α, β and γ NS3 proteins in Sf9 cells was further examined here by fluorescent microscopic analysis of the proteins expressed as eGFP fusions. Using membrane flotation assays it was shown that these fusion proteins associated with the membranous components of the cell analogous to the wild-type NS3 proteins. The addition of the eGFP protein to the C-terminus of NS3 did not therefore influence the membrane association of the protein and the localisation of the NS3-eGFP fusion proteins should therefore be representative of wild-type NS3 localisation. The addition of the eGFP protein to NS3 allowed for direct fluorescent imaging of NS3 in live unfixed cells. Laser scanning confocal fluorescence microscopy was used to examine the localisation of the proteins within insect cells.

All three NS3-eGFP proteins were detected at the plasma membrane of cells as discrete foci of fluorescence. This concurs with previous immunofluorescent localisation studies in Sf9 cells, where NS3 was found to be associated with the outer membrane in unfixed cells (Van Niekerk *et al.*, 2001a). Cells displayed a uniform or homogenous fluorescence of the cell surface in contrast to the distinct areas of bright fluorescence observed here. This may represent localisation to specific domains within the cell membrane, such as lipid rafts. Both rotavirus NSP4 (Storey *et al.*, 2007) and BTV NS3 (Bhattacharya & Roy, 2008) have been shown to associate with lipid rafts, and this interaction may be important in the final assembly of progeny virions as well as transport and release of the virus from the cell.

A distinct punctuate perinuclear fluorescence was also observed for all three NS3-eGFP fusion proteins in Sf9 cells. This may represent localisation to the internal membrane systems within the cell, i.e. the ER, the ER-Golgi intermediate compartment (ERGIC) and/or the Golgi apparatus. The majority of eukaryotic integral membrane proteins are cotranslationally inserted into the ER membrane. The ER then serves as a gateway for proteins where they may then be targeted to particular cellular membranes, including all the compartments of the secretory pathway and the plasma membrane.

Studies of the localisation of viroporins have shown that the majority of the protein in cells resides intracellularly in the membranes of the ER, ERGIC and/or Golgi, while only a small amount can

be detected at the plasma membrane (Gonzalez & Carrasco, 2003). Examples of viroporins that show this localisation pattern include HIV-1 Vpu (Gonzalez & Carrasco, 2003), coronavirus E protein (Corse & Machamer, 2000; Nal *et al.*, 2005; Liao *et al.*, 2006) and enterovirus 2B protein (De Jong *et al.*, 2004; Sánchez-Martínez *et al.*, 2008). This localisation to the components of the secretory pathway may be significant to the functions of these viroporins.

In coronavirus the localisation to, and membrane permeabilising effect of, the E protein to the secretory pathway has been proposed to be involved in the mechanism by which this protein enhances virus release. The E protein is a small membrane permeabilising protein involved in the release of the virus from infected cells (Madan *et al.*, 2005a). Immunofluorescence staining of the E protein in coronavirus-infected cells, showed both a granular or punctuate fluorescence within cells and some fluorescence on the cell surface. This distribution within the cell was shown, in a variety of studies, to be association of the E protein with the ER, ER-Golgi intermediate and/or Golgi complex (Corse & Machamer, 2000; Nal *et al.*, 2005; Liao *et al.*, 2006). It was proposed that localisation of the E protein to the ER-Golgi intermediate and Golgi could disrupt ionic gradients in these compartments promoting the exit of the virus through the transport pathway, and this may be the mechanism by which the E protein enhances virus release (Liu *et al.*, 2007). In the case of HIV-1, the viroporin Vpu localises to the ER and Golgi, and to a lesser extent to the plasma membrane. In addition to its membrane permeabilising effect on the cell membrane, Vpu is thought to induce modification of the secretory pathway causing impaired trafficking of cellular membrane proteins (Gonzalez & Carrasco, 2003). The anti-apoptotic function of the enterovirus viroporin 2B has additionally been associated with its effects on the secretory pathway. Here the association of 2B with the ER and Golgi membrane and the subsequent membrane permeability increase results in a reduction in Ca^{2+} levels in these organelles. This perturbs the Ca^{2+} dependant apoptotic signalling that normally occurs between the ER and mitochondria, with the result that cell death is delayed and viral replication continues (Van Kuppeveld *et al.*, 2005).

Computational analysis revealed a potential nuclear localisation signal in the AHSV-2(82/61) NS3 amino acid sequence. Examination of the localisation of this protein, as an eGFP fusion, revealed that this protein was present in the nucleus. This localisation appears to be unique to AHSV-2(82/61) NS3, as an NLS was not predicted in any other NS3 proteins, and no nuclear localisation of AHSV-3 and AHSV-4 NS3-eGFP was observed. The biological significance of this, if any, remains to be investigated.

In summary, the preliminary results presented here show that the α, β and γ NS3 proteins potentially differ in their ability to permeabilise Vero cells. When expressed in insect cells the proteins show a similar subcellular localisation, association with membranes and cytotoxicity.

Although no significant differences between the recombinant α, β and γ NS3 proteins in insect cells could be identified, the findings presented here should form a good starting point for more detailed investigations. Of particular interest would be the potential association of NS3 with the secretory pathway, and association of the N- and C-terminal regions of NS3 with other viral proteins. This should then further our understanding of the role of NS3 in virus induced membrane permeabilisation and virus release.

CHAPTER 5: CONCLUDING REMARKS

The primary aim of this study was to further characterise the role that the AHSV NS3 protein plays in the AHSV life cycle and host cell interactions. In the first part of this study, the involvement of NS3 in several parameters during AHSV infection of mammalian cells, including virus yield, virus release, cytopathicity and membrane permeability, was examined. The strategy used to achieve this was based on *in vitro* reassortment of the genome segment 10 encoding NS3 between parental virus strains that showed quantitative differences in these parameters. The parental virus strains used during reassortment encoded NS3 proteins representative of each of the three NS3 phylogenetic clades (α, β and γ). Two parameters of these parental viruses, the amount of virus released and the degree of membrane permeabilisation induced, were found to be associated with the genome segment encoding NS3. The induction of cytopathic effects was not associated with NS3 alone and the results showed a possible involvement of NS3 together with NS1. Differences in the parental viruses such as their effect on cell viability and protein synthesis within cells could not be related to their encoded NS3 proteins. Each of these aspects, and their implications for future research, will be discussed here in the context of what is currently known about AHSV and the prototype orbivirus, BTV.

The finding that the amount of virus released was associated with NS3 is significant, as this influences the spread of the virus to other target cells within or between organs and so may have an impact on pathogenesis. This also agrees with a previous study by Martin *et al.* (1998) in which it was shown that viruses encoding NS3 from the β and γ clades differed in the timing of virus release. The role played by NS3 in the release mechanism of AHSV remains to be elucidated although it is likely to be similar to that proposed for BTV (Roy, 2008). AHSV may be released from mammalian cells by both a lytic or non-lytic budding mechanism (Stoltz *et al.*, 1996). It would be of interest to investigate whether the ratio of lytic to non-lytic release in these cells is affected by the different NS3 proteins. Another intriguing question in orbivirus research is the differences in release in mammalian and insect cells. In BTV-infected mammalian cells mature virions remain cell-associated, as has been commonly observed with reoviruses and, in the majority, are released by cell lysis. This may explain the high levels of CPE observed in BTV-infected mammalian cells. However, there is also support for the egress of virions as enveloped particles by budding at the cell membrane (Hyatt *et al.*, 1989). In insect cells virus release occurs mainly by budding in both AHSV and BTV, and although persistent infections are established no apparent CPE is observed (Eaton *et al.*, 1990; Martin *et al.*, 1998). This may be due to a number of factors, including the mechanism of virus release. It would be interesting to compare the mode of release of the parental and reassortant strains in mammalian and insect cells. This could be achieved by ultrastructural electron microscopic investigations of infected cells.

Vero cells infected with viruses encoding the NS3 proteins from the α, β and γ clades also showed distinct differences in membrane permeability. Using reassortants these differences

could clearly be associated with NS3. This lends support to the classification of NS3 as a viroporin. Membrane permeabilisation may impact both the virus and the infected cell as reviewed in chapter 1. Several factors may also influence viroporin permeabilisation activity including cell type, other functions of the protein and interactions with other viral or host proteins. Many viroporins are multifunctional and the other activities or functions of the protein may affect their permeabilisation activity. For example, picornavirus 3A blocks ER-to-Golgi transport of cellular proteins and may therefore prevent targeting of 3A itself to plasma membrane. Other viral proteins may also directly or indirectly affect viroporin activity in a variety of ways such as being necessary for the localisation of the viroporin to the plasma membrane, or having anti- or pro-apoptotic functions themselves (Madan *et al.*, 2008). The activity of viroporins may therefore be weakened or enhanced in the context of viral infection. Differences observed in the membrane permeabilising effects of the α, β and γ NS3 proteins may then be directly due to differences in their membrane permeabilisation activities and/or due to differences in their interactions with other viral or host proteins that affect their membrane permeabilising properties.

The cytopathic effect on Vero cells of the reassortant viruses generated here could not be associated with NS3 alone, but possibly with both NS3 and NS1. In BTV it is thought that NS1 could be a major determinant of cytopathogenesis, and that modifying the ratio of NS1 to NS3 can shift the mechanism of viral release from a lytic process to one of non-lytic budding from the cell surface (Owens *et al.,* 2004). The possible involvement of NS3 and NS1 in AHSV cytopathology, and the relative levels of expression of AHSV NS1 and NS3 in the different strains, should be investigated. NS3 is probably a component of a complex system influencing cytopathology involving virus tropism, the velocity of virus replication and release. Also affecting this would be host cell factors, in a recent study it was shown that 250 host factors or proteins are required during HIV-1 infection (Brass *et al.*, 2008). The cell innate defence responses such as apoptosis, the interferon response and RNA interference (De Vries *et al.*, 2008) may additionally be involved.

Although genomic reassortment studies have provided important information for many segmented viruses, this approach does have some drawbacks. This includes the necessity to screen large numbers of progeny viruses from crosses to identify reassortants and the unexplained preferential selection of certain genome segments. The recent development of a reverse genetics system for BTV (Boyce *et al.*, 2008) should makes it feasible to in future design and recover viruses containing specific mutations, or reassortants with desired combinations of gene segments. The use of RNA interference techniques should also prove useful in providing key information, as has been shown for rotavirus (Zambrano *et al.*, 2008). For studies as to the specific role played by each of the viral proteins in the viral life cycle it would also be more appropriate to use equine endothelial and *Culicoides* cell lines.

In chapter 3 the AHSV-2 (γ) NS3 protein was expressed as a recombinant in an inducible prokaryotic system that has been found to be ideally suited to the identification and analysis of virally-encoded membrane active proteins (Studier, 1991; Browne *et al.*, 2000). The results showed that NS3 was cytolytic to these cells and this activity could be related to membrane permeabilisation induced by the protein. A series of truncated AHSV-2 NS3 mutants were additionally expressed and analysed in this same system, and the results indicated that the HDs within the protein are responsible for this activity and that the presence of both HDs is critical to this. The full length AHSV-2 NS3 protein was also compared to BTV and EEV NS3 in this system. Differences in the cytolytic and membrane permeabilising activities were observed that, although cannot be related to the activities of these proteins in host cells, imply potential differences in structural stability and association with membranes of specific cell types, which in turn may impact on cytotoxicity

In chapter 4 the NS3 proteins from AHSV-2, AHSV-3 and AHSV-4 (i.e. from the γ, β and α NS3 clades) were expressed in the BAC-TO-BAC expression system as both wild-type proteins and C-terminal eGFP (enhanced green fluorescent protein) fusions. The potential impact of the sequence variation between these NS3 proteins on structure and function was then examined by comparing properties such as membrane permeabilisation, cytotoxicity, membrane association and localisation. As an initial comparison, the membrane permeabilising effect of the baculovirus expressed wild-type NS3 on Vero cells following exogenous addition was monitored. The α, β and γ NS3 proteins differed in their permeabilisation effect on Vero cells in a manner that could linked to that induced by the parental AHSV strains encoding these proteins. To further explore these apparent differences in permeabilising activity of the NS3 proteins, the effect on insect cell viability following *in vivo* recombinant expression was compared. Trypan blue viability assays showed that, in this system, all three proteins were equivalently cytotoxic. Membrane association assays additionally revealed that all three proteins associated with the membranous components of these cells. Future experiments to compare these proteins could be carried out in a mammalian cells through the use of an inducible recombinant expression system. The association of NS3 with the permeabilising properties of the parental and reassortant virus generated in this study could also be analysed by investigating the effect of siRNA knockdown of NS3 expression during AHSV infection of Vero cells. This technique had been used with great success by Zambrano and coworkers (2008) to examine the role of NSP4, and other viral proteins, in rotavirus induced permeabilisation of cells. Additionally the targeting of NS3 to the outer membrane in AHSV infected cells could be abrogated through the use of the membrane traffic inhibitor, Brefeldin A, and the effect on membrane permeabilisation monitored. In this case indirect immunofluorescent labelling of NS3 with monospecific antibodies could be used to

confirm blocking of the outer membrane targeting of NS3. This type of approach is described by Ruiz *et al.* (2005).

In this study the subcellular localisation of the AHSV-2, AHSV-3 and AHSV-4 NS3 proteins was examined through recombinant expression as C-terminal eGFP fusions in the baculovirus expression system. Live cell confocal imaging of infected insect cells showed that NS3 localised to the plasma membrane, and as distinct punctuate foci in the perinuclear region. This suggests localisation to the internal membrane systems of cells and would require further investigation. This could be achieved by co-localisation studies via immunfluorescent labelling of NS3 and specific cellular markers in AHSV infected cells. As outlined in the discussion in chapter 4, localisation to the ER, ERGIC and/or Golgi may have important implications for the function of AHSV NS3 during the viral life cycle. In a study by Bansal and coworkers (1998) BTV NS3 was was also found to be localised to the ER and Golgi.

In summary, NS3 plays a role in virus release, membrane permeabilisation and cytopathology making it a multifunctional pleiotropic protein in the virus life cycle. A greater understanding of the factors and events that contribute to the virulence and pathogenesis of AHSV are vital in developing strategies that may prevent, or lesser the impact of, African horsesickness disease.

Parts of the results presented in this thesis have been published:

Meiring, T.L., Huismans, H. and van Staden, V. (2009). Genome segment reassortment identifies non-structural protein NS3 as a key protein in African horsesickness virus release and alteration of membrane permeability. *Arch Virol* **154**, 263-271.

Parts of the results presented in this thesis are in preparation for publication:

Meiring, T.L., Teixeira, L., Fick, W.C., Huismans, H. and van Staden, V. Membrane destabilising activity of the orbivirus non-structural protein NS3 is mediated by the transmembrane domains. To be submitted.

Non-peer reviewed publication:

Huismans, H., van Staden, V., Fick, W.C., van Niekerk, M., Meiring, T.L. 2004. A comparison of different orbivirus proteins that could affect virulence and pathogenesis. *Vet Ital* **40**, 417-425

Parts of the results in thesis have been presented at scientific meetings:

NATIONAL CONFERENCES:

Van de Merwe, E., R. van der Sluis, T.L. Meiring, A.N. Hall, H. Huismans, V. van Staden. 2008. Conserved residues in non-structural protein NS3 of African horsesickness virus influence subcellular localisation. Microscopy Society of Southern Africa (MSSA), July 2008, Gabarone, Botswana (Presentation)

Meiring, T.L., Huismans, H., van Staden, V. 2008. Using genetic reassortants of African horsesickness virus (AHSV) to study the role of non-structural protein NS3 in viral phenotypic properties in Vero cells. 20th Congress of the South African Genetics Society (SAGS), April 2008, Pretoria, RSA. (Presentation)

Meiring, T.L, van Staden, V., Huismans, H. 2006. Correlating the cytolytic effect of viral infection and single viral protein expression for three orbiviruses. 19th Congress of the SAGS, April 2006, Bloemfontein, RSA. (Presentation)

Meiring, T.L, Teixeira, L., Fick, W.C., van Staden, V., Huismans, H. 2005. Identification of regions of non-structural protein NS3 involved in membrane destabilisation in different orbiviruses. South African Society for Biochemistry and Molecular Biology XIX th Conference, January 2005, Stellenbosch, RSA. (Poster)

Meiring, T.L, Teixeira, L., Fick, W.C., van Staden, V., Huismans, H. 2004. Membrane destabilisation activity of non-structural protein 3 (NS3) of different orbiviruses. Combined South African Society of Microbiology and 18th SAGS congress, April 2004, Stellenbosch, RSA. (Poster)

INTERNATIONAL CONFERENCES:

Tracy Meiring, Henk Huismans and Vida van Staden 2008. Using African horse sickness virus reassortants to study the role of non-structural protein NS3 in several phenotypic properties of the virus. XIV International Virology Congress, International Union of Microbiological Sciences, August 2008, Istanbul, Turkey. (Presentation)

Tracy Meiring, Henk Huismans and Vida van Staden 2006. Membrane topology of African horsesickness virus non-structural protein NS3. 9th dsRNA Virus Symposium, October 2006, Cape Town, RSA. (Poster)

Vida van Staden, Tracy Meiring, Wilma Fick and Henk Huismans 2005. Cytotoxicity and membrane permeabilising activity of non-structural protein NS3 of different orbiviruses. Virology Africa, November 2005, Cape Town, RSA. (Presentation)

Vida van Staden, Tracy Meiring, Luisa Teixeira, Wilma Fick and Henk Huismans 2005. Membrane destabilization activity of non-structural protein NS3 of different orbiviruses. XIII International Virology Congress, International Union of Microbiological Sciences, July 2005, San Francisco, USA. (Poster)

Vida van Staden, Michelle van Niekerk, Tracy Meiring and Henk Huismans 2003. The effect of sequence variation in AHSV non-structural protein NS3 on viral and protein phenotypic properties. 3rd International Symposium on Bluetongue, 26 to 29 October 2003, Taormina, Italy. (Presentation)

Van Staden, V., van Niekerk, M, Meiring, T.L., Huismans, H. 2003. An investigation into the effect of sequence variation in AHSV non-structural protein NS3 on viral and protein phenotypic properties. 8th International Symposium on Double-Stranded RNA viruses, September 2003, Lucca, Italy. (Presentation)

Huismans, H., van Staden, V., Fick, W.C., van Niekerk, M., Meiring, T.L. 2003. A comparison of different orbivirus proteins that could affect virulence and pathogenesis. Bluetongue virus Workshop 2003, Sardinia, Italy. (Presentation)

REFERENCES

Aldabe, R., Barco, A. & Carrasco, L. (1996). Membrane permeabilization by poliovirus proteins 2B and 2BC. *J Biol Chem* **271**, 23134-23137.

Arroyo, J., Boceta, M., González, Michel, M. & Carrasco, L. (1995). Membrane permeabilization by different regions of the human immunodeficiency virus type 1 transmembrane glycoprotein gp41. *J Virol* **69**, 4095-4102.

Au, K. S., Mattion, N. M. & Estes, M. K. (1993). A subviral particle binding domain on the rotavirus nonstructural glycoprotein NS28. *Virology* **194**, 665-673.

Balasuriya, U. B., Nadler, S. A., Wilson, W. C., Pritchard, L. I., Smythe, A. B., Savini, G., Monaco, F., de Santis, P., Zhang, N., Tabachnick, W. J. & MacLachlan, N. J. (2008). The NS3 proteins of global strains of bluetongue virus evolve into regional topotypes through negative (purifying) selection. *Vet Microbiol* **126**, 91-100.

Ball, J. M., Tian, P., Zeng, C. Q., Morris, A. P. & Estes, M. K. (1996). Age-dependent diarrhea induced by a rotaviral nonstructural glycoprotein. *Science* **272**, 101-104.

Bansal, O. B., Stokes, A., Bansal, A., Bishop, D. & Roy, P. (1998). Membrane organization of bluetongue virus non-structural glycoprotein NS3. *J Virol* **72**, 3362-3369.

Batten, C. A., Maan, S., Shaw, A. E., Maan, N. S. & Mertens, P. P. (2008). A European field strain of bluetongue virus derived from two parental vaccine strains by genome segment reassortment. *Virus Res*.

Beaton, A. R., Rodriguez, J., Reddy, Y. K. & Roy, P. (2002). The membrane trafficking protein calpactin forms a complex with bluetongue virus protein NS3 and mediates virus release. *Proc Natl Acad Sci U S A* **99**, 13154-13159.

Bechinger, B. (2008). A dynamic view of peptides and proteins in membranes. *Cell Mol Life Sci* **19**, 3028-3039.

Bentley, L., Fehrsen, J., Jordaan, F., Huismans, H. & du Plessis, D. H. (2000). Identification of antigenic regions on VP2 of African horsesickness virus serotype 3 by using phage-displayed epitope libraries. *J Gen Virol* **81**, 993-1000.

Berkova, Z., Crawford, S. E., Blutt, S. E., Morris, A. P. & Estes, M. K. (2007). Expression of rotavirus NSP4 alters the actin network organization through the actin remodeling protein cofilin. *J Virol* **81**, 3545-3553.

Berkova, Z., Crawford, S. E., Trugnan, G., Yoshimori, T., Morris, A. P. & Estes, M. K. (2006). Rotavirus NSP4 induces a novel vesicular compartment regulated by calcium and associated with viroplasms. *J Virol* **80**, 6061-6071.

Berkova, Z., Morris, A. P. & Estes, M. K. (2003). Cytoplasmic calcium measurement in rotavirus enterotoxin-enhanced green fluorescent protein (NSP4-EGFP) expressing cells loaded with Fura-2. *Cell Calcium* **34**, 55-68.

Bhattacharya, B. & Roy, P. (2008). Bluetongue virus outer capsid protein VP5 interacts with membrane lipid rafts via a SNARE domain. *J Virol* **82**, 10600–10612.

Bodelón, G., Labrada, L., Martínez-Costas, J. & Benavente, J. (2002). Modification of late membrane permeability in avian reovirus-infected cells. *J Biol Chem* **277**, 17789-17796.

Borghan, M. A., Mori, Y., El-Mahmoudy, A. B., Ito, N., Sugiyama, M., Takewaki, T. & Minamoto, N. (2007). Induction of nitric oxide synthase by rotavirus enterotoxin NSP4: implication for rotavirus pathogenicity. *J Gen Virol* **88**, 2064-2072.

Bowie, J. U. (2005). Solving the membrane protein folding problem. *Nature* **438**, 581-589.

Boyce, M., Celma, C. C. & Roy, P. (2008). Development of reverse genetics systems for bluetongue virus: recovery of infectious virus from synthetic RNA transcripts. *J Virol* **82**, 8339-8348.

Brass, A. L., Dykxhoorn, D. M., Benita, Y., Yan, N., Engelman, A., Xavier, R. J., Lieberman, J. & Elledge, S. J. (2008). Identification of host proteins required for HIV infection through a functional genomic screen. *Science* **319**, 921-926.

Bremer, C. W. (1976). A gel electrophoretic study of the protein and nucleic acid components of African horsesickness virus. *Onderstepoort J Vet Res* **43**, 193-199.

Brignati, M. J., Loomis, J. S., Wills, J. W. & Courtney, R. J. (2003). Membrane association of VP22, a herpes simplex virus type 1 tegument protein. *J Virol* **77**, 4888–4898.

Briones, C., de Vicente, A., Molina-París, C. & Domingo, E. (2006). Minority memory genomes can influence the evolution of HIV-1 quasispecies *in vivo*. *Gene* **384**, 129-138.

Browne, E. P., Bellamy, A. R. & Taylor, J. A. (2000). Membrane-destabilizing activity of rotavirus NSP4 is mediated by a membrane-proximal amphipathic domain. *J Gen Virol* **81**, 1955-1959.

Bugarcic, A. & Taylor, J. A. (2006). Rotavirus nonstructural glycoprotein NSP4 is secreted from the apical surfaces of polarized epithelial cells. *J Virol* **80**, 12343-12349.

Burrage, T. G. & Laegried, W. W. (1994). African horse sickness: pathogenesis and immunity. *Comp Immunol Microbiol Infect Dis* **17**, 275-285.

Burrage, T. G., Trevejo, R., Stone-Marschat, M. & Laegreid, W. W. (1993). Neutralizing epitopes of African horsesickness virus serotype 4 are located on VP2. *Virology* **196**, 799-803.

Butan, C., van der Zandt, H. & Tucker, P. A. (2004). Structure and assembly of the RNA binding domain of bluetongue virus non-structural protein 2. *J Biol Chem* **279**, 37613-37621.

Carrasco, L. (1995). Modification of membrane permeability by animal viruses. *Adv Virus Res* **45**, 61-112.

Cheung, L., McLain, L., Hollier, M. J., Reading, S. A. & Dimmock, N. J. (2005). Part of the C-terminal tail of the envelope gp41 transmembrane glycoprotein of human immunodeficiency virus type 1 is exposed on the surface of infected cells and is involved in virus-mediated cell fusion. *J Gen Virol* **86**, 131-138.

Chuma, T., Le Blois, H., Sanchez-Vizcaino, J. M., Diaz-Laviada, M. & Roy, P. (1992). Expression of the major core antigen VP7 of African horsesickness virus by a recombinant baculovirus and its use as a group-specific diagnostic reagent. *J Gen Virol* **73 (Pt 4)**, 925-931.

Chwetzoff, S. & Trugnan, G. (2006). Rotavirus assembly: an alternative model that utilizes an atypical trafficking pathway. *Curr Top Microbiol Immunol* **309**, 245-261.

Ciarlet, M., Liprandi, F., Conner, M. E. & Estes, M. K. (2000). Species specificity and interspecies relatedness of NSP4 genetic groups by comparative NSP4 sequence analyses of animal rotaviruses. *Arch Virol* **145**, 371-383.

Ciccaglione, A. R., Costantino, A., Marcantinio, C., Equestre, M., Geraci, A. & Rapicetta, M. (2001). Mutagenesis of hepatitus C virus E1 protein affects its membrane-permeabilizing activity. *J Gen Virol* **82**, 2243-2250.

Ciccaglione, A. R., Marcantinio, C., Costantino, A., Equestre, M., Geraci, A. & Rapicetta, M. (1998). Hepatitis C virus E1 protein induces modification of membrane permeability in *E. coli* cells. *Virology* **250**, 1-8.

Coetzer, J. A. & Erasmus, B. J. (1994). African horsesickness. In *Infectious Diseases of Livestock with Special Reference to Southern Africa*, pp. 460-475. Edited by J. A. Coetzer, C. R. Thomson & R. C. Tustin. New York: Oxford University Press.

Coetzer, J. A. W. & Guthrie, A. J. (2004). African horsesickness. In *Infectious Diseases Of Livestock*, pp. 1231-1246. Edited by J. A. W. Coetzer & R. C. Tustin. Cape Town: Oxford University Press.

Cokol, M., Nair, R. & Rost, B. (2000). Finding nuclear localization signals. *EMBO Rep* **1**, 411-415.

Corse, E. & Machamer, C. E. (2000). Infectious bronchitis virus E protein is targeted to the Golgi complex and directs release of virus-like particles. *J Virol* **74**, 4319 - 4326.

Cowley, J. A. & Gorman, B. M. (1987). Genetic reassortants for identification of the genome segment coding for the bluetongue virus hemagglutinin. *J Virol* **61**, 2304-2306.

Cuadras, M. A., Bordier, B. B., Zambrano, J. L., Ludert, J. E. & Greenberg, H. B. (2006). Dissecting rotavirus particle-raft interaction with small interfering RNAs: insights into rotavirus transit through the secretory pathway. *J Virol* **80**, 3935-3946.

De Jong, A. S., Melchers, W. J. G., Glaudemans, D. H. R. F., Peter H. G. M. Willems & van Kuppeveld, F. J. M. (2004). Mutational analysis of different regions in the coxsackievirus 2B protein. *J Biol Chem* **279**, 19924–19935.

De Jong, A. S., Wessels, E., Dijkman, H. B. P. M., Galama, J. M. D., Melchers, W. J. G., Willems, P. H. G. M. & van Kuppeveld, F. J. M. (2003). Determinants for membrane association and permeabilization of the coxsackievirus 2B protein and the identification of the golgi complex as the target organelle. *J Biol Chem* **278**, 1012–1021.

De Vries, W., Haasnoot, J., van der Velden, J., van Montfort, T., Zorgdrager, F., Paxton, W., Cornelissen, M., van Kuppeveld, F., de Haan, P. & Berkhout, B. (2008). Increased virus replication in mammalian cells by blocking the intracelleluar innate defence responses. *Gene Therapy* **15**, 545-552.

De Waal, P. J. & Huismans, H. (2005). Characterization of the nucleic acid binding activity of inner core protein VP6 of African horse sickness virus. *Arch Virol* **150**, 2037-2050.

DeDiego, M. L., Álvarez, E., Almazán, F., Rejas, M. T., Lamirande, E., Roberts, A., Shieh, W., Zaki, S. R., Subbarao, K. & Enjuanes, L. (2007). A severe acute respiratory syndrome coronavirus that lacks the E gene is attenuated in vitro and in vivo. *J Virol* **81**, 1701-1713.

Delmas, O., Durand-Schneider, A. M., Cohen, J., Colard, O. & Trugnan, G. (2004a). Spike protein VP4 assembly with maturing rotavirus requires a postendoplasmic reticulum event in polarized caco-2 cells. *J Virol* **78**, 10987-10994.

Delmas, O., Gardet, A., Chwetzoff, S., Breton, M., Cohen, J., Colard, O., Sapin, C. & Trugnan, G. (2004b). Different ways to reach the top of a cell. Analysis of rotavirus assembly and targeting in human intestinal cells reveals an original raft-dependent, Golgi-independent apical targeting pathway. *Virology* **327**, 157-161.

DeMaula, C. D., Jutila, M. A., Wilson, D. W. & MacLachlan, N. J. (2001). Infection kinetics, prostacyclin release and cytokine-mediated modulation of the mechanism of cell death during bluetongue virus infection of cultured ovine and bovine pulmonary artery and lung microvascular endothelial cells. *J Gen Virol* **82**, 787-794.

DeMaula, C. D., Leutenegger, C. M., Jutila, M. A. & MacLachlan, N. J. (2002). Bluetongue virus-induced activation of primary bovine lung microvascular endothelial cells. *Vet Immunol Immunopathol* **86**, 147-157.

Dennehy, P. H. (2008). Rotavirus vaccines: an overview. *Clin Microbiol Rev* **21**, 198-208.

Devaney, M. A., Kendall, J. & Grubman, M. J. (1988). Characterization of a nonstructural phosphoprotein of two orbiviruses. *Virus Res* **11**, 151-164.

Domingo, E., Escarmis, C., Sevilla, N., Moya, A., Elena, S. F., Quer, J., Novella, I. S. & Holland, J. J. (1996). Basic concepts in RNA virus evolution. *FASEB Journal* **10**, 859-864.

Domingo, E. & Holland, J. J. (1997). RNA virus mutations and fitness for survival. *Annu Rev Microbiol* **51**, 151-178.

Dowling, W., Denisova, E., Lamonica, R. & Mackow, E. (2000). Selective membrane permeabilization by the rotavirus VP5 protein is abrogated by mutations in an internal hydrophobic domain *J Virol* **74**, 6368-6376.

Du Plessis, M., Cloete, M., Aitchison, H. & van Dijk, A. A. (1998). Protein aggregation complicates the development of baculovirus-expressed African horsesickness virus serotype 5 VP2 subunit vaccines. *Onderstepoort J Vet Res* **65**, 321-329.

Eaton, B. T., Hyatt, A. D. & Brookes, S. M. (1990). The replication of bluetongue virus. *Curr Top Microbiol Immunol* **162**, 89-118.

Erasmus, B. J. (1998). African horse sickness. In *US Animal Health Association, Committee on Foreign Animal Disease Foreign animal diseases: the gray book*, 6 edn, p. Part IV. Richmond, VA: US Animal Health Assoc.

Estes, M. K. (2001). Rotaviruses and their replication. In *Fields virology*, 4 edn, pp. 1747–1785. Edited by D. M. Knipe, P. M. Howley, D. E. Griffin, R. A. Lamb, M. A. Martin, B. Roizman & S. E. Straus. Philadelphia, PA: Lippincott Williams & Wilkins.

Fillmore, G. C., Lin, H. & Li, J. K. (2002). Localization of the single-stranded RNA-binding domains of bluetongue virus nonstructural protein NS2. *J Virol* **76**, 499-506.

Firth, A. E. (2008). Bioinformatic analysis suggests that the Orbivirus VP6 cistron encodes an overlapping gene. *Virol J* **5**, 48.

Forzan, M., Marsh, M. & Roy, P. (2007). Bluetongue virus entry into cells. *J Virol* **81**, 4819-4827.

Forzan, M., Wirblich, C. & Roy, P. (2004). A capsid protein of nonenveloped Bluetongue virus exhibits membrane fusion activity. *Proc Natl Acad Sci U S A* **101**, 2100-2105.

Franco, R., Bortner, C. D. & Cidlowski, J. A. (2006). Potential roles of electrogenic ion transport and plasma membrane depolarization in apoptosis. *J Membr Biol* **209**, 43–58.

French, T. J., Inumaru, S. & Roy, P. (1989). Expression of two related non-structural proteins of bluetongue virus (BTV) type 10 in insect cells by a recombinant baculovirus: Production of polyclonal ascitic fluid and characterization of the gene product in BTV-infected BHK cells. *J Virol* **63**, 3270-3278.

Garry, R. F., Bishop, J. M., Parker, S., Westbrook, K., Lewis, G. & Waite, M. R. (1979). Na^+ and K^+ concentrations and the regulation of protein synthesis in Sindbis virus-infected chick cells. *Virology* **96**, 108-120.

Ghosh, M. K., Borca, M. V. & Roy, P. (2002a). Virus-derived tubular structure displaying foreign sequences on the surface elicit CD4+ Th cell and protective humoral responses. *Virology* **302**, 383-392.

Ghosh, M. K., De'riaud, E., Saron, M. F., Lo-Man, R., Henry, T., Jiao, X., Roy, P. & Leclerc, C. (2002b). Induction of protective antiviral cytotoxic T cells by a tubular structure capable of carrying large foreign sequences. *Vaccine* **20**, 1369-1377.

Gomez-Villamandos, J. C., Sanchez, C., Carrasco, L., Laviada, M. M., Bautista, M. J., Martinez-Torrecuadrada, J., Sanchez-Vizcaino, J. M. & Sierra, M. A. (1999). Pathogenesis of African horse sickness: ultrastructural study of the capillaries in experimental infection. *J Comp Pathol* **121**, 101-116.

Gonzalez, M. A. & Carrasco, L. (2001). Human immunodeficiency virus type 1 vpu protein affects Sindbis virus glycoprotein processing and enhances membrane permeabilization. *Virology* **279**, 201-209.

Gonzalez, M. E. & Carrasco, L. (2003). Viroporins. *FEBS Lett* **552**, 28-34.

Gould, E. A. & Higgs, S. (2009). Impact of climate change and other factors on emerging arbovirus diseases. *Trans R Soc Trop Med Hyg* **103**, 109-121.

Greene, I. P., Wang, E., Deardorff, E. R., Milleron, R., Domingo, E. & Weaver, S. C. (2005). Effect of alternating passage on adaptation of sindbis virus to vertebrate and invertebrate cells. *J Virol* **79**, 14253-14260.

Grimes, J. M., Burroughs, J. N., Gouet, P., Diprose, J. M., Malby, R., Zientara, S., Mertens, P. P. & Stuart, D. I. (1998). The atomic structure of the bluetongue virus core. *Nature* **395**, 470-478.

Guinea, R. & Carrasco, L. (1994). Influenza virus M2 protein modifies membrane permeability in *E. coli* cells. *FEBS Letters* **343**, 242-246.

Halaihel, N., Lievin, V., Ball, J. M., Estes, M. K., Alvarado, F. & Vasseur, M. (2000). Direct inhibitory effect of rotavirus NSP4(114-135) peptide on the Na(+)-D-glucose symporter of rabbit intestinal brush border membrane. *J Virol* **74**, 9464-9470.

Han, Z. & Harty, R. N. (2004). The NS3 protein of bluetongue virus exhibits viroporin-like properties. *J Biol Chem* **279**, 43092-43097.

Hassan, S. H., Wirblich, C., Forzan, M. & Roy, P. (2001). Expression and functional characterization of bluetongue virus VP5 protein: role in cellular permeabilization. *J Virol* **75**, 8356-8367.

Hassan, S. S. & Roy, P. (1999). Expression and functional characterization of bluetongue virus VP2 protein: role in cell entry. *J Virol* **73**, 9832-9842.

Hatherell, T. (2007). An investigation into the subcellular localisation of nonstructural protein NS3 of African horsesickness virus. Pretoria: University of Pretoria.

Hou, Z., Huang, Y., Huan, Y., Pang, W., Meng, M., Wang, P., Yang, M., Jiang, L., Cao, X. & Wu, K. K. (2008). Anti-NSP4 antibody can block rotavirus-induced diarrhea in mice. *J Pediatr Gastroenterol Nutr* **46**, 376-385.

Howell, P. G. (1962). The isolation and identification of further antigenic types of African horse sickness virus. *Onderstepoort J Vet Res* **29**, 139–149.

Howerth, E. W. & Tyler, D. E. (1988). Experimentally induced bluetongue virus infection in white-tailed deer: ultrastructural findings. *Am J Vet Res* **49**, 1914-1922.

Huang, H., Schroeder, F., Estes, M. K., McPherson, T. & Ball, J. M. (2004). Interaction(s) of rotavirus non-structural protein 4 (NSP4) C-terminal peptides with model membranes. *Biochem J* **380**, 723-733.

Huang, H., Schroeder, F., Zeng, C., Estes, M. K., Schoer, J. & Ball, J. A. (2001). Membrane interactions of a novel viral enterotoxin: rotavirus non-structural glycoprotein NSP4. *Biochemistry* **40**, 4169-4180.

Huismans, H. (1979). Protein synthesis in bluetongue virus-infected cells. *Virology* **92**, 385-396.

Huismans, H. & Els, H. J. (1979). Characterization of the tubules associated with the replication of three different orbiviruses. *Virology* **92**, 397-406.

Hyatt, A. D., Eaton, B. T. & Brookes, S. M. (1989). The release of bluetongue virus from infected cells and their superinfection by progeny virus. *Virology* **173**, 21-34.

Hyatt, A. D., Gould, A. R., Coupar, B. & Eaton, B. T. (1991). Localization of the non-structural protein NS3 in bluetongue virus-infected cells. *J Gen Virol* **72**, 2263-2267.

Hyatt, A. D., Zhao, Y. & Roy, P. (1993). Release of bluetongue virus-like particles from insect cells is mediated by BTV non-structural protein NS3/NS3A. *Virology* **193**, 592-603.

Isherwood, B. J. & Patel, A. H. (2005). Analysis of the processing and transmembrane topology of the E2p7 protein of hepatitis C virus. *J Gen Virol* **86**, 667-676.

Iturriza-Gómara, M., Isherwood, B., Desselberger, U. & Gray, J. J. (2001). Reassortment *in vivo*: Driving force for diversity of human rotavirus strains isolated in the United Kingdom between 1995 and 1999. *J Virol* **75**, 3696-3705.

Jourdan, N., Maurice, M., Delautier, D., Quero, A. M., Servin, A. L. & Trugnan, G. (1997). Rotavirus is released from the apical surface of cultured human intestinal cells through nonconventional vesicular transport that bypasses the Golgi apparatus. *J Virol* **71**, 8268-8278.

Kahlon, J., Siugiyama, K. & Roy, P. (1983). Molecular basis of bluetongue virus neutralization. *J Virol* **48**, 627-632.

Kar, A. K., Bhattacharya, B. & Roy, P. (2007). Bluetongue virus RNA binding protein NS2 is a modulator of viral replication and assembly. *BMC Mol Biol* **8**, 4.

Kirkwood, C. D. & Palombo, E. A. (1997). Genetic characterization of the rotavirus nonstructural protein, NSP4. *Virology* **236**, 258-265.

Koekemoer, J. J., Potgieter, A. C., Paweska, J. T. & van Dijk, A. A. (2000). Development of probes for typing African horsesickness virus isolates using a complete set of cloned VP2-genes. *J Virol Methods* **88**, 135-144.

Krogh, A., Larsson, B., von Heijne, G. & Sonnhammer, E. L. (2001). Predicting transmembrane protein topology with a hidden Markov model: application to complete genomes. *J Mol Biol* **305**, 567-580.

Kuo, L. & Masters, P. S. (2003). The small envelope protein E is not essential for murine coronavirus replication. *J Virol* **77**, 4597-4608.

Laegreid, W. W., Burrage, T. G., Stone-Marschat, M. & Skowronek, A. (1992a). Electron microscopic evidence for endothelial infection by African horsesickness virus. *Vet Pathol* **29**, 554-556.

Laegreid, W. W., Skowronek, A., Stone-Marschat, M. & Burrage, T. (1993). Characterization of virulence variants of African horsesickness virus. *Virology* **195**, 836-839.

Laegreid, W. W., Stone-Marschat, M., Skowronek, A. & Burrage, T. (1992b). Infection of endothelial cells by African horse sickness viruses. In *Bluetongue, African Horse Sickness, and Related Orbiviruses*, pp. 807-814. Edited by T. E. Walton & B. I. Osburn. Florida: CRC Press.

Lama, J. & Carrasco, L. (1995). Mutations in the hydrophobic domain of poliovirus protein 3AB abrogate its permeabilising activity. *FEBS Letters* **367**, 5-11.

Lambert, C. & Prange, R. (2001). Dual topology of the hepatitis B virus large envelope protein: determinants influencing post-translational pre-S translocation. *J Biol Chem* **276**, 22265-22272.
Liao, Y., Yuan, Q., Torres, J., Tam, J. P. & Liu, D. X. (2006). Biochemical and functional characterization of the membrane association and membrane permeabilizing activity of the severe acute respiratory syndrome coronavirus envelope protein. *Virology* **349** 264-275.
Liu, D. X., Yuan, Q. & Liaob, Y. (2007). Coronavirus envelope protein: a small membrane protein with multiple functions. *Cell Mol Life Sci* **64**, 2043 - 2048.
Loewy, A., Smyth, J., von Bonsdorff, C. H., Liljestrom, P. & Schlesinger, M. J. (1995). The 6-kilodalton membrane protein of Semliki Forest virus is involved in the budding process. *J Virol* **69**, 469-475.
Lopez, T., Camacho, M., Zayas, M., Najera, R., Sanchez, R., Arias, C. F. & Lopez, S. (2005). Silencing the morphogenesis of rotavirus. *J Virol* **79**, 184-192.
Lundin, M., Monne, M., Widell, A., von Heijne, G. & Persson, M. A. (2003). Topology of the membrane-associated hepatitis C virus protein NS4B. *J Virol* **77**, 5428-5438.
Lymperopoulos, K., Noad, R., Tosi, S., Nethisinghe, S., Brierley, I. & Roy, P. (2006). Specific binding of Bluetongue virus NS2 to different viral plus-strand RNAs. *Virology* **353**, 17-26.
Maass, D. R. & Atkinson, P. H. (1990). Rotavirus proteins VP7, NS28, and VP4 form oligomeric structures. *J Virol* **64**, 2632-2641.
MacLachlan, N. J. (1994). The pathogenesis and immunology of bluetongue virus infection of ruminants. *Comp Immunol Microbiol Infect Dis* **17**, 197-206.
MacLachlan, N. J., Balasuriya, U. B., Davis, N. L., Collier, M., Johnston, R. E., Ferraro, G. L. & Guthrie, A. J. (2007). Experiences with new generation vaccines against equine viral arteritis, West Nile disease and African horse sickness. *Vaccine* **25**, 5577-5582.
Madan, V., Castello, A. & Carrasco, L. (2008). Viroporins from RNA viruses induce caspase-dependent apoptosis. *Cell Microbiol* **10**, 437-451.
Madan, V., Garcia Mde, J., Sanz, M. A. & Carrasco, L. (2005a). Viroporin activity of murine hepatitis virus E protein. *FEBS Lett* **579**, 3607-3612.
Madan, V., Sánchez-Martínez, S., Vedovato, N., Rispoli, G., Carrasco, L. & Nieva, J. L. (2007). Plasma membrane-porating domain in poliovirus 2B protein. A short peptide mimics viroporin activity. *J Mol Biol* **374**, 951-964.
Madan, V., Sanz, M. A. & Carrasco, L. (2005b). Requirement of the vesicular system for membrane permeabilization by Sindbis virus. *Virology* **332**, 307-315.
Mahbub Alam, M., Kobayashi, N., Ishino, M., Naik, T. N. & Taniguchi, K. (2006). Analysis of genetic factors related to preferential selection of the NSP1 gene segment observed in mixed infection and multiple passage of rotaviruses. *Arch Virol* **151**, 2149-2159.
Maree, F. F. & Huismans, H. (1997). Characterization of tubular structures composed of nonstructural protein NS1 of African horsesickness virus expressed in insect cells. *J Gen Virol* **78**, 1077-1082.
Maree, S., Durbach, S. & Huismans, H. (1998). Intracellular production of African horsesickness virus core-like particles by expression of the two major core proteins, VP3 and VP7, in insect cells. *J Gen Virol* **79 (Pt 2)**, 333-337.
Marheineke, K., Grünewald, S., Christie, W. & Reiländer, H. (1998). Lipid composition of *Spodoptera frugiperda* (Sf9) and *Trichoplusia ni* (Tn) insect cells used for baculovirus infection. *FEBS Lett* **441**, 49-52.
Martin, L. A., Meyer, A. J., O'Hara, R. S., Fu, H., Mellor, P. S., Knowles, N. J. & Mertens, P. P. (1998). Phylogenetic analysis of African horse sickness virus segment 10: sequence variation, virulence characteristics and cell exit. . *Arch Virol (Suppl)* **14**, 281-293.
Martinez-Torrecuadrada, J. L. & Casal, J. I. (1995). Identification of a linear neutralization domain in the protein VP2 of African horse sickness virus. *Virology* **210**, 391-399.
Martinez-Torrecuadrada, J. L., Diaz-Laviada, M., Roy, P., Sanchez, C., Vela, C., Sanchez-Vizcaino, J. M. & Casal, J. I. (1996). Full protection against African horsesickness (AHS) in horses induced by baculovirus-derived AHS virus serotype 4 VP2, VP5 and VP7. *J Gen Virol* **77 (Pt 6)**, 1211-1221.
Martinez-Torrecuadrada, J. L., Iwata, H., Venteo, A., Casal, I. & Roy, P. (1994). Expression and characterization of the two outer capsid proteins of African horsesickness virus: the role of VP2 in virus neutralization. *Virology* **202**, 348-359.
Martinez-Torrecuadrada, J. L., Langeveld, J. P., Meloen, R. H. & Casal, J. I. (2001). Definition of neutralizing sites on African horse sickness virus serotype 4 VP2 at the level of peptides. *J Gen Virol* **82**, 2415-2424.
Martinez-Torrecuadrada, J. L., Langeveld, J. P., Venteo, A., Sanz, A., Dalsgaard, K., Hamilton, W. D., Meloen, R. H. & Casal, J. I. (1999). Antigenic profile of African horse sickness virus serotype 4 VP5 and identification of a neutralizing epitope shared with bluetongue virus and epizootic hemorrhagic disease virus. *Virology* **257**, 449-459.
Maruri-Avidal, L., Lopez, S. & Arias, C. F. (2008). Endoplasmic reticulum chaperones are involved in the morphogenesis of rotavirus infectious particles. *J Virol* **82**, 5368-5380.

Matsumoto, T., Takahashi, H. & Fujiwara, H. (2004). Targeted nuclear import of open reading frame 1 protein is required for *in vivo* retrotransposition of a telomere-specific non-long terminal repeat retrotransposon. *Mol Cell Biol* **24**, 105-122.

McGinnes, L. W., Reitter, J. N., Gravel, K. & Morrison, T. G. (2003). Evidence for mixed membrane topology of the Newcastle disease virus fusion protein. *J Virol* **77**, 1951-1963.

Meiswinkel, R. (1998). The 1996 outbreak of African horse sickness in South Africa--the entomological perspective. *Arch Virol Suppl* **14**, 69-83.

Mellor, P. S. & Hamblin, C. (2004). African horse sickness. *Vet Res* **35**, 445-466.

Mellor, P. S., Rawlings, P., Baylis, M. & Wellby, M. P. (1998). Effect of temperature on African horse sickness virus infection in *Culicoides*. *Arch Virol Suppl* **14**, 155-163.

Melton, J. V., Ewart, G. D., Weir, R. C., Board, P. G., Lee, E. & Gage, P. W. (2002). Alphavirus 6 K proteins form ion channels. *J Biol Chem* **277**, 46923-46931.

Mertens, P. (2004). The dsRNA viruses. *Virus Res* **101**, 3-13.

Mertens, P. P. & Diprose, J. (2004). The bluetongue virus core: a nano-scale transcription machine. *Virus Res* **101**, 29-43.

Mertens, P. P. C., Brown, F. & Sangar, D. V. (1984). Assignment of the genome segments of bluetongue virus type I to the proteins which they encode. *Virology* **135**, 207-217.

Miller, S., Sparacio, S. & Bartenschlage, R. (2006). Subcellular localization and membrane topology of the Dengue virus type 2 non-structural protein 4B. *J Biol Chem* **281**, 8854–8863.

Mir, K. D., Parr, R. D., Schroeder, F. & Ball, J. M. (2007). Rotavirus NSP4 interacts with both the amino- and carboxyl-termini of caveolin-1. *Virus Res* **126**, 106–115.

Mirazimi, A., Nilsson, M. & Svensson, L. (1998). The molecular chaperone calnexin interacts with the NSP4 enterotoxin of rotavirus in vivo and in vitro. *J Virol* **72**, 8705-8709.

Mirazimi, A. & Svensson, L. (1998). Carbohydrates facilitate correct disulfide bond formation and folding of rotavirus VP7. *J Virol* **72**, 3887-3892.

Miwa, N., Uebi, T. & Kawamura, S. (2008). S100-annexin complexes - biology of conditional association. *FEBS Journal* **275**, 4945-4955.

Modrof, J., Lymperopoulos, K. & Roy, P. (2005). Phosphorylation of bluetongue virus nonstructural protein 2 is essential for formation of viral inclusion bodies. *J Virol* **79**, 10023-10031.

Monastyrskaya, K., Booth, T., Nel, L. & Roy, P. (1994). Mutation of either of two cysteine residues or deletion of the amino or carboxy terminus of nonstructural protein NS1 of bluetongue virus abrogates virus-specified tubule formation in insect cells. *J Virol* **68**, 2169-2178.

Moody, M. D. & Joklik, W. K. (1989). The function of reovirus proteins during the reovirus multiplication cycle: analysis using monoreassortants. *Virology* **173**, 437-446.

Mortola, E., Noad, R. & Roy, P. (2004). Bluetongue virus outer capsid proteins are sufficient to trigger apoptosis in mammalian cells. *J Virol* **78**, 2875-2883.

Murphy, A. & Roy, P. (2008). Manipulation of the bluetongue virus tubules for immunogen delivery. *Future Microbiol* **3**, 351-359.

Nagaleekar, V. K., Tiwari, A. K., Kataria, R. S., Bais, M. V., Ravindra, P. V. & Kumar, S. (2007). Bluetongue virus induces apoptosis in cultured mammalian cells by both caspase-dependent extrinsic and intrinsic apoptotic pathways. *Arch Virol* **152**, 1751-1756.

Nal, B., Chan, C., Kien, F., Siu, L., Tse, J., Chu, K., Kam, J., Staropoli, I., Crescenzo-Chaigne, B., Escriou, N., van derWerf, S., Yuen, K. Y. & Altmeyer, R. (2005). Differential maturation and subcellular localization of severe acute respiratory syndrome coronavirus surface proteins S, M and E. *J Gen Virol* **86**, 1423 - 1434.

Newton, K., Meyer, J. C., Bellamy, A. R. & Taylor, J. A. (1997). Rotavirus nonstructural glycoprotein NSP4 alters plasma membrane permeability in mammalian cells. *J Virol* **71**, 9458-9465.

O'Brien, J. A., Taylor, J. A. & Bellamy, A. R. (2000). Probing the structure of rotavirus NSP4: a short sequence at the extreme C terminus mediates binding to the inner capsid particle. *J Virol* **74**, 5388-5394.

O'Hara, R. S., Meyer, A. J., Burroughs, J. N., Pullen, L., Martin, L. A. & Mertens, P. P. (1998). Development of a mouse model system, coding assignments and identification of the genome segments controlling virulence of African horse sickness virus serotypes 3 and 8. *Arch Virol (Suppl)* **14**, 259-279.

Owens, R. J., Limn, C. & Roy, P. (2004). Role of an arbovirus nonstructural protein in cellular pathogenesis and virus release. *J Virol* **78**, 6649-6656.

Paclet, M., Henderson, L. M., Campion, Y., Morel, F. & Dagher, M. (2004). Localization of Nox2 N-terminus using polyclonal antipeptide antibodies. *Biochem J* **382**, 981-986.

Pappas, C., Aguilar, P. V., Basler, C. F., Solorzano, A., Zeng, H., Perrone, L. A., Palese, P., Garcia-Sastre, A., Katz, J. M. & Tumpey, T. M. (2008). Single gene reassortants identify a critical role for PB1, HA, and NA in the high virulence of the 1918 pandemic influenza virus. *Proc Natl Acad Sci U S A* **105**, 3064-3069.

Parks, C. L., Latham, T., Cahill, A., O'Neill R, E., Passarotti, C. J., Buonagurio, D. A., Bechert, T. M., D'Arco, G. A., Neumann, G., Destefano, J., Arendt, H. E., Obregon, J., Shutyak, L., Hamm, S., Sidhu, M. S., Zamb, T. J. & Udem, S. A. (2007). Phenotypic properties resulting from directed gene segment reassortment between wild-type A/Sydney/5/97 influenza virus and the live attenuated vaccine strain. *Virology* **367**, 275-287.

Parr, R. D., Storey, S. M., Mitchell, D. M., McIntosh, A. L., Zhou, M., Mir, K. D. & Ball, J. M. (2006). The rotavirus enterotoxin NSP4 directly interacts with the caveolar structural protein caveolin-1. *J Virol* **80**, 2842-2854.

Paterson, R. G., Takeda, M., Ohigashi, Y., Pinto, L. H. & Lamba, R. A. (2003). Influenza B virus BM2 protein is an oligomeric integral membrane protein expressed at the cell surface. *Virology* **306**, 7-17.

Pierce, C. M., Balasuriya, U. B. & MacLachlan, N. J. (1998). Phylogenetic analysis of the S10 gene of field and laboratory strains of bluetongue virus from the United States. *Virus Res* **55**, 15-27.

Potgieter, A. C., Cloete, M., Pretorius, P. J. & van Dijk, A. A. (2003). A first full outer capsid protein sequence data-set in the Orbivirus genus (family Reoviridae): cloning, sequencing, expression and analysis of a complete set of full-length outer capsid VP2 genes of the nine African horsesickness virus serotypes. *J Gen Virol* **84**, 1317-1326.

Potgieter, A. C., Steele, A. D. & van Dijk, A. A. (2002). Cloning of complete genome sets of six dsRNA viruses using an improved cloning method for large dsRNA genes. *J Gen Virol* **83**, 2215-2223.

Purse, B. l. V., Mellor, P. S., Rogers, D. J., Samuel, A. R., Mertens, P. P. & Baylis, M. (2005). Climate change and the recent emergence of bluetongue in Europe. *Nat Rev Microbiol* **3**, 171-181.

Quan, M., van Vuuren, M., Howell, P. G., Groenewald, D. & Guthrie, A. J. (2008). Molecular epidemiology of the African horse sickness virus S10 gene. *J Gen Virol* **89**, 1159-1168.

Ramig, R. F., Garrison, C., Chen, D. & Bell-Robinson, D. (1989). Analysis of reassortment and superinfection during mixed infection of Vero cells with bluetongue virus serotypes 10 and 17. *J Gen Virol* **70**, 2595-2603.

Rodriguez-Sanchez, B., Fernandez-Pinero, J., Sailleau, C., Zientara, S., Belak, S., Arias, M. & Sanchez-Vizcaino, J. M. (2008). Novel gel-based and real-time PCR assays for the improved detection of African horse sickness virus. *J Virol Methods* **151**, 87-94.

Roner, M. R. & Mutsoli, C. (2007). The use of monoreassortants and reverse genetics to map reovirus lysis of a ras-transformed cell line. *J Virol Methods* **139**, 132-142.

Roy, P. (1996). Orbivirus structure and assembly. *Virology* **216**, 1-11.

Roy, P. (2008). Functional mapping of bluetongue virus proteins and their interactions with host proteins during virus replication. *Cell Biochem Biophys* **50**, 143-157.

Roy, P., Bishop, D. H., Howard, S., Aitchison, H. & Erasmus, B. (1996). Recombinant baculovirus-synthesized African horsesickness virus (AHSV) outer-capsid protein VP2 provides protection against virulent AHSV challenge. *J Gen Virol* **77**, 2053-2057.

Roy, P., Mertens, P. P. & Casal, I. (1994). African horse sickness virus structure. *Comp Immunol Microbiol Infect Dis* **17**, 243-273.

Ruiz, M. C., Diaz, Y., Pena, F., Aristimuno, O. C., Chemello, M. E. & Michelangeli, F. (2005). Ca^{2+} permeability of the plasma membrane induced by rotavirus infection in cultured cells is inhibited by tunicamycin and brefeldin A. *Virology* **333**, 54-65.

Sailleau, C., Moulay, S. & Zientara, S. (1997). Nucleotide sequence comparison of the segments S10 of the nine African horsesickness virus serotypes. *Arch Virol* **142**, 965-978.

Sambrook, J. & Russell, D. W. (2001). *Molecular Cloning, a laboratory manual*. Cold Spring Harbour: Cold Spring Laboratory Press.

Sánchez-Martínez, S., Huarte, N., Maeso, R., Madan, V., Carrasco, L. & Nieva, J. L. (2008). Functional and structural characterization of 2B viroporin membranolytic domains. *Biochemistry* **47**, 10731-10739.

Sanz, M. A., Madan, V., Carrasco, L. & Nieva, J. L. (2003). Interfacial domains in sindbis virus 6K protein. *J Biol Chem* **278**, 2051-2057.

Sanz, M. A., Perez, L. & Carrasco, L. (1994). Semliki Forest virus 6 K protein modifies membrane permeability after inducible expression in *Escherichia coli* cells. *J Biol Chem* **269**, 12106-12110.

Sapin, C., Colard, O., Delmas, O., Tessier, C., Breton, M., Enouf, V., Chwetzoff, S., Ouanich, J., Cohen, J., Wolf, C. & Trugnan, G. (2002). Rafts promote assembly and atypical targeting of a nonenveloped virus, rotavirus, in Caco-2 cells. *J Virol* **76**, 4591-4602.

Seo, N. S., Zeng, C. Q., Hyser, J. M., Utama, B., Crawford, S. E., Kim, K. J., Hook, M. & Estes, M. K. (2008). Inaugural article: integrins alpha1beta1 and alpha2beta1 are receptors for the rotavirus enterotoxin. *Proc Natl Acad Sci U S A* **105**, 8811-8818.

Silvestri, L. S., Tortorici, M. A., Vasquez-Del Carpio, R. & Patton, J. T. (2005). Rotavirus glycoprotein NSP4 is a modulator of viral transcription in the infected cell. *J Virol* **79**, 15165-15174.

Skowronek, A. J., LaFranco, L., Stone-Marschat, M. A., Burrage, T. G., Rebar, A. H. & Laegreid, W. W. (1995). Clinical pathology and hemostatic abnormalities in experimental African horsesickness. *Vet Pathol* **32**, 112-121.

Smit, C. C. (1999). Identification of critical functional domains of nonstructural protein NS3 of African horsesickness virus. MSc Thesis. Pretoria: University of Pretoria.

Stoltz, M. A., van der Merwe, C. F., Coetzee, J. & Huismans, H. (1996). Subcellular localization of the nonstructural protein NS3 of African horsesickness virus. *Onderstepoort J Vet Res* **63**, 57-61.

Stone-Marschat, M. A., Moss, S. R., Burrage, T. G., Barber, M. L., Roy, P. & Laegreid, W. W. (1996). Immunization with VP2 is sufficient for protection against lethal challenge with African horsesickness virus Type 4. *Virology* **220**, 219-222.

Storey, S. M., Gibbons, T. F., Williams, C. V., Parr, R. D., Schroeder, F. & Ball, J. M. (2007). Full-Length, Glycosylated NSP4 is Localized to Plasma Membrane Caveolae by a Novel Raft Isolation Technique. *J Virol* **81**, 5472-5483.

Studier, F. W. (1991). Use of bacteriophage T7 lysozyme to improve an inducible T7 expression system. *J Mol Biol* **219**, 37-44.

Studier, F. W. & Moffat, B. A. (1986). Use of bacteriophage T7 RNA polymerase to direct selective high-level expression of cloned genes. *J Mol Biol* **189**, 113-130.

Tauscher, G. I. & Desselberger, U. (1997). Viral determinants of rotavirus pathogenicity in pigs: production of reassortants by asynchronous coinfection. *J Virol* **71**, 853-857.

Taylor, J. A., O'Brien, J. A. & Yeager, M. (1996). The cytoplasmic tail of NSP4, the endoplasmic reticulum-localized non-structural glycoprotein of rotavirus, contains distinct virus binding and coiled coil domains. *Embo J* **15**, 4469-4476.

Teixeira, L. M. (2005). The cytotoxicity of the nonstructural protein NS3 of equine encephalosis virus. MSc Thesis. Pretoria: University of Pretoria.

Theiler, A. (1921). African horsesickness. *Department of Agriculture Sci Bulletin* **19**, 1-32.

Tian, P., Hu, Y., Schilling, W. P., Lindsay, D. A., Eiden, J. & Estes, M. K. (1994). The nonstructural glycoprotein of rotavirus affects intracellular calcium levels. *J Virol* **68**, 251-257.

Tini, M., Jewell, U. R., Camenisch, G., Chilov, D. & Gassmann, M. (2002). Generation and application of chicken egg-yolk antibodies. *Comp Biochem Phys* **Part A 131**, 569–574.

Turnbull, P. J., Cormack, S. B. & Huismans, H. (1996). Characterization of the gene encoding core protein VP6 of two African horsesickness virus serotypes. *J Gen Virol* **77 (Pt 7)**, 1421-1423.

Uitenweerde, J. M., Theron, J., Stoltz, M. A. & Huismans, H. (1995). The multimeric nonstructural NS2 proteins of bluetongue virus, African horsesickness virus, and epizootic hemorrhagic disease virus differ in their single-stranded RNA-binding ability. *Virology* **209**, 624-632.

Ulug, E. T., Garry, R. F. & Bose, H. R., Jr (1996). Inhibition of $Na^{+}K^{+}$ATPase activity in membranes of Sindbis virus-infected chick cells. *Virology* **216**, 299-308.

Van Dijk, A. A. & Huismans, H. (1988). In vitro transcription and translation of bluetongue virus mRNA. *J Gen Virol* **69** 573-581.

Van Kuppeveld, F. J. M., de Jong, A. S., Melchers, W. J. G. & Willems, P. H. G. M. (2005). Enterovirus protein 2B po(u)res out the calcium: a viral strategy to survive? *Trends in Microbiology* **13**, 41-44.

Van Niekerk, M. (2001). Association of nonstructural protein NS3 of African horsesickness virus with cytotoxicity and virus virulence. PhD Thesis. Pretoria: University of Pretoria.

Van Niekerk, M., Freeman, M., Paweska, J. T., Howell, P. G., Guthrie, A. J., Potgieter, A. C., van Staden, V. & Huismans, H. (2003). Variation in the NS3 gene and protein in South African isolates of bluetongue and equine encephalosis viruses. *J Gen Virol* **84**, 581-590.

Van Niekerk, M., Smit, C. C., Fick, W. C., van Staden, V. & Huismans, H. (2001a). Membrane association of African horsesickness virus nonstructural protein NS3 determines its cytotoxicity. *Virology* **279**, 499-508.

Van Niekerk, M., van Staden, V., van Dijk, A. A. & Huismans, H. (2001b). Variation of African horsesickness virus nonstructural protein NS3 in southern Africa. *J Gen Virol* **82**, 149-158.

Van Staden, V. & Huismans, H. (1991). A comparison of the genes which encode non-structural protein NS3 of different orbiviruses. *J Gen Virol* **72**, 1073-1079.

Van Staden, V., Smit, C. C., Stoltz, M. A., Maree, F. F. & Huismans, H. (1998). Characterization of two African horse sickness virus non-structural proteins, NS1 and NS3. *Arch Virol Suppl* **14**, 251-258.

Van Staden, V., Stoltz, M. A. & Huismans, H. (1995). Expression of nonstructural protein NS3 of African horsesickness virus (AHSV): evidence for a cytotoxic effect of NS3 in insect cells, and characterization of the gene products in AHSV infected Vero cells. *Arch Virol* **140**, 289-306.

Venter, G. J., Graham, S. D. & Hamblin, C. (2000). African horse sickness epidemiology: vector competence of south african Culicoides species for virus serotypes 3, 5 and 8. *Med Vet Entomol* **14**, 245-250.

Von Heijne, G. (1996). Principles of membrane protein assembly and structure. *Prog Biophys Mol Biol* **66**, 113-139.

Von Teichman, B. F. & Smit, T. K. (2008). Evaluation of the pathogenicity of African Horsesickness (AHS) isolates in vaccinated animals. *Vaccine* **26**, 5014-5021.

Watanabe, T., Watanabe, S., Ito, H., Kida, H. & Kawaoka, Y. (2001). Influenza A virus can undergo multiple cycles of replication without M2 ion channel activity. *J Virol* **75**, 5656–5662.

Wirblich, C., Bhattacharya, B. & Roy, P. (2006). Nonstructural protein 3 of bluetongue virus assists virus release by recruiting ESCRT-I protein Tsg101. *J Virol* **80**, 460-473.

Wohlsein, P., Pohlenz, J. F., Davidson, F. L., Salt, J. S. & Hamblin, C. (1997). Immunohistochemical demonstration of African horse sickness viral antigen in formalin-fixed equine tissues. *Vet Pathol* **34**, 568-574.

Wu, X., Chen, S. Y., Iwata, H., Compans, R. W. & Roy, P. (1992). Multiple glycoproteins synthesized by the smallest RNA segment (S10) of bluetongue virus. *J Virol* **66**, 7104-7112.

Xu, A., Bellamy, A. R. & Taylor, J. A. (1998). BiP (GRP78) and endoplasmin (GRP94) are induced following rotavirus infection and bind transiently to an endoplasmic reticulum-localized virion component. *J Virol* **72**, 9865-9872.

Xu, A., Bellamy, A. R. & Taylor, J. A. (2000). Immobilization of the early secretory pathway by a virus glycoprotein that binds to microtubules. *Embo J* **19**, 6465-6474.

Zambrano, J. L., Diaz, Y., Pena, F., Vizzi, E., Ruiz, M. C., Michelangeli, F., Liprandi, F. & Ludert, J. E. (2008). Silencing of rotavirus NSP4 or VP7 expression reduces alterations in Ca^{2+} homeostasis induced by infection of cultured cells. *J Virol* **82**, 5815-5824.

Zhang, M., Zeng, C. Q., Dong, Y., Ball, J. M., Saif, L. J., Morris, A. P. & Estes, M. K. (1998). Mutations in rotavirus nonstructural glycoprotein NSP4 are associated with altered virus virulence. *J Virol* **72**, 3666-3672.

Zhang, M., Zeng, C. Q., Morris, A. P. & Estes, M. K. (2000). A functional NSP4 enterotoxin peptide secreted from rotavirus-infected cells. *J Virol* **74**, 11663-11670.

APPENDIX A

Nucleotide sequence alignments of reassortant virus genome segments

VP2 gene (Segment 2)

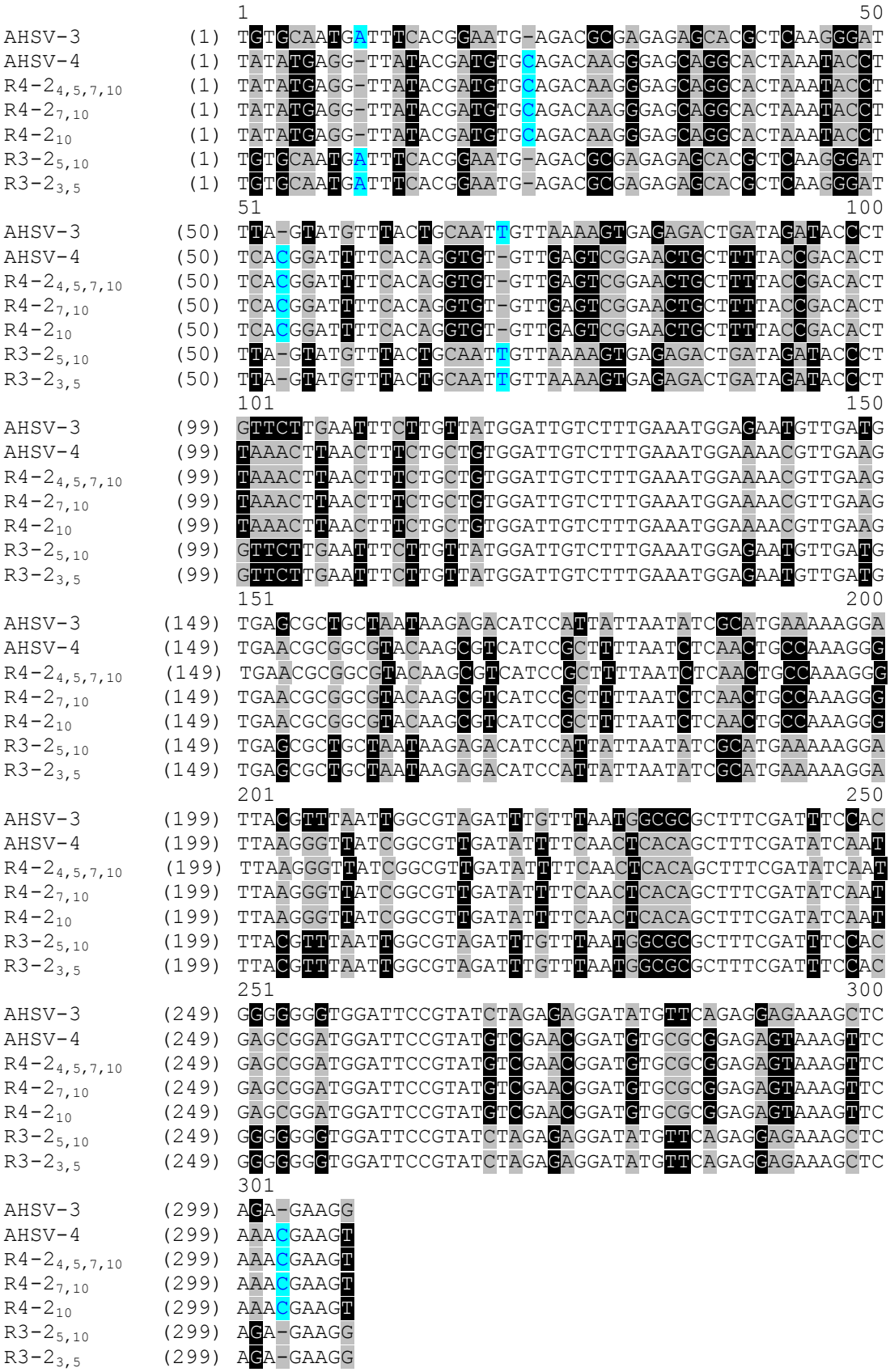

VP3 gene (Segment 3)

```
                    1                                                  50
AHSV-2          (1) ATTTAAAAGCAACCATTCTCACTCCATCCCTCTCCTCTTCTGTGTACACA
AHSV-3          (1) ATTTAAAAGCGACCATCCTCACTCCATCCCTCTCCTCCTCCGTGTACACA
AHSV-4          (1) ATTTAAAAGCGACCATTCTCACTCCATCCCTCTCCTCCTCTGTGTACACA
R4-2(4,5,7,10)  (1) ATTTAAAAGCGACCATTCTCACTCCATCCCTCTCCTCCTCTGTGTACACA
R4-2(7,10)      (1) ATTTAAAAGCGACCATTCTCACTCCATCCCTCTCCTCCTCTGTGTACACA
R4-2(10)        (1) ATTTAAAAGCGACCATTCTCACTCCATCCCTCTCCTCCTCTGTGTACACA
R3-2(5,10)      (1) ATTTAAAAGCGACCATCCTCACTCCATCCCTCTCCTCCTCCGTGTACACA
R3-2(3,5)       (1) ATTTAAAAGCAACCATTCTCACTCCATCCCTCTCCTCTTCTGTGTACACA
                    51                                                 100
AHSV-2         (51) TAAGGCATTGCCGTCAGTATCTCGTCGGGCGGCCGTGAATCAAAGAATTT
AHSV-3         (51) TAAGGCATTGCCGTCAGTATCTCGTCGGGCGGCCGCGAATCAAAAAATTT
AHSV-4         (51) TAAGGCATTGCCGTCAGTATCTCGTCGGGCGGCCGTGAATCAAAAAATTT
R4-2(4,5,7,10) (51) TAAGGCATTGCCGTCAGTATCTCGTCGGGCGGCCGTGAATCAAAAAATTT
R4-2(7,10)     (51) TAAGGCATTGCCGTCAGTATCTCGTCGGGCGGCCGTGAATCAAAAAATTT
R4-2(10)       (51) TAAGGCATTGCCGTCAGTATCTCGTCGGGCGGCCGTGAATCAAAAAATTT
R3-2(5,10)     (51) TAAGGCATTGCCGTCAGTATCTCGTCGGGCGGCCGCGAATCAAAAAATTT
R3-2(3,5)      (51) TAAGGCATTGCCGTCAGTATCTCGTCGGGCGGCCGTGAATCAAAAAATTT
                    101                 127
AHSV-2        (101) AATCTTGATGTTCCGTAACATACCACC
AHSV-3        (101) AATCTTGATATTCCGTAACATACCACC
AHSV-4        (101) AATCTTGATATTCCGTAACATACCGCC
R4-2(4,5,7,10)(101) AATCTTGATATTCCGTAACATACCGCC
R4-2(7,10)    (101) AATCTTGATATTCCGTAACATACCGCC
R4-2(10)      (101) AATCTTGATATTCCGTAACATACCGCC
R3-2(5,10)    (101) AATCTTGATATTCCGTAACATACCACC
R3-2(3,5)     (101) AATCTTGATGTTCCGTAACATACCACC
```

NS1 gene (segment 5)

```
                      1                                                  50
AHSV-2          (1)   CCAGTGGTTGATTCAAAAATTGCTGAACTAACGGGAGGCACAGATGTATT
AHSV-3          (1)   CCAGTGGTTGATTCAAAAATTGCTGAACTAACAGGAGGCATAGATGTATT
AHSV-4          (1)   CCAGTGGTTGATTCAAAAATCGCTGAACTAACAGGAGGCACGGATGTATT
R4-2(4,5,7,10   (1)   CCAGTGGTTGATTCAAAAATTGCTGAACTAACGGAGGCACAGATGTATT
R4-2(7,10       (1)   CCAGTGGTTGATTCAAAAATCGCTGAACTAACAGGAGGCACGGATGTATT
R4-2(10         (1)   CCAGTGGTTGATTCAAAAATCGCTGAACTAACAGGAGGCACGGATGTATT
R3-2(5,10       (1)   CCAGTGGTTGATTCAAAAATTGCTGAACTAACGGAGGCACAGATGTATT
R3-2(3,5        (1)   CCAGTGGTTGATTCAAAAATTGCTGAACTAACGGAGGCACAGATGTATT
                      51                                                 100
AHSV-2         (51)   TTATACACGTGCGTATGTACATGCGGACAATCACAAAGCGCCAAATGTCA
AHSV-3         (51)   TTATACACGTGCGTATGTACATGCGGACAATCACAAAGTGCCAAATGTCA
AHSV-4         (51)   TTATACACGTGCGTATGTACATGCGGACAATCACAAAGTGCCAAATGTCA
R4-2(4,5,7,10  (51)   TTATACACGTGCGTATGTACATGCGGACAATCACAAAGCGCCAAATGTCA
R4-2(7,10      (51)   TTATACACGTGCGTATGTACATGCGGACAATCACAAAGTGCCAAATGTCA
R4-2(10        (51)   TTATACACGTGCGTATGTACATGCGGACAATCACAAAGTGCCAAATGTCA
R3-2(5,10      (51)   TTATACACGTGCGTATGTACATGCGGACAATCACAAAGCGCCAAATGTCA
R3-2(3,5       (51)   TTATACACGTGCGTATGTACATGCGGACAATCACAAAGCGCCAAATGTCA
                      101                                                150
AHSV-2        (101)   GAGATTTGATGATGAATGAAGTCTTCAGGAAGATTGATGATCATTGGGTG
AHSV-3        (101)   GAGATTTGATGATGAATGAAGTCTTCAGGAAGATCGATGATCATTGGGTG
AHSV-4        (101)   GAGATTTGATGATGAATGAAGTCTTCAGGAAGATTGATGATCATTGGGTG
R4-2(4,5,7,10 (101)   GAGATTTGATGATGAATGAAGTCTTCAGGAAGATTGATGATCATTGGGTG
R4-2(7,10     (101)   GAGATTTGATGATGAATGAAGTCTTCAGGAAGATTGATGATCATTGGGTG
R4-2(10       (101)   GAGATTTGATGATGAATGAAGTCTTCAGGAAGATTGATGATCATTGGGTG
R3-2(5,10     (101)   GAGATTTGATGATGAATGAAGTCTTCAGGAAGATTGATGATCATTGGGTG
R3-2(3,5      (101)   GAGATTTGATGATGAATGAAGTCTTCAGGAAGATTGATGATCATTGGGTG
                      151                                                200
AHSV-2        (151)   ATTCAGAAGTGTCATACAACGAAGGAAGCGATTACCGTAACTGCAATTCA
AHSV-3        (151)   ATTCAGAAGTGTCATACAACGAAGGAAGCGATTACCGTAACTGCAATTCA
AHSV-4        (151)   ATTCAGAAGTGTCATACCACGAAGGAAGCGATTACTGTAACTGCAATTCA
R4-2(4,5,7,10 (151)   ATTCAGAAGTGTCATACAACGAAGGAAGCGATTACCGTAACTGCAATTCA
R4-2(7,10     (151)   ATTCAGAAGTGTCATACCACGAAGGAAGCGATTACTGTAACTGCAATTCA
R4-2(10       (151)   ATTCAGAAGTGTCATACCACGAAGGAAGCGATTACTGTAACTGCAATTCA
R3-2(5,10     (151)   ATTCAGAAGTGTCATACAACGAAGGAAGCGATTACCGTAACTGCAATTCA
R3-2(3,5      (151)   ATTCAGAAGTGTCATACAACGAAGGAAGCGATTACCGTAACTGCAATTCA
                      201                                                250
AHSV-2        (201)   AATCCAGAGGTCGATCAGAGGTGATGGACAGTGGGATACTCCGATGTTTC
AHSV-3        (201)   GATCCAGAGGTCGATCAGAGGTGATGGGCAGTGGGATACTCCGATGTTTC
AHSV-4        (201)   GATTCAGAGGTCGATCAGAGGTGATGGGCAGTGGGATACTCCGATGTTTC
R4-2(4,5,7,10 (201)   AATCCAGAGGTCGATCAGAGGTGATGGACAGTGGGATACTCCGATGTTTC
R4-2(7,10     (201)   GATTCAGAGGTCGATCAGAGGTGATGGGCAGTGGGATACTCCGATGTTTC
R4-2(10       (201)   GATTCAGAGGTCGATCAGAGGTGATGGGCAGTGGGATACTCCGATGTTTC
R3-2(5,10     (201)   AATCCAGAGGTCGATCAGAGGTGATGGACAGTGGGATACTCCGATGTTTC
R3-2(3,5      (201)   AATCCAGAGGTCGATCAGAGGTGATGGACAGTGGGATACTCCGATGTTTC
                      251                                                300
AHSV-2        (251)   ACCAATCAATGGCTCTGTTGACACGATTGATTGTTTATTGGTTAACGGAT
AHSV-3        (251)   ACCAATCAATGGCTCTGTTAACACGATTGATTGTTTATTGGTTAACGGAT
AHSV-4        (251)   ACCAATCAATGGCTCTGTTAACACGATTGATTGTTTATTGGTTAACGGAT
R4-2(4,5,7,10 (251)   ACCAATCAATGGCTCTGTTGACACGATTGATTGTTTATTGGTTAACGGAT
R4-2(7,10     (251)   ACCAATCAATGGCTCTGTTAACACGATTGATTGTTTATTGGTTAACGGAT
R4-2(10       (251)   ACCAATCAATGGCTCTGTTAACACGATTGATTGTTTATTGGTTAACGGAT
R3-2(5,10     (251)   ACCAATCAATGGCTCTGTTGACACGATTGATTGTTTATTGGTTAACGGAT
R3-2(3,5      (251)   ACCAATCAATGGCTCTGTTGACACGATTGATTGTTTATTGGTTAACGGAT
```

```
                      301                                                 350
AHSV-2          (301) GTGACTGAGAGAAGCGCTATCTTTCGGCTGACTTGTTTCGCAATCTTCGG
AHSV-3          (301) GTGACTGAGAGAAGCGCTATCTTTCGGCTGACTTGTTTCGCAATCTTCGG
AHSV-4          (301) GTGACTGAGAGAAGTGCTATCTTTCGGCTGACTTGTTTCGCGATCTTCGG
R4-2(4,5,7,10)  (301) GTGACTGAGAGAAGCGCTATCTTTCGGCTGACTTGTTTCGCAATCTTCGG
R4-2(7,10)      (301) GTGACTGAGAGAAGTGCTATCTTTCGGCTGACTTGTTTCGCGATCTTCGG
R4-2(10)        (301) GTGACTGAGAGAAGTGCTATCTTTCGGCTGACTTGTTTCGCGATCTTCGG
R3-2(5,10)      (301) GTGACTGAGAGAAGCGCTATCTTTCGGCTGACTTGTTTCGCAATCTTCGG
R3-2(3,5)       (301) GTGACTGAGAGAAGCGCTATCTTTCGGCTGACTTGTTTCGCAATCTTCGG
                      351                                                 399
AHSV-2          (351) ATGTAAGCCAACAGCTCGAGGTAGATATATTGATTGGGACGATCTTGGA
AHSV-3          (351) ATGTAAGCCAACAGCTCGAGGTAGATATATTGACTGGGATGATCTTGGA
AHSV-4          (351) ATGTAAGCCGACGGCTCGAGGTAGATATATTGATTGGGATGATCTTGGA
R4-2(4,5,7,10)  (351) ATGTAAGCCAACAGCTCGAGGTAGATATATTGATTGGGACGATCTTGGA
R4-2(7,10)      (351) ATGTAAGCCGACGGCTCGAGGTAGATATATTGATTGGGATGATCTTGGA
R4-2(10)        (351) ATGTAAGCCGACGGCTCGAGGTAGATATATTGATTGGGATGATCTTGGA
R3-2(5,10)      (351) ATGTAAGCCAACAGCTCGAGGTAGATATATTGATTGGGACGATCTTGGA
R3-2(3,5)       (351) ATGTAAGCCAACAGCTCGAGGTAGATATATTGATTGGGACGATCTTGGA
```

VP5 gene (Segment 6)

```
                        1                                                  50
AHSV-3            (1)   TGAAGAAGCTGTGCAGGAGATGTTGGATTTAAGTGCCGAGGTCATCGAAA
AHSV-4            (1)   TGATGAAGCGATTCAGGAGATGCTCGACTTAAGCGCAGAAGTGATTGAGA
R4-2(4,5,7,10)    (1)   TGATGAAGCGATTCAGGAGATGCTCGACTTAAGCGCAGAAGTGATTGAGA
R4-2(7,10)        (1)   TGATGAAGCGATTCAGGAGATGCTCGACTTAAGCGCAGAAGTGATTGAGA
R4-2(10)          (1)   TGATGAAGCGATTCAGGAGATGCTCGACTTAAGCGCAGAAGTGATTGAGA
R3-2(5,10)        (1)   TGAAGAAGCTGTGCAGGAGATGTTGGATTTAAGTGCCGAGGTCATCGAAA
R3-2(3,5)         (1)   TGAAGAAGCTGTGCAGGAGATGTTGGATTTAAGTGCCGAGGTCATCGAAA
                        51                                                 100
AHSV-3           (51)   CGGCGGCTGAGGAGGTGCCAATCTTTGGCGCAGGCGCAGCAAATGTTGTT
AHSV-4           (51)   CTGCGTCGGAGGAGGTACCAATTTTTGGCGCTGGGGCGGCGAACGTTATC
R4-2(4,5,7,10)   (51)   CTGCGTCGGAGGAGGTACCAATTTTTGGCGCTGGGGCGGCGAACGTTATC
R4-2(7,10)       (51)   CTGCGTCGGAGGAGGTACCAATTTTTGGCGCTGGGGCGGCGAACGTTATC
R4-2(10)         (51)   CTGCGTCGGAGGAGGTACCAATTTTTGGCGCTGGGGCGGCGAACGTTATC
R3-2(5,10)       (51)   CGGCGGCTGAGGAGGTGCCAATCTTTGGCGCAGGCGCAGCAAATGTTGTT
R3-2(3,5)        (51)   CGGCGGCTGAGGAGGTGCCAATCTTTGGCGCAGGCGCAGCAAATGTTGTT
                        101                                                150
AHSV-3          (101)   GCGACGACACGCGCAATCCAAGGGGGTCTAAAGTTGAAGGAGATAATAGA
AHSV-4          (101)   GCCACAACCCGAGCAATACAGGGGGGGTTAAAACTAAAGGAAATTGTTGA
R4-2(4,5,7,10)  (101)   GCCACAACCCGAGCAATACAGGGGGGGTTAAAACTAAAGGAAATTGTTGA
R4-2(7,10)      (101)   GCCACAACCCGAGCAATACAGGGGGGGTTAAAACTAAAGGAAATTGTTGA
R4-2(10)        (101)   GCCACAACCCGAGCAATACAGGGGGGGTTAAAACTAAAGGAAATTGTTGA
R3-2(5,10)      (101)   GCGACGACACGCGCAATCCAAGGGGGTCTAAAGTTGAAGGAGATAATAGA
R3-2(3,5)       (101)   GCGACGACACGCGCAATCCAAGGGGGTCTAAAGTTGAAGGAGATAATAGA
                        151                                185
AHSV-3          (151)   TAAACTCACAGGGATTGATCTCTCTCATTTGAAAG
AHSV-4          (151)   TAAGCTTACGGGAATAGACTTGAGTCATTTGAAGG
R4-2(4,5,7,10)  (151)   TAAGCTTACGGGAATAGACTTGAGTCATTTGAAGG
R4-2(7,10)      (151)   TAAGCTTACGGGAATAGACTTGAGTCATTTGAAGG
R4-2(10)        (151)   TAAGCTTACGGGAATAGACTTGAGTCATTTGAAGG
R3-2(5,10)      (151)   TAAACTCACAGGGATTGATCTCTCTCATTTGAAAG
R3-2(3,5)       (151)   TAAACTCACAGGGATTGATCTCTCTCATTTGAAAG
```

VP7 gene (Segment 7)

```
                      1                                                  50
AHSV-2          (1)   GGACCAAGTAAAGTGCAGACGGGACCTTATGCAGGAGCGGCTGAGGTGCA
AHSV-3          (1)   GGACCAAGCAAAGTACAGACGGGACCTTATGCAGGAGCAGTTGAGGTGCA
AHSV-4          (1)   GGACCAAGCAAAGTGCAAACGGGACCTTATGCAGGAGCGGTAGAGGTGCA
R4-24,5,7,10    (1)   GGACCAAGTAAAGTGCAGACGGGACCTTATGCAGGAGCGGCTGAGGTGCA
R3-25,10        (1)   GGACCAAGCAAAGTACAGACGGGACCTTATGCAGGAGCAGTTGAGGTGCA
R3-23,5         (1)   GGACCAAGCAAAGTACAGACGGGACCTTATGCAGGAGCAGTTGAGGTGCA
                      51                                                 100
AHSV-2         (51)   ACAGTCTGGCAGATATTATGTACCGCAAGGTCGAACACGTGGTGGGTACA
AHSV-3         (51)   ACAATCTGGCAGATATTACGTACCGCAAGGTCGAACACGTGGTGGGTACA
AHSV-4         (51)   ACAATCTGGCAGATATTACGTACCGCAAGGTCGAACACGTGGTGGGTACA
R4-24,5,7,10   (51)   ACAGTCTGGCAGATATTATGTACCGCAAGGTCGAACACGTGGTGGGTACA
R3-25,10       (51)   ACAATCTGGCAGATATTACGTACCGCAAGGTCGAACACGTGGTGGGTACA
R3-23,5        (51)   ACAATCTGGCAGATATTACGTACCGCAAGGTCGAACACGTGGTGGGTACA
                      101                                                150
AHSV-2        (101)   TCAATTCAAATATTGCTGAAGTGTGTATGGATGCGGGTGCTGCGGGACAG
AHSV-3        (101)   TTAATTCAAATATTGCTGAAGTGTGTATGGATGCAGGCGCTGCGGGACAG
AHSV-4        (101)   TCAATTCAAATATTGCTGAGGTGTGTATGGATGCAGGTGCTGCGGGACAG
R4-24,5,7,10  (101)   TCAATTCAAATATTGCTGAAGTGTGTATGGATGCGGGTGCTGCGGGACAG
R3-25,10      (101)   TTAATTCAAATATTGCTGAAGTGTGTATGGATGCAGGCGCTGCGGGACAG
R3-23,5       (101)   TTAATTCAAATATTGCTGAAGTGTGTATGGATGCAGGCGCTGCGGGACAG
                      151                                                200
AHSV-2        (151)   GTCAATGCGCTGCTAGCCCCAAGGAGGGGGGACGCAGTCATGATCTATTT
AHSV-3        (151)   GTCAATGCGCTGCTAGCCCCAAGGAGGGGGGACGCAGTCATGATCTATTT
AHSV-4        (151)   GTCAATGCGCTGTTAGCCCCAAGGAGGGGGGACGCAGTCATGATCTATTT
R4-24,5,7,10  (151)   GTCAATGCGCTGCTAGCCCCAAGGAGGGGGGACGCAGTCATGATCTATTT
R3-25,10      (151)   GTCAATGCGCTGCTAGCCCCAAGGAGGGGGGACGCAGTCATGATCTATTT
R3-23,5       (151)   GTCAATGCGCTGCTAGCCCCAAGGAGGGGGGACGCAGTCATGATCTATTT
                      201                                                250
AHSV-2        (201)   CGTTTGGAGACCGCTGCGTATATTCTGTGATCCTCAAGGTGCATCACTCG
AHSV-3        (201)   TGTTTGGAGACCATTGCGTATATTTTGTGATCCTCAAGGTGCGTCACTTG
AHSV-4        (201)   CGTTTGGAGGCCGTTGCGTATATTTTGTGATCCTCAGGGTGCGTCACTTG
R4-24,5,7,10  (201)   CGTTTGGAGACCGCTGCGTATATTCTGTGATCCTCAAGGTGCATCACTCG
R3-25,10      (201)   TGTTTGGAGACCATTGCGTATATTTTGTGATCCTCAAGGTGCGTCACTTG
R3-23,5       (201)   TGTTTGGAGACCATTGCGTATATTTTGTGATCCTCAAGGTGCGTCACTTG
                      251
AHSV-2        (251)   AGAGCGCTCC
AHSV-3        (251)   AAAGCGCTCC
AHSV-4        (251)   AGAGCGCTCC
R4-24,5,7,10  (251)   AGAGCGCTCC
R3-25,10      (251)   AAAGCGCTCC
R3-23,5       (251)   AAAGCGCTCC
```

NS2 gene (Segment 8)

```
                      1                                                  50
AHSV-2          (1)   AGCTTAATGATTACTGAGAGTGGAATTGAGGTAACGCAAAACCGATGGGA
AHSV-3          (1)   AGTTTAATGATTACTGAGAGTGGAATTGAGGTAACGCAAAACCGATGGGA
AHSV-4          (1)   AGTTTAATGATTACTGAAAGTGGAATTGAGGTCACGCAAAACCGATGGGA
R4-24,5,7,10    (1)   AGTTTAATGATTACTGAAAGTGGAATTGAGGTCACGCAAAACCGATGGGA
R4-27,10        (1)   AGTTTAATGATTACTGAAAGTGGAATTGAGGTCACGCAAAACCGATGGGA
R4-210          (1)   AGTTTAATGATTACTGAAAGTGGAATTGAGGTCACGCAAAACCGATGGGA
R3-25,10        (1)   AGTTTAATGATTACTGAGAGTGGAATTGAGGTAACGCAAAACCGATGGGA
R3-23,5         (1)   AGTTTAATGATTACTGAGAGTGGAATTGAGGTAACGCAAAACCGATGGGA
                      51                                                 100
AHSV-2         (51)   GGAGTGGAGCTTTGAGGCGTTAACACCAGTACCCATGGCTGTGGCGGTGA
AHSV-3         (51)   GGAGTGGAGTTTTGAAGCGTTAACACCAGTACCAATGGCAGTGGCGGTGA
AHSV-4         (51)   AGAGTGGAGTTTTGAAGCGTTAACACCAGTACCAATGGCTGTGGCGGTCA
R4-24,5,7,10   (51)   AGAGTGGAGTTTTGAAGCGTTAACACCAGTACCAATGGCTGTGGCGGTCA
R4-27,10       (51)   AGAGTGGAGTTTTGAAGCGTTAACACCAGTACCAATGGCTGTGGCGGTCA
R4-210         (51)   AGAGTGGAGTTTTGAAGCGTTAACACCAGTACCAATGGCTGTGGCGGTCA
R3-25,10       (51)   GGAGTGGAGTTTTGAAGCGTTAACACCAGTACCAATGGCAGTGGCGGTGA
R3-23,5        (51)   GGAGTGGAGTTTTGAAGCGTTAACACCAGTACCAATGGCAGTGGCGGTGA
                      101                                                150
AHSV-2        (101)   ATGTAGGGAGAGGCTCGTTTGACACTGAGATTAAATATGTGAGAGGAAGC
AHSV-3        (101)   ATGTAGGGAGAGGCTCGTTTGACACTGAGATTAAATATGTGAGAGGAAGC
AHSV-4        (101)   ACGTAGGGAGAGGCTCGTTTGACACTGAGATTAAATATGTGAGAGGAAGC
R4-24,5,7,10  (101)   ACGTAGGGAGAGGCTCGTTTGACACTGAGATTAAATATGTGAGAGGAAGC
R4-27,10      (101)   ACGTAGGGAGAGGCTCGTTTGACACTGAGATTAAATATGTGAGAGGAAGC
R4-210        (101)   ACGTAGGGAGAGGCTCGTTTGACACTGAGATTAAATATGTGAGAGGAAGC
R3-25,10      (101)   ATGTAGGGAGAGGCTCGTTTGACACTGAGATTAAATATGTGAGAGGAAGC
R3-23,5       (101)   ATGTAGGGAGAGGCTCGTTTGACACTGAGATTAAATATGTGAGAGGAAGC
                      151                                                200
AHSV-2        (151)   GGTGCAGTTCCACCTTATACGAAGAATGGAATGGATCGAAGAGCGATGCC
AHSV-3        (151)   GGTGCGGTTCCACCTTATACGAAGAATGGAATGGATCGAAGAGCGATGCC
AHSV-4        (151)   GGTGCGGTTCCACCTTATACGAAGAATGGAATGGACCGAAGAGCGATGCC
R4-24,5,7,10  (151)   GGTGCGGTTCCACCTTATACGAAGAATGGAATGGACCGAAGAGCGATGCC
R4-27,10      (151)   GGTGCGGTTCCACCTTATACGAAGAATGGAATGGACCGAAGAGCGATGCC
R4-210        (151)   GGTGCGGTTCCACCTTATACGAAGAATGGAATGGACCGAAGAGCGATGCC
R3-25,10      (151)   GGTGCGGTTCCACCTTATACGAAGAATGGAATGGATCGAAGAGCGATGCC
R3-23,5       (151)   GGTGCGGTTCCACCTTATACGAAGAATGGAATGGATCGAAGAGCGATGCC
                      201                                                250
AHSV-2        (201)   TTCTTTACCAGGAATAACCACTTTGGATGTTGGAGTTAGAGATTTGCGTT
AHSV-3        (201)   TTCTTTACCAGGAATAACAACTTTGGATGTTGGAGTTAGAGATTTGCGTT
AHSV-4        (201)   TTCTTTACCAGGAATAACAACTTTGGATGTTGGAGTTAGAGATTTGCGTT
R4-24,5,7,10  (201)   TTCTTTACCAGGAATAACAACTTTGGATGTTGGAGTTAGAGATTTGCGTT
R4-27,10      (201)   TTCTTTACCAGGAATAACAACTTTGGATGTTGGAGTTAGAGATTTGCGTT
R4-210        (201)   TTCTTTACCAGGAATAACAACTTTGGATGTTGGAGTTAGAGATTTGCGTT
R3-25,10      (201)   TTCTTTACCAGGAATAACAACTTTGGATGTTGGAGTTAGAGATTTGCGTT
R3-23,5       (201)   TTCTTTACCAGGAATAACAACTTTGGATGTTGGAGTTAGAGATTTGCGTT
                      251                                                300
AHSV-2        (251)   TAAAGATGAAGGAGAACAGGGAGGCAGAAAGGGAGAAGATGGAACGAGCC
AHSV-3        (251)   TAAAGATGAAGGAGAACAGGGAGGCAGAAAGGGAGAAGATGGAACGAGCC
AHSV-4        (251)   TAAAGATGAAGGAGAACAGGGAGGCAGAAAGGGAGAAGATGGAACGAGCC
R4-24,5,7,10  (251)   TAAAGATGAAGGAGAACAGGGAGGCAGAAAGGGAGAAGATGGAACGAGCC
R4-27,10      (251)   TAAAGATGAAGGAGAACAGGGAGGCAGAAAGGGAGAAGATGGAACGAGCC
R4-210        (251)   TAAAGATGAAGGAGAACAGGGAGGCAGAAAGGGAGAAGATGGAACGAGCC
R3-25,10      (251)   TAAAGATGAAGGAGAACAGGGAGGCAGAAAGGGAGAAGATGGAACGAGCC
R3-23,5       (251)   TAAAGATGAAGGAGAACAGGGAGGCAGAAAGGGAGAAGATGGAACGAGCC
```

```
                      301                                                 350
AHSV-2          (301) CTAAGTGGTGGGCTCGATATGGGAAGCTGTAGAATGTATGGGGGAGGAAG
AHSV-3          (301) CTGAGTGGTGGGCTCGATATGGGAAGCTGTAGAATGTATGGGGGAGGAAG
AHSV-4          (301) CTAAGTGGTGGGCTCGATATGGGGAGCTGTAGAATGTATGGAGGAGGAAG
R4-24,5,7,10    (301) CTAAGTGGTGGGCTCGATATGGGGAGCTGTAGAATGTATGGAGGAGGAAG
R4-27,10        (301) CTAAGTGGTGGGCTCGATATGGGGAGCTGTAGAATGTATGGAGGAGGAAG
R4-210          (301) CTAAGTGGTGGGCTCGATATGGGGAGCTGTAGAATGTATGGAGGAGGAAG
R3-25,10        (301) CTGAGTGGTGGGCTCGATATGGGAAGCTGTAGAATGTATGGGGGAGGAAG
R3-23,5         (301) CTGAGTGGTGGGCTCGATATGGGAAGCTGTAGAATGTATGGGGGAGGAAG
                      351                                                 400
AHSV-2          (351) AAATGACGTGCGTGAGATTACCTTGGATGAGGCCGGACCATCACGTACGC
AHSV-3          (351) AAATGATGTGCGTGAGATCACCTTGGATGAGGCTGGACCATCGCGTACAC
AHSV-4          (351) AAATGATGTGCGTGAGATCACCTTGGATGAGGCCGGACCATCACGTACAC
R4-24,5,7,10    (351) AAATGATGTGCGTGAGATCACCTTGGATGAGGCCGGACCATCACGTACAC
R4-27,10        (351) AAATGATGTGCGTGAGATCACCTTGGATGAGGCCGGACCATCACGTACAC
R4-210          (351) AAATGATGTGCGTGAGATCACCTTGGATGAGGCCGGACCATCACGTACAC
R3-25,10        (351) AAATGATGTGCGTGAGATCACCTTGGATGAGGCTGGACCATCGCGTACAC
R3-23,5         (351) AAATGATGTGCGTGAGATCACCTTGGATGAGGCTGGACCATCGCGTACAC
                      401                                                 450
AHSV-2          (401) CAAGGAGACTTTCTGTTCAGAGCAATGAAAGCCGTTCAGATGATGTGGCG
AHSV-3          (401) CAAGGAAACTTTCTGTTCAGAGCAATGAAAGTCGTTCAGATGATGTGGCA
AHSV-4          (401) CGAGGAAACTTTCTGTTCAGAGTAATGAAAGTCGTTCAGACGATGTGGCA
R4-24,5,7,10    (401) CGAGGAAACTTTCTGTTCAGAGTAATGAAAGTCGTTCAGACGATGTGGCA
R4-27,10        (401) CGAGGAAACTTTCTGTTCAGAGTAATGAAAGTCGTTCAGACGATGTGGCA
R4-210          (401) CGAGGAAACTTTCTGTTCAGAGTAATGAAAGTCGTTCAGACGATGTGGCA
R3-25,10        (401) CAAGGAAACTTTCTGTTCAGAGCAATGAAAGTCGTTCAGATGATGTGGCA
R3-23,5         (401) CAAGGAAACTTTCTGTTCAGAGCAATGAAAGTCGTTCAGATGATGTGGCA
                      451                                                 500
AHSV-2          (451) CGAAGACATGCTGAGTTGGTAGAGATGGAGCGATTAAGAATGATGAAGAA
AHSV-3          (451) CGAAGACATGCTGAGTTGGTGGAGATGGAGCGATTAAGAATGATGAAGAA
AHSV-4          (451) CGAAGACATGCTGAGTTGGTGGAGATGGAGCGACTAAGAATGATGAAGAA
R4-24,5,7,10    (451) CGAAGACATGCTGAGTTGGTGGAGATGGAGCGACTAAGAATGATGAAGAA
R4-27,10        (451) CGAAGACATGCTGAGTTGGTGGAGATGGAGCGACTAAGAATGATGAAGAA
R4-210          (451) CGAAGACATGCTGAGTTGGTGGAGATGGAGCGACTAAGAATGATGAAGAA
R3-25,10        (451) CGAAGACATGCTGAGTTGGTGGAGATGGAGCGATTAAGAATGATGAAGAA
R3-23,5         (451) CGAAGACATGCTGAGTTGGTGGAGATGGAGCGATTAAGAATGATGAAGAA
                      501                                                 550
AHSV-2          (501) CGAACCAGTACGTACAGAGAGTATGTGGTGTCAAAGTGATAGTGATGATC
AHSV-3          (501) TGAACCAGTACGTACAGAGAGTATGTGGTGTCAAAGTGATAGTGATGATC
AHSV-4          (501) TGAACCAGTACGTACAGAGAGTATGTGGTGTCAAAGTGAAAGTGATGATC
R4-24,5,7,10    (501) TGAACCAGTACGTACAGAGAGTATGTGGTGTCAAAGTGAAAGTGATGATC
R4-27,10        (501) TGAACCAGTACGTACAGAGAGTATGTGGTGTCAAAGTGAAAGTGATGATC
R4-210          (501) TGAACCAGTACGTACAGAGAGTATGTGGTGTCAAAGTGAAAGTGATGATC
R3-25,10        (501) TGAACCAGTACGTACAGAGAGTATGTGGTGTCAAAGTGATAGTGATGATC
R3-23,5         (501) TGAACCAGTACGTACAGAGAGTATGTGGTGTCAAAGTGATAGTGATGATC
                      551                                 584
AHSV-2          (551) AATCTGATGAGGATCACGAGATTGGGAGTACAGA
AHSV-3          (551) AATCTGATGAGGATCACGAGGTTGGGAGTACAGA
AHSV-4          (551) AATCTGATGAGGATCACGAGGTTGGGAGTACAGA
R4-24,5,7,10    (551) AATCTGATGAGGATCACGAGGTTGGGAGTACAGA
R4-27,10        (551) AATCTGATGAGGATCACGAGGTTGGGAGTACAGA
R4-210          (551) AATCTGATGAGGATCACGAGGTTGGGAGTACAGA
R3-25,10        (551) AATCTGATGAGGATCACGAGGTTGGGAGTACAGA
R3-23,5         (551) AATCTGATGAGGATCACGAGGTTGGGAGTACAGA
```

VP6 gene (Segment 9)

```
                      113                                                 162
AHSV-2          (113) GATAGGACAGGCGGCCGCAGCGGAGATTCAAAAACTGAGGGAGAGGAGGC
AHSV-3          (113) GATAGGATTGGCGGCTGCAGCGGAAATTCAAAAACTGAGGGAGAGGAGGC
AHSV-4          (113) GATAGGACAGGCGGCTGCAGCGGAAATTCAAAAACTGAGGGAGAGGAGGC
R4-24,5,7,10    (113) GATAGGACAGGCGGCTGCAGCGGAAATTCAAAAACTGAGGGAGAGGAGGC
R4-27,10        (113) GATAGGACAGGCGGCTGCAGCGGAAATTCAAAAACTGAGGGAGAGGAGGC
R4-210          (113) GATAGGACAGGCGGCTGCAGCGGAAATTCAAAAACTGAGGGAGAGGAGGC
R3-25,10        (113) GATAGGATTGGCGGCTGCAGCGGAAATTCAAAAACTGAGGGAGAGGAGGC
R3-23,5         (113) GATAGGATTGGCGGCTGCAGCGGAAATTCAAAAACTGAGGGAGAGGAGGC
                      163                                                 212
AHSV-2          (163) AAAGGCTGGAGGGGGCGATAGACGGATTGGAGGATTAGCCACGCAGGAGA
AHSV-3          (163) GAAGGCTGGAGGGGGCGATAGACGGATTGGAGGATTAGCAACGCAGGAGA
AHSV-4          (163) GAAGGCTGGAGGGGGCGATAGACGGATTGGAGGATTAGCAACGCAGGAGA
R4-24,5,7,10    (163) GAAGGCTGGAGGGGGCGATAGACGGATTGGAGGATTAGCAACGCAGGAGA
R4-27,10        (163) GAAGGCTGGAGGGGGCGATAGACGGATTGGAGGATTAGCAACGCAGGAGA
R4-210          (163) GAAGGCTGGAGGGGGCGATAGACGGATTGGAGGATTAGCAACGCAGGAGA
R3-25,10        (163) GAAGGCTGGAGGGGGCGATAGACGGATTGGAGGATTAGCAACGCAGGAGA
R3-23,5         (163) GAAGGCTGGAGGGGGCGATAGACGGATTGGAGGATTAGCAACGCAGGAGA
                      213                                                 262
AHSV-2          (213) TTGCAGACTTTGTGAAGAAGAAGATCGGAGTTGAAGTTCAGGTGTTCTCT
AHSV-3          (213) TTGCAGACTTTGTGAAGAAGAAGATCGGAGTTGAAGTTCAGGTGTTTTCT
AHSV-4          (213) TTGCAGACTTTGTGAAGAAGAAGATCGGAGTTGAAGTTCAGGTGTTTTCT
R4-24,5,7,10    (213) TTGCAGACTTTGTGAAGAAGAAGATCGGAGTTGAAGTTCAGGTGTTTTCT
R4-27,10        (213) TTGCAGACTTTGTGAAGAAGAAGATCGGAGTTGAAGTTCAGGTGTTTTCT
R4-210          (213) TTGCAGACTTTGTGAAGAAGAAGATCGGAGTTGAAGTTCAGGTGTTTTCT
R3-25,10        (213) TTGCAGACTTTGTGAAGAAGAAGATCGGAGTTGAAGTTCAGGTGTTTTCT
R3-23,5         (213) TTGCAGACTTTGTGAAGAAGAAGATCGGAGTTGAAGTTCAGGTGTTTTCT
                      263                                                 312
AHSV-2          (263) AAAGGAATGAGCAACTTATTTACTGTAGATAAGTCATTGCTTGAGCGGGG
AHSV-3          (263) AAAGGAATGAGCAACTTATTTACTGTAGATAAGTCATTGCTTGAGCGGGG
AHSV-4          (263) AAAGGAATGAGCAACTTATTTACTGTAGATAAGTCATTGCTTGAGCGGGG
R4-24,5,7,10    (263) AAAGGAATGAGCAACTTATTTACTGTAGATAAGTCATTGCTTGAGCGGGG
R4-27,10        (263) AAAGGAATGAGCAACTTATTTACTGTAGATAAGTCATTGCTTGAGCGGGG
R4-210          (263) AAAGGAATGAGCAACTTATTTACTGTAGATAAGTCATTGCTTGAGCGGGG
R3-25,10        (263) AAAGGAATGAGCAACTTATTTACTGTAGATAAGTCATTGCTTGAGCGGGG
R3-23,5         (263) AAAGGAATGAGCAACTTATTTACTGTAGATAAGTCATTGCTTGAGCGGGG
                      313
AHSV-2          (313) TGGGTTAGGG
AHSV-3          (313) TGGGTTAGGG
AHSV-4          (313) TGGGTTAGGA
R4-24,5,7,10    (313) TGGGTTAGGA
R4-27,10        (313) TGGGTTAGGA
R4-210          (313) TGGGTTAGGA
R3-25,10        (313) TGGGTTAGGG
R3-23,5         (313) TGGGTTAGGG
```

NS3 gene (Segment 10)

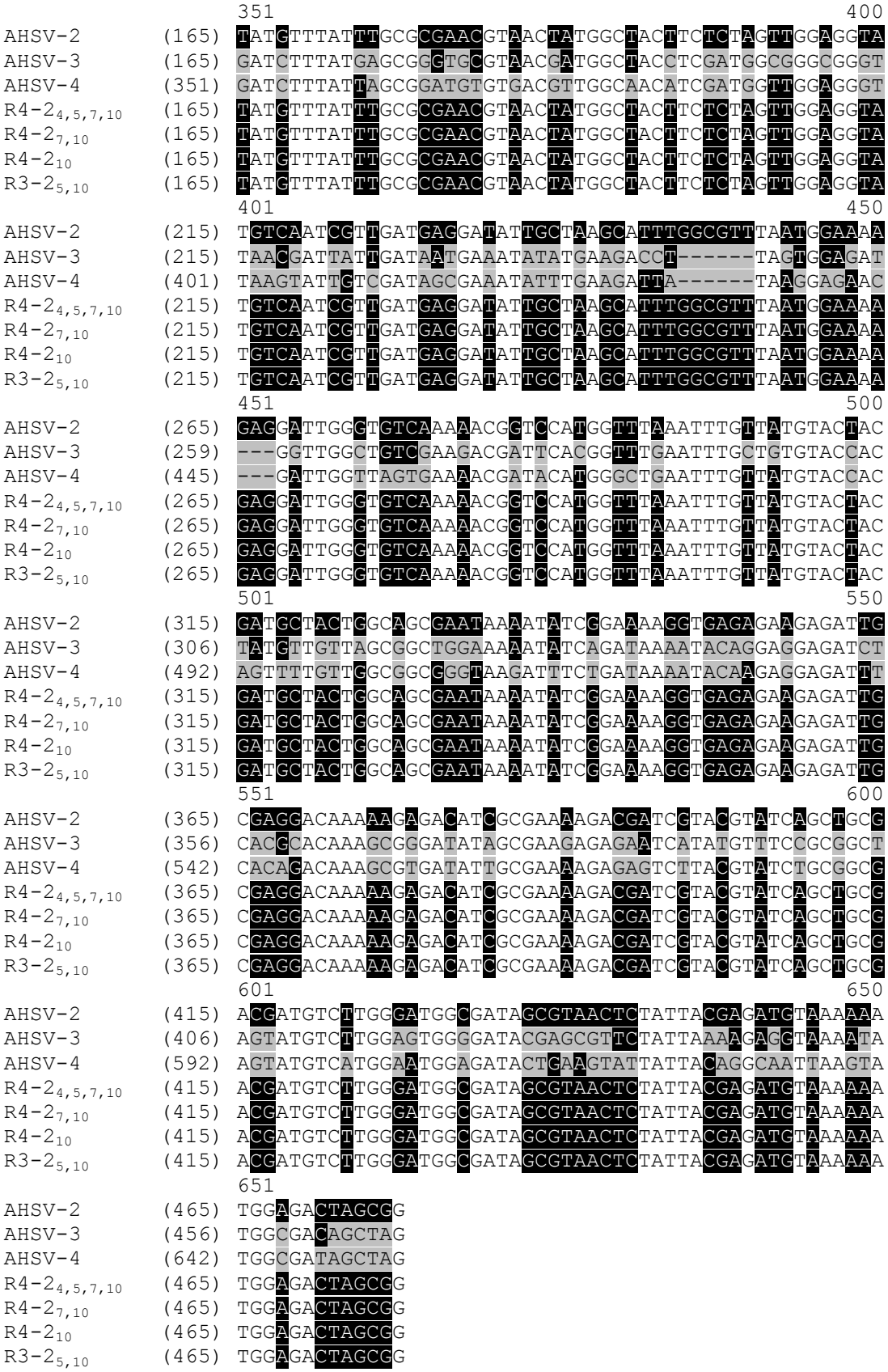

APPENDIX B

Amino acid sequence alignment of NS3 of AHSV-2, AHSV-3 and AHSV-4. Dots indicate identity to AHSV-2 82/61 NS3.

```
                  1                                                  50
AHSV-2 82/61      MNLASISQSYMSHNENERSIVPYIPPPY-HPTAPALAVSASQMETMSLGI
AHSV-3 M322/97    .S..T.AEN..M..G.Q.A....V....AYAN..TLGGQ.GE..S.....
AHSV-4 HS39/97    ....T.AKN.SM..GESGA....V....NFAS..TFSQRT....SV....
                  51                                                 100
AHSV-2 82/61      LNQAMSSSAGASGALKDEKAAFGAVAEALRDPEPIRKIKRRVGIQTLKTL
AHSV-3 M322/97    .......TT...R...........M...........Q..KH..LR...H.
AHSV-4 HS39/97    .......TT..............M...........Q..KQ...R...N.
                  101                                                150
AHSV-2 82/61      KVELSGMRRKKLILKIIMFICANVTMATSLVGGMSIVDEDIAKHLAFDGK
AHSV-3 M322/97    .I..AS...RYA..RVVI.MSGC......MA..LT.I.NE.YED.SG..-
AHSV-4 HS39/97    .M..AT.....SA...MI..SGC..L...M...L....DE.LRDYKNND-
                  151                                                200
AHSV-2 82/61      GDWVSKTVHGLNLLCTTMLLAANKISEKVREEIARTKRDIAKRQSYVSAA
AHSV-3 M322/97    --.L...I.............G...D.IQ...S.........E......
AHSV-4 HS39/97    --.LM..I.........V....G...D.MQ...S.........E......
                  201              220
AHSV-2 82/61      TMSWDGDSVTLLRDVKYGD-
AHSV-3 M322/97    S...S..TSV..KE.....S
AHSV-4 HS39/97    S...S..TEM..QGI...ES
```